UNIVERSITÄT
DES
SAARLANDES

Effect of obesity on blood-brain barrier integrity in ischemic brain using mouse model

Dissertation

Zur Erlangung des Grades

Des Doktors der Naturwissenschaften

Der Naturwissenschaftlich-Technischen Fakultät

Der Universität des Saarlandes

Von

M.Sc. Shatha Ramadhan Zaidan

Saarbrücken

2020

Tag des Kolloquiums:

15.06.2020

Dekan:

Univ.-Prof. Dr. Guido Kickelbick

Mitglieder des Prüfungsausschusses:

Prof. Dr. Claus-Michael Lehr (dem Vorsitzenden)

Prof. Dr. Claus Jacob (Berichterstatter)

Prof. Dr. Caroline Gaucher (Berichterstatter)

Dr. Stefan Böttcher (Akademischen Mitarbeiter)

Erklärung

Ich erkläre hiermit an Eides statt, dass ich die vorliegende Arbeit selbständig und ohne unerlaubte fremde Hilfe angefertigt, andere als die angegebenen Quellen und Hilfsmittel nicht benutzt habe. Die aus fremden Quellen direkt oder indirekt übernommenen Stellen sind als solche kenntlich gemacht.

Die Arbeit wurde bisher in gleicher oder ähnlicher Form keinem anderen Prüfungsamt vorgelegt und auch nicht veröffentlicht.

Die vorliegende Arbeit wurde von April 2016 bis June 2020 unter Anleitung von Herrn Prof. Dr. Claus Jacob in der Fachrichtung Pharmazie (Bioorganische Chemie) der Naturwissenschaftlich- Technischen Fakultät der Universität des Saarlandes angerfertigt.

Saarbrücken, Datum

(Unterschrift)

I Dedicate This to Haydar .....my husband

to Zainab ..... my lovely daughter

and to my family

Acknowledgement

I would like to show my gratitude to ***Prof. Dr. Claus Jacob*** for sharing his pearls of wisdom with me during the course of this research.

I would also thank ***Prof. Dr. Tobias Hartmann*** for comments that greatly improved the manuscript.

I thank ***Dr. Marcus Grimm*** and ***Dr. Heike Grimm*** and my colleagues from AG Hartmann and Bioorganic chemistry of the University of Saarland, who provided insight and expertise that greatly assisted the research, even if they may not entirely agree with all of the interpretations/conclusions of this dissertation.

Table of contents

Abbreviations

%	percent
° C	Degree Celsius
µg	Micrograms
µl	Microliter
µM	Micro molar
ACE	Angiotensin converting enzyme
AD	Alzheimer's disease
AICD	APP intracellular domain
APLP	Amyloid precursor-like protein
APOE	Apolipoprotein E
APP	Amyloid precursor protein
Aβ	Amyloid-β
BACE1	β-site APP cleaving enzyme 1
BCA	Bicinchoninic acid
BSA	Bovine serum albumin
$CaCl_2$	calcium chloride
cDNA	Complementary DNA
CO_2	Carbon dioxide
CTF	C-terminal fragment
dd	Double-distilled
DHA	Docosahexaenoic acid
DMEM	Dulbecco's Modified Eagels Medium
DMSO	Dimethyl sulfoxide
DNA	Deoxyribonucleic acid
DPPC	Diacyl-phosphatidylcholine
E. coli	*Escherichia coli*

ECE	Endothelin converting enzymes
EDTA	Ethylenediaminetetraacetic acid
EPA	Eicosapentaenoic acid
et al.	and more
FAD	Familial Alzheimer's disease
FCS	Fetal calf serum
FRET	Fluorescence resonance energy transfer
g	Grams
GSK3	Glycogen Synthase kinase 3β
H_2O	Water
HCl	hydrochloric acid
HDAC	Histone deacetylase
HMGCR	Hydroxymethylglutaryl coenzyme
HPLC	High performance liquid chromatography
HRP	Horseradish peroxidase
IDE	Insulin-degrading enzyme
KCl	potassium chloride
KD	Knockdown
kDa	kilo-Dalton
LDH	Lactate dehydrogenase
M	Molar
MEF	Mouse embryonic fibroblast
MEM	Minimum essential medium
mg	milligram
$MgCl_2$	magnesium chloride
min	minutes
ml	milliliter
MMP	Matrix metalloproteinase

ns	not significant
N2a	Neuro-2a
NaCl	sodium chloride
NaOH	sodium hydroxide
ng	nanograms
nm	nanometer
nM	nanomolar
OD	Optical density
PBS	Phosphate buffered saline
PC	Phosphatidylcholine
qRT-PCR	Quantitative real time polymerase chain reaction
RNA	Ribonucleic acid
ROS	Reactive Oxygen Species
RT	Room temperature
sAPPα	Soluble APP fragment after the cleavage by α-secretase
sAPPβ	Soluble APP fragment after the cleavage by β-secretase
SDS-Page	Sodium dodecyl sulfate polyacrylamide gel electrophoresis
SEAP	Secretory alkaline phosphatase
sec	Seconds
LRP	Soluble lipoprotein receptor-related protein
TBS	Tris-buffered saline
U / min	revolutions per minute
v	Volt
v / v	Volume / volume
WT	Wildtype

List of tables

List of figures

Abstract:

Obesity is a primary risk factor for vascular diseases because of adipose tissue accumulation. This accumulation can significantly aggravate any injury to the blood-brain barrier (BBB), leading to disruption in BBB integrity that may cause both; enhancement in production of amyloid-β (Aβ) peptides through the amyloidogenic pathway and, impairment of the clearance of the peptide. Subsequent senile plaque accumulation between neurons and impaired clearance of Aβ in addition to intracellularly localized neurofibrillary tangles have been shown to be one of the main causes of and a hallmark of Alzheimer's disease, a progressive neurodegenerative disease. The amyloidogenic pathway consists of cleavage of a membrane protein which is amyloid precursor protein (APP) via β-secretase followed by γ-secretase, which then produces Aβ and the soluble amyloid precursor protein (sAPPβ). In the amyloidogenic pathway, sAPPβ translocates to the extracellular space and APP intracellular domain (AICD) to the nucleus, whereas the non-amyloidogenic pathway involves sequential APP proteolysis by α-secretase and γ-secretase. We aimed to study factors influencing Aβ degradation in order to try to reduce its deteriorating effects on the ischemic brain. The brain is a cholesterol-rich organ, and in the ischemic brain, cholesterol balance is altered due to loss of the BBB integrity, leading to the accumulation of Aβ as previously described in earlier studies. Therefore, the influence of cholesterol on Aβ deposition and degradation have been studied in this thesis from different perspectives, including the many enzymes involved in Aβ degradation on the cell membrane and extracellular space. In order to detect the potent enzymes involved in Aβ peptide degradation, mouse Neuro 2a (N2a) cells were used to quantify Aβ degradation both intracellularly (by quantifying the remaining peptide using living N2a cells) and extracellularly (by detecting Aβ in culture medium of the same cell line with or without cholesterol). Results obtained from this study showed that a reduction of about 20% was detected for intracellular and extracellular Aβ due to the effects of degrading enzymes, including the insulin-degrading enzyme (IDE) and neprilysin. IDE, which is a primary Aβ peptide degradation-related enzyme, was taken into consideration exclusively in this study because other enzymes have already been previously studied. The elimination of IDE in N2a IDE knockdown cells resulted in a reduction in Aβ intracellular degradation up to 5%, while it reached 20% when IDE was functioning. Moreover, extracellular Aβ even increased to about 25% in N2a IDE knockdown cells, emphasizing the important role of IDE in Aβ degradation in addition to the influence of cholesterol as an IDE modulator. Furthermore, cholesterol effects on IDE were revealed from different experiments in which cholesterol influenced the activity of IDE by up-regulating its gene expression, levels, and stability. In a sequel to earlier findings, APP, Aβ, and

AICD effects have been studied to determine the impact of these proteins on gene expressions of key regulators involved in the cholesterol biosynthetic pathway and because the transcriptional impact of these proteins on cholesterol biosynthesis have not been studied while, it need to be uncovered. Results obtained from gene expression analysis showed that deletion of APP and AICD by using mouse embryogenic fibroblasts MEF APP/APLP2 -/- and MEF ΔCT15, respectively, when compared with MEF WT, caused downregulation of cholesterol gene expression, whereas deletion of Aβ by using MEF PS1/2 -/- cells produced an upregulation of cholesterol gene expression.

As part of this thesis, the effects of selected substances or compounds on Aβ's aggregation or deposition was conducted using circular dichroism spectrometry to determine the changes in Aβ's secondary structure. Aggregation of this protein occurs once a decrease in its α-helix formation or an increase in the number of β-sheets within its structure occurs. These two secondary structural elements have been used as an indication of Aβ aggregation, in which the peptide in its native form, is folded and functioning properly (high α-helix) or when it is misfolded (less α-helix). β-sheet formation and accumulation increases and finally, this accumulation forms plaques that deteriorate in adjacent neurons, leading to cell apoptosis. Detection of α-helices by CD spectrometry was done at wavelengths of 208, 222, and 193 nm, β-sheets were detected at 218 and 192 nm, and random coils were detected at a wavelength of 205 nm. The influence of vitamins C and E, potassium, and sodium tellurite and sulfite have been observed at a concentration of 20 µM for each of them. Selenium compounds showed enhancement at 15 µM. Finally, sodium sulfide, lithium, sodium, copper, and zinc chlorides, Gallic, *p*-coumaric, sinapic, and vanillic acids, hesperidin, naringin, catechin, and flavones enhanced α-helix formation at a lower concentration of 5 µM as compared to a control mix of Aβ without additives. Finally, no effect from various compounds on AICD accumulation was observed.

From another aspect, Aβ may play a role in the innate immune system as an antimicrobial peptide. This role is controversial and has been considered in this study by evaluation of its assumed effects on the *Steinernema feltiae*, *Escherichia coli*, *Candida albicans*, and *Saccharomyces cerevisiae* strains. Limited Aβ effects on these cells' viability has been detected. This effect can be attributed to Aβ's toxic properties rather than its antimicrobial characteristics. This aspect needs to be studied more extensively.

Zusammenfassung:

Durch die Vermehrung von Fettgewebe ist Übergewicht ein Hauptrisikofaktor für Gefäßkrankheiten. Diese Vermehrung beeinträchtigt die Integrität der Blut-Hirn Schranke, was zur Steigerung der Produktion von Amyloid-β (Aβ) Peptiden in der amyloidogenen Prozessierung und zur Einschränkung Aβ-Clearance führt. Folglich sammeln sich senile Plaques zwischen den Neuronen, die zusammen mit einer gestörten Clearance von Aβ, und intrazellulären neurofibrillären Tangles als Hauptauslöser und Kennzeichen der neurodegenerativen Alzheimer-Krankheit ausgemacht wurden. Die amyloidogene Prozessierung besteht aus der Spaltung des Transmembranproteins Amyloid Precurser Protein (APP) zunächst durch die β-Sekretase gefolgt von der ɣ-Sekretase, wobei Aβ und das lösliche Amyloid Precursor Protein (sAPP) entstehen. Hierbei translozíert das sAPP in den Extrazellulärraum und die APP intracellular domain (AICD) nach intrazellulär. Die nicht-amyloidogene Prozessierung umfasst die sequentielle Proteolyse durch α-Sekretase und ɣ-Sekretase. Unser Ziel war es, Einflussfaktoren auf die Aβ-Degradation zu untersuchen, um die negative Aβ-Wirkung auf das ischämische Gehirn zu reduzieren. Das Gehirn ist ein cholesterolreiches Organ. Im ischämischen Zustand ist das Cholesterolgleichgewicht durch die eingeschränkte Integrität der Blut-Hirn-Schranke verändert. Dies führt zu Aβ-Ansammlung, wie bereits in früheren Untersuchungen beschrieben. Deswegen wird in der vorliegenden Dissertation der Einfluss des Cholesterols auf Aβ-Ablagerung und Degradation mit verschiedenen Herangehensweisen untersucht. Eingeschlossen sind dabei die vielen Enzyme, die Aβ in der Plasmamembran und im Extrazellulärraum degradieren. Um die Aβ-degradierenden Enzyme auszumachen, wurden Neuro 2a (N2a) - Mauszellen zur Quantifizierung der intrazellulären Aβ-Degradation (Messung des verbleibenden Peptids in lebenden N2a-Zellen) und der extrazellulären (Messung des Aβs in Zellkulturmedium derselben Zelllinie mit oder ohne Cholesterol) benutzt. Aus diesen Untersuchungen ergab sich eine Reduktion des intra- und extrazellulären Aβs um 20%, die von Aβ-degradierenden Enzymen, darunter Insulin-degrading enzyme (IDE) und Neprilysin, vermittelt wird. Da andere Enzyme bereits in vorangegangenen Studien untersucht wurden, wird hier ausschließlich das IDE als wichtiges Aβ-degradierendes Enzym berücksichtigt. Die Eliminierung von IDE in N2a-IDE-Knockdown-Zellen führte zu einer Verminderung intrazellulären Aβs um bis zu 5%, wohingegen es bei voller IDE-Funktion bis zu 20% sind. Zudem stieg das extrazelluläre Aβ um etwa 25%

an, wodurch die wichtige Rolle des IDE in der Aβ-Degradation und den Einfluss des Cholesterols als IDE-Modulator unterstrichen wird. Darüberhinaus zeigten verschiedene Experimente, dass Cholesterol die IDE-Aktivität steigert durch Steigerung der Genexpression, Erhöhung der Spiegel und der Stabilität. Auf Grundlage früherer Ergebnisse wurden APP, Aβ und AICD untersucht, um deren Einfluss auf die Genexpression der regulatorischen Enzyme der Cholesterolbiosynthese zu ermitteln. Ergebnisse daraus stellten dar, dass eine Deletion von APP und AICD in embryogenen Maus-Fibroblasten MEF APP/APLPp2 -/- bzw. MEF ΔCT15 verglichen mit MEF WT zu einer Herunterregulation der Cholesterol-Genexpression führten, wohingegen die Deletion von Aβ in MEF PS1/2 -/- eine Hochregulation zur Folge hatte.

Ein Teil dieser Doktorarbeit untersucht die Effekte ausgewählter Substanzen auf die Aβ-Aggregation und Ablagerung mittels Circulardichroismus-Spektroskopie (CD-Spektroskopie), um Veränderungen der Sekundärstruktur festzustellen. Eine Aggregation dieses Proteins zeichnet sich durch eine verringerte Ausprägung der α-Helix-Konformation oder eine vermehrte Anzahl an β-Faltblättern in seiner Struktur aus. Diese beiden Elemente der Sekundärstruktur dienten als Indikatoren der Aβ-Aggregation, in der das Peptid in seiner nativen Form vorliegt, gefaltet und funktionsfähig (hohe α-Helix-Anteile) oder wenn es fehlgefaltet ist (geringere α-Helix-Anteile). β-Faltblatt-Bildung und Anhäufung führt letztendlich zur Plaquebildung, welche benachbarte Neurone beeinträchtigen und deren Apoptose herbeiführen. In der CD-Spektroskopie wurden α-Helices bei den Wellenlängen 208, 222 und 193 nm, β-Faltblätter bei 218 und 192 nm und Random coils bei 205 nm detektiert. Der Einfluss von Vitamin C und E, Kalium, Natriumtellurit und Natriumsulfit wurde je bei einer Konzentration von 20 µM beobachtet. Caesiumchlorid und Selen zeigten eine Verbesserung bei einer Konzentration von 15 µM. Letztendlich verbesserten Natriumsulfid, Lithium, Natrium, Kupfer und Zinkchlorid sowie Gallussäure, Ferulasäure, *p*-Cumarsäure, Sinapinsäure und Vanillinsäure, Hesperidin, Naringin, Catechin und Flavone die α-Helix-Ausbildung bei Konzentrationen von 5µM verglichen mit einer Aβ-Kontrolle ohne Additive. Zudem wurde ein unerwarteter Effekt verschiedener Substanzen auf die AICD-Akkumulation beobachtet.

Ein anderer Aspekt des Aβs ist die mögliche Rolle im angeborenen Immunsystem als antimikrobielles Peptid. Diese Rolle ist umstritten und wurde in meiner Untersuchung durch die Effekte auf *Steinernema feltiae*, *Escherichia coli*, *Candida albicans* und *Saccharomyces cerevisiae* spcc. bewertet. Begrenzte Effekte des Aβs auf das

Zellüberleben konnten gezeigt werden. Diese Effekte sind jedoch eher auf die toxische Wirkung des Aβ zurückzuführen, als auf seine antimikrobiellen Eigenschaften. Dieser Aspekt benötigt weitere intensive Untersuchungen.

Chapter I

Introduction

Obesity is a primary risk factor for ischemic stroke because of the impairment in blood flow or even clotting due to the accumulation of adipose tissue in these patients. Additionally, ischemic stroke mediates the progressive neurodegenerative disease, Alzheimer's disease (AD). Upon stroke due to obesity, a disruption occurs in the blood-brain barrier (BBB), a barrier protecting the brain from harmful substances and controlling the intake of required substances for proper brain function, which underlies imbalance of cholesterol levels and homeostasis in the brain, main constitute of the brain (25% of total brain mass), and accumulation of amyloid β peptide, a hall mark of AD which is a product of the proteolytic cleavage of amyloid precursor protein (APP) along with APP intracellular domain (AICD). The aggregation of the insoluble form of the amyloid beta (Aβ) peptide is considered to play a significant role in neurodegeneration that leads to neuronal apoptosis and the main cause of senile plaques which have been considered toxic to surrounding neurons. The accumulation of amyloid β occurs primarily when the clearance of the peptide from the brain is obstructed due to reduced expression of lipoprotein receptor protein (LRP1), a key factor involved in the clearance of Aβ, as a consequence to the loss of BBB integrity.

1.1 Problem statement

Accumulation of Aβ is a primary risk factor in developing AD implications and hence, disaggregation or degradation of such peptide is a target of many investigations to minimize its burden on the nervous system. One of the approaches is by studying enzymes responsible for degrading Aβ such as neprilysin (nep), insulin degrading enzyme (IDE), and matrix metallopeptidase 9 (MMP9) because these enzymes are secreted inside the brain while drug resistance occurs due to the presence of efflux pumps, ATP-binding cassette subfamily b1 (ABCB1), on the surface of endothelium, cells that are connected tightly by tight junctions to form BBB. However, the impact of cholesterol on the enzymatic activity of IDE, as a therapeutic target of AD, in degrading Aβ is un-studied yet, which is the interest of this study as well as transcriptional impacts of APP, AICD and Aβ on cholesterol homeostasis. Transctiptional studies have been performed on APOE and its isoforms (ε2, ε3, and ε4) with focus on ε4 allele as it is

associated with the early onset of Alzheimer's. However, transcriptional functions of APP, AICD, and Aβ in regulating cholesterol biosynthesis have not been studied which are one of the interests in the current investigation. Additionally, Aβ generation induced by microorganism's infiltration to the brain have been suggested as a response of innate immune system in which Aβ plays the role of antimicrobial peptide (AMP). The latter hypothesis has been examined in the current study to determine the antimicrobial function potential of Aβ. Finally, nutrients from different sources which can help in maintaining Aβ in its monomer state, soluble form of the peptide that can be cleared out of the brain, have been studied *in vitro* to overcome the drug delivery implications due to the efflux pumps across BBB. These nutrients can cross BBB through channels or transporters to play a role in reducing the harmful aggregation of Aβ.

1.2 Research aims

- To examine the transcriptional impact of APP, AICD and Aβ on cholesterol *de novo* biosynthesis pathway.
- To study the combined role of cholesterol and IDE in degrading Aβ.
- To examine the antimicrobial activity of Aβ subsequent to microorganism's inflammation.
- To examine the influence of nutrients from different sources in suppressing Aβ deposition.

1.3 Research objectives

To achieve these aims, following research objectives would be utilized:

- To study the impact of APP and its derivatives; Aβ, and AICD on the transcription of genes involved in cholesterol biosynthesis pathway by employing mouse embryonic fibroblasts cells (MEF) and qRT-PCR technique. MEF WT (wild type) as control, MEF APP/APLP2 -/- which are lacking APP and APLP2 (amyloid precursor like protein-2), MEF APPΔCTF15 (ΔΔ) lack to last 15 amino acids of APP C-terminal which do not express AICD, and MEF PS1/2 -/- that do not express Aβ, and MEF PS1res which express human Aβ only.
- To study the impact of cholesterol on the enzymatic activity of IDE in degrading Aβ through utilizing neuroblastoma cells (N2A) and western blot technique.

- To study the impact of cholesterol on IDE gene expression (qRT-PCR), level and stability (western blot).
- To examine the antimicrobial activity of Aβ by measuring the impact of the peptide on the viability of bacteria and fungus strands and nematode utilizing Alamarblue assay.
- To investigate the therapeutic potential or harmful impact of some nutrients and phytochemicals that can cross the blood brain barrier by channels or transporters, on the accumulation of Aβ by employing circular dichroism (CD) technique in studying the changes in secondary structure elements of the peptide, α-helix and β-sheet. These chemicals include: vitamins (ascorbic acid and α-tocotrienol), salts (lithium chloride, rubidium chloride, sodium chloride, cupric chloride, zinc chloride, sodium sulfide, sodium sulfite, sodium selenite, and sodium selenite), phytochemicals: Gallic acid, *p*-coumaric acid, sinapic acid, vanilic acid, hesperidin, naringin, and catechin hydrate, and flavones and selenoflavones.

This thesis is divided into five chapters. Chapter One contains an overview of the completed work and thesis structure. In Chapter Two, previous studies, which have been performed relevant to the interest of the study, are reviewed. Chapter Three contains a detailed presentation of the cell lines, materials and test methods which have been utilized during the experimental course of the study. Results of the experimental plan are illustrated in Chapter Four. This chapter contains the discussion of these results too. Finally, chapter Five, summarizes the main conclusions of the study as well as the recommendations for future work.

Supporting literatures are listed in the Bibliography section of the thesis, and detailed results are shown in the Appendix. Figure 1, presents the plan of the study.

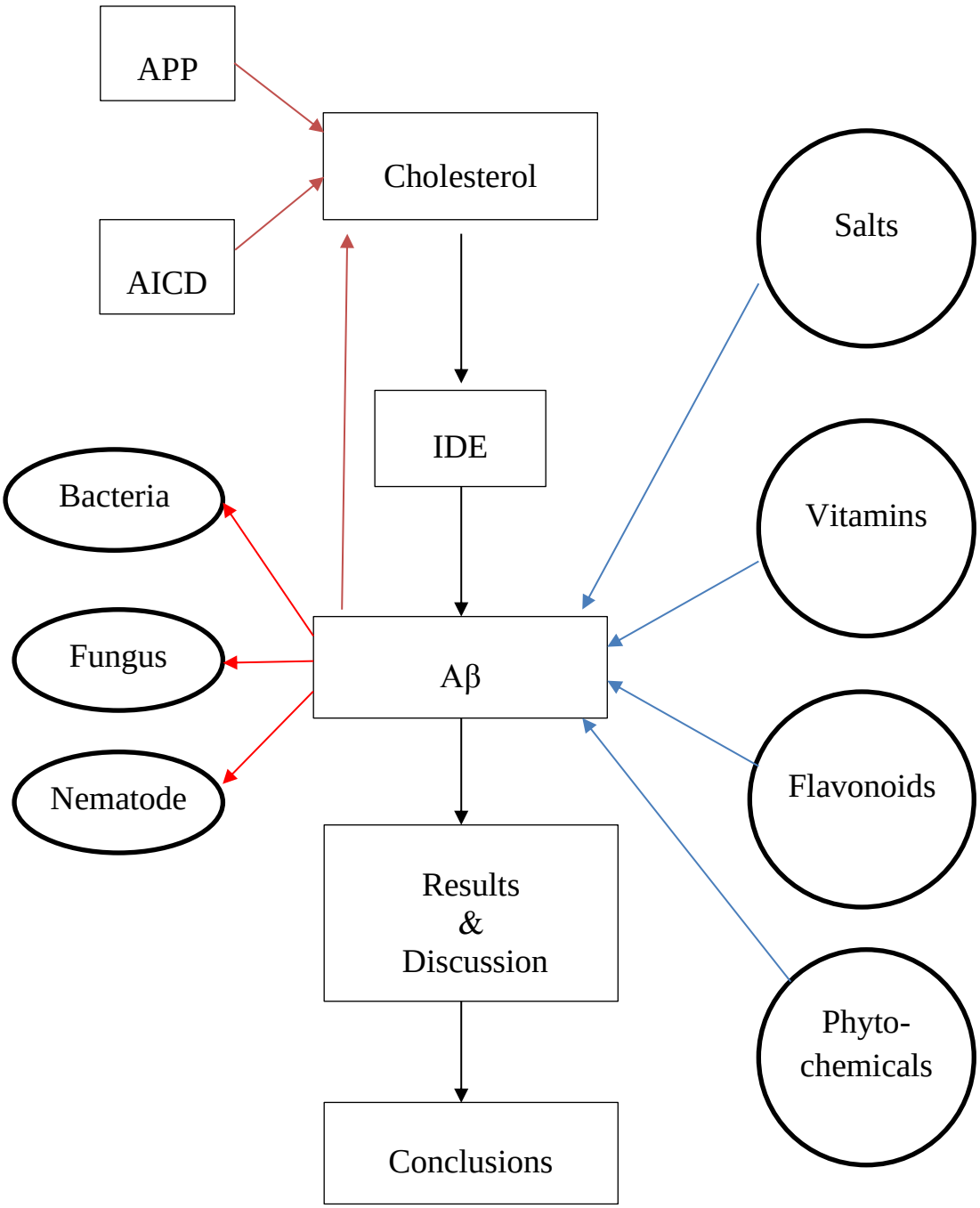

Figure 1: Research plan of the study.

Chapter II

Literature review

2.1 Overview

Obesity is defined according to World Health Organization (WHO) as abnormal or excessive fat accumulation that impairs health and is measured by body mass index (BMI), a simple weight-for-height index that is used to classify overweight and obesity. It can be measured as a ratio of body weight (kg) to the squared body height in meters (kg/m^2). Individuals with a BMI $\geq$25 are classified as overweight persons, while persons with $\geq$30 are considered obese (WHO, 2000). In Germany, around 30% of the elderly population (≥64 years) were obese in 2014 (Germany extended 2014 from worldobesity.org), while in Iraq it was around 23% in 2006 according to the same study. This rate is likely to increase and reach epidemic proportions. Obesity is a risk factor for ischemic stroke and vascular cognitive impairment (Andrew et al., 2015 and Seunghan et al., 2003) and increases AD progression (Gorelick et al., 2011) via aggravation of BBB injury (Tucsek et al., 2014). The capillary lengths in mouse is 0.6 km while, in the human brains is 650 km, which represent >85% of total cerebral blood vessel length, that provides the largest surface area of endothelial cells (120 cm^2/g of the brain) for solute transport exchange between blood and brain (Zlokovic, 2008). The estimated distance between the BBB and neurons is 8 μm on average, in which the diffusion of molecules from capillaries to neurons across the brain interstitial space occurs promptly (Montagne et al., 2017).

2.2 Blood brain barrier integrity

As the name implies, this barrier is between the brain on one side and blood on the other one. The function of the BBB is to maintain the brain by stringent regulation of cell, molecular, and ion transport and xenobiotic efflux (Abbott et al., 2006; Tietz and Engelhardt, 2015). The adequate neuronal and synaptic peoformance is maintained by BBB through controlling the constitution of the internal neuronal milieu (Zhao et al., 2015). This barrier consists of endothelial cells and blood vessel walls that are tightly connected through tight junctions (Daneman and Prat, 2015) as shown in Figure 2 (Boonstra et al., 2015). As shown in the same figure the differences between blood vessels in the body and brain in which tight junctions are preventing free transport of blood substances into the brain. The existance of tight junctions, and the expression of

specific polarized transport systems that mediate the transport of nutrients to the brain parenchyma, efflux of toxic metabolites from the brain, and regulation of the migration of circulating immune cells are displaying a unique phenotype BBB endothelial cells (Luissint et al., 2012; Wallez and Huber, 2008).

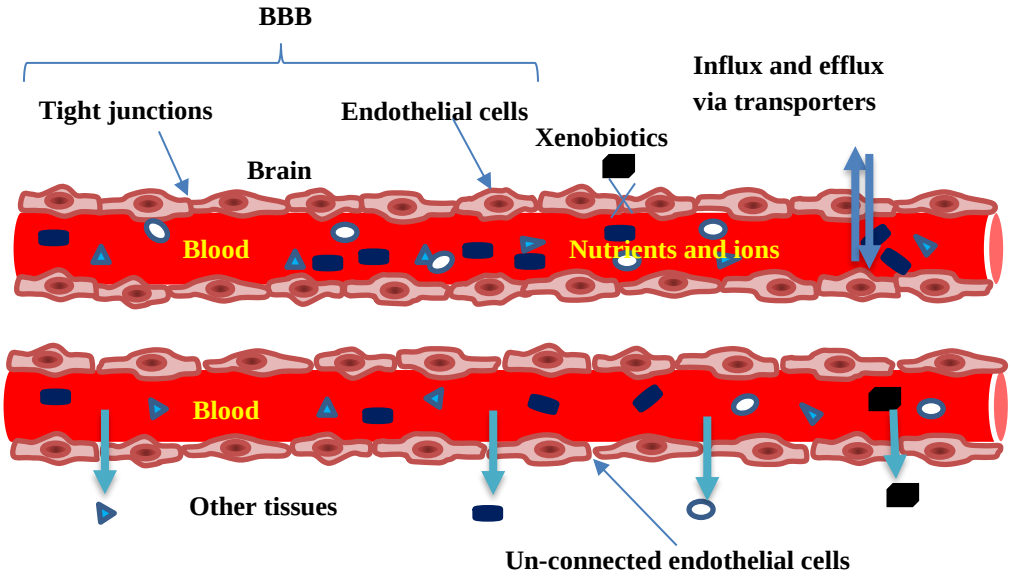

Figure 2: Composition of Blood brain barrier (BBB) (up), where endothelial cells are strictly connected by tight junction which prevent free transport of molecules, ions and xenobiotics from the blood to the brain. Normal endothelial cells (down) are un-connected.

A tight junction consists of a complex combination of both transmembrane and cytoplasmic accessory proteins and is linked to the actin-based cytoskeleton, thus allowing it to form a seal with the cytoskeleton (Liu et al., 2012; Bauer et al., 2011). The first proteins that constitute a tight junction are occludin (molecular weight 60–65 kDa) and claudin (molecular weight 20–24 kDa) followed by junctional adhesion molecules (molecular weight 40 kDa) in addition to cytoplasmic accessory proteins and the zonula occludens (ZO) protein family (molecular weight 160 kDa), (Sandoval and Witt, 2008). Figure 3 shows a schematic view of tight junction. This protein combination preserves and maintains the brain.

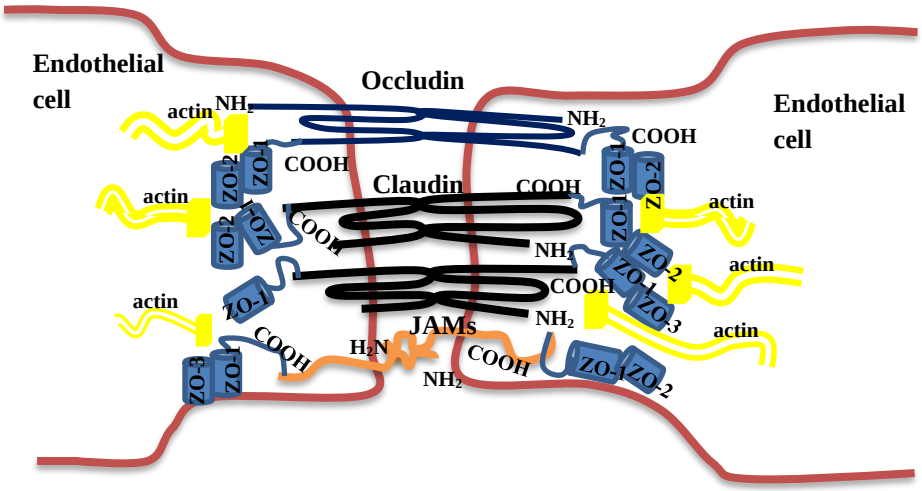

Figure 3: Schematic view of proteins that structuring tight junction, occludin, claudin, junctional adhesion molecules and ZO family and actin proteins (Redzic, 2011 with modifications).

Additionally, in order to integrate the BBB's full function, there is a group of ATP-binding cassette (ABC) family of transporters (ABC-A1, -C1, and -G1) (Juan et al., 2013). Obesity in aging increases BBB disruption, inflammation, and oxidative stress (Tucsek et al., 2014), and the influx of serum cholesterol through the BBB leads to accumulation of Alzheimer's hall-mark peptide, Aβ (Gosselet, 2011). Cholesterol was taken into consideration in this study because it is the main lipid in the brain (O'Brien and Sampson, 1965).

2.3 Cholesterol in the brain

Cholesterol is an essential ingredient of cell membranes in mammalians. It is necessary for the cell membrane's bilayer function and organization because of its structure, which consists of a fused rigid ring system, a polar hydroxyl group, and a hydrocarbon tail. Therefore, it can increase order within the membrane and thereby affect membrane fluidity, especially in lipid rafts (Grimm et al. 2013). Cholesterol is localized in sizable levels in the brain, where it comprises 25% of the total body cholesterol (Dietschy and Turkey, 2004; Dietschy, 2009; Bjorkhem, 2006) at a content of 15-30 mg/g tissue in the brain whereas in other tissues, the content is 2-3 mg/g tissue (Petrov et al, 2016). Figure 4 shows cholesterol's chemical structure.

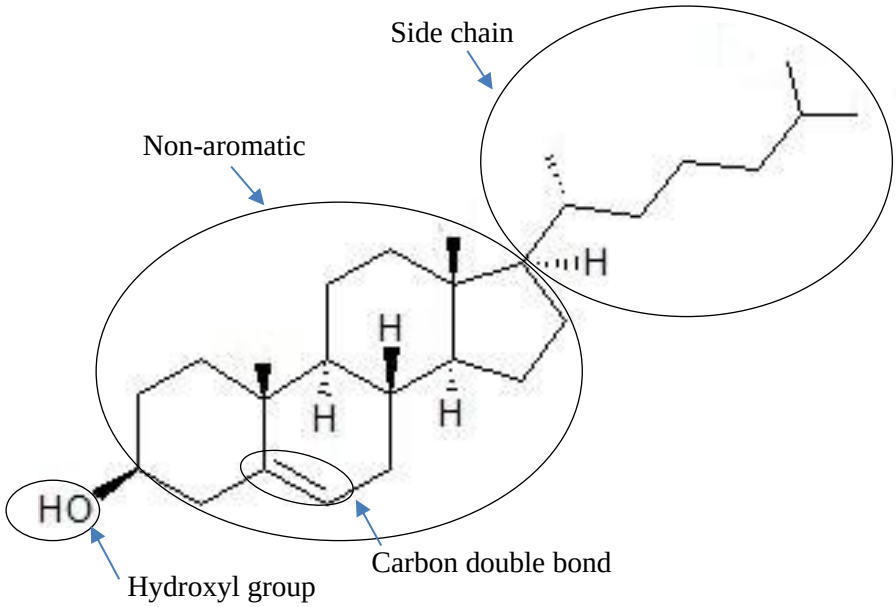

Figure 4: Chemical structure of cholesterol, $C_{27}H_{46}O$, molecular weight 386.664 g/mol (picture from https://pubchem.ncbi.nlm.nih.gov/cpmpound/cholesterol#section=Top with modifications).

2.3.1 Cholesterol biosynthesis pathway

Cholesterol homeostasis is maintained by sterol regulatory element-binding proteins (SREBPs), which are transcription factors involved in regulating cholesterol biosynthesis genes (Arenas et al, 2017 and Zhang and Liu, 2015). At low cholesterol concentrations, sterol sensing domains (SSDs) catalyzes SREBP cleavage activating protein (SCAP) to escort the in-active form of SREBP to the Golgi complex where, a sequential cleavage of SREBP by site-1 and site-2 proteases (S1P and S2P) occurs to form the mature SREBP (m-SREBP). The active form of SREBP (m-SREBP) is translocated to the nucleus to upregulate gene expression of cholesterol synthesis pathway by binding to sterol regulatory elements (SRE) in the promoter region of about 30 genes (Petrov et al, 2016). At high cholesterol level, insulin-induced gene 1 and 2 (INSIG-1 and INSIG-2), consolidated proteins in the endoplasmic reticulum (ER), inhibit SCAP from escorting SREBP to the Golgi complex and hence downregulating cholesterol biosynthesis.

Cholesterol biosynthesis is a multi-step process which involves the formation of Acetoacetyl Co-A from two moles of Acetyl-Coenzyme-A then to form 3-hydroxy-3-methylglutaryl-CoA by HMG-COA synthase (encoded by HMGCS1 gene) in the first step (Mohamed et al, 2015). Then, mevalonate pathway starts by HMG-COA reductase

(encoded by HMGCR gene) which is a rate-limit step in the cholesterol pathway. Isopentenyl pyrophosphate (IPP) is then produced after a series of enzymatic reaction of mevalonate pathway. Squalene is produced by condensation of six IPP molecules and regulated by many enzymes. Squalene cyclization to lanosterol and further steps (19-step process; Zhang and Liu, 2015) ends with production of cholesterol (Petrov et al, 2016; Zhang and Liu, 2015; Hung et al, 2013; and Ye and DeBose Boyd, 2011).

2.4 Alzheimer's Disease

AD is defined as a neurodegenerative disorder of the central nervous system and is characterized by a progressive loss of short-term memory accompanied by a gradual loss of cognitive functions (Ross and Poirier, 2004). AD is the most common cause of dementia in the elderly, accounting for 60% to 70% of all dementia cases. It can be determined by a neuropathological diagnosis as a consequence of the presence of neurofibrillary tangles and senile plaques (Xu, et al., 2013). Furthermore, mostly the second element of dementia after AD is vascular dementia in aged pateints (Khan et al., 2016). Definition of vascular dementia is the loss of cognitive function as a consequence of ischemic and hypoperfusive or haemorrhagic brain lesions because of cerebrovascular disease or cardiovascular pathology (Khan et al., 2016). Although extensive research has been conducted about AD and several outcomes have been disclosed, however there is a need to determine the accurate trigger factors of physiological changes which develop AD with exception of some genetic factors such as defined genetic mutations that leads to scarce and inherited forms of AD (Xu, et al., 2013). Epidemiological studies predicted that 24.3 million people have dementia worldwide at present with an increase of 4.6 million new cases of dementia diagnosed every year (one new case every seven seconds). Moreover, some anticipations pointed out that the number of demented people will double every 20 years to 81.1 million by 2040 (Ferri et al., 2010).

2.4.1 Risk factors

AD is a multifactorial disorder determined by the interaction of genetic and environmental factors. One of the genetic factors that may be responsible for the initiation of AD is mutations in the amyloid precursor protein (APP) and the presenilin-1 and -2 (PS1 and 2, respectively) genes (Xu et al., 2013). The APOE gene has three

common forms (ε2–4) in which the APOE ε4 allele mediates cholesterol metabolism by providing the characteristics for a protein that carries cholesterol in the bloodstream (Arbor et al., 2016). Individuals acquire one of the aforementioned forms of the APOE gene from parents (Kim et al., 2009). The risk of AD is increased in individuals who inherit one APOE ε4 gene as well as the early onset of the disease compared to those who inherit the ε2 or 3 form of the APOE gene. The risk is even higher when APOE-ε4 gene is inherited from both parents (Xu et al., 2013). Furthermore, the obesity-related alpha-ketoglutarate-dependent dioxygenase gene may increase the risk of developing AD due to the interaction with APOE-ε4 (Xu et al., 2013). Likewise, relatives of AD pateints of the first-degree (parent, brother, or sister) are candidate to develop the disease more than those who do not have such relative (Xu et al., 2013). Sporadic AD represents the majority of cases (95%) in which several studies have suggested a lifespan-dependent relationship of obesity with AD. Additionally, elevated cholesterol levels at midlife has also been reported to be associated with an increased risk of the AD at late-life (Xu et al., 2013).

2.4.2 Amyloid precursor protein processing

The principal pathological AD hallmarks are the formation and aggregation of senile plaques and neurofibrillary tangles at a higher rate in the brain of AD pateints when compared with healty individuals at identical ages (Saito et al., 2013). Amyloid-β (Aβ) peptide of the 39–43 amino-acid is the predominant constituent of senile plaques (Murphy and LeVine III, 2010). Aβ is generated as a final product of sequential proteolytic processing of amyloid protein precursor (APP). Aβ40 and Aβ42 peptides are popularly produced in human and murine brains (Younkin, 1998). In the amyloidogenic pathway, a sequential proteolytic cleavage of APP is mediated by β-secretase (β-site APP cleaving enzyme 1 or BACE1) followed by the γ-secretase complex, which is consisted of four core subunits of presenilins PS1 or 2, anterior pharynx defective 1 (APH-1), presenilin enhancer 2 (PEN2), and nicastrin (Baranello et al., 2016). First cleavage event by β-secretase is occurred the luminal domain of APP which produces soluble APPβ (sAPPβ) and membrane-bound APP carboxyl-terminal fragment (CTFβ or C99; Grimm et al., 2008). C99 contains an intact Aβ sequence which is cleaved by γ-secretase to generate Aβ, which is released to the extracellular space at which point it accumulates to form senile plaques and APP intracellular domains (AICD) (Saito et al., 2013). Considerable studies demonstrated that the membrane

microdomains (lipid rafts) are the locations in which amyloidogenic APP processing occurs (Saito et al., 2013; Rushworth and Hooper, 2011; Vetrivel and Thinakaran, 2010; Kim et al. 2006). However, it is obscure how APP is translocated to lipid rafts and the molecular mechanism underlying such translocation. Membrane microdomains are rich in cholesterol and sphingolipids such as ceramide, gangliosides, glycerophospholipids, and sterols (Seghezza et al., 2014). The approximate diameter of lipid rafts has been determined to be roughly around 50 nm on average (Saito et al., 2013). Golgi apparatus is forming lipid rafts and then transported to the plasma membrane at which point the main function is composing a floor for cell signaling, pathogen entry, cell adhesion, and protein sorting (Pike, 2003). The biochemical definition of lipid rafts is the detergent-resistant membrane (DRM) fraction (Saito et al., 2013). Figure 5 shows amyloidogenic and non-amyloidogenic processing of APP.

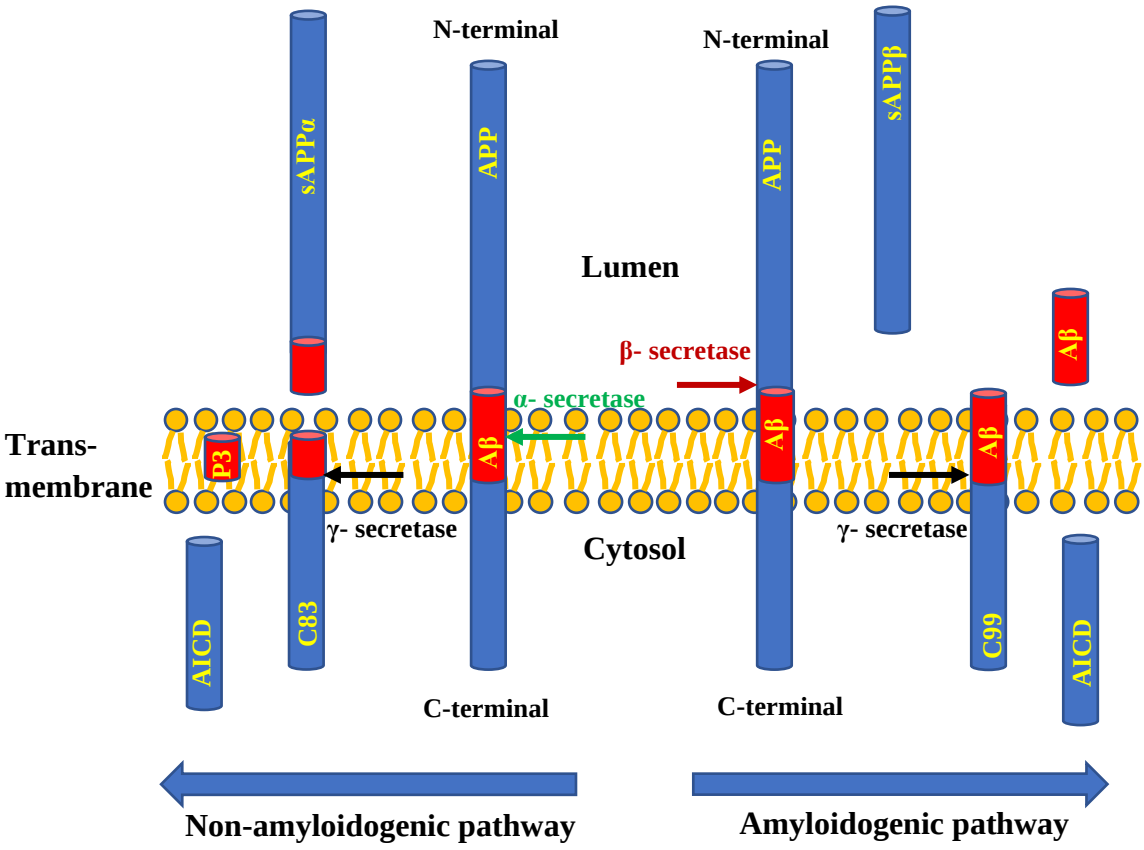

Figure 5: Amyloidogenic and non-amyloidogenic processing of APP. β-secretase and γ- secretase processing leading to producing Aβ and AICD. Accumulation of Aβ is the reason of senile plaques. While in non-amyloidogenic processing of APP, α-secretase and γ-secretase are producing P3 protein and AICD (Swomley et. al., 2014 with modifications).

The role of AICD in gene regulation is still controversial (Mett, 2017; Mueller et al., 2008) since AICD, upon cleavage, is released to the nucleus. The cytosolic adaptor Fe65, a brain-enriched and member of family of multidomain adaptor proteins, interacts with AICD and translocate to the nucleus. Following the cleavage of APP, the Fe65 adaptor protein rescues AICD from rapid degradation (Cao and Sudhof, 2001). Additionally, the translocation of AICD to the nucleus is showed to be mediated by Fe65 through studying mutated AICD protein which is lacking interaction site with Fe65. Such protein remained largely cytosolic indicating the essential role of Fe65 (Kimberly et al., 2001). The supposed involvement of AICD in transcription has been investigated by employing a fusion protein consisting of the DNA-binding domain of the yeast Gal4 transcription factor and C-terminal APP domain, and it revealed that such a protein could activate transcription from the Ga14 dependent reporter plasmid only to a small extent (Cao and Sudhof, 2001; Slomnicki and Lesniak, 2008).

2.4.3 Interaction between cholesterol and APP

Several studies have shown that the transcriptional impact of APP on SREBP1/2, HMGCR, and HMGCS genes where, cholesterol biosynthesis process was inhibited as a result of increased expression of APP (Pierrot et al, 2013). APP-KO astrocytes have shown to up-regulate mRNA expression of HMGCR as compared to wild-type (Fong et al, 2018). However, the gene expression of HMGCR exhibited no changes in AD brains of human and mouse models (Mohamed et al, 2015). Furthermore, the role of Aβ was shown to down-regulate cholesterol biosynthesis due to the inhibited maturation of SREBP (Kant et al, 2019; Chang et al, 2017; Mohamed et al, 2015; and Grimm et al, 2007) and HMGCR (Beel et al, 2010). AICD has shown to down-regulate LRP-1 gene expression and thus reducing cellular cholesterol uptake (Zhang and Liu, 2015; Hung et al, 2013; and Beel et al, 2010)

2.5 Aβ degradation

Participation of cholesterol in the process of Aβ clearance have been studied recently and shown that cholesterol may regulate Aβ degrading enzymes (Wong et al., 2014). One of such enzymes is IDE which transported (after synthesis) to the cell membrane by the secretory pathway and then, it either remains there or is secreted (Wong et al., 2014). Lipid rafts are the domains where IDE is localized (Bulloj et al., 2008). IDE is

a thiol zinc metalloendopeptidase (110 kDA) located in the cytosol, peroxisomes, endosomes, and on the cell surface (Saido and Leissring, 2012). Substrates of IDE comprise small proteins of diverse sequence such as insulin, Aβ, amylin, atrial natriuretic factor, and calcitonin, most of such substrates tend to form β-pleated sheet-rich amyloid fibrils (Shen et al., 2006). Furthermore, degrading activity of several cell lines have been screened, results revealed that IDE participated as a mjor degrading enzyme of Aβ (Qiu et al., 1998). Additionally, IDE degrading activity has been compared with neprilysin (NEP) activity in degrading intracellular Aβ by transfecting cDNA of IDE and NEP into stable human cell line which expressing APP, results demonstrated that IDE significantly lowered the levels of soluble and insoluble Aβ, whereas NEP minimized only the insoluble levels of Aβ (Farris et al., 2004). In line with this result, it was proven in another study that IDE was principal protease capable of down-regulation the levels of secreted Aβ extracellularly (Qiu et al., 1998). NEP, an 86 kDa protein, is also known as a neutral endopeptidase (Wang et al., 2006). NEP is expressed in both pre-post-synaptic brain neuronal plasma membranes (Barnes et al., 1992) and is involved in Aβ degradation. Similarly, endothelin-converting enzyme (ECE), is a membrane-bound type II metalloprotease that degrades Aβ (Eckman et al., 2000). There is evidence that angiotensin-converting enzyme (ACE), also known as dipeptidyl carboxypeptidase, can significantly inhibit Aβ aggregation, deposition, and cytotoxicity (Hu et al., 2001). A study with plasmin, tissue plasminogen activator (tPA), and urokinase-type plasminogen activator (uPA)-serine proteases have shown that tPA may be activated by Aβ in AD and enhance Aβ degradation (Ledesma et al., 2000). Matrix metalloproteinases (MMPs) belong to the family of zinc-dependent enzymes and are released into the extracellular space (Baranello et al., 2016). MMP-2 degrades Aβ1-40 and Aβ1-42 peptides *in vitro* (Roher et al., 1994). MMP-3 indirectly cleaves Aβ by activating MMP-9 (Baranello et al., 2016). MMP-9 degrades Aβ at important sites in order to facilitate β-sheet formation (Backstrom et al., 1996).

A non-enzymatic pathway in Aβ clearance from the brain is also enrolled via different mechanisms. The BBB removes Aβ from the brain largely via the age-dependent, scavenger lipoprotein receptor-1 (LPR1) (Shibata et al., 2000). The main role of this receptor is cholesterol transport and metabolism. Another mechanism of Aβ removal from the brain was shown to be via activation of microglia by Aβ plaque formation (Frautschy et al., 1997) and clearance by phagocytosis. In addition to the aforementioned mechanisms, the flowing of interstitial fluid (ISF) along periarterial

spaces until meeting the cerebrospinal fluid (CSF) and then drain into the cervical lymph nodes is another mechanism of Aβ clearance (Weller et al., 2000) where, at which point an accumulation of Aβ in ISF drainage pathway was found. Such aggregation is attributed to the increased Aβ generation, lowered solubility of Aβ, or impedance of Aβ drainage along periarterial interstitial fluid (ISF) drainage pathways resulting from aging factors in cerebral arteries (Weller et al., 2000). Figure 6 provides a schematic view of these mechanisms.

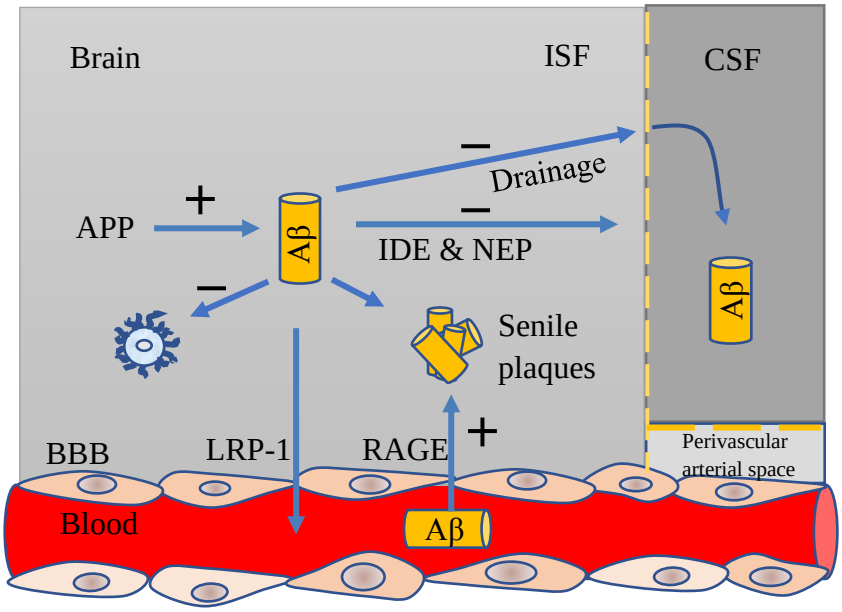

Figure 6: Schematic view of non-enzymatic mechanisms involved in Aβ clearance by lipoprotein receptor-1 (LRP-1), phagocytosis by microglia and drainage by ISF (Yoon et al., 2012 with modifications).

2.6 Impact of metals on Aβ

Metals have been shown to accumulate in the brains of AD patients. (Robinson and Bishop, 2001)). It has been revealed that when copper (Cu^{2+}) has been implicated, a Cu^{2+}-binding site on Aβ42 with a very-high-affinity of binding is mediating the precipitation of Aβ as well as increasing the the tendency of this peptide to self-aggregate in aqueous solutions (Kitazawa et al., 2016). This affinity is less in Aβ1-40 (Atwood et al., 2000). In contrast, another study demonstrated that Cu^{2+} prevented accumulation of Aβ1-42 *in vitro* (Mold et al., 2012). In line with this study, it was reported that zinc (Zn^{2+}) caused a rapid precipitation of soluble Aβ1-40 into protease-resistant, amyloid-like aggregates *in vitro* (Bush and Tanzi, 2002). Iron (Fe) levels have

been shown to rise significantly with age in both humans and mice (Maynard et al., 2005).

2.7 Oxidative stress induced by Aβ

Oxidative stress defined as the consequence increased reactive oxygen species (ROS) levels and impeded endogenous antioxidant mechanisms (Padurariu et al., 2013). It has been reported that Aβ impairs mitochondrial redox activity and increases reactive redox species (RRS) generation (Kadowaki et al., 2005), attacks cell membranes, initiates lipoperoxidation, and damages sensitive membrane proteins. The membrane barrier function and ion homeostasis are compromised (Henseley et al., 1994; Behl et al., 1994). Several studies have also suggested that Aβ-induced oxidative stress leads to apoptotic-associated neuronal cell death (Cheignon et al., 2018). Soluble Aβ has been linked to an increase in hydrogen peroxide (H_2O_2) levels thus inducing the formation of mitochondrial ROS (Massaad, 2011) as shown in Figure 7.

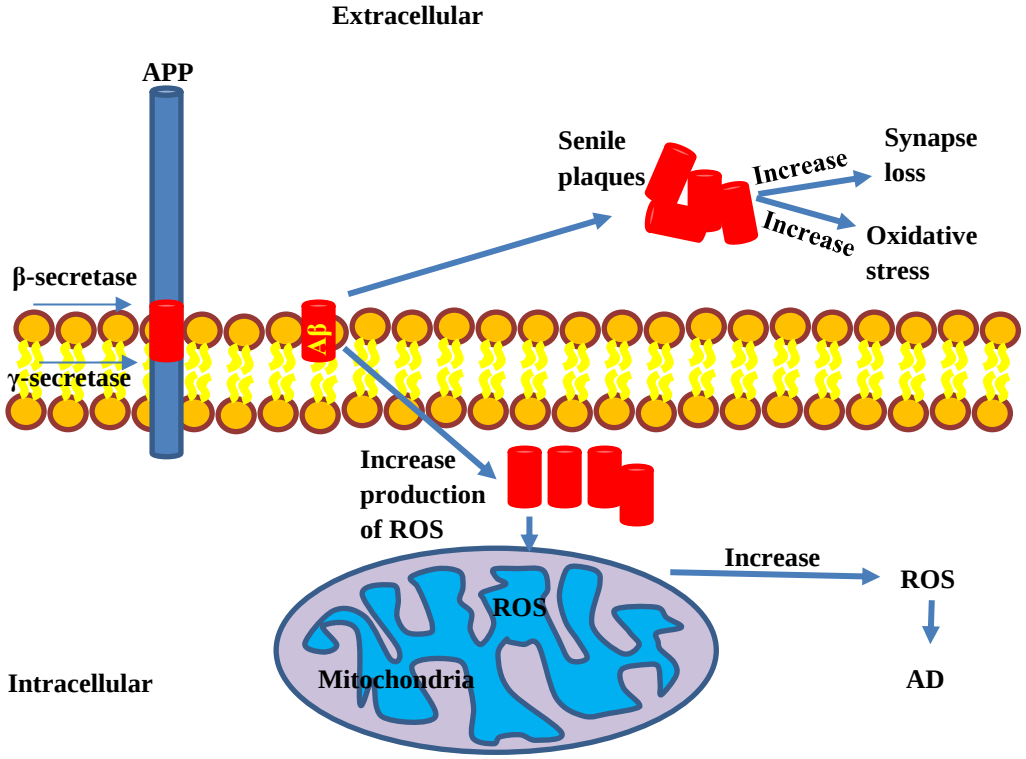

Figure 7: Aβ plaques and oxidative stress, β- and γ- secretase cleave APPs and produce Aβ peptide. Outside cells, these proteins can lead to synapse loss and oxidative stress. Inside cells, Aβ accumulation can increase the generation of ROS, causing neurotoxicity and cell death (Ghasemi et. al., 2015 with modifications).

2.8 Impact of phytochemicals

2.8.1 Flavonoids

Flavonoids are polyphenolic compounds possessing a C15 skeleton in which either two benzene rings are joined by a linear three carbon atoms chain or a chromane ring bears a secondary aromatic ring B at the second, third, or fourth position (Anand and Singh, 2012) as shown in Figure 8. Over 4,000 different flavonoids have been described (Hollman and Katan, 1999). Flavonoids are classified into six categories: (1) flavones; (2) flavonols; (3) flavanones; (4) isoflavones; (5) flavanols; and (6) anthocyanins (Hollman and Katan, 1999). It was found that dietary flavonols could contribute significantly to the antioxidant defense systems present in blood plasma (Hollman and Katan, 1999). Furthermore, limiting Aβ production by inhibiting BACE1 activity (β-secretase) was achieved by using isoliquiritigenin from *Glycyrrhiza uralensis*. Several processes of design, synthesis, and evaluation of hydroxy chalcones (simple chemical scaffold compound which is occurring naturally) to determine the inhibitory activities against BACE1 which was governed to a greater extent by the hydroxyl substituent on the chalcone's A- and B-rings (Ma et al., 2011). Tau is a microtubule-binding protein that regulates the microtubule assembly and stability in neuronal cells. Aβ induces tau protein hyper-phosphorylation, which promotes microtubule instability and contributes to its neurotoxic effects by activating apoptotic pathways (Fath et al., 2002; Ballatore et al., 2007). Glycogen synthase kinase-3α and -β (GSK-α and GSK-β) are involved in tau protein hyperphosphorylation (Hanger et al., 1992). Inhibition of GSK-3β was achieved by different types of flavonoids (Anand and Singh, 2012; Ravishankar et al., 2009).

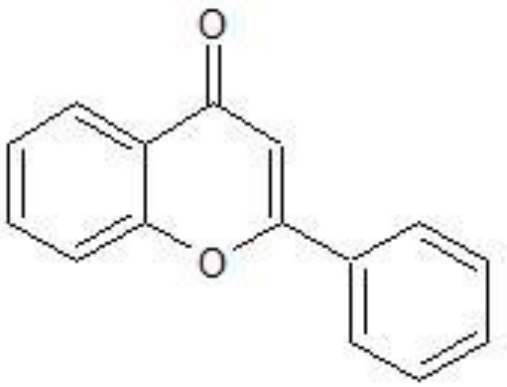

Figure 8: Chemical structure of flavone backbone. $C_{15}H_{10}O_2$ (Pubchem, https://pubchem.ncbi.nlm.nih.gov/compound/flavone#section=2D-Structure)

2.8.2 Selenium and selenoproteins

Selenocysteine is a naturally occurring amino acid in both eukaryotic and prokaryotic organisms (Wikipedia). Its chemical structure is shown in Figure 9. It can be found in bread, cereals, seafood, cruciferous vegetables (mainly broccoli), and especially Brazil nuts (Santos et al., 2014). Selenium and selenium compounds (sodium selenate [Na_2SeO_4], selenite [Na_2SeO_3], and selenoproteins) were shown to act as antioxidant compounds, which work in combination with the free radical scavenger enzyme glutathione peroxidase (GSH-Px) to catalyze the reduction of hydrogen peroxide and phospholipid hydroperoxides generated *in vivo* by ROS and hence protecting lipids (Santos et al., 2014; Rayman, 2000; Aaseth et al., 2016). Finally, in a different study, it was found that longtime supplementation of mice with Na_2SeO_4 were identified at one or more time points, especially iron and zinc, whose levels were significantly and persistently decreased after six-month Se supplementation. Untreated mice with Na_2SeO_4 supplementation showed deposition of Fe and Zn leading to increased Aβ production, elevated oxidative stress, and cell death (Zheng et al., 2016). Na_2SeO_3 can inhibit Aβ production by decreasing γ- secretase (Pillai et al., 2014). The recommended intake for men is 80 µg/day and women 57 µg/day to maintain selenium in equilibrium, that is selenium intake equals selenium excretion in urine and feces, (Pillai et al., 2014).

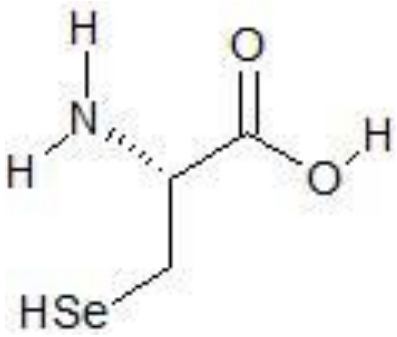

Figure 9: Chemical structure of selenocysteine (Pubchem, https://pubchem.ncbi.nlm.nih.gov/compound/6326983#section=Top).

2.8.3 Vitamin C and Vitamin E

Ascorbic acid is a six-carbon compound related to glucose. It can be found in several natural resources such as citrus fruits and many vegetables. Vitamin C is the active form of ascorbic acid which plays a role as a reducing agent and coenzyme in several metabolic pathways. Ascorbic acid is considered as a powerful antioxidant of the first-

line which participate beneficially in several impacts on redox oxidative and mitochondrial pathways in the immune system, inflammatory pathways, endothelial integrity, and lipoprotein metabolism (Monacelli et al., 2017). Additionally, a line of evidence have demonstrated that ascorbic acid may maintain BBB integrity and hence prevent the onset of AD, in a stroke model (Monacelli et al., 2017). Furthermore, BBB disruption was also impeded by ascorbic acid through upregulating the expression of the tight junction proteins, occludin and claudin-5 (Monacelli et al., 2017). Identical results have been reported for vitamin E's effects as an antioxidant (Sung et al., 2003; Nishida et al., 2009; Grimm et al., 2015).

Chapter III
Materials and Methods

3.1 Materials

Different materials from various sources were used, and hence they are arranged in this section according to their type or use.

3.1.1 Apparatus, reagents and solutions used in the study

Apparatus and relevant accessories, chemical reagents, solutions, compounds, peptides, and disposable materials that were used in this study are listed in Appendix (A).

3.1.2 Primers used in gene expression detection by RT-PCR

Detection of gene expression have been carried out by quantitative real-time polymerase chain reaction (qRT-PCR), and primers needed for the detection of genes involved in the research plan are listed in Tables 1 and 2 for murine and human genes, respectively. The primer source was Eurofins Genomics.

Table 1: Sequences of forward and reverse primers used in RT-PCR for murine genes

Oligo-name	Forward primer (5' ->3')	Reverse Primer (5' ->3')
Actb	CCTAGGCACCAGGGTGTGAT	TCTCCATGTCGTCCCAGTTG
Fdft1	CTGGAAGACCAACAGGAAGG	ACGGCCACATCTACGTTCTC
Fdps	TGAAGATCCTGATGGAGATGG	CAGCTGCATTTGTTGTCCTG
Hmgcr	ATCGAGCCACGACCTAATGA	TAAGCTGGGATATGCTTGGC
Hmgcs1	GGCAGAAAGAGGGAAAGGAT	GGCAGAAAGAGGGAAAGGAT
Hmgcs2	GGTGGATGGGAAGCGTCTA	GGTTGTTTCCAGCTTGCTTC
IDE	GCTACGTGCAGAAGGACCTC	TGGACGTATAGCCTCGTGGT
Lss	CTGCAGAAGGCTCACGAGTT	CAGTCCAGTGTGCTGAAGGA
Mvd	CCAAGAGCAGGACTTTCAGG	CCTGGAGGTGTCATTGAGGT

Mvk	GGGACGATGTTCTTCCTTGAA	TCTCAGGGAACTTGGTCAGC
Pmvk	GCGAGCACCTACAAGGAGAC	CACTCACCAGCCAGATAGGC
Polr2	AAGCGGATCACCACTCCTTA	TGAGCAAAGGGTCTGTCTCC
Sqle	GTTGTTGCGGATGGACTCTT	GGGTTGACCAGAACAAGCTC

Table 2: Sequences of forward and reverse primers used in RT-PCR for human genes

Oligo-name	**Forward primer (5' ->3')**	**Reverse Primer (5' ->3')**
ACTB	CTTCCTGGGCATGGAGTC	AGCACTGTGTTGGCGTACAG
IDE	AAGCAGGCTGCATTAGGAATTA	CCTCTGTCAAGGGAGCTGAAC
TBP	CGGAGAGTTCTGGGATTGT	GGTTCGTGGCTCTCTTATC

3.1.3 Cell lines

Different cell lines were used for achieving research goals. Types of cell lines used in the study with brief descriptions of each are listed in Table 3.

Table 3: Cell lines used as a part of the study

Name	**Source**
MEF APP / APLP2 -/-	Mouse fibroblastoma generated without expression of APP and APLP2 (Heber et al.,2000)
MEF APPΔCTF15 (ΔΔ)	Mouse fibroblastoma lack of the last 15 amino acids of APP C-terminal (Ring et al, 2007)
MEF PS1/2 -/-	Mouse fibroblastoma generated without expression of PS1 and PS2 (Herrmann et al.,2000)
MEF PS1res	Generated by Dr. Eva Hesser (Plasmid construct cloning by Dr. Marcus Grimm), Zeosin-resistant
MEF WT	Wild type mouse fibroblast cell line

N2a IDE KD	N2a mouse neuroblastoma, lack of sh-RNA function, generated by Janine Mett (Experimental neurology, University of Saarland)
N2a WT	Wild type, mouse neuroblastoma (Klebe et al., 1970)

3.1.4 Lipids, Plasmids, Antibodies, and Kits

Cholesterol (3β-hydroxy-5-chlesterol) was used in addition to PC 18:0 (1,2-distearoyl-*sn*-glycero-3-phosphocholine), which was used for comparison purposes (Avanti). The plasmid pEZX-PG04-IDE-Gluc (GenCopoeia) was used for measuring IDE promoter activity. A primary monoclonal (not for IDE detection), ST1120, and secondary antibodies (polyclonal) used for the western blot are listed in Table 4. Table 5 contains a list of kits that were used in this thesis.

Table 4: Primary and secondary antibodies

Name	Epitope / use	Source
G210	Free C-terminus of Aβ40 for Aβ40 immunoprecipitation	Beyreuther (Heidelberg)
G211	Free C-terminus of Aβ42 for Aβ42 immunoprecipitation	Beyreuther (Heidelberg)
P0260	Mouse IgG, HRP-coupled secondary antibody for western blot	DAKO
ST1120	N-terminus IDE for IDE immunoprecipitation, IDE activity and IDE western blot	Merck Millipore
W02	Human APP (5-10 amino acids of Aβ) for total Aβ immunoprecipitation and Aβ western blot	Beyreuther (Heidelberg)
W4011	Rabbit IgG, HRP- coupled secondary body for western blot	Promega

Table 5: list of kits used in the study

Name	Use	Source
High capacity cDNA RT	cDNA synthesis	Applied Biosystems
Secrete-Pair Dual Luminescence Assay	IDE promoter activity	GenCopoeia

3.1.5 Computer software utilized as a part of data analysis

Data analyses obtained by different experiments were performed using the software listed in Table 6.

Table 6: Computer programs used in data analysis

Name	Source
Analyst 1.5	AB Sciex
Excel	Microsoft
Image Gauge V3.45	Fuji Science lab
Piko Real 2.1	Thermo Scientific

3.2 Methods

Preparation of cells, solutions, and compounds with corresponding protocols are described in the following sections. Description of testing methods, parameters, and test conditions are also presented. Unless otherwise indicated, all preparatory and testing protocols were performed according to Mett (Experimental Neurology Department, University of Saarland; Mett, 2017).

3.2.1 Cell Cultures

The cell culture protocol followed that of Doering, 2010. To avoid contamination, a laminar flow sterile workbench was used under sterile conditions. The culturing protocol consisted of several steps:

I. PBS solution: 137 mM NaCl
2.7 mM KCl
8.1 mM $Na_2HPO_4.2H_2O$
1.5 mM KH_2PO_4
pH adjusted to 7.5 with HCl.

II. Cell cultivation in 10 ml cell culture medium, and cells were maintained at 37 °C, 5% CO_2, and 95% atmospheric humidity in 10 cm cell culture dishes.

III. Cells were washed with 5 ml phosphate buffered saline (PBS) upon achieving about 90% to 100% confluency.

IV. Incubation of cell cultures with 1.5 ml trypsin/ethylenediaminetetraacetic acid (EDTA) solution for 2 to 3 min to separate growing cells from the bottom of culture dish.

V. Addition of 8.5 ml of fresh medium after trypsin/EDTA incubation.

VI. According to the cell line undergoing cultivation, distribution of 0.5 to 3 ml according to cell line (Table 7) of the cell suspension on new culture dishes for further cultivation and brought to 10 ml final volume with fresh medium.

VII. Seeding cells on new 10 cm dishes or 6, 12, 24, or 96 well plates according to the experiments of interest.

Table 7: Cell culture media.

Cell line	Cell culture media	Hygromycin B 400 µg/ml	Zeocin 300 µg/ml
N2a WT	DMEM 0.1 mM MEM amino acid solution 10 % (v/v) FCS	-	-
N2a IDE-KD	100U/ ml Penicillin 0.1 mg/ml Streptomycin	+	-

Cells were stored long-term at –80 °C in liquid nitrogen according to the following protocol:

I. preparation of freezing solution A:
30% (v/v) FCS in DMEM

and freezing solution B:

30% (v/v) FCS
20% (v/v) DMSO in DMEM

II. Washing of 60% to 80% confluent cells with 5 ml PBS.
III. Separation from bed of 10 cm dish with 1.5 ml trypsin/EDTA solution.
IV. Adding 4.5 ml culture medium and transferring to Falcon tube.
V. Centrifugation at 355 g for 5 min.
VI. Resuspension of cell pellets in 1.5 ml of freezing solution A.
VII. Addition 1.5 ml of freezing solution B and aliquoting into two cryogenic vessels.
VIII. Storage in a freezer box that contains isopropanol at –80 °C; this will lead to a gradual decrease in temperature at a rate of 1 °C/min.

Re-cultivation of the cells can be carried out according to the following procedure:

I. Thaw-freeze cycles of culture at room temperature.
II. Dilution in 8.5 ml fresh, prewarmed culture medium.
III. Centrifugation for 5 min. at 355 g.
IV. Resuspension of cell pellets in 10 ml cell culture medium.
V. Transfer to 10 cm cell culture dishes.

3.2.2 Cell incubation with cholesterol

Incubation of cells with cholesterol was carried out according to Grimm et al., 2013 in which N2a cells were incubated for 18 h + 6 h with Aβ40. Additionally, 6 h before incubation, the fetal calf serum in the culture medium was reduced to 0.1 %. Furthermore, to increase solubility of cholesterol in the aqueous culture medium, the ethanol-containing lipids and the medium in glass tubes were heated to 37 °C. The final concentration of cholesterol in the pre-warmed medium was 100 µM, and the batches were vortexed after removing old culture medium.

3.2.3 Quantification of gene expression by qRT-PCR

qRT-PCR is commonly applied in molecular biology in order to quantify the genes under consideration expressions. As a combined technique, it starts from isolation of total RNA from a specific sample followed by reverse transcription to obtain cDNA,

and then amplification via PCR of gene sequences under consideration by using particular sets of primers designed for those genes. Furthermore, the fluorescent cyanine dye, SYBR green, was used to quantify the amplified gene products at the point at which they were bound to double-stranded DNA that emitted light upon excitation. Quantification can be accomplished by measuring the emitted light of the dye. Finally, the results were normalized and analyzed according to $2^{-\Delta\Delta CT}$- method (Rao et al., 2013; Livak and Schmittgen, 2001).

3.2.3.1 Total RNA Isolation

The process of RNA isolation was conducted according to manufacturer's instructions (Life Technologies, issue December 2012).

Total ribonucleic acid (RNA) was isolated from cultured cells according to the following protocol:

I. Complete removal of culture medium.
II. Addition of 1ml TRIzol reagent per 6 well and scraping of cells with a rubber scraper from the bed of the cell culture dish.
III. Addition of 200 µl chloroform, transfer to 1.5 ml Eppendorf reaction vessels, and incubation at room temperature for 5 min.
IV. Shaking for 15 sec followed by incubation at room temperature for 3 min.
V. Centrifugation for 15 min at 13,800 g and 4 °C.
VI. After centrifugation, different layers can be seen: (1) the first layer in the bottom contains DNA and is red; (2) The middle layer contain proteins; and (3) the upper aqueous layer contains RNA.
VII. Transfer of the upper layer into a new 1.5 ml Eppendorf.
VIII. Mixing with 500 µl isopropanol and incubation for 10 min at room temperature.
IX. Centrifugation at 13800 xg and 4 °C for 10 min in order to cause RNA pellet formation that was precipitated at the bottom of the vessel.
X. Discard supernatant. Washing of pellets with 1 ml of 75% ethanol.
XI. Centrifugation at 5400 xg for 5 min at 4 °C.
XII. Discard the supernatant followed by air drying RNA for 5 min.
XIII. Incubation for 10 min in 100 µl nuclease-free water at 55 °C.

After that, isolated RNA's purity and concentration was determined using a Nano Drop spectrophotometer. Knowing that, the maximum absorbance of nucleic acids and proteins was read at 260 and 280 nm, respectively. Thus, the purity of the isolated RNA can be calculated as the ratio of absorbance for nucleic acids at 260 nm to the absorbance of proteins at 280 nm. As an indication of pure isolated RNA, the ratio should be is 2.2. Therefore, a ratio of >2 was used to indicate pure RNA in this study. Furthermore, the calculation of isolated RNA concentration depends on an absorbance at 260 nm in which an absorbance of 1 at this wavelength corresponds to a concentration of 40 µg/ml of pure RNA. For future use or long-term storage, isolated RNA can be kept at –80 °C.

3.2.3.2 Reverse Transcription of Isolated RNA

Synthesis of cDNA was carried out according to manufacturer's instructions (Thermo Fisher Scientific, Issue March 2016).

Isolated RNA from the previous step was used to synthesize complementary DNA. The synthesis process required the use of the High Capacity cDNA Reverse Transcription kit from Life Technologies according to manufacturer's instructions in a Primus 25 Advanced PCR cycler as shown in Table 8. The cycler was operated according to the program shown in Table 9.

Table 8: preparing solution for cDNA synthesis

2 µg	**Isolated RNA**
2µl	10x RT buffer
0,8µl	25x dNTP mix
2µl	10x RT Random primer
1µl	MultiScribe reverse transcriptase 4,2µl
4,2µl	Nuclease-free water
Total	**10 µl (RNA concentration 0.2 µg/µl)**

Table 9: Program of cDNA cycler

step	duration	Temperature	cycles
1	10min	25 ℃	**1**
2	120min	37 ℃	**1**
3	5min	85 ℃	**1**
4	constant	8 ℃	

After those steps, the cDNA obtained was then diluted in nuclease-free water 1:10 and stored at -20 ℃.

3.2.3.3 Real-Time Polymerase Chain Reaction

Amplification of cDNA obtained from previous step is performed by RT-PCR with gene-specific primers and SYBR green dye. The PikoReal PCR system, manufactured by Thermo Scientific, was used to measure gene expression in which batches prepared for RT-PCR were pipetted into 96-well plates, and fluorescence of emitted light from the SYBR green dye were measured. Every well contained the following:

I. 2.5 µl cDNA
II. µl nuclease water
III. 0.25 µl forward primer
IV. 0.25 µl reverse primer
V. 5 µl SYBR Green master mix.

The program of PCR is shown in Table 10.

Table 10. Program for qRT-PCR

Step	Process	Duration, s	Temperature, °C	No. of cycles
1	Denaturation	20	95	1
2	Denaturation	3	95	
3	Attachment / elongation	30	60	40
4	Melting curve analysis		60–95	1

Finally, the data was normalized to one or more housekeeping genes such as β-actin or the TATA binding box protein (TBP) by applying $2^{-\Delta\Delta CT}$ method (Rao et al., 2013; Livak and Schmittgen 2001).

3.2.4 Western Blot method

This technique is used extensively to detect specific proteins in a mixture of proteins from a sample by using sodium dodecyl sulfate-polyacrylamide gel electrophoresis (SDS-PAGE) to separate proteins according to their size. After that, the separated proteins are transferred onto a nitrocellulose membrane and stained primary and secondary antibodies specific to their respective proteins. This technique consists of cell preparation (cell lysis) followed by gel electrophoresis, blotting, blocking, treatment with primary followed by secondary antibodies, and finally, treatment with reagents to visualize the enzyme and quantify the amount of protein. The subsequent paragraphs provide details for the cell preparation from tissue and protein extraction, including details of western blotting experiments.

3.2.4.1 Determination of protein concentration

In order to determine protein concentrations, the bicinchoninic acid (BCA) method, first described by Smith and co-workers in 1985 as a two steps reaction, was used. In the first step, the protein reduces Cu^{2+} to Cu^{1+} in an alkaline environment (Smith et al. 1985). In the second step of the reaction, BCA reacts with the newly formed Cu^{1+} ions to form a purple colored BCA-Cu^{1+}complex that has an absorbance at 560 nm. The BCA reaction solution consists of 4% (w/v) $CuSO_4.5H_2O$ and BCA 1:39 (v/v). Samples were pipetted in triplicate into the wells of a 96-well plate, and 10 µl of lysates were used for protein determinations. Also, to prepare references for the calculations of protein concentration, serial dilutions of bovine serum albumin (BSA) prepared in water at 12 different concentrations (0.1 to 1.1 mg/ml) were used. Samples incubated at 37 °C for 15 min after 200 µl of BCA reaction solution. Samples were then shaken at 200 rpm at room temperature for an additional 15 min. Absorbances were then measured at 560 nm in a plate photometer, and the protein concentration in the samples were computed using a standard BCA curve. Figure 10 shows an example of this method.

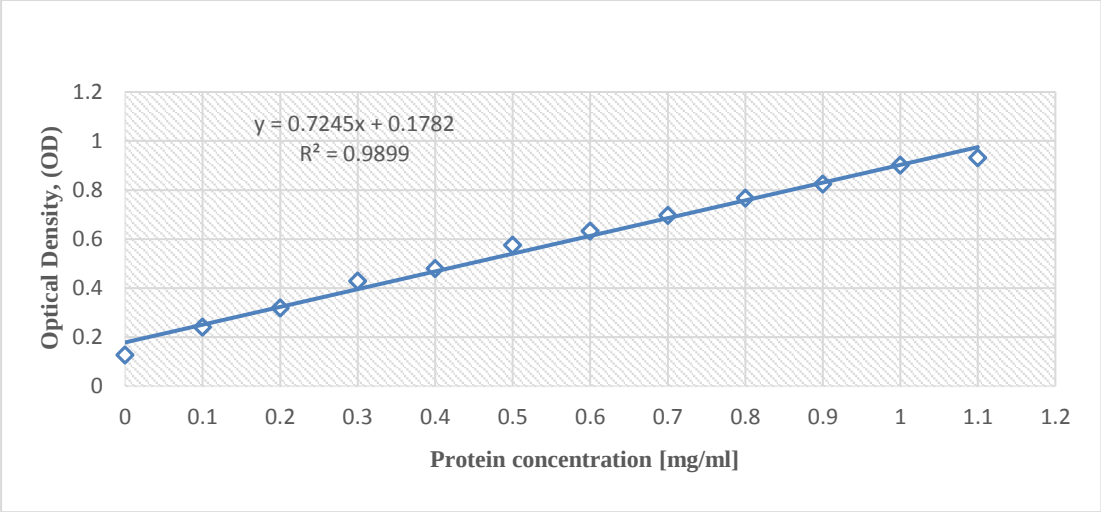

Figure 10: Protein concentration and linearity according to the BCA method.

3.2.4.2 Protein separation by SDS-PAGE

Protein electrophoresis via SDS-PAGE entails the separation of proteins according to their molecular weight within an electric field. The separation was carried out in 10%–20% Tris-Tricine gradient gels by applying an electrical voltage. Proteins prepared in the previous step were used for this technique. Fifteen microliters of 3x protein sample buffer was added. Other samples were mixed with 1/3 volume 3x protein sample buffer. After that, samples were incubated for 5 min at 98 °C in a heating block in order to denature the proteins. The SDS contained in the protein sample buffer masks the intrinsic charges of the proteins with a negative charge, which in the electric field leads to the movement of the proteins towards the anode. The denatured samples were then centrifuged for a few seconds and loaded onto the gel pockets using a Hamilton capillary syringe. In addition, 5 µl of the protein size standard page ruler was applied to each gel, which allowed the subsequent estimation of the sample proteins' molecular weights. The electrophoretic separation of the proteins took place in a chamber filled with running buffer by applying an electrical voltage of 120 V over a period of 60 to 90 min. The composition of the running and protein sample buffers are described below:

a. 1X running buffer for SDS-Page:

I. 100 mM Tris/HCl pH 8.25 to 8.5

II. pH 6.8 100 mM tricine

III. 0.1% (w/v) SDS in ddH_2O

b. 3X protein sample buffer:

I. 187.5mM Tris/HCl pH

II. 6% (w/v) SDS

III. 30% (v/v) glycerin

IV. 15% (v/v) β-mercaptoethanol

V. 0.03% (w/v) Bromophenol in ddH_2O

3.2.4.3 Transfer of proteins

In this step, proteins separated in the previous step were then transferred to a nitrocellulose membrane. This can be performed by applying an external electrical voltage, which enables the protein detection using specific antibodies. Tris-tricine gel was placed on a nitrocellulose membrane and wrapped on both sides with two layers of Whatman filter paper and a sponge. The whole assembly was suspended in a plastic tank filled with transfer buffer. Negatively charged proteins transfer by SDS occurred toward the anode at 38 0 mA and 4 °C. Depending on the molecular weight of the proteins to be transferred, the transfer time may vary from 1 to 2 h for small peptides such as Aβ. However, the default time was set to 3 h. The transfer buffer consisted of several ingredients:

I. 25 mM Tris / HCl pH8,7

II. 192 mm glycine

III. 20% (v/v) methanol

IV. 0.025% (w/v) SDS in ddH_2O.

3.2.4.4 Immunological detection of proteins

In this step, proteins were detected using specific antibodies in which specific binding of the primary antibody to its epitope occurs. The primary antibody can then be recognized by the secondary antibody, which is coupled to the enzyme, horseradish

peroxidase (HRP). An enzymatic reaction results in a light reaction that occurs upon contact of the ECL (enhanced chemiluminescence) reaction solution with the horseradish peroxidase. The light reaction will enable the preparation of labeled proteins on photosensitive films. Before the treatment with primary antibody, the membrane is incubated in blocking solution in order to reduce the amount of nonspecific protein binding during subsequent steps in the assay using inert protein or nonionic detergent. When using the anti-amyloid primary antibody, W02, the nitrocellulose membrane was heated prior to blocking for 5 min in PBS in a microwave oven at 700 W (Ida et al., 1996). This was followed by three washing steps and incubation of the membrane with the respective primary antibody. After washing again three times, the membrane was incubated for 1 h with the appropriate secondary antibody and then washed an additional three times after which the ECL reaction solution was pipetted onto the membrane, resulting in an HRP-catalyzed chemiluminescent reaction. The membrane was placed between two copy sheets without air bubbles and exposed in a darkroom on an ECL hypersensitive film. Finally, bands were evaluated using the computer software Image Gauge V3.45.

3.2.5 Determination of Aβ degradation

Western blotting was used to measure the remaining Aβ in living cells and culture medium. The cells were seeded in 24-well plates till confluency which correspond with a cell number of 0.24×10^6 cells / well and treated as previously described with and without the addition of cholesterol. Following that step, cells were incubated with cholesterol in combination with 0.5 μg/ml of human Aβ40. Also, total degradation was measured in cell lysates and in the conditioned medium from incubated cells. The localization of Aβ degrading proteases was also considered by measuring the activity of intracellular and extracellular degrading enzyme activities. In order to measure activities, Aβ40 was added to the sample material in a glass bottle and shaken at 37 °C and 300 rpm.

Since the antibody W02 used in the western blot analysis exclusively detected human Aβ, only the supplemented human Aβ40 was detected with the use of murine cells. When using human cells, endogenous Aβ detection was experimentally excluded.

3.2.6 Evaluation of the effects of cholesterol on IDE activity

Fluorometric measurements were used for IDE enzymatic activity assessments.

Internally quenched fluorogenic substrates are commonly used in this type of measurement. This particular method consisted of a fluorophore and a quencher linked by an amino acid sequence and mimicking a substrate of the respective enzyme, which contained the enzyme's interface. Fluorescence resonance energy transfer (FRET) between the quenching moiety and the fluorophore prevents fluorescence emission. After hydrolysis of the substrate, a fluorophore is excited at a certain wavelength due to the spatial separation of the two groups. The resulting fluorescence can be measured using a suitable detector in real time. Prior to the start of experiment, it is essential to determine the optimum measurement parameters by scanning the excitation and emission first for the substrate Mca-RPPGFSAFK (Dnp)-OH. Fluorescence was measured using an incremental 5 nm excitation wavelength increase for each step.

To study the direct influences of cholesterol on the IDE-enzyme activity, the recombinant human IDE was analyzed after *in vitro* incubation with the cholesterol. Assay buffer B for IDE used in this experiment consists of:

I. 100 mM Tris/HCl, pH 7.5
II. 50 mM NaCl
III. 10 µM $ZnCl_2$ in ddH_2O without inhibitors

The experimental procedure is described below:

I. Addition of recombinant human IDE 50 ng/200 µl of assay buffer IDE-B in small glass bottles with 100 µM of cholesterol.
II. Shaking at 37 °C and 300 U/min for 15 min.
III. Pipetting triplicate 50 µl aliquots of the mixture into black 96-well plates.
IV. Adding the substrate Mca-RPPGFSAFK (Dnp)-OH at a final concentration of 5 µM.
V. Continuous recording of the emitted fluorescence at excitation and emission wavelengths of 320 and 405 nm, respectively, in a Safire2 fluorimeter.

3.2.7 Impact of cholesterol on IDE promoter activity

(According to the manufacturer's instructions, secreted-pair dual luminescence assay kit by GeneCopoeia, version 2013)

IDE promoter activity was measured using a luciferase activity. This can be conducted by measuring a reporter enzyme's activity; therefore, the promoter activity is measured indirectly, and cases in which the promoter under study (IDE in this case) is regulating the transcription of the reporter can be measured. Thus, cells need to be first transfected by the reporter enzyme. The transfection process may include variations that can affect transfection efficiency; therefore, a second reporter gene under the control of active promoter is used. Co-transfection of the second promoter is needed in addition to normalization of data obtained from measuring activity of second reporter gene's activity to the standard reporter enzyme's activity. Measuring IDE promoter activity was preceded by a step in which cells were transfected using Lipofectamine transfection 2000 and plasmid pEZX-PG04-IDE-Gluc according to the following protocol:

I. Incubation of OptiMEM (7.5 ml) with plasmid DNA (16 µg) for 5 min at room temperature in a 1.5 ml Eppendorf reaction tube.
II. Incubation of OptiMEM with Lipofectamine 2000 (36µl) in another 1.5 ml Eppendorf tube.
III. Combining the two mixtures for 20 min at room temperature.
IV. Washing cells of 70%–80% confluency with OptiMEM and presenting OptiMEM to cells being transfected.
V. Reducing OptiMEM to about 50% according to manufacturer's instruction (Invitrogen, version July 2005) for achieving increased transfection efficiency.
VI. Addition of the plasmid DNA, Lipofection 2000, and OptiMEM mixture to cells and incubating the cells and mixture for 4 to 6 h at 37 °C.
VII. Replacing transfection medium with new culture medium.
VIII. Transfected cells were used for an expression period of 48 to72 h for subsequent experiments.

After this step, the IDE promoter controls the reporter gene, which encodes the secreted Gaussia luciferase. Furthermore, the constitutively active cytomegalovirus (CMV) promoter controls the secretion of the standard reporter enzyme alkaline phosphatase (SEAP) gene that is contained in the same plasmid. After 24 h of transfection, cells were seeded in 24-well plates, and after an additional 24 h, incubation with substrate was done. Gaussia luciferase and the secreted embryonic alkaline phosphatase (SEAP)

reporter activities were measured using the culture medium and were done using a Secrete-Pair Dual Luminescence Assay kit according to the manufacturer's instructions with white 96-well plates. Signal detection was performed in an Infinite M1000 pro-fluorometer / luminometer. Normalization of signals was carried out as the ratio of Gaussia luciferase signals to SEAP signals for the respective sample.

3.2.8 Evaluation the impact of cholesterol on IDE stability

The experimental protocol was based on the thesis of Haupenthal (Haupenthal, 2016).

Determination of IDE protein stability with and without cholesterol was achieved by inhibiting IDE protein biosynthesis with cycloheximide and then quantified by western blotting. A comparison between the results obtained for the control and cholesterol treated samples was established in order to determine whether protein stability increased or decreased. Thus, the test was carried out using confluent N2a cells on a 6-well plate according to the following procedure:

I. After cells reached confluency on 6-well plate, they were washed once with 1% FCS and then FCS concentration in the media was reduced to 0.1%.
II. Incubation with 20 µg/ml cycloheximide for 8 h.
III. Removal of culture medium and cell incubation for an additional 16 h with cycloheximide and cholesterol.
IV. Centrifugation of the collected media at 13,000 rpm for 5 min.
V. Collection of the supernatant for extracellular IDE testing after removal of dead cells, storage at –80 °C.
VI. Washing wells once with PBS on ice.
VII. Adding 200 µl lysis buffer containing 10% protease inhibitors.
VIII. Leaving on ice for 30 min followed by scraping cells and pipetting the scraped cells several times.
IX. Collecting in Eppendorf tubes followed by centrifugation at 13,000 for 5 min.
X. Using the supernatant for the BCA assay standard after removing pellets.
XI. Applying western blotting and blocking using 10% skimmed milk in TBS with 0.2% Tween 20 for 1 h at room temperature.

3.2.9 Preparation of monomeric Aβ

The protocol of producing monomerized peptide was according to Stine (Stine et al., 2011). Homogeneous unaggregated Aβ40 peptide was produced by using strong solvent to prevent any structural changes prior to incubation with additives. Monomerization was carried out according the following protocol:

I. Prepare a 1 mM Aβ solution by adding 2.217 ml of hexafluoro-2-propanpl (HFIP) directly to the vial containing 10 mg lyophilized powder of peptide through the rubber septum using a 2.5 mL glass Hamilton syringe with a Teflon plunger and sharp (not blunt-end) needle.
II. After the peptide is completely dissolved, pierce the septum with a syringe needle to release the vacuum.
III. Incubate the Aβ–HFIP solution at room temperature (RT) for at least 30 min.
IV. Uncap the glass vial (pliers work well), and remove the rubber septum being careful not to allow the HFIP to come in contact with the septum. Have a rack of 0.5 mL or 1.7 mL micro-centrifuge tubes ready.
V. Using a positive-displacement repeating pipette, aliquot the solution into 10 μL (0.045 mg for Aβ40) or 100 μL (0.45 mg for Aβ40) aliquots in either 0.5 mL or 1.7 mL microcentrifuge tubes.
VI. Allow HFIP to evaporate in the open tubes overnight in the fume hood.
VII. Transfer tubes to a SpeedVac and dry down for 1 h without heating to remove any remaining traces of HFIP and moisture.

The previous steps should be carried out in a fume hood, then:

VIII. Remove tubes from SpeedVac. The resulting peptide should be a thin clear film at the bottom of the tubes.
IX. Store dried peptide films over desiccant in glass jars at −20 °C.
X. Prior to use, remove peptide film from −20 °C freezer and allow sample to thaw till RT.
XI. Prepare a 5 mM Aβ DMSO stock by adding 20 μL fresh dry dimethyl sulfoxide (DMSO) to 0.45 mg Aβ40 peptide (2 μl to 0.045 mg Aβ40). Pipette thoroughly, scraping down the sides of the tube near the bottom to ensure complete resuspension of peptide film.
XII. Vortex well (~30 sec) and pulse in a microcentrifuge to collect solution at the bottom of the tube.

XIII. Sonicate 5 mM Aβ DMSO solution for 10 min in a bath sonicator.

XIV. To this Aβ aliquot, add ice-cold H_2O to a final concentration of 100 µM Aβ.

XV. Vortex for 15 sec and use immediately.

3.2.10 Viability of nematodes

A homogeneous mixture of *Steinernema feltiae* was prepared by suspending 200 mg of powder in 50 mL of distilled water at 27 ºC to restore the nematodes. The suspension was then kept at RT for 30 min. Subsequently, viable nematodes were counted under the microscope (0 h) at a 4-fold magnification (TR 200, VWR International, Belgium). After that, previously prepared Aβ was added to well plates at a concentration of 1, 1.5, and 2 µM and incubated in the dark at RT for 24 h. Thereafter live and dead nematodes were counted under the microscope (24 h). Each concentration was replicated three times per experiment, and each experiment was conducted three times.

The viability of the nematodes was assessed then according to the following formula:

$$\text{Viability} = \frac{V_{24h}}{V_{0h}} * 100 \qquad \text{eq.1}$$

Where:

V_{24h} = number of live nematodes after 24 h
V_{0h} = number of live nematodes at 0 h.

3.2.11 Cell viability test using AlamarBlue

The AlamarBlue test has been used frequently for the determination of cell viability and cytotoxicity in a wide spectrum of cell lines, including bacteria, yeast, fungi, protozoa and cultured mammalian and piscine cells (Rampersad, 2012). Detection of cell viability for selected strands of bacteria by AlamarBlue to test the antimicrobial activity of Aβ have been carried out by using resazurin dye (7-Hydroxy3H-phenoxazin-3-one 10-oxide). The process is explained in the publication of G-biosciences "AlamarBlue dye in its oxidized form is blue in color and non-fluorescent. In AlamarBlue assay reagent, the growing cells cause a chemical reduction of the AlamarBlue dye from non-fluorescent blue to fluorescent red. The continued growth of viable cells maintains a reducing environment (fluorescent, red) and inhibition of growth maintains an oxidized environment (non-fluorescent, blue), which can be detected using a fluorescence or absorbance detector" (G-Biosciences, 2016).

Rampersad stated: “In addition to mitochondrial reductases, other enzymes (such as the diaphorase (EC 1.8.1.4, dihydrolipoamine dehydrogenase), NAD(P)H: quinone oxidoreductase (EC 1.6.99.2) and flavin reductase (EC 1.6.99.1) located in the cytoplasm and the mitochondria may be able to reduce AlamarBlue” (Rampersad, 2012).

3.2.11.1 Preparation of inoculum

The preparation of inoculum is done by using a direct broth suspension of isolated colonies selected from 18 to 24-h agar plates. After that, the turbidity of the suspension can be adjusted to be equivalent to a 0.5 McFarland turbidity standard. Approximately, 1.5 x 10^8 CFU/mL (colony forming unit), is expected according to this standard for *Escherichia coli*. After adjustment of suspension, inoculums were diluted in broth to a final concentration according to the cell types. Finally, mixing with the antimicrobial agent (Aβ) for the concentrations under consideration was done. Furthermore, a tube with broth only without bacteria and another tube with growth control without the antimicrobial agent were used as a control. After that, incubation of tubes for 16 to 20 h at 35 ±2°C in an ambient air incubator was done (M. Balouiri et al, 2016).

3.2.11.2 Preparation of AlamarBlue

The preparation of AlamarBlue was achieved by dissolving high purity resazurin in PBS (pH 7.4) to 0.15 mg/mL. The solution was filtered through a 0.2 µm filter into a sterile, light protected container. The resazurin solution can be stored at 4 °C for immediate use or at –20 °C for long-term storage, protected from light (G-Biosciences, 2016).

3.2.11.3 Detection of viable cells

The quantification of viable cells was performed by preparing pre-adjusted tubes of cells and antimicrobial agent (Aβ), in opaque-welled 96-well plates of a final volume of 100 µl per well. After that, 20 µl resazurin solution to each well has been added. After incubation for 1 hour at 37 °C, the absorbance was recorded using microplate reader EL 800 Bioscience instrumentation and 570 nm and 630 nm filters. The percent differences between treated and control cells were then calculated according to the following equation:

$$\% \text{ reduction} = \frac{(O2\ x\ A1)-(O1\ x\ A2)}{(O2\ x\ P1)-(O1\ x\ P2)}\ x\ 100 \qquad \text{eq.2}$$

In which:

O1 = molar extinction coefficient (*E*) of oxidized AlamarBlue at 570 nm. = 80586

O2 = *E* of oxidized AlamarBlue at 630 nm. = 34798

A1 = absorbance of test wells at 570 nm

A2 = absorbance of test wells at 630 nm.

P1 = absorbance of positive growth control well (cells + AlamarBlue, without Aβ) at 570 nm

P2 = absorbance of positive growth control well (cells + AlamarBlue, without Aβ) at 630 nm.

3.2.12 Evaluation of Aβ aggregation by circular dichroism spectrometry

Circular dichroism (CD) spectrometry measures the differences in absorption between right- and left-handed circularly polarized light over a range of wavelengths. The differences occur due to the protein and peptide chirality. Thus, conformational changes of Aβ40 can be detected using this technique. CD has been applied extensively to the structural characterization of peptides because it is not the sum of the CD spectra of the individual residues or bases but is greatly influenced by the three-dimensional structure of the peptide itself. Likewise, each peptide has a specific CD signature, and this has the advantage of detecting elements of a specific peptide's structure and determining changes in the peptide's structure. Peptide aggregation then can be determined by monitoring changes in the peptide's secondary structure elements such as the α-helix (wavelength –208, –222, and +193 nm), β-sheet (wavelength –218 and +195 nm), and random coil (wavelength –205 nm). Highly aggregated peptides show an increase in the secondary structure's β-sheet element. The CD spectra in the far-UV range (190–260 nm) can be used to predict the formation of each secondary structural element in protein's structure. This method was used to assess changes in Aβ's secondary structure, which is incubated with selected compounds, and their impact on the peptide's accumulation.

3.2.12.1 Preparation of compounds

Preparation was conducted according to the work of Wiedemann et al., 2013.

Chemical compounds were dissolved in Tris to a concentration of 1 mM as a stock solution. Afterward, different concentrations of compounds were added to the peptide. The concentrations used in this study were 10, 15, and 20 μM as final concentrations. Three-hundred milliliters of solution was then loaded in the CD spectrometer cuvette, and the spectrum measured at different time intervals to monitor changes in the secondary structure of the peptide upon incubation with compounds. Unless stated otherwise, three replicates were examined for every compound, and a spectrum for the monomerized peptide without the compound was used as the control. Analysis of data obtained from the CD spectrum was carried out according to Wiedemann et, al., 2013 and Micsonai et al., 2015. The experiments were carried out in the Laboratory of the Institute of Bioorganic Chemistry in Saarbruecken.

3.2.12.2 Data analysis and plotting

Acquired data by CD spectrometry was analysed and plotted by a web server-based called CD analysis and Plotting tool (CAPITO; https://capito.nmr.leibniz-fli.de//). It is assumed that for a given protein, the CD spectrum is the resultant of linear combination of basis spectra and, elements of the secondary structure for the given protein increases characteristcs of bands in wavelengh and intensity (Wiedemann et al, 2013) as shown in the following equation:

$[\theta]_\lambda = \sum f_n + S_{\lambda n} + noise$ eq.3

Where:

λ: wavelength in nm

[θ]: molar ellipticity

f_n: fraction of each secondary structure, *n* and,

$S_{\lambda n}$: ellipticity at each wavelength of each n^{th} secondary structure.

The sum of all fractions is 1.

The result of the predicted secondary structure is compared with the 3D structure database of known proteins provided in proteins CD data bank (PCDDB) for more reliable results. Input data of CAPITO server is either; millidegrees (mdeg); mean residue extinction coeffiecient ($\Delta\epsilon$ in M^{-1} cm^{-1}) or; mean residue ellipticity ([θ] in deg cm^2 $dmol^{-1}$). In the current study the default input has been used (mdeg). Furthermore, test parameters such as cuvette pathlengh was set to 1 mm, protein concentration (10

µM, 15 µM, and 20 µM). After that, the server runs Chou-Fasman-algorithm to predict the secodary structure of the peptide. Results are shown in a graph represents the spectral data into Δϵ or [θ] as a function of wavelength. Figure 11 shows a sample of secondary structure elements prediction of 100% α-helix, 100% β-sheet, and 100% Random coil (irregular).

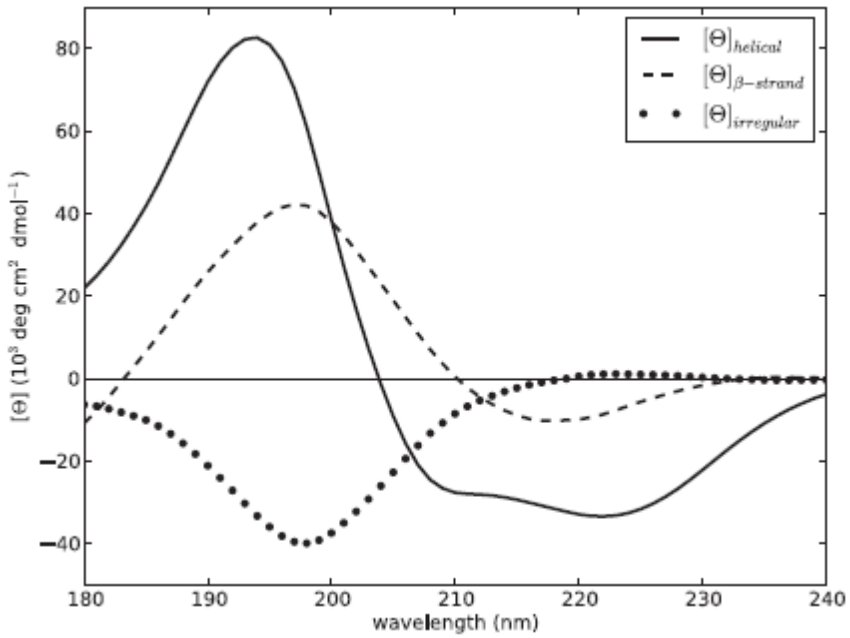

Figure 11: Sample of pure secondary structure elements (α-helix, β-sheet, or random coil) of a protein.

Besides the prediction of secondary structure elements, folding state of the protein being tested is estimated as a plot of spectral values at 200 nm versus 222 nm and according to PCDDB entries as shown in Figure 12.

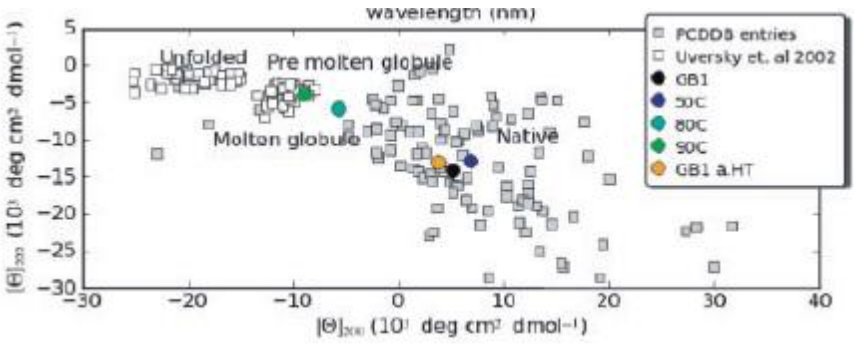

Figure 12: Estimation of folding state of sample protein. Uncolored squares represent entries by PCCDB whereas, colored circles represent the results obtained during experiment at different concentrations (for example).

3.2.13 Statistical analysis

All results were presented as boxplots and followed by table containing statistical parameters, average, confidence interval (CI), standard deviation and standard error of the mean (SEM). Statistical significance was analyzed using the Student's two-tailed t-test for normally distributed data and non-parametric test which is Mann-Whitney U test for not normally distributed data. Test of normal distribution of the data was performed by Shapiro-Wilk test, while Leven's test was conducted to examine the equality of variances. Analyses of results and statistical tests were performed with SPSS software (IBM SPSS statistics data editor) version 25. Statistical significance was defined as $p \leq 0.05$.

Chapter IV

Results and Discussion

4.1 Results

4.1.1 Influence of APP, AICD, and Aβ on cholesterol homeostasis

Transcriptional effects of APP and its proteolytic fragments on the expression of cholesterol bio-synthesis genes and sterol regulatory binding protein (SREBP-1) and related genes, which are summarized in Table 11, were determined by employing qRT-PCR in quantifying the gene expression as the first interest of the study. Cholesterol bio-synthesis process was reviewed in section 2.3.1 whereas, the impact of full length APP and its proteolytic fragments on cholesterol homeostasis was studied previously as shown in section 2.4.3. However, information regarding the direct impact of APP on gene expression of enzymes involved in cholesterol bio-synthesis process is still needed.

Table 11: Detailed names of genes involved in the study.

Gene	Name
HMGCS1	3-Hydroxy-3-MethylGlutaryl-CoA Synthase 1
HMGCS2	3-Hydroxy-3-MethylGlutaryl-CoA Synthase 2
HMGCR	3-Hydroxy-3-MethylGlutaryl-CoA Reductase
MVK	MeValonate Kinase
PMVK	PhosphoMeValonate Kinase
MVD	MeValonate (diphospho) Decarboxylase
FDPS	Farnesyl DiphosPhate Synthase
FDFT	Farnesyl-Diphoshate FarnesylTransferase
SQLE	SQuaLene Epoxidase
LSS	LanoSterol Synthase (2,3-oxidosqualene-lanosterol cyclase)
SREBF1	Sterol Regulatory Element Binding transcription Factor 1
SREBF2	Sterol Regulatory Element Binding transcription Factor 2
SCAP	Sterol regulatory element-binding protein Cleavage-Activating Protein
INSIG	Insulin Induced Gene 1
S1P	Site-1 Protease

4.1.1.1 Impact of APP

Mouse embryonic fibroblasts-wild type (MEF-WT) was used as a control and compared with the results of MEF cells which are lacking amyloid precursor protein APP and APP homologues, APLP2 (MEF APP/APLP2-/-) as samples of the test. Results are shown in Figure 13 and statistics are summarized in Table 12.

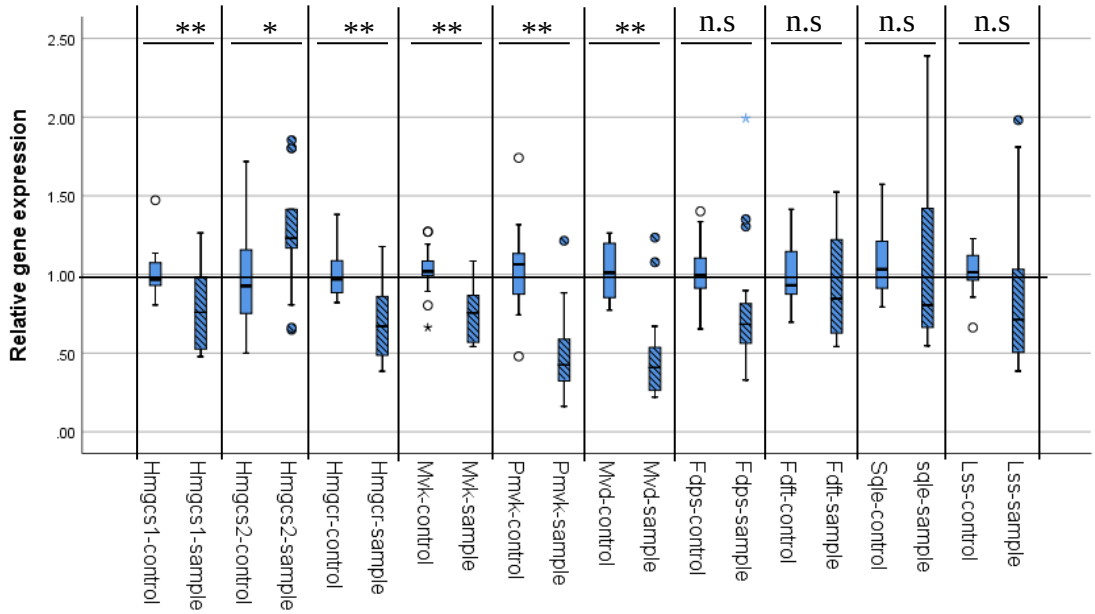

Figure 13: Quantitative determination of gene expression for genes involved in cholesterol biosynthesis pathway by using the real-time reverse transcriptase polymerase chain reaction (qRT-PCR) technique (n=13-16). β-actin was used as a housekeeping gene. Results were normalized to the housekeeping gene, and control and quantitative detection of gene expressions were calculated by employing the $2^{-\Delta\Delta}$ method. Mouse embryonic fibroblasts- wild type cells MEF WT (control) and mouse embryonic fibroblasts lacking APP and APLP2, MEF APP/APLP2 -/- (sample). Boxplots represent; minimum, first quartile, median, third quartile, and maximum. Outliers represent 1.5 (circle) and 2 (star) times' interquartile range. Horizontal line represent mean of controls. Statistical significance was determined using Student's unpaired two-sided t-test (* $p \leq 0.05$, ** $p \leq 0.01$, *** $p \leq 0.001$, and n.s., not significant).

Detailed results are shown in tables B-1 - B-5, B-10 – B-13, B-24, and B-32 – B-34, in the appendix.

Table 12: Descriptive statistics of quantified MEF-WT (control) and MEF APP/APLP2 -/- (sample) genes.

Gene		Mean	95% CI for mean		Std. deviation	SEM	p	n
			Lower	Upper				
Hmgcs1	Control	1.0098	0.9276	1.0919	0.15420	0.03855	0.007	16
	Sample	0.7735	0.6256	0.9214	0.27761	0.06940		16
Hmgcs2	Control	0.9567	0.7543	1.1590	0.33483	0.09286	0.044	13
	Sample	1.2653	1.0231	1.5075	0.40082	0.11117		13
Hmgcr	Control	1.0105	0.9277	1.0934	0.15546	0.03886	0.000109	16
	Sample	0.6937	0.5667	0.8207	0.23838	0.05960		16
Mvk	Control	1.0206	0.9253	1.1158	0.16500	0.04410	0.000195	14
	Sample	0.7457	0.6473	0.8442	0.17052	0.04557		14
Pmvk	Control	1.0559	0.8751	1.2368	0.29925	0.08300	0.000060	13
	Sample	0.5041	0.3352	0.6731	0.27964	0.07756		13
Mvd	Control	1.0134	0.9228	1.1040	0.17003	0.04251	7.239E-7	16
	Sample	0.4797	03214	0.6381	0.29717	0.07429		16
Fdps	Control	1.0188	0.9121	1.1254	0.19255	0.04972	0.085	15
	Sample	0.7936	0.5500	1.0372	0.43994	0.11359		15
Fdft	Control	1.0255	0.8964	1.1546	0.21363	0.05925	0.303	13
	Sample	0.9112	0.7127	1.1097	0.32848	0.09110		13
Sqle	Control	1.0693	0.9413	1.1972	0.21168	0.05871	0.702	13
	Sample	1.1495	0.7214	1.5776	0.70842	0.19648		13
Lss	Control	1.0131	0.9314	1.0949	0.14162	0.03785	0.490	14
	Sample	0.9049	0.5846	1.2251	0.55467	0.14824		14

Similarly, gene expression of sterol regulatory element binding protein (SREBP-1) genes are shown in Figure 14, while Table 13 summarizes the statistics of these genes.

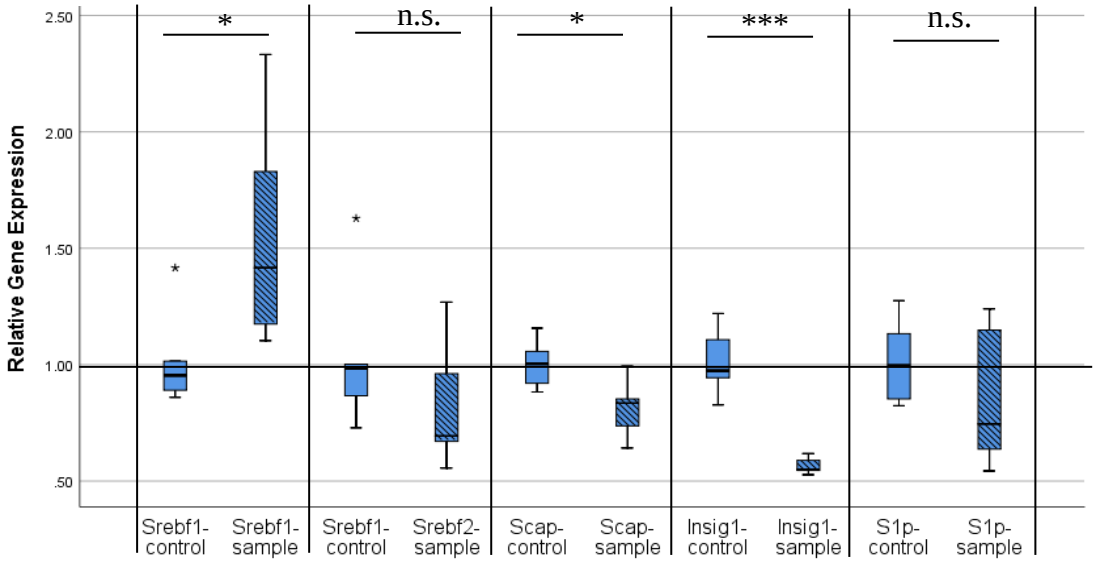

Figure 14: Quantitative determination of gene expression for genes involved in SREBP-1 and related genes by using the real-time reverse transcriptase polymerase chain reaction (qRT-PCR) technique (n=6). β-actin was used as a housekeeping gene. Results

were normalized to the housekeeping gene, and control and quantitative detection of gene expressions were calculated by employing the $2^{-\Delta\Delta}$ method. Mouse embryonic fibroblasts- wild type cells MEF WT (control) and mouse embryonic fibroblasts lacking APP and APLP2, MEF APP/APLP2 -/- (sample). Boxplots represent; minimum, first quartile, median, third quartile, and maximum. Outliers represent 1.5 (circle) and 2 (star) times' interquartile range. Horizontal line represents mean of controls. Statistical significance was determined using Student's unpaired two-sided t-test (* $p \leq 0.05$, ** $p \leq 0.01$, *** $p \leq 0.001$, and n.s., not significant).

Table 13: Descriptive statistics of quantified MEF-WT (control) and MEF APP/APLP2 -/- (sample) genes.

Gene		Mean	95% CI for mean		Std. deviation	SEM	p	n
			Lower	Upper				
Srebf1	Control	1.0148	0.8001	1.2295	0.20460	0.08353	0.029	6
	Sample	1.5453	1.0538	2.0368	0.46830	0.19118		6
Srebf2	Control	1.0327	0.7074	1.3580	0.30997	0.12654	0.205	6
	Sample	0.8076	0.5321	1.0831	0.26256	0.10719		6
Scap	Control	1.0039	0.9010	1.1069	0.09806	0.04003	0.014	6
	Sample	0.8159	0.6911	0.9406	0.11887	0.04853		6
Insig1	Control	1.0077	0.8632	1.1522	0.13771	0.05622	0.000356	6
	Sample	0.5633	0.5280	0.5987	0.03370	0.01376		6
S1p	Control	1.0126	0.8270	1.1982	0.17689	0.07221	0.243	6
	Sample	0.8432	0.5453	1.1412	0.28395	0.11592		6

Results in the figures above shows downregulation in the transcription of cholesterol bio-synthesis genes, but not for HMGCS2 and SREBF1, in case of APP absence. More results are shown in Table B-27 and B-40 – B-42 in the appendix.

4.1.1.2 Impact of AICD

In the same manner, the effect of AICD absence was investigated by mediating MEF APPΔCT15 that is lacking the last 15 amino acids of the APP C-terminus Figure 15 for cholesterol biosynthesis and Table 14 for relevant statistics. Details associated with this figure are presented in the appendix in Tables B-1 – B-9, B-23, and B-29 – B-31.

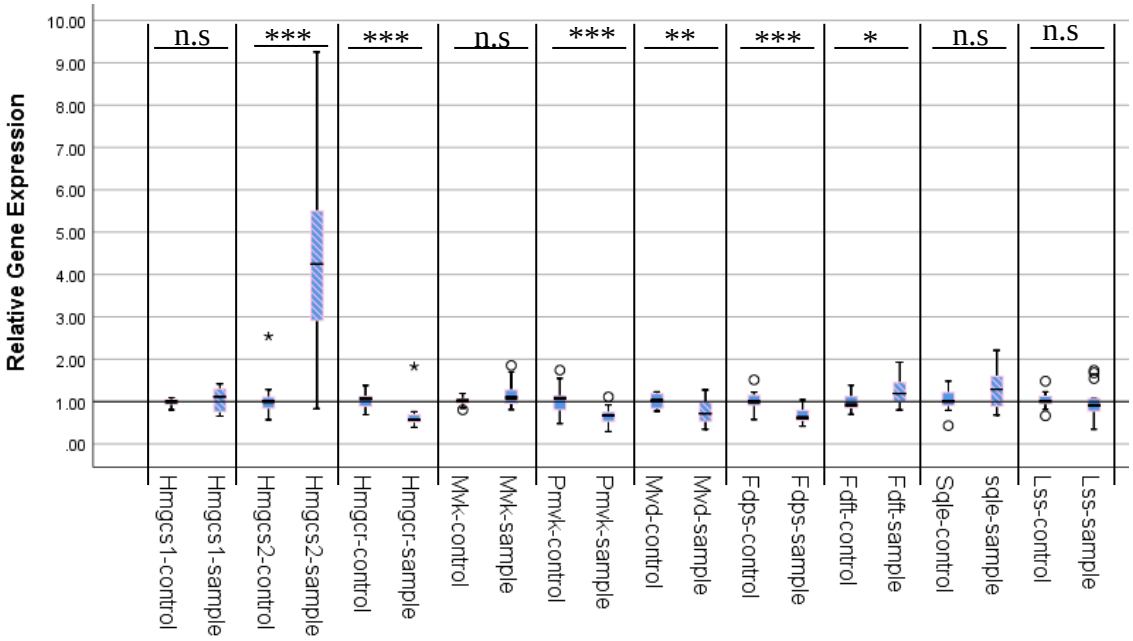

Figure 15: Quantitative determination of gene expression for genes involved in cholesterol biosynthesis pathway by using the real-time reverse transcriptase polymerase chain reaction (qRT-PCR) technique (n=13-15). β-actin was used as a housekeeping gene. Results were normalized to the housekeeping gene and control, and quantitative detection of gene expressions were calculated by employing the $2^{-\Delta\Delta}$ method. Mouse embryonic fibroblasts- wild type cells MEF WT (control) and MEF APPΔCT15 that is lacking the last 15 amino acids of the APP C-terminus (sample). Boxplots represent; minimum, first quartile, median, third quartile, and maximum. Outliers represent 1.5 (circle) and 2 (star) times' interquartile range. Horizontal line represents mean of controls. Statistical significance was determined using Student's unpaired two-sided t-test (* $p \leq 0.05$, ** $p \leq 0.01$, *** $p \leq 0.001$, and n.s., not significant).

Table 14: Descriptive statistics of quantified MEF-WT (control) and MEF APPΔCT15 (sample) genes.

Gene		Mean	95% CI for mean		Std. deviation	SEM	p	n
			Lower	Upper				
Hmgcs1	Control	0.9761	0.9286	1.0236	0.08223	0.02198	0.374	14
	Sample	1.0484	0.8847	1.2121	0.28347	0.07576		14
Hmgcs2	Control	1.0697	0.8025	1.3370	0.46288	0.12371	0.000231	14
	Sample	4.3969	2.9603	5.8336	2.48826	0.66501		14
Hmgcr	Control	1.0138	0.9188	1.1088	0.17147	0.04427	0.001	15
	Sample	0.6629	0.4746	0.8512	0.34005	0.08780		15
Mvk	Control	1.0043	0.9442	1.0644	0.10408	0.02782	0.054	14
	Sample	1.1807	1.0071	1.3543	0.30062	0.08035		14

Pmvk	Control	1.0478	0.8527	1.2429	0.33791	0.09031	0.001	14
	Sample	0.6567	0.5281	0.7852	0.22262	0.05950		14
Mvd	Control	1.0090	0.9131	1.1049	0.16611	0.04439	0.009	14
	Sample	0.7450	0.5726	0.9173	0.29845	0.07976		14
Fdps	Control	1.0228	0.9018	1.1439	0.2163	0.05645	0.000056	15
	Sample	0.6782	0.5825	0.7739	0.17282	0.04462		15
Fdft	Control	0.9939	0.8643	1.1235	0.21445	0.05948	0.033	13
	Sample	1.2477	1.0400	1.4555	0.34377	0.09534		13
Sqle	Control	1.0185	0.8590	1.1780	0.26397	0.07321	0.069	13
	Sample	1.2996	1.0209	1.5783	0.46116	0.12790		13
Lss	Control	1.0196	0.9072	1.1320	0.19464	0.05202	0.869	14
	Sample	0.999	0.7709	1.2288	0.39656	0.10598		14

The impact of AICD on SREBP-1 and related genes are shown in Figure 16 and Table 15 for relevant statistics. Details shown in Tables B-26, B-38 and B-39 in the appendix.

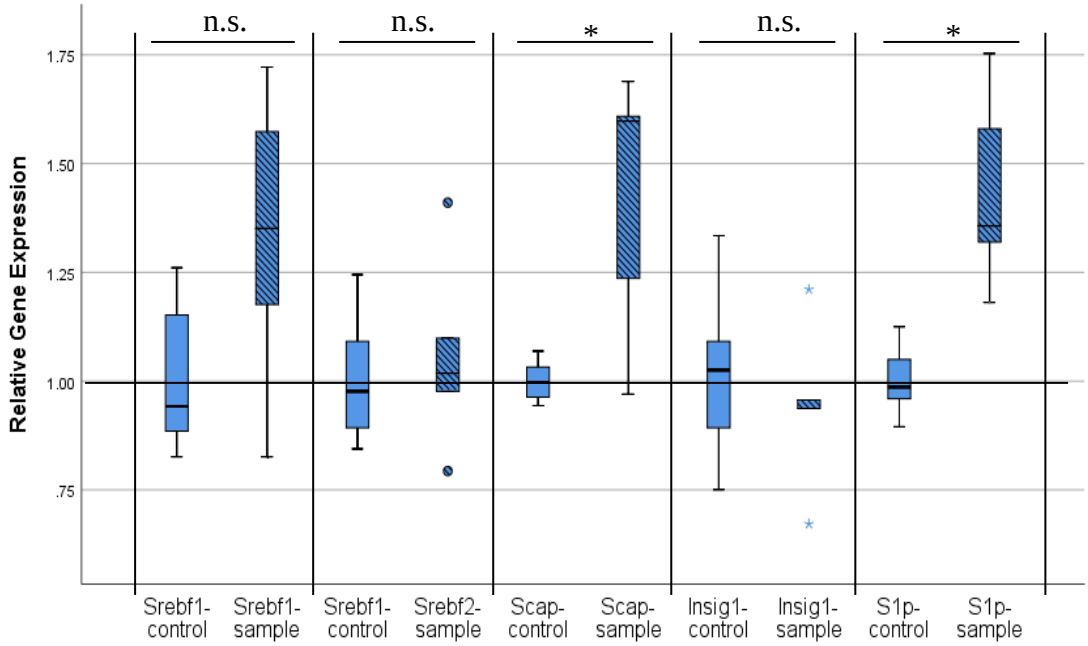

Figure 16: Quantitative determination of gene expression for genes involved in SREBP-1 and related genes by using the real-time reverse transcriptase polymerase chain reaction (qRT-PCR) technique (n=5). β-actin was used as a housekeeping gene. Results were normalized to the housekeeping gene, and control and quantitative detection of gene expressions were calculated by employing the $2^{-\Delta\Delta}$ method. Mouse embryonic fibroblasts- wild type cells MEF WT (control) and MEF APPΔCT15 that is lacking the last 15 amino acids of the APP C-terminus (sample). Boxplots represent; minimum, first quartile, median, third quartile, and maximum. Outliers represent 1.5 (circle) and 2 (star) times' interquartile range. Horizontal line represents mean of controls. Statistical significance was determined using Student's unpaired two-sided t-test (* $p \leq 0.05$, and n.s., not significant).

Table 15: Descriptive statistics of quantified MEF-WT (control) and MEF APPΔCT15 (sample) genes.

Gene		Mean	95% CI for mean		Std. deviation	SEM	p	n
			Lower	Upper				
Srebf1	Control	1.0131	0.7834	1.2428	0.18502	0.08274	0.112	5
	Sample	1.3297	0.8946	1.7648	0.35041	0.15671		5
Srebf2	Control	1.0100	0.8097	1.2103	0.16132	0.07214	0.700	5
	Sample	1.0595	0.7791	1.3399	0.22584	0.10100		5
Scap	Control	1.0010	0.9379	1.0641	0.05083	0.02273	0.037	5
	Sample	1.4203	1.0397	1.8009	0.30650	0.13707		5
Insig1	Control	1.0188	0.7462	1.2913	0.21948	0.09816	0.594	5
	Sample	0.9465	0.7096	1.1835	0.19082	0.08534		5
S1p	Control	1.0031	0.8939	1.1123	0.08794	0.03933	0.010	5
	Sample	1.4381	1.1561	1.7200	0.22708	0.10155		5

Significant decrease in the expression of rate-limit enzyme, HMGCR, was detected with a non-significant increase of SREBP-1 and related genes.

4.1.1.3 Impact of Aβ

Finally, the transcriptional regulation of Aβ was studied in MEF PS1res cells (control), which are lacking mouse PS1 and PS2 but expressing human PS1 and MEF PS1/PS2 -/- that are lacking mouse PS1 and PS2 (sample), as shown in Figure 17, statistical analysis of the obtained results are summarized in Table 16. More details shown in Tables B-14 – B-22, B-25 and B-35 – B-37 in the appendix.

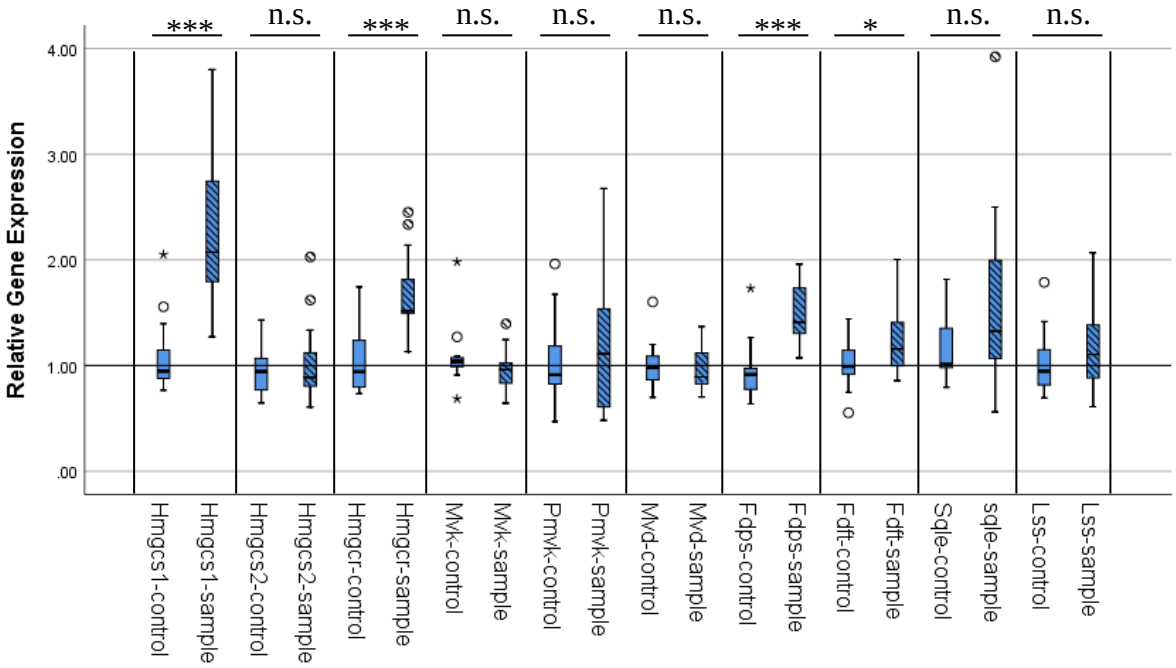

Figure 17: Quantitative determination of gene expression for genes involved in cholesterol biosynthesis pathway by using the real-time reverse transcriptase

polymerase chain reaction (qRT-PCR) technique (n=10-14). β-actin was used as a housekeeping gene. Results were normalized to the housekeeping gene, and control and quantitative detection of gene expressions were calculated by employing the $2^{-\Delta\Delta}$ method. Mouse embryonic fibroblasts cells which are lacking mouse PS1 / PS2 and expressing human PS1 MEF PS1res (control) and MEF PS1/PS2 -/- which are lacking mouse PS1 and PS2 (sample). Boxplots represent; minimum, first quartile, median, third quartile, and maximum. Outliers represent 1.5 (circle) and 2 (star) times' interquartile range. Horizontal line represent mean of controls. Statistical significance was determined using Student's unpaired two-sided t-test (* $p \leq 0.05$, *** $p \leq 0.001$, and n.s., not significant).

Table 16: Descriptive statistics of quantified MEF PS1res. (control) and MEF PS1/PS2 -/- (sample) genes.

Gene		Mean	95% CI for mean		Std. deviation	SEM	T.Test	n
			Lower	Upper				
Hmgcs1	Control	1.0888	0.8836	1.2940	0.35539	0.09498	0.000059	14
	Sample	2.3597	1.8780	2.8414	0.83434	0.22299		14
Hmgcs2	Control	0.9613	0.8143	1.1084	0.23144	0.06681	0.593	12
	Sample	1.0355	0.7724	1.2986	0.41406	0.11953		12
Hmgcr	Control	1.0371	0.8701	1.2040	0.28912	0.07727	0.000080	14
	Sample	1.6571	1.4238	1.8904	0.40407	0.10799		14
Mvk	Control	1.0893	0.9093	1.2693	0.29780	0.08260	0.234	13
	Sample	0.9640	0.8311	1.0969	0.21991	0.06099		13
Pmvk	Control	1.0434	0.7795	1.3072	0.43658	0.12109	0.407	13
	Sample	1.2397	0.8065	1.6729	0.71686	0.19882		13
Mvd	Control	1.0029	0.8647	1.1412	0.22885	0.06347	0.726	13
	Sample	0.9714	0.8357	1.1071	0.22455	0.06228		13
Fdps	Control	0.9538	0.7939	1.1137	0.27693	0.07401	0.000038	14
	Sample	1.4861	1.3177	1.6545	0.29161	0.07793		14
Fdft	Control	1.0055	0.8748	1.1362	0.22640	0.06051	0.037	14
	Sample	1.2538	1.0471	1.4604	0.35796	0.09567		14
Sqle	Control	1.1540	0.9326	1.3754	0.32953	0.09936	0.122	11
	Sample	1.6495	1.0225	2.2765	0.93324	0.28138		11
Lss	Control	1.0435	0.8035	1.2834	0.33541	0.10607	0.467	10
	Sample	1.1700	0.8684	1.4717	0.42172	0.13336		10

Rate-limit enzyme, HMGCR, showed a statisticly significant upregulation induced by the absence of Aβ. Likewise, the impact of Aβ on SREBP-1 and relevant genes are elucidated in Figure 18, while statistical analysis results are detailed in Table 17. More details are shown in Tables B-28 and B-43 – B-45

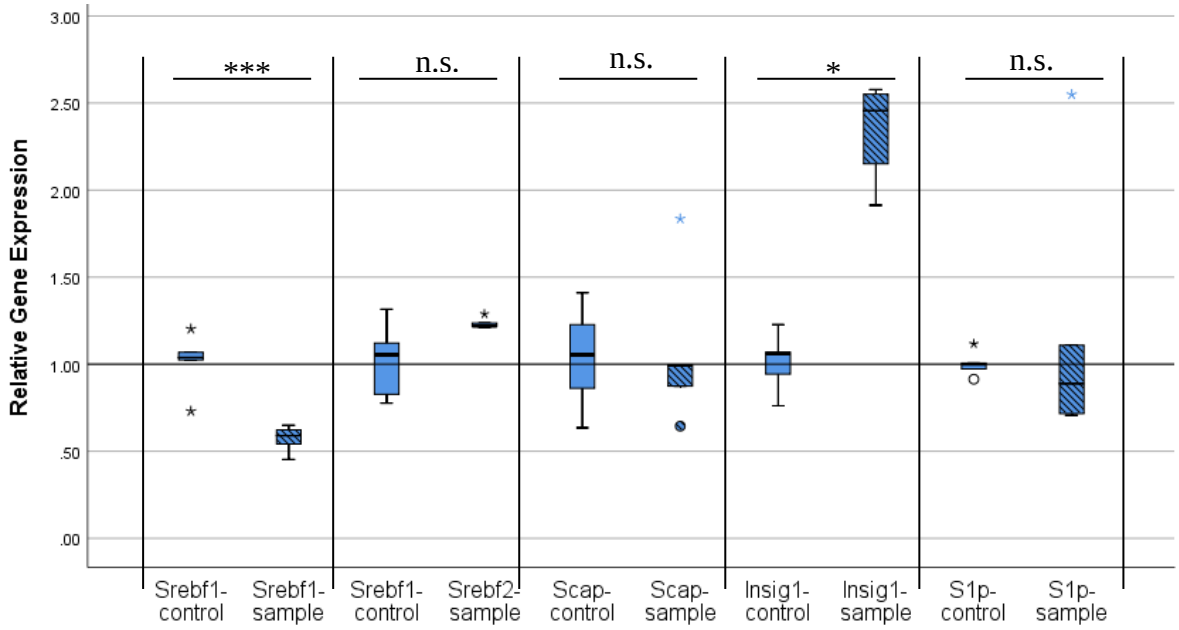

Figure 18: Quantitative determination of gene expression for genes involved in SREBP-1 and related genes by using the real-time reverse transcriptase polymerase chain reaction (qRT-PCR) technique (n=5). β-actin was used as a housekeeping gene. Results were normalized to the housekeeping gene, and control and quantitative detection of gene expressions were calculated by employing the $2^{-\Delta\Delta}$ method. Mouse embryonic fibroblasts cells which are lacking mouse PS1 / PS2 and expressing human PS1 MEF PS1res (control) and MEF PS1/PS2 -/- which are lacking mouse PS1 and PS2 (sample). Boxplots represent; minimum, first quartile, median, third quartile, and maximum. Outliers represent 1.5 (circle) and 2 (star) times' interquartile range. Horizontal line represents mean of controls. Statistical significance was determined using Student's unpaired two-sided t-test (* $p \leq 0.05$, *** $p \leq 0.001$, and n.s., not significant).

Table 17: Descriptive statistics of quantified MEF PS1res. (control) and MEF PS1/PS2 -/- (sample) genes.

Gene		Mean	95% CI for mean		Std. deviation	SEM	p	n
			Lower	Upper				
Srebf1	Control	1.0132	0.7982	1.2282	0.17317	0.07744	0.001	5
	Sample	0.5709	0.4749	0.6669	0.07733	0.03458		5
Srebf2	Control	1.0192	0.7448	1.2936	0.22100	0.09883	0.094	5
	Sample	1.2349	1.1957	1.2740	0.03152	0.01409		5
Scap	Control	1.0380	0.6615	1.4145	0.30323	0.13561	0.904	5
	Sample	1.0683	0.5072	1.6294	0.45188	0.20209		5
Insig1	Control	1.0125	0.7975	1.2275	0.17314	0.07743	0.030	5
	Sample	2.3509	1.8696	2.8322	1.31266	0.58704		5
S1p	Control	1.0021	0.9102	1.0941	0.07409	0.03313	0.596	5
	Sample	1.1943	0.2323	2.1564	0.77479	0.34650		5

4.1.2 Influence of cholesterol on Aβ degradation

In the second phase of the study, the proposed function of cholesterol as a triggering factor for the enzymes involved in the process of Aβ degradation was examined. This was achieved by using neuroblastoma 2a cells (N2a) with the emphasis on the enzymatic activity of IDE. The reason of studying IDE is because this enzyme can degrade Aβ in the trans-membrane and the secreted IDE can degrade Aβ in the cytosol. Due to the fact that Aβ can be found on cell membrane and between cells (extracellular space), the impact of cholesterol was then studied in living N2a cells and culture medium, respectively, by quantifying the Aβ remaining after incubation with cholesterol on western blots.

4.1.2.1 Impact of cholesterol on Aβ degradation in living N2a cells

Determination of total Aβ degradation in living neuroblastoma 2a WT cells was measured by western blot technique as previously described in the methods section (3.2.4). The human sequence of synthetic peptide was incubated for 6 h with N2a cells at a concentration of 0.5 µg/ml with and without cholesterol (100 µM) in reduced culture medium (cholesterol in culture medium is neglected) to study its impact on Aβ degradation. Results of this experiment are shown in Figure 19, while Table 18 contains statistical analysis outcomes.

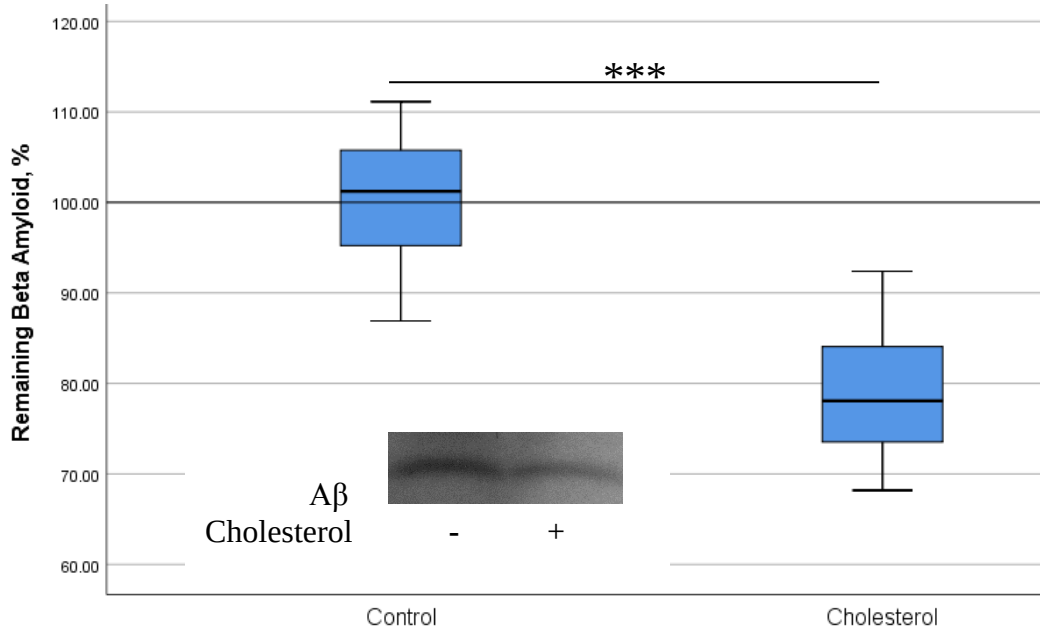

Figure 19: Impact of cholesterol on Aβ40 degradation in living N2a cells. Confluent mouse neuroblastoma N2a cells were incubated with reduced culture medium (DMEM / 0.1% FCS) for 6 h. Culture medium is reduced to control cell number. After that cells

were then incubated with ethanol (control) or with cholesterol and ethanol (sample) at a concentration of 100 µM for 18 h. The human Aβ40 peptide sequence at a concentration of 0.5 µg/ml was added to control and sample and incubated for 6 h before quantification. Western blot analysis was used to quantify the remaining Aβ40 peptides using the W02 antibody (n=16).
Boxplots represent; minimum, first quartile, median, third quartile, and maximum. Horizontal line represents mean of control. Statistical significance was determined using Student's unpaired two-sided t-test (*** $p \leq 0.001$).

More details are shown if Figures C-1 – C-3 and Tables C-1 – C-6 in the appendix.

Table 18: Descriptive statistics of the remaining Aβ in N2a living cells.

		Control	Cholesterol
Mean		100.0175	79.2825
95% CI for mean	Lower	96.3137	75.5786
	Upper	103.7214	82.9863
Std. deviation		6.95080	6.95080
SEM		1.73770	1.73770
p		2.0426E-9	
n		16	16

Degraded Aβ was increased to around 20% with statisticaly significant result as shown by the reduction of recombinant human Aβ due to the presence of cholesterol.

4.1.2.2 Impact of cholesterol on Aβ degradation in N2a cells' culture medium

Quantification of the non-degraded amyloid peptide was carried out by Western Blot using the W02 antibody to detect the human synthetic peptide in the culture medium of N2a WT cells as already described. Different incubation times were first examined to choose the best incubation time for future experiments. Moreover, the human amyloid peptide concentration was set at 0.5 µg/ml as shown in Figure 20. Because this procedure had been already established (Mett, 2017) therefore, the experiment was carried out once. According to these results, incubation time was set to 24 h. Detailed results are shown in Figures C-4 – C-7 and Tables C-7 – C-14 in the appendix.

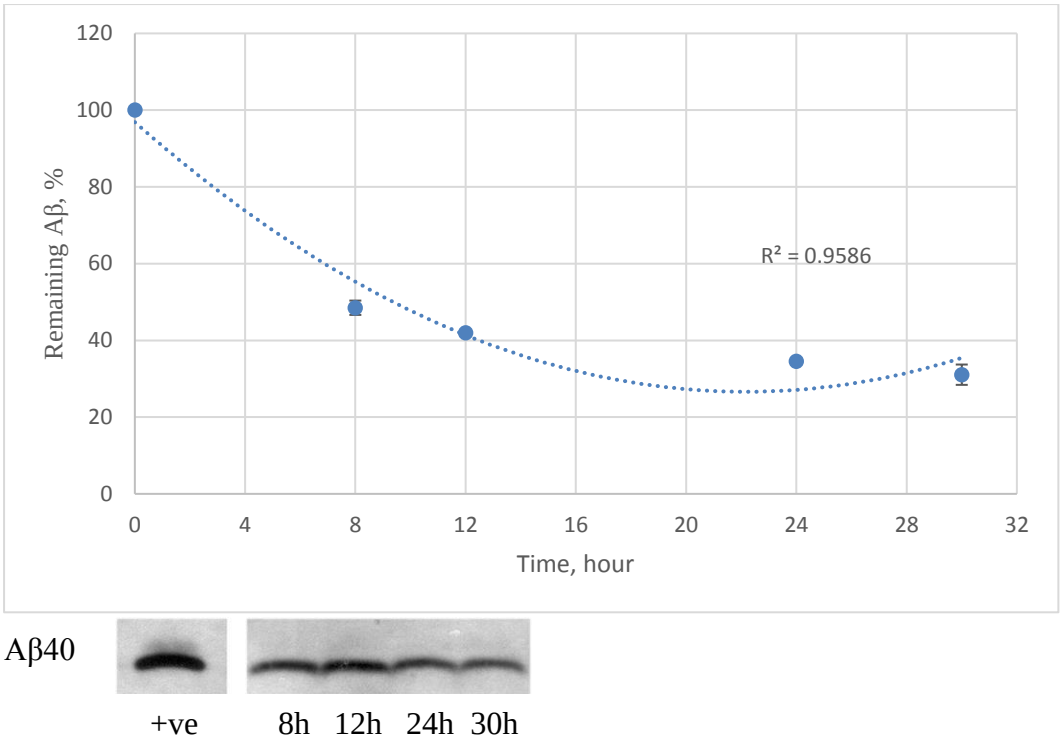

Figure 20: Effect of incubation time on Aβ40 degradation in culture media of N2a WT cells. Confluent mouse neuroblastoma N2a cells were incubated with reduced culture medium (DMEM / 0.1 % FCS) for 24 h. The human Aβ40 peptides sequence were incubated with the cells at a concentration of 0.5 µg/ml. The cells were tested at different times. Western blot analysis with the W02 antibody was used to quantify the remaining Aβ peptides.
Error bars represent the standard deviation (±2.6, 0.85, 0.4, and 3.7 %) for incubation times of 8, 12, 24, and 30 h, respectively.

The influence of cholesterol at a concentration of 100 µM on Aβ40 in the culture medium on N2a WT cells was measured as shown in Figure 21 and summarized statistics in Table 19.

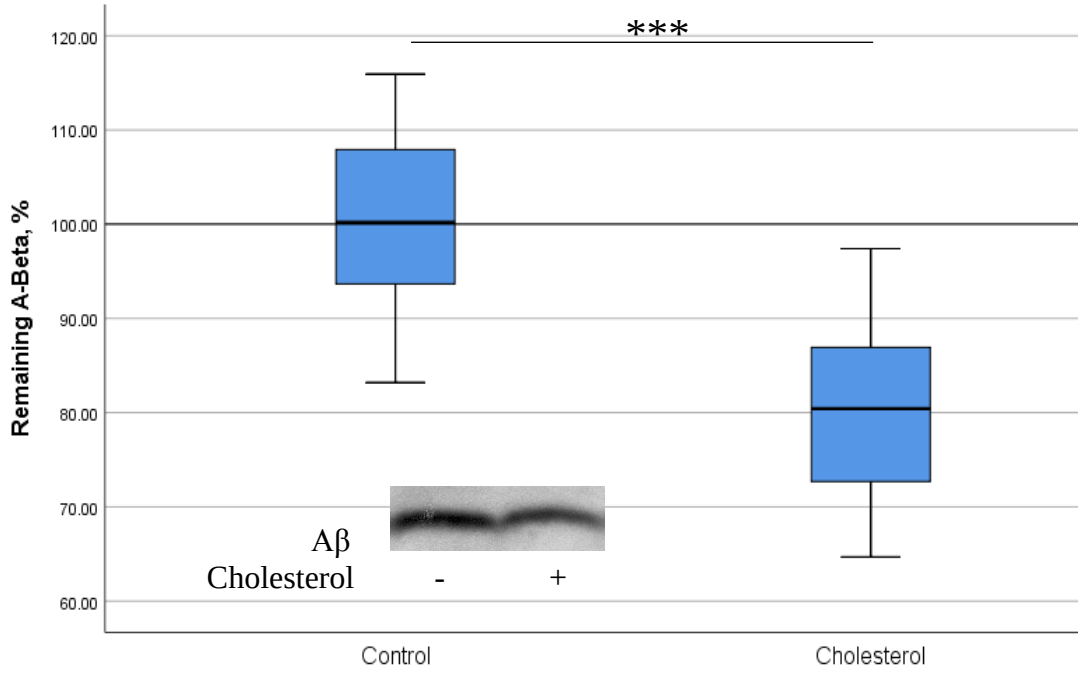

Figure 21: Influence of cholesterol on Aβ40 degradation in culture media of N2a WT cells. Confluent mouse neuroblastoma N2a cells were incubated with reduced culture medium (DMEM / 0.1 % FCS) for 24 h. The human Aβ40 peptides sequence at a concentration of 0.5 µg/ml were incubated with the reduced culture medium only for 24 h with the addition of ethanol (control) or cholesterol and ethanol (sample) at a concentration of 100 µM. Western blot analysis with the W02 antibody was used to quantify the remaining Aβ peptides (n=13).

Boxplots represent; minimum, first quartile, median, third quartile, and maximum. Horizontal line represent mean of control. Statistical significance was determined using Student's unpaired two-sided t-test (*** $p \leq 0.001$).

Table 19: Statistics of the remaining Aβ40 in N2a culture medium.

		Control	Cholesterol
Mean		100.0302	80.5698
95% CI for mean	Lower	94.0189	74.5585
	Upper	106.0415	86.5811
Std. deviation		9.94759	9.94759
SEM		2.75896	2.75896
p		0.000043	
n		13	13

Obviously, the impact of secreted IDE on the degradation of Aβ is shown in the extracellular space in the previous figure. However, in order to confirm the hypothesis that IDE is the main Aβ degrading enzyme in the extracellular space, the same

experiment was repeated but with the introduction of IDE knockdown N2a cells. Experiments were carried out with living cells and with culture medium to compare the results as shown in Figure 22 and relevant statistics in Table 20 (Detailed results are shown in Figures C-8 – C-10 and Tables C-15 – C-20 in the appendix), and Figure 23 and pertinent statistics in Table 21 (Detailed of results are presented in Figures C-11 – C-13 and Tables C-21 – C-26 in the appendix), respectively.

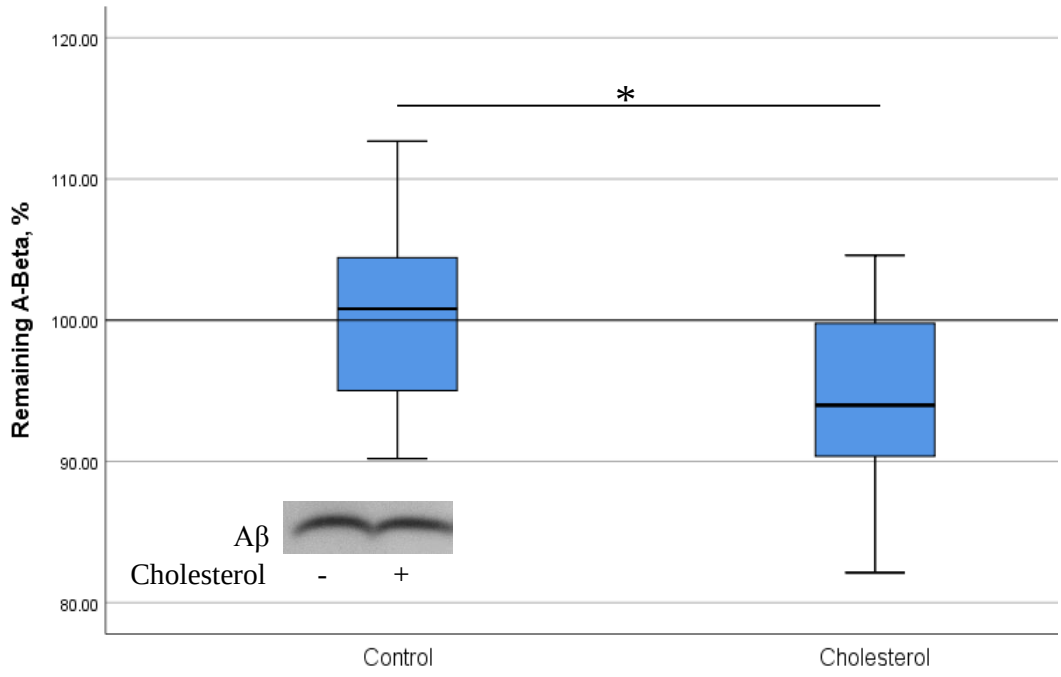

Figure 22: Impact of cholesterol on Aβ40 degradation in living N2a IDE knockdown cells. Confluent mouse neuroblastoma N2a IDE knockdown cells were incubated with reduced culture medium (DMEM / 0.1% FCS) for 6 h to control cell number, then incubated with ethanol (control) or with cholesterol and ethanol at a concentration of 100 µM (sample) for 18 h. The human Aβ40 peptide sequence at a concentration of 0.5 µg/ml was added to control and sample and incubated for 6 h before quantification. Western blot analysis was used to quantify the remaining Aβ40 peptides using the W02 antibody (n=16).
Boxplots represent; minimum, first quartile, median, third quartile, and maximum. Horizontal line represent mean of control. Statistical significance was determined using Student's unpaired two-sided t-test (* $p \leq 0.05$).

Impeded activity of IDE resulted in a limited degradation potential of Aβ to only 5% intracellularly.

Table 20: Statistics of the remaining Aβ40 in living N2a IDE knockdown cells.

		Control	Cholesterol
Mean		100.0911	94.7089
95% CI for mean	Lower	96.8235	91.4414
	Upper	103.3586	97.9765
Std. deviation		6.13206	6.13206
SEM		1.53302	1.53302
p		0.019	
n		16	16

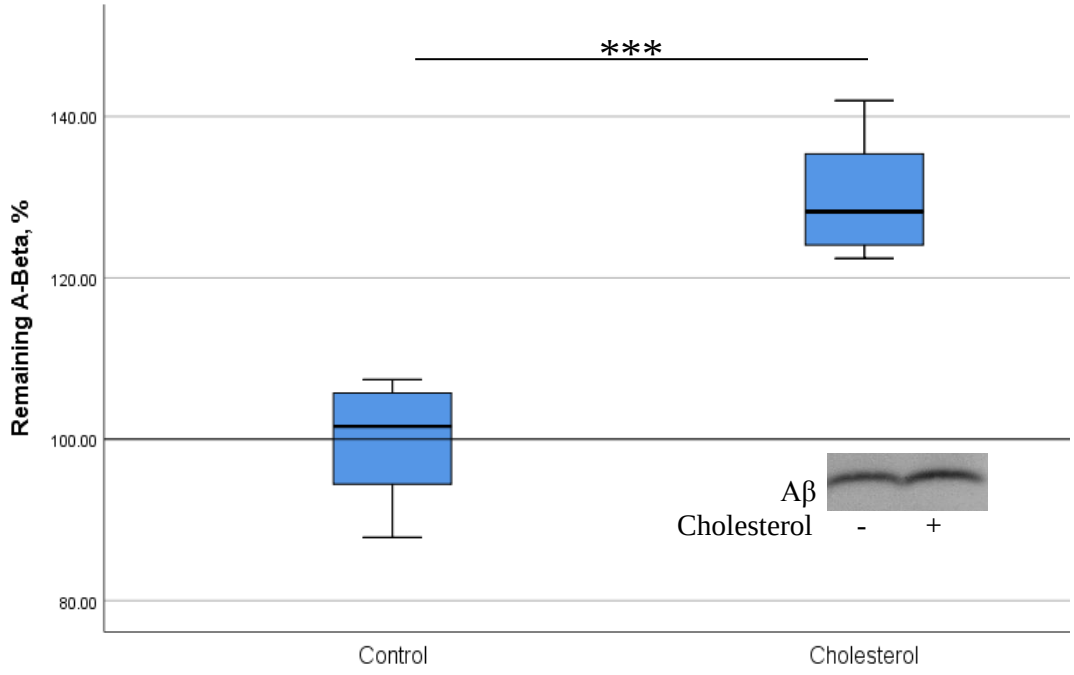

Figure 23: Influence of cholesterol on Aβ40 degradation in culture media of N2a IDE knock down (KD) cells. Confluent mouse neuroblastoma N2a KD cells were incubated with reduced culture medium (DMEM / 0.1 % FCS) for 24 h. The human Aβ40 peptides sequence at a concentration of 0.5 µg/ml were incubated with the reduced culture medium only, for 24 h with the addition of ethanol (control) or cholesterol (sample) at a concentration of 100 µM. Western blot analysis with the W02 antibody was used to quantify the remaining Aβ peptides (n=13).

Boxplots represent; minimum, first quartile, median, third quartile, and maximum. Horizontal line represent mean of control. Statistical significance was determined using Student's unpaired two-sided t-test (*** $p \leq 0.001$).

Significant increase in the accumulation of Aβ (29%) is achieved due to the absence of IDE.

Table 21: Statistics of the remaining Aβ40 in culture medium of N2a IDE knockdown cells.

		Control	Cholesterol
Mean		100.0199	129.7801
95% CI for mean	Lower	95.8446	125.6048
	Upper	104.1952	133.9554
Std. deviation		6.90937	9.94759
SEM		1.91631	2.75896
P		7.6624E-11	
N		13	13

4.1.2.3 Effects of cholesterol on IDE gene expression

According to the results obtained in the previous section, cholesterol exhibited an obvious role in up-regulating IDE enzymatic activity. In order to investigate whether cholesterol influences IDE at the transcriptional level, IDE gene expressions (IDE59) were analyzed in the presence of cholesterol using qRT-PCR. The investigation was carried out using N2a-WT cells which are incubated cholesterol at a concentration of 100 µM, for 18 h, then total RNA and subsequent cDNA was isolated as described previously. Two housekeeping genes were employed in the investigation: (1) β-actin and (2) Polr2 (Figure 24 and Table 22 for relevant statistics). More details are shown in Tables B-46 – B-52 in the appendix.

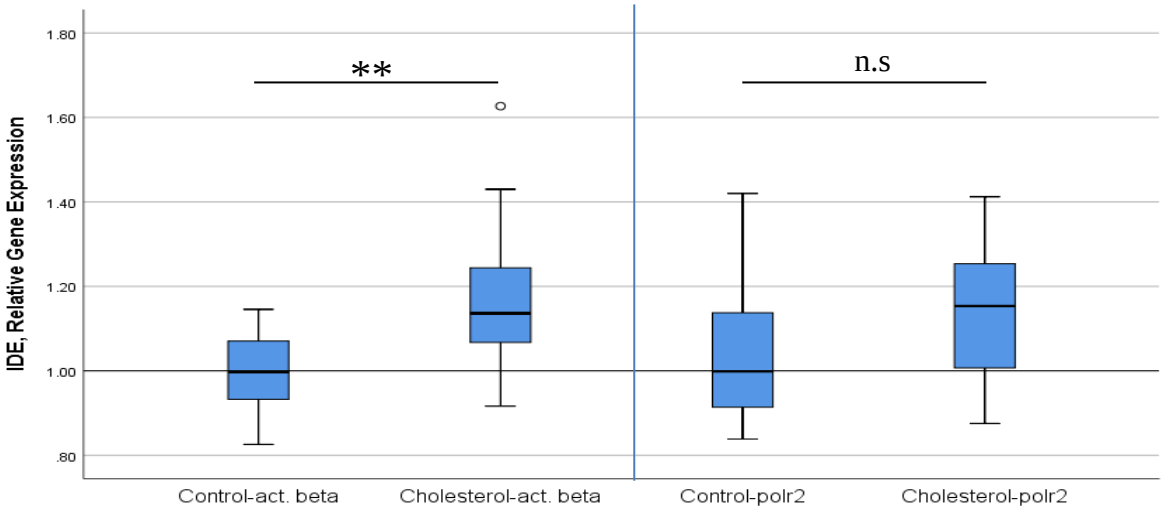

Figure 24: Effects of cholesterol on IDE gene expression as compared with β-actin and Polr2 housekeeping gene used as a control in N2a cell culture medium. Mouse

neuroblastoma cells were incubated with cholesterol at a concentration of 100 µM. RT-PCR analysis was used to quantify IDE gene expression (n=12). Results were normalized to the housekeeping gene and control (no cholesterol) and quantitative detection of gene expression was calculated using the $2^{-\Delta\Delta}$ method. Significance level, ** $p \leq 0.01$, n.s = not significant.

Table 22: Statistics of IDE gene expression test.

Housekeeping Gene		Mean	95% CI for mean		Std. deviation	SEM	p	n
			Lower	Upper				
β-actin	Control	1.0040	0.9527	1.0554	0.09267	0.02393	0.004	15
	Sample	1.1722	1.0673	1.2771	0.18941	0.049891		15
Polr2	Control	1.0358	0.9368	1.1347	0.16378	0.04542	0.115	13
	Sample	1.1430	1.0398	1.2462	0.17080	0.04737		13

Upregulation of IDE gene expression was statisticaly significant with β-actin and non-significant with Polr2 housekeeping genes due to the influence of cholesterol.

4.1.2.3.1 Effects of cholesterol on IDE promoter activity

Cholesterol's effects on increased IDE gene expression were demonstrated by measuring IDE promoter activity using N2a WT cells incubated with and without cholesterol (control). The process included transient transfection with a reporter plasmid that contained the gene encoding Gaussia luciferase controlled by the IDE promoter, whereas the gene encoding SEAP was controlled by the active promoter as previously described in the methods section. Gaussia luciferase and SEAP signals were determined for the incubated cells' culture medium, and the resulting data were normalized as a ratio of the measurement of Gaussia luciferase for each sample to that of SEAP activity. Figure 25 summarizes normalized results of cholesterol's effects on the IDE promoter, whereas Table 23 displays relevant statistics (see Appendix D for more details).

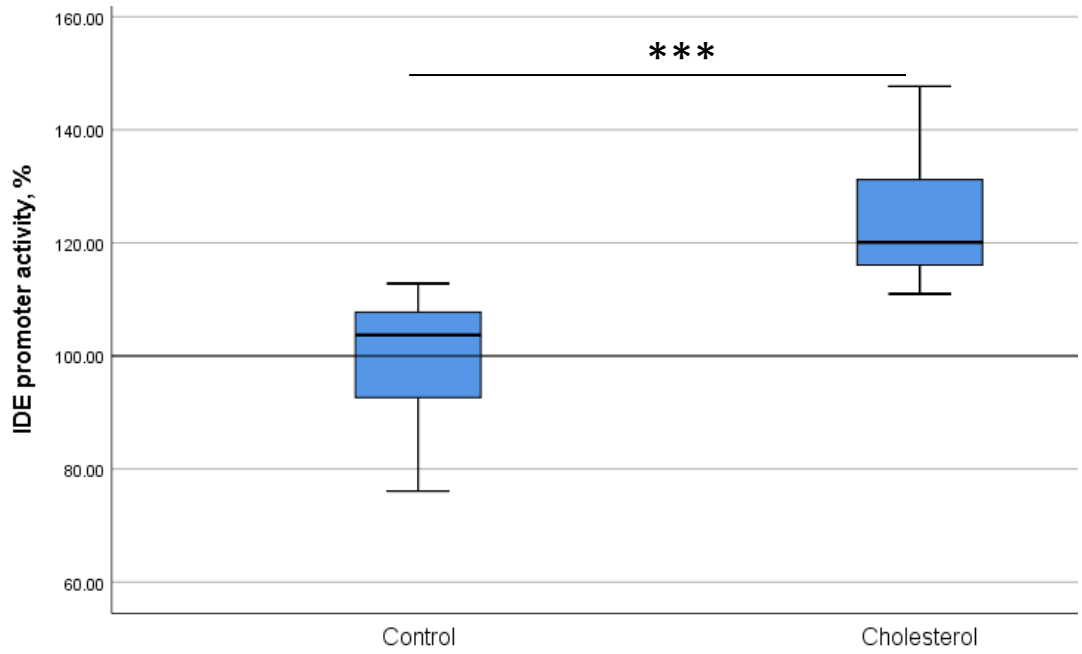

Figure 25: Influence of cholesterol on IDE59 promoter activity in N2a WT cells. Confluent mouse neuroblastoma wild type cells were incubated with Opti-MEM medium, lipofectamine (transfection reagent), and vector solution for 6 h, then incubated with reduced medium (DMEM / 0.1 % FCS) to control cell number and ethanol (control) or ethanol and cholesterol (sample) at a concentration of 100 µM, for 16 h. Incubation media then collected and the assay solution was prepared according to the manufacturer's instructions (n=12).

Boxplots represent; minimum, first quartile, median, third quartile, and maximum. Horizontal line represents mean of control. Statistical significance was determined using Student's unpaired two-sided t-test (*** $p \leq 0.001$).

Table 23: Statistics of IDE59 promoter activity in N2a WT cells.

		Control	Cholesterol
Mean		100.0350	123.7650
95% CI for mean	Lower	92.7980	116.7650
	Upper	107.2718	131.0018
Std. deviation		11.38992	11.38992
SEM		3.28799	3.28799
p		0.000041	
n		12	12

Obvious enhancement in the transcriotion of IDE gene is shown (24%) as a consequence of cholesterol's impact.

4.1.2.4 Effects of cholesterol on IDE protein levels

In order to measure cholesterol's effects on IDE membrane and extracellular protein levels, western blots technique was employed to quantify IDE protein in N2a WT cells as shown in Figure 26 and statistics in Table 24 for intracellular IDE protein level, whereas Figure 27 and dependent statistics in Table 25, demonstrates the influence of cholesterol on extracellular IDE protein level.

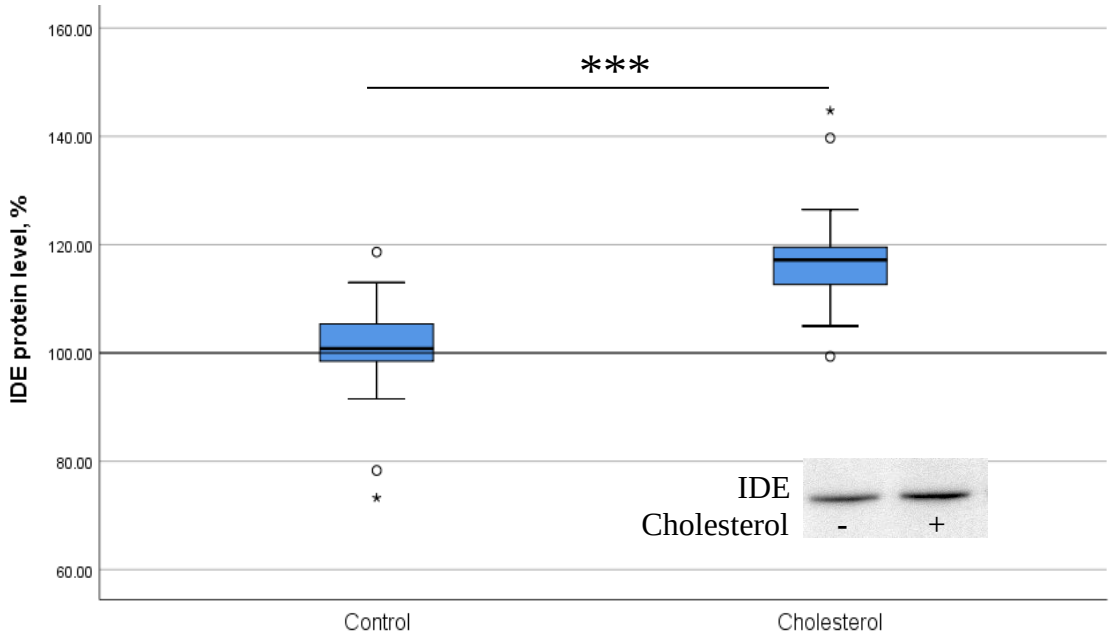

Figure 26: Influence of cholesterol on IDE protein level in N2a WT cells lysate. Confluent mouse neuroblastoma cells were cultured in reduced culture medium (DMEM / 0.1 FCS) for 6 h, then incubated with ethanol (control) or cholesterol and ethanol (sample) at a concentration of 100 µM, for 18 h, in reduced culture medium. Cell lysate were quantified by western blot using ST1120 secondary antibody (n=15). Boxplots represent; minimum, first quartile, median, third quartile, and maximum. Horizontal line represent mean of control. Statistical significance was determined using Student's unpaired two-sided t-test (*** $p \leq 0.001$).

Table 24: Statistics of IDE protein level in N2a WT cells lysate.

		Control	Cholesterol
Mean		100.0278	117.9722
95% CI for	Lower	93.3877	111.3321
	Upper	106.6679	124.6123
Std. deviation		11.99049	11.99049
SEM		3.09593	3.09593
p		0.000323	
N		15	15

Details are shown in Figures C-14, 16, 17 and Tables C-27, 29, 31, 33-35 in the appendix.

Cholesterol has induced the increase of IDE level to about 18% in the cytosol of N2a cells as shown in the previous figure with sitatisticaly highly significant result.

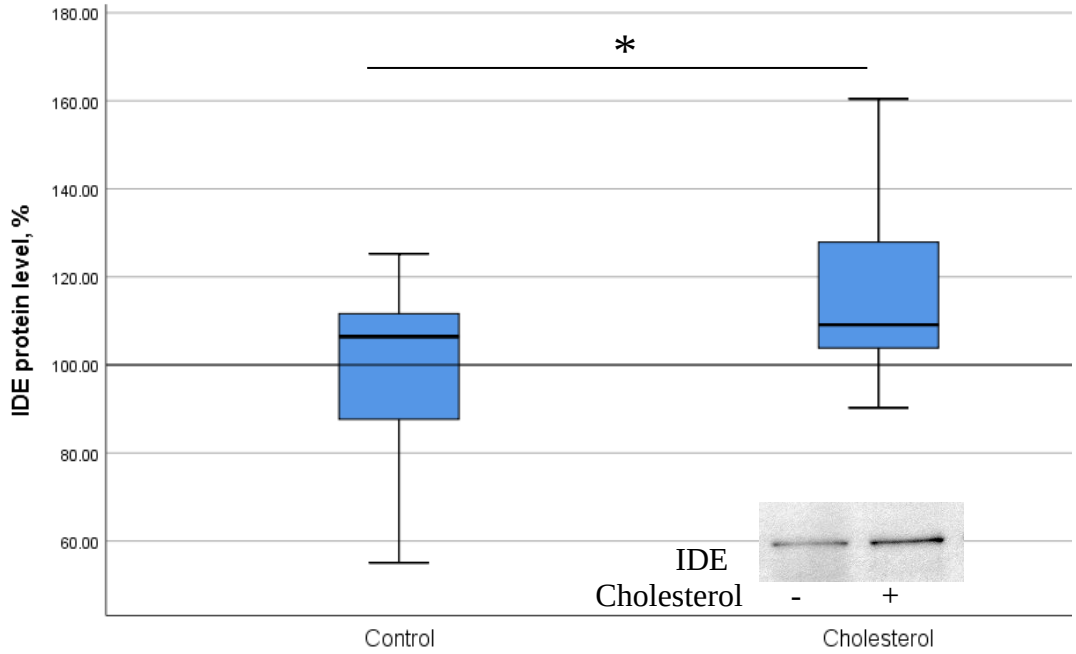

Figure 27: Influence of cholesterol on IDE protein level in N2a WT cells culture medium. Confluent mouse neuroblastoma cells were cultured in reduced culture medium (DMEM / 0.1 FCS) for 6 h, then incubated with ethanol (control) or cholesterol (sample) at a concentration of 100 µM, for 18 h, in reduced culture medium. Culture medium was quantified by western blot using ST1120 secondary antibody (n=14). Boxplots represent; minimum, first quartile, median, third quartile, and maximum. Horizontal line represent mean of control. Statistical significance was determined using Student's unpaired two-sided t-test (* $p \leq 0.05$).

Table 25: Statistics of IDE protein level in N2a WT cells culture medium.

		Control	Cholesterol
Mean		100.0029	115.4971
95% CI for mean	Lower	89.6251	105.1194
	Upper	110.3806	125.8749
Std. deviation		17.97381	17.97381
SEM		4.80370	4.80370
P		0.031	
N		14	14

Details are shown in Figure C-15-17 and Tables C-28, 30, 32, 36-38 in the appendix. Protein level of IDE is increased at a rate of around 15% due to the presence of cholesterol in the extracellular space of N2a cells.

4.1.2.5 Effects of cholesterol on IDE protein stability

Maintaining the folded (stable) state of IDE proteins in the presence of cholesterol was investigated to study cholesterol's effects on IDE protein conformation by using cycloheximide (inhibitor of protein biosynthesis). Western blotting was used to quantify intracellular (Figure 28 and statistics in Table 26) and extracellular (Figure 29 and statistics in Table 27) IDE proteins in the presence of cholesterol.

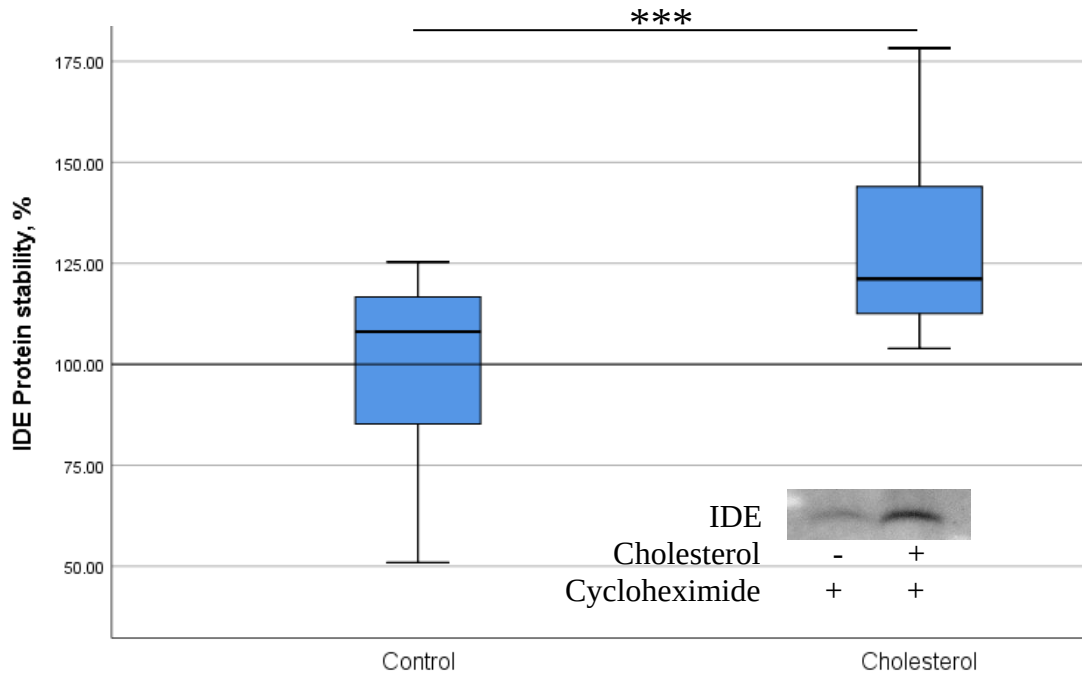

Figure 28: Effect of cholesterol on IDE protein stability in N2a WT cells lysate (n=15). Confluent N2a WT cells were cultured in reduced culture medium (DMEM / 0.1 % FCS), then with cycloheximide at a concentration of 20 µg/ml, for 8 h. After that cells were incubated with cycloheximide and with ethanol (control) or with ethanol and cholesterol at a concentration of 100 µM (sample), for 16 h in reduced culture medium. Detection by western blot analysis was used to quantify IDE level in lysate. Asterisks show statistical significance compared to control (*** $p \leq 0.001$).

Table 26: Statistics of IDE protein stability in N2a WT cells lysate.

		Control	Cholesterol
Mean		100.0040	129.1960
95% CI for mean	Lower	88.4172	117.6092
	Upper	111.5908	140.7828
Std. deviation		20.92303	20.92303
SEM		5.40230	5.40230
p		0.001	
n		15	15

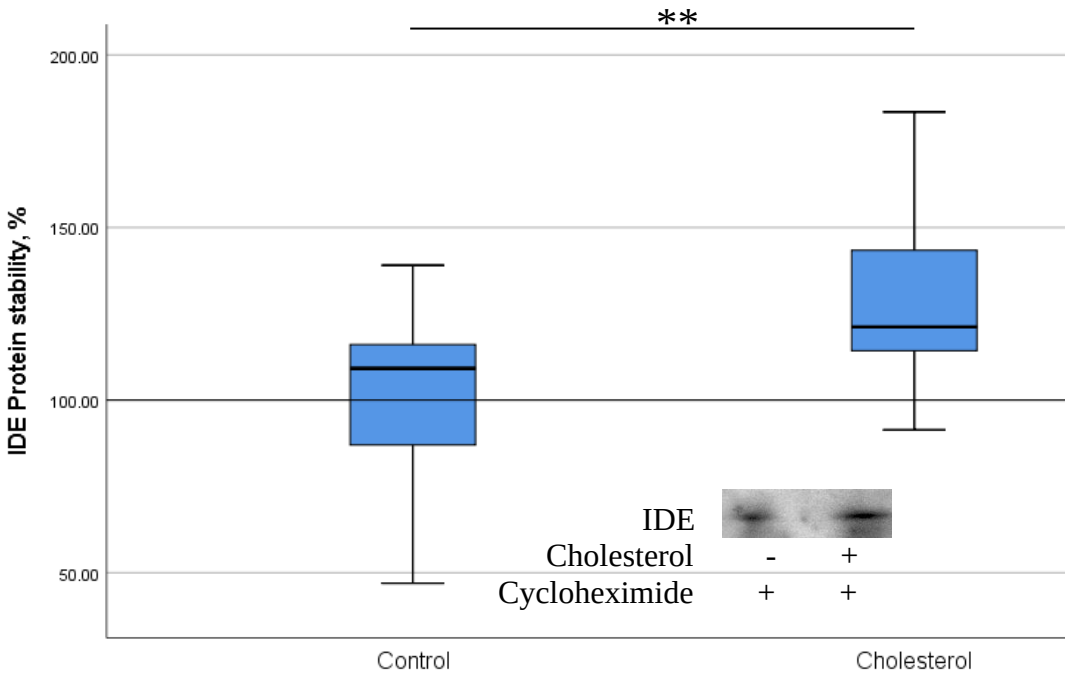

Figure 29: Effect of cholesterol on IDE protein stability in N2a WT cells culture medium. Confluent N2a WT cells were cultured in reduced culture medium (DMEM / 0.1 % FCS), then with cycloheximide at a concentration of 20 µg/ml, for 8 h. After that cells were incubated with cycloheximide and with ethanol (control) or with ethanol and cholesterol at a concentration of 100 µM (sample), for 16 h in reduced culture medium. Detection by western blot analysis was used to quantify IDE level in culture medium (extracellular) (n=15). Asterisks show statistical significance compared to control (** $p \leq 0.01$).

Table 27: Statistics of IDE protein stability in N2a WT cells culture medium.

		Control	Cholesterol
Mean		100.0318	130.3682
95% CI for mean	Lower	85.0444	115.3808
	Upper	115.0192	145.3556
Std. deviation		27.06376	27.06376
SEM		6.98783	6.98784
p		0.005	
n		15	15

Results showed that cholesterol participated in enhancing the resistance of IDE to cycloheximide and hence increasing its stability at a rate of around 29% and 30% in intracellular and exracellular space of N2a cells, respectively. Detailed results of intracellular IDE are presented in Figures C-18 – C-20 and Tables C-39 – C- 44, while extracellular IDE details are shown in Figures C-21 – C-23 and Tables C-45 C-50 in the appendix.

4.1.2.6 Effects of cholesterol on IDE activity

The direct effects of cholesterol on IDE activity were measured for the purpose of studying the role of cholesterol on IDE from different aspects. Enzymatic activity of recombinant human IDE in the presence of cholesterol was evaluated after incubation for 15 min. After that period, the Mca-RPPGFSAFK (Dnp)-OH substrate was added and the enzymatic activity was measured. Furthermore, PC 18:0 was utilized to confirm the role of lipids on IDE activity. Figure 30 shows the results of cholesterol, and cholesterol and PC 18:0. Activation of IDE occurs in the presence of PC 18:0 with higher fluorescence intensity (starting at around 1000 AU) and by cholesterol with less extent (around 400 AU) while, ethanol (control) showed no impact on IDE activity. More details are shown in the Appendix E.

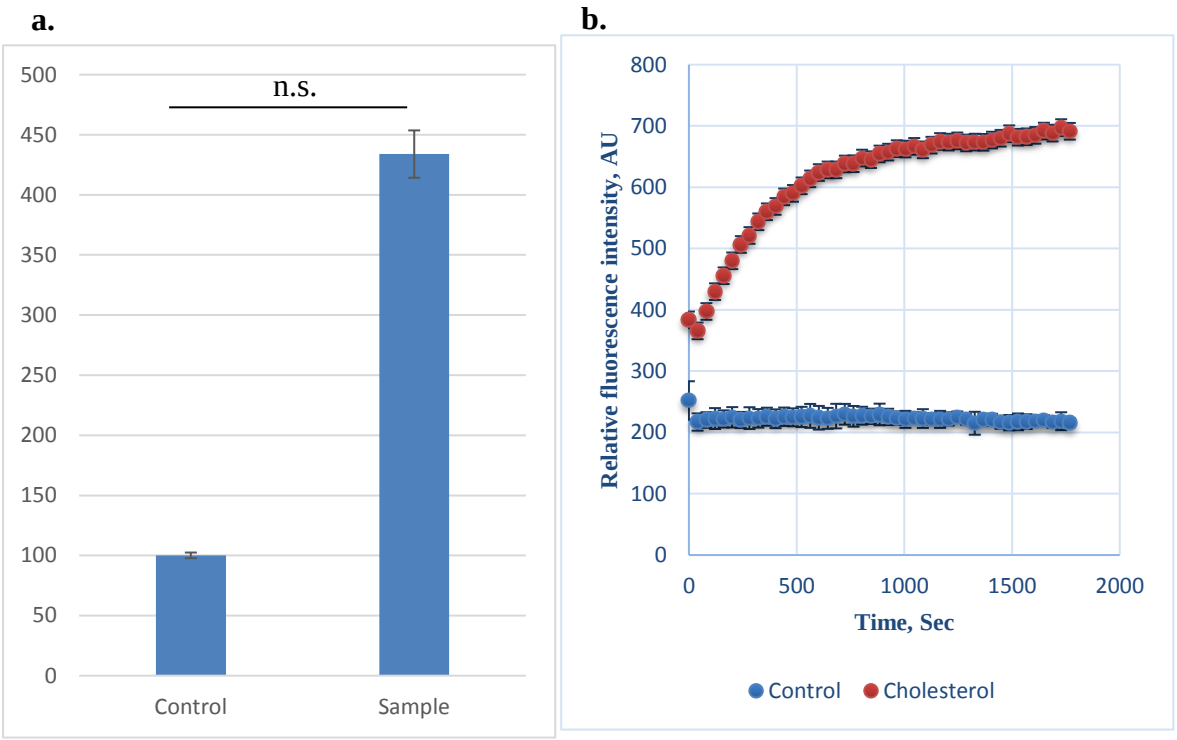

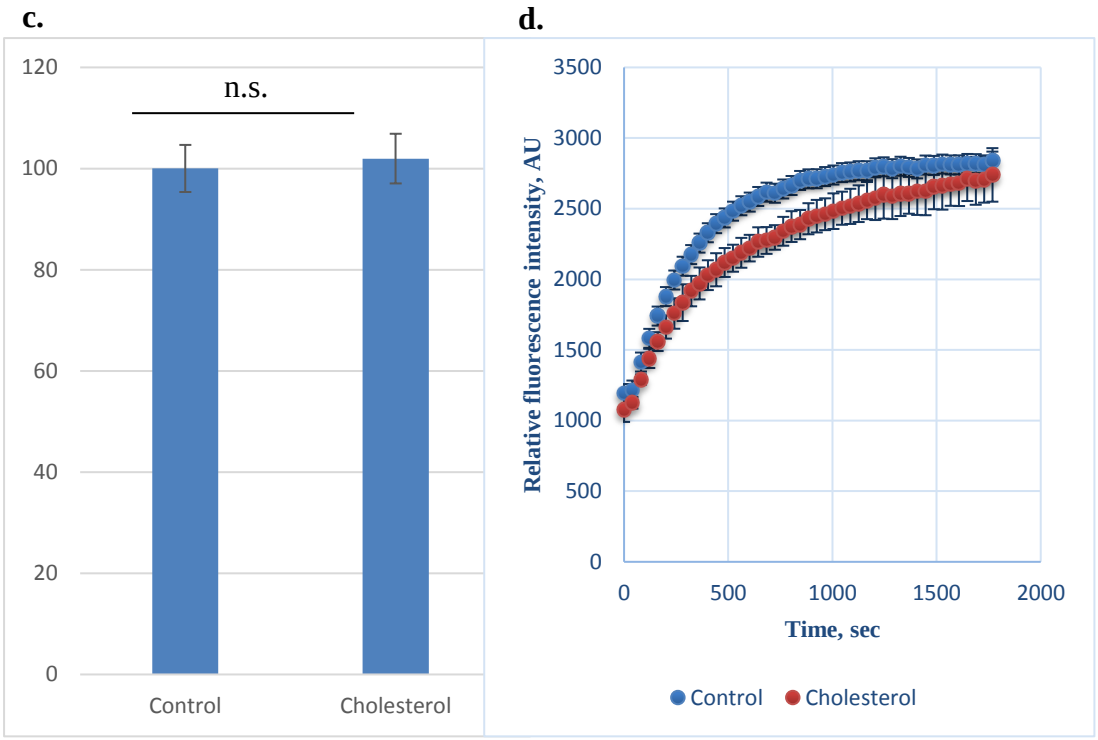

Figure 30: Effect of cholesterol on IDE protein activity. Recombinant human IDE enzyme was pre-incubated with ethanol (control) or ethanol and cholesterol at a concentration of 100 µM (sample) for 15 min. *in vitro*, then substrate Mca-RPPGFSAFK (Dnp) -OH was added and fluorescence was measured (a.) and slope (b.), and (c) with the addition of PC18:0 at a concentration of 150 µM to the control and sample and the slope (d.). The vast difference in fluorescence intensity in (b) and (d) is due to the use of PC 18:0. Error bars represent the standard deviation of the mean (n = 3). n.s. = not significant.

Obvious increase in IDE activity is observed due to the impact of cholesterol and PC18:0 lipid.

4.1.3 Antimicrobial activity of Aβ

As the third aim of the study, viability of nematode in the presence of Aβ are shown in Figure 31 at different Aβ concentrations in addition to negative and positive (ethanol) controls for comparison purposes. Obviously, it can be seen in Figure 31 that the peptide has not affected viability of *S. feltiae* regardless of the peptide concentration. Table 28 displays the statistics of the test.

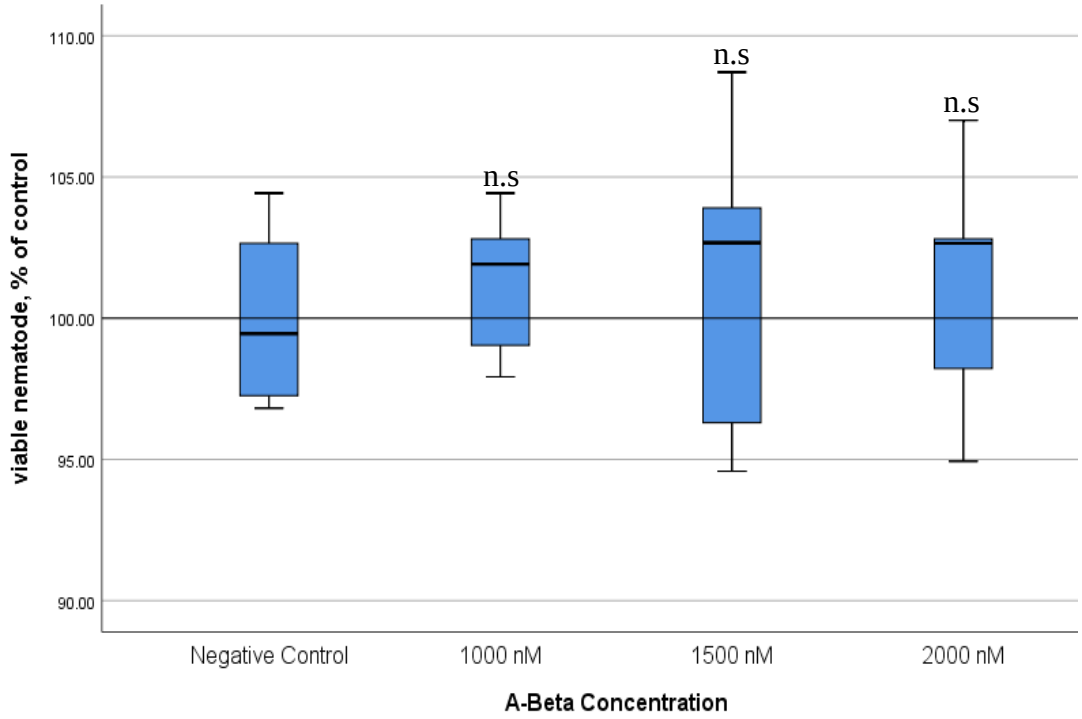

Figure 31: Antimicrobial activity of Aβ against *S. feltiae*. Three concentrations of Aβ (1000, 1500, and 2000 nM) were incubated with nematodes in addition to the control sample (0 Aβ). Three independent experiments (n=9) were carried out at every concentration.

Boxplots represent; minimum, first quartile, median, third quartile, and maximum. Horizontal line represents mean of control. n.s. = not significant.

Table 28: Statistics of *S. feltiae* viability test.

Aβ concentration, nM		**0**	**1000**	**1500**	**2000**
Mean		100.0013	101.1786	101.1161	100.7040
95% CI for mean	Lower	97.83	99.3965	97.2274	97.5793
	Upper	102.18	102.9607	105.0048	103.8287
Std. deviation		2.82787	2.31846	5.05902	4.06508
SEM		0.94262	0.77282	1.68634	1.35503
T.Test			0.348	0.574	0.676
n		9	9	9	9

Similarly, results from bacteria strands and fungus are shown in Figure 32 a., b. and c. for *Escherichia coli, Candida albicans, and Saccharomyces cerevisiae* respectively. Five concentrations of Aβ were used using sequential dilution method, these concentrations were 3000 nM, 1500 nM, 750 nM, 375 nM and 187 nM. All results

were normalized to the control sample in which there was no added recombinant Aβ in the well.

a.

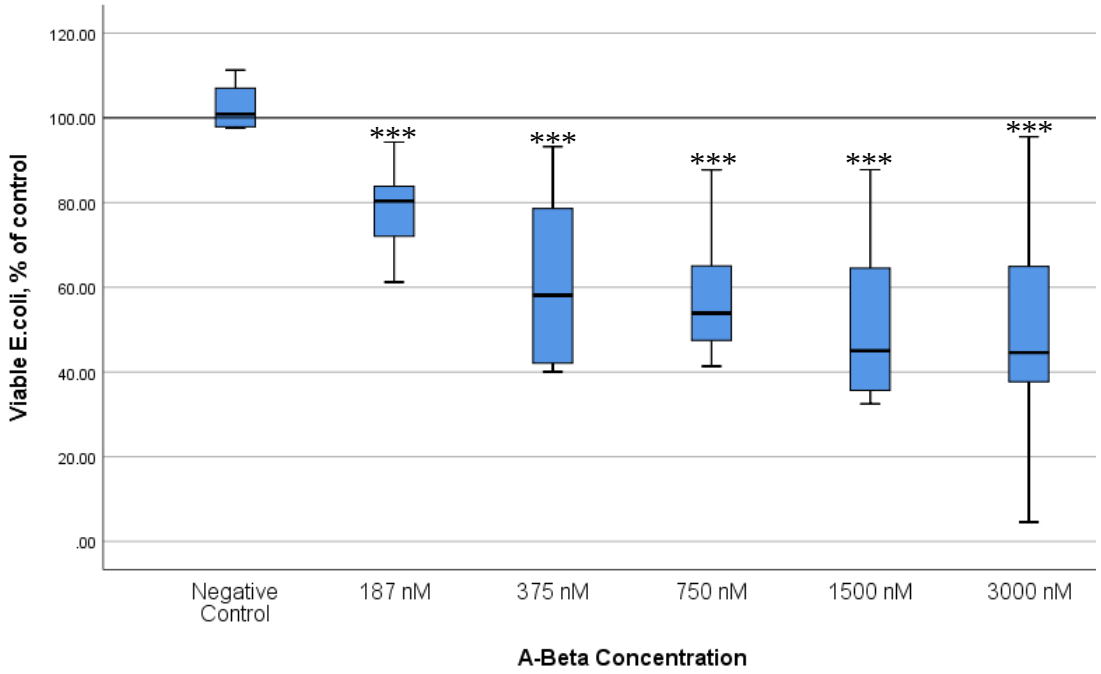

Aβ concentration,		0	187	375	750	1500	3000
Mean		102.9292	78.1608	61.5008	57.2950	51.4975	50.7442
95% CI for mean	Lower	95.4633	71.8063	49.5002	48.8441	38.8846	34.7015
	Upper	110.3951	84.5153	73.5015	65.7459	64.1104	66.7868
Std. deviation		6.01285	10.00125	18.88761	13.30083	19.85126	25.24928
SEM		2.68903	2.88711	5.45238	3.83962	5.730565	7.28884
p			0.000129	0.000007	0.000003	0.002*	0.000433
n		5	12	12	12	12	12

*) Mann-Whitney U test was used because the data were not normally distributed.

b.

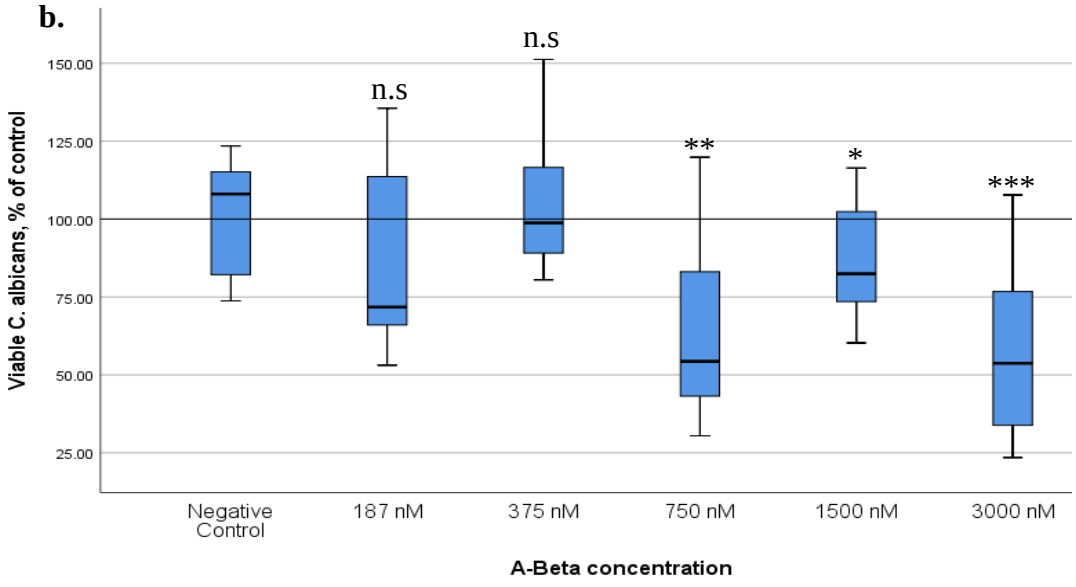

Aβ concentration,		0	187	375	750	1500	3000
Mean		99.7840	87.2408	104.1708	64.3667	86.3508	57.1833
95% CI for mean	Lower	86.5305	69.0147	91.4171	46.4137	75.1576	39.4122
	Upper	113.0375	105.4670	116.9245	82.3196	97.5440	74.9545
Std. deviation		18.52706	28.68589	20.07289	28.25588	17.61682	27.96983
SEM		5.85877	8.28090	5.79454	8.15677	5.08554	8.07419
p			0.248	0.603	0.003	0.097	0.001
n		10	12	12	12	12	12

c.

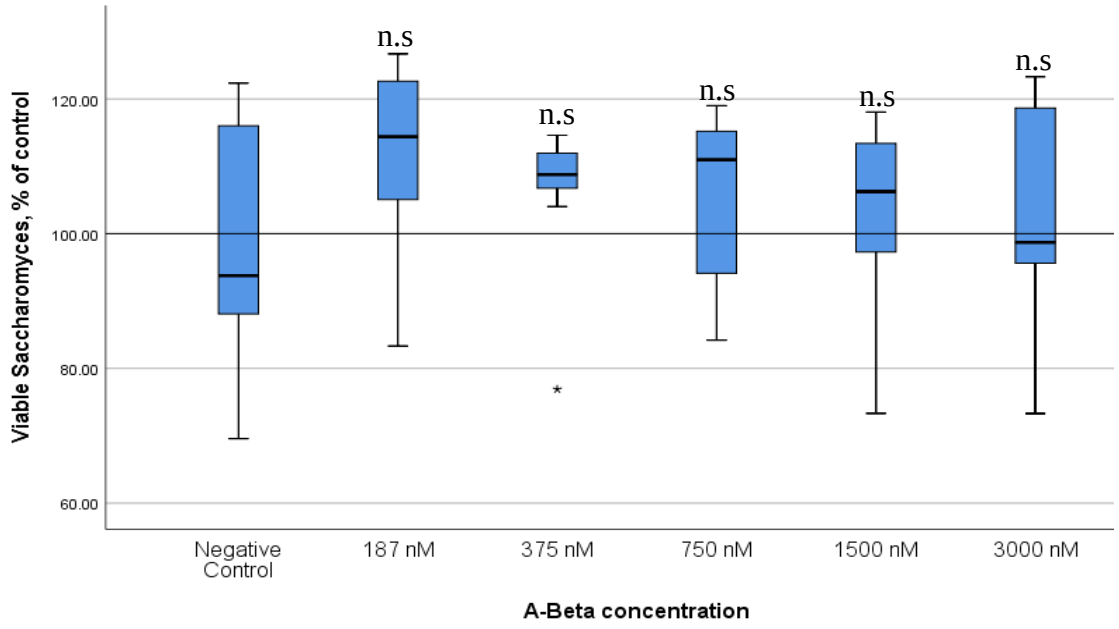

Aβ concentration,		0	187	375	750	1500	3000
Mean		99.9782	111.8676	106.1550	105.5400	103.9416	103.3108
95% CI of mean	Lower	87.4803	106.2109	98.4696	98.0413	98.3170	93.7119
	Upper	112.4760	117.5243	113.8404	105.9783	109.5662	112.9097
Std. deviation		18.60329	12.42705	10.74348	11.80218	12.68588	15.88450
SEM		5.60910	2.71181	3.397387	3.40700	2.704639	4.40557
P			0.076	0.944*	0.409	0.703*	0.640
N		11	21	10	12	22	13

*) Mann-Whitney U test was used because the data were not normally distributed.

Figure 32: Antimicrobial activity of Aβ against (**a)** *E. coli* at 0.5 x 10^6 cells per well, (**b**) *C. albicans* at 2.5 x 10^3 cells per well, and (**c**) *S. cerevisiae* at 0.5 x 10^6 cells per well. Five concentrations of Aβ (3000, 1500, 750, 375, and 187 nM) were incubated with these strands in addition to the negative and positive controls (mixture of 10,000 units penicillin, 10 mg streptomycin and 25 µg amphotericin). Three individual experiments for every concentration were investigated. Boxplots represent; minimum,

first quartile, median, third quartile, and maximum. Outliers represent 1.5 (circle) and 2 (star) times' interquartile range. Horizontal line represents mean of controls. Statistical significance was determined using Student's unpaired two-sided t-test (* $p \leq 0.05$, ** $p \leq 0.01$, *** $p \leq 0.001$, and n.s., not significant).

Results with *E. coli* indicated a dose-dependent effects on cell viability. While, it can be noted that the standard deviation is high in the results of *C. albicans*, this can be attributed to biological or technical variability. Finally, results with *S. cerevisiae* revealed no inhibition on cell growth except for a slight enhancement.

4.1.4 Nutrients as a therapeutic target against Aβ

In the previous sections, Aβ has been investigated to determine factors affecting its degradation and clearance from cells and hence prevent the early onset of AD. It has been examined as an AMP. In this section, *in vitro* studies have been considered which comprise the use of chemical compounds that can assist in preventing Aβ accumulation. Organic and inorganic substances have been used to study their impact on Aβ aggregation. CD spectrometry has been employed for this purpose where recombinant human Aβ40 has been monomerized (details in section 3.2.9) for further using as control or to incubate with a specific compound. Changes in Aβ's secondary structure have been used as an indicator of accumulation as previously described in section 3.2.12.2. Conformational switching from α-helix or random coil to a β-sheet is considered an indicator of peptide misfolding and aggregation (Serpell, 1999; Adessi and Soto, 2002; Funke and Willbold, 2012; Nie et al., 2011). The compound that maintains Aβ in a monomerized state or impairs β-sheet accumulation has been suggested as a therapeutic compound or supplement for curing AD. Spectra at 222 nm are an indication of the α-helical secondary structure, while spectra at 212 and 205 nm are an indication of β-sheet and random coils, respectively (Birthwhistle, 2012). Various groups of compounds representing humans' daily dietary intake has been selected in order to examine their impact on Aβ accumulation as shown in the next sub-sections.

4.1.4.1 Impact of Vitamin C and Vitamin E

Ascorbic acid (CAS no. 50-81-7; molecular weight 176.12 g/mol; Figure 33 a.) and α-tocotrienol ($C_{29}H_{44}O_2$, Cas no. 58864-81-6, molecular weight 424.66 g/mol; Figure 33

b.) was incubated with 10 µM of Aβ for 24 h, and changes in the secondary structure are shown in Figure 34 a and b, respectively.

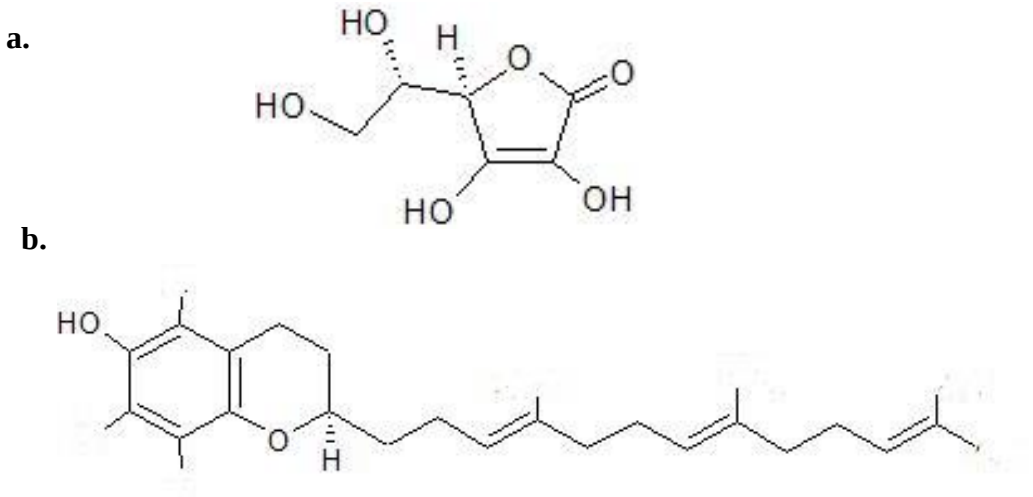

Figure 33: Chemical structure of (a.) L-ascorbic acid and (b.) α-tocotrienol.

Every CD signal data set was analyzed and presented in two panels in the same figure; the first panel (upper panel) represents CD signals distributed along the far UV range (190–260 nM), and the second panel (lower panel) shows the peptide's predicted state at these wavelengths. The peptide in its native state is folded and unfolded when conformational changes, including stacking or accumulation of β-sheets, occur. Generaly, higher doses of ascorbic acid or α-tocotrienol has reduced the accumulation of β-sheets.

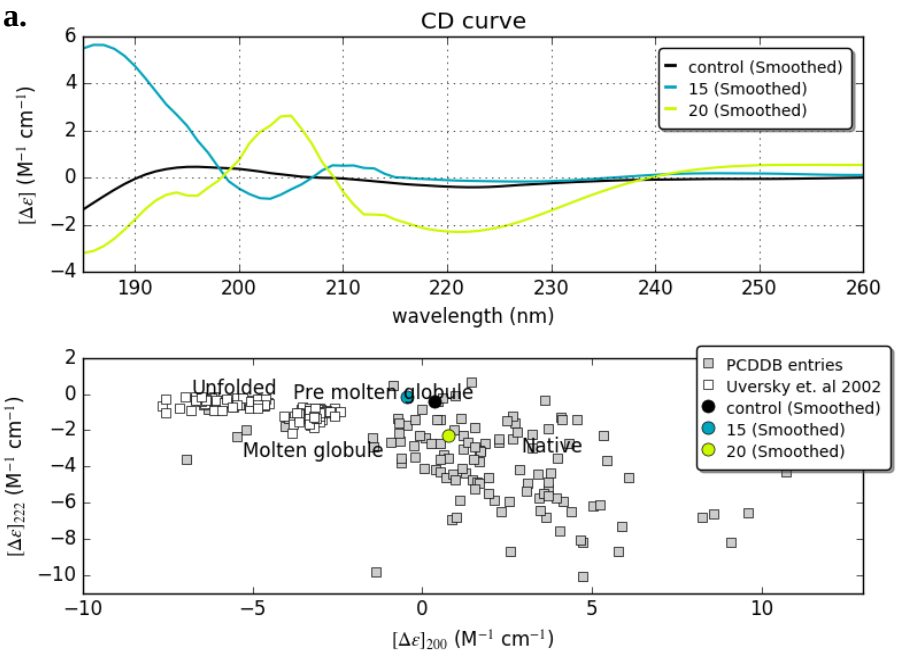

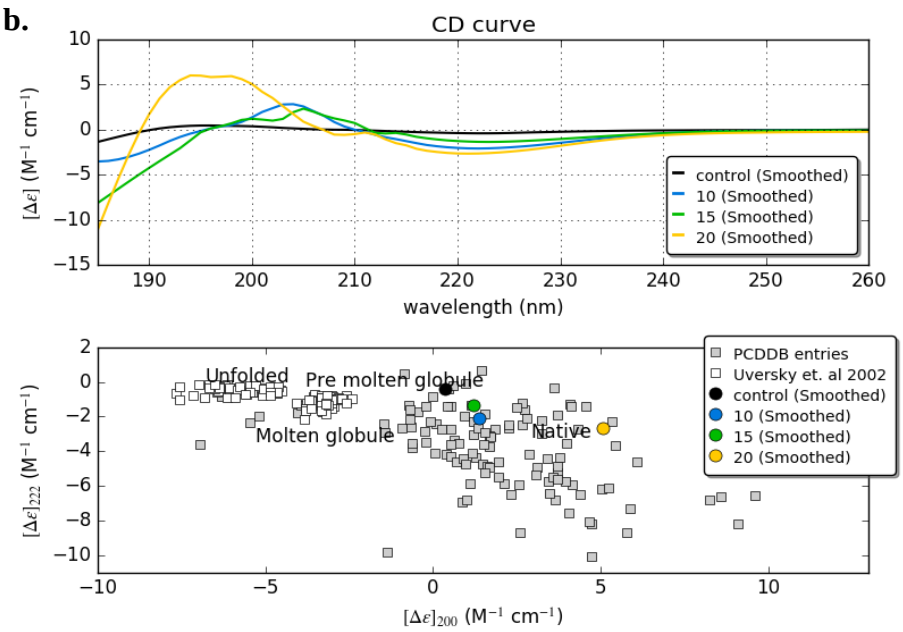

Figure 34: Changes in Aβ's secondary structure resulting from the effects of (**a**) L-Ascorbic acid and (**b**) $C_{29}H_{44}O_2$ (both at 15 and 20 µM as shown above) CD spectrum and (lower panel) prediction of peptide state. Spectra at 222 or 208 nm indicate α-helix, while spectra at 212 nm indicate β-sheet, and at 205 nm indicates a random coil.

4.1.4.2 Effects of tellurite compounds

Potassium tellurate hydrate ($K_2TeO_4.H_2O$, Cas No. 314041-10-6, molecular weight, 269.79 g/mol) and sodium tellurite (Na_2TeO_3, Cas no. 10102-20-2, molecular weight 221.577 g/mol) were used in the study of Aβ accumulation. CD signals are shown in Figure 35 a and b, respectively.

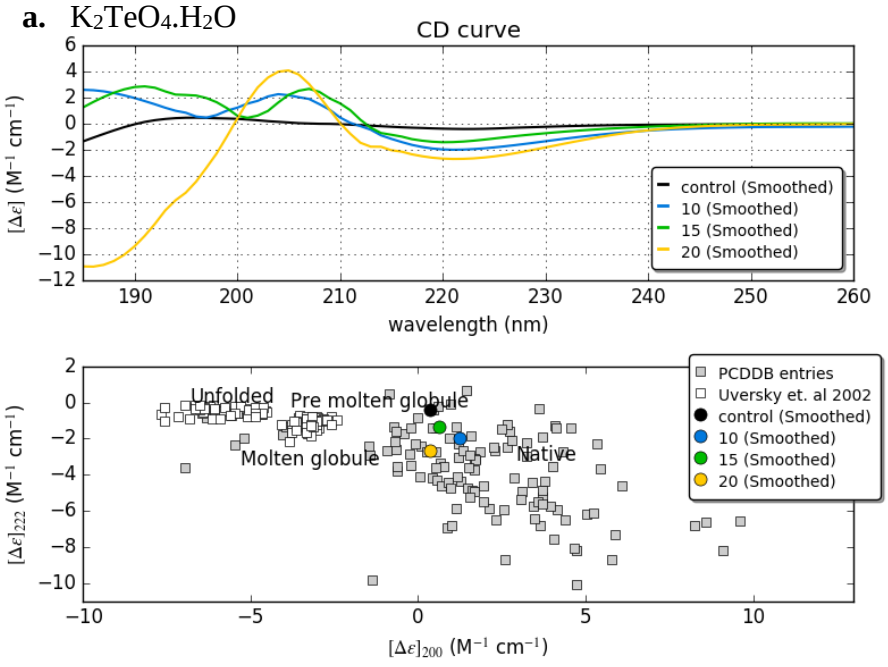

b. Na_2TeO_3

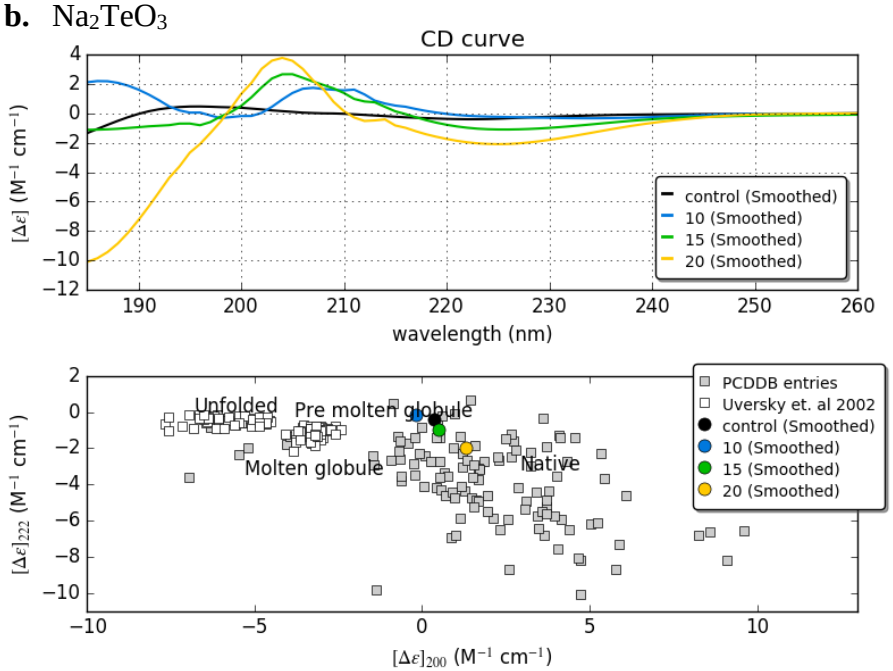

Figure 35: Effects of (**a**) $K_2TeO_4.H_2O$ and (**b**) Na_2TeO_3, on Aβ aggregation. Ten micromolar of Aβ was incubated with each compound at concentrations of 10, 15, and 20 µM. Control represents Aβ alone.

Higher concentrations of potassium tellurate hydrate and sodium tellurite have reduced the accumulation of Aβ.

4.1.4.3 Effect of chloride compounds

A series of selected chloride compounds were used in the experiments, in which these compounds' characteristics are presented in Table 29.

Table 29: Properties of chloride compounds.

Compound name	Molecular formula	CAS no.	Molecular weight, g/mol
Lithium Chloride	LiCl	7447-41-8	42.39
Rubidium Chloride	RbCl	7791-11-9	120.918
Sodium Chloride	NaCl	7647-14-5	58.44
Cupric Chloride	$CuCl_2$	7447-39-4	134.446
Zinc Chloride	$ZnCl_2$	766-85-7	136.28

The results show an enhancement in α-helix at the lower concentration (5 µM) of each compound as shown in Figure 36 a–e, while an increase in chloride concentration (>5 µM) resulted in a negligible impact on the peptide's secondary structure.

a. LiCl

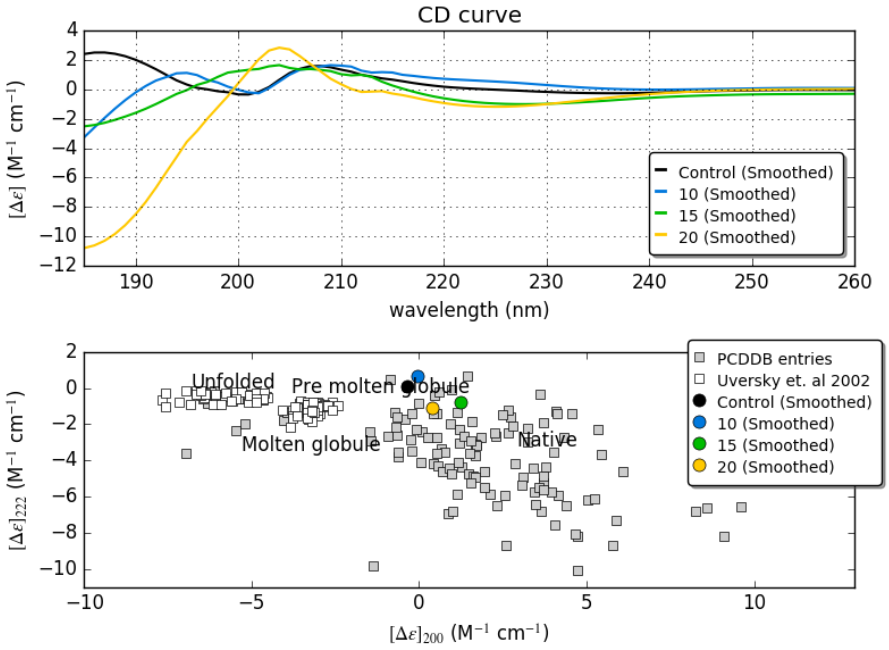

b. RbCl

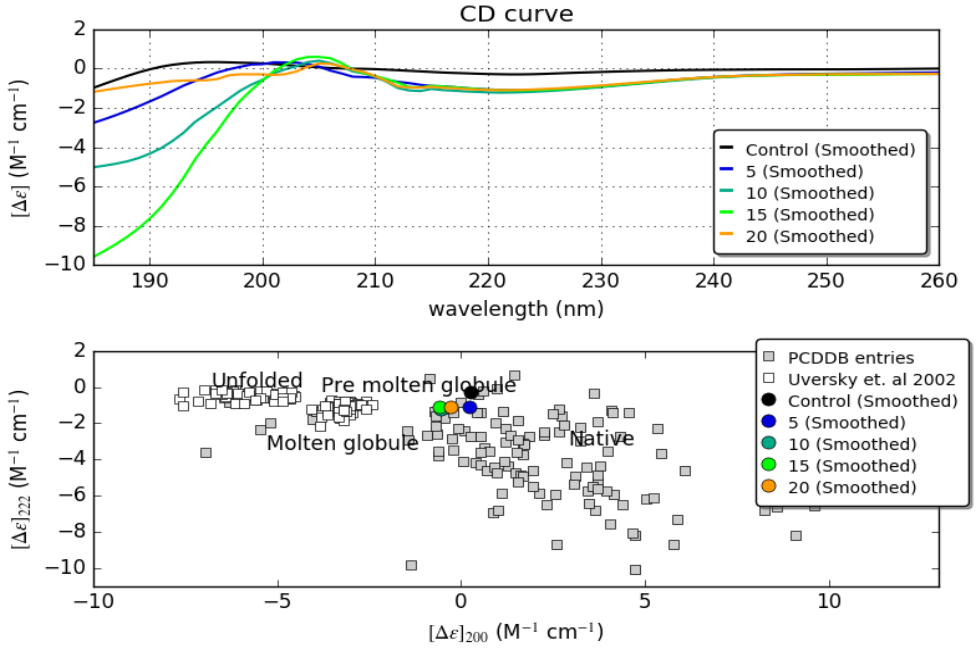

c. NaCl

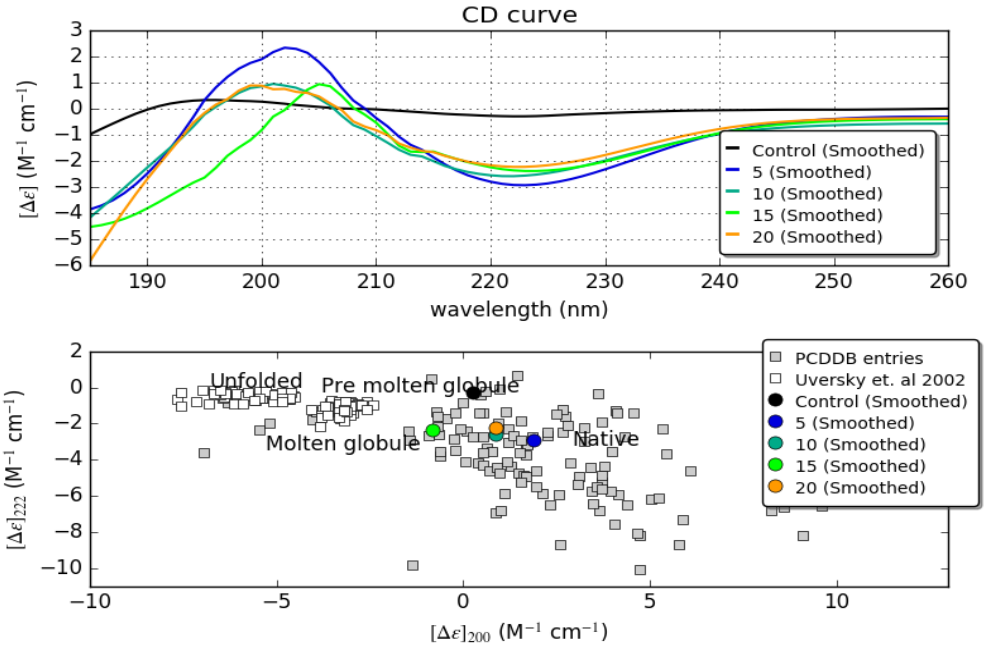

d. $CuCl_2$

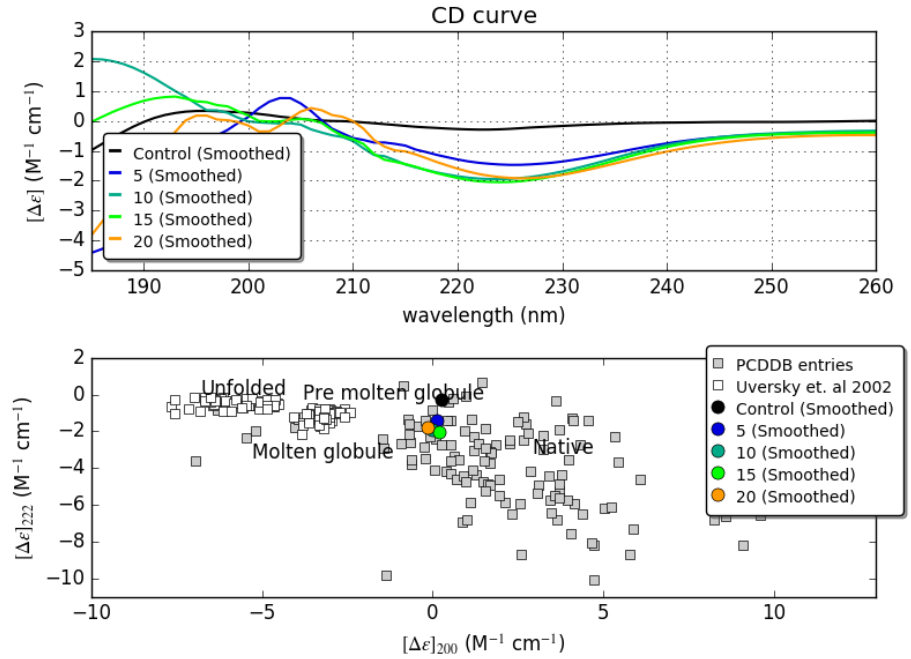

e. $ZnCl_2$

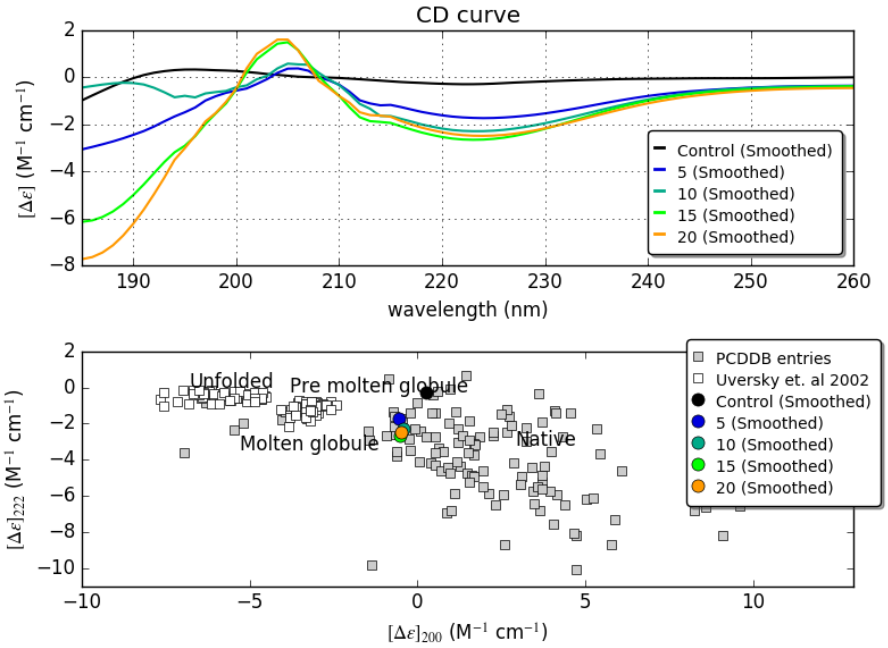

Figure 36: Effects of (**a**) LiCl, (**b**) RbCl, (**c**) NaCl, (**d**) $CuCl_2$, and (**e**) $ZnCl_2$ on Aβ aggregation. Ten micromolar Aβ was incubated with each compound used at concentrations of 5, 10, 15, and 20 µM. Control represents Aβ alone.

Results showed that the accumulation of Aβ is reduced at low concentrations excep for lithium and rubidium chlorides.

4.1.4.4 Effects of sulfur compounds

Sodium sulfide (Na_2S, CAS no. 1313-82-2, Molecular weight 79.048 g/mol), sodium sulfite (Na_2SO_3, CAS no. 7757-83-7, Molecular weight 126.037 g/mol), and sodium sulfate (Na_2SO_4, CAS no. 7757-82-6, molecular weight 142.036 g/mol) were introduced to the study of Aβ aggregation. Different effects caused by each one of these chemicals were noticed when added at different concentrations to Aβ as shown in Figure 37 a.-c.

a. Na_2S

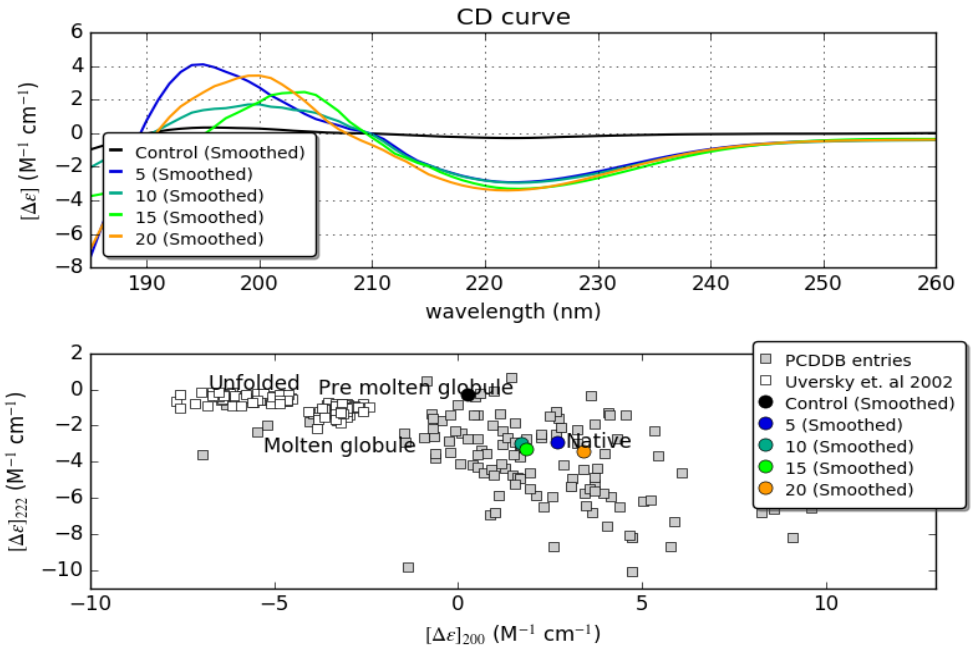

b. Na_2SO_3

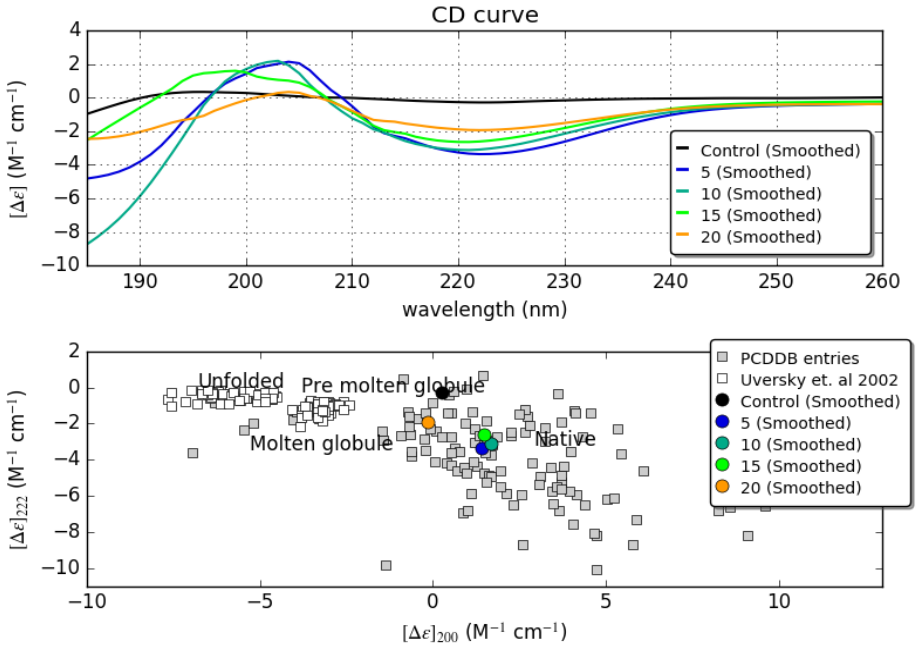

c. Na_2SO_4

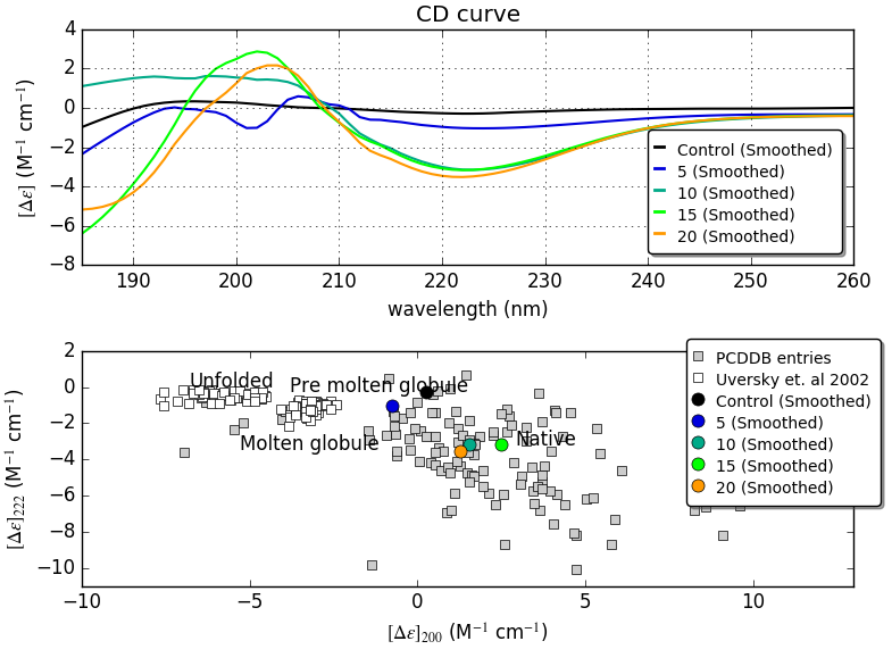

Figure 37: Effects of (**a**) Na_2S, (**b**) Na_2SO_3, and (**c**) Na_2SO_4, on Aβ aggregation. Ten micromolar Aβ was incubated with each compound that were used at concentrations of 5, 10, 15, and 20 µM. Control represents Aβ alone.

Accumulation of Aβ has been reduced at low concentrations of sulfur compounds.

4.1.4.5 Selenium compounds

Sodium selenite (Na_2SeO_3, CAS no. 10102-18-8, molecular weight 172.94 g/mol) and sodium selenate (Na_2SeO_4, CAS no. 10102-23-5, molecular weight 188.95 g/mol) effects are shown in Figure 38 a and b, respectively.

a. Na_2SeO_3

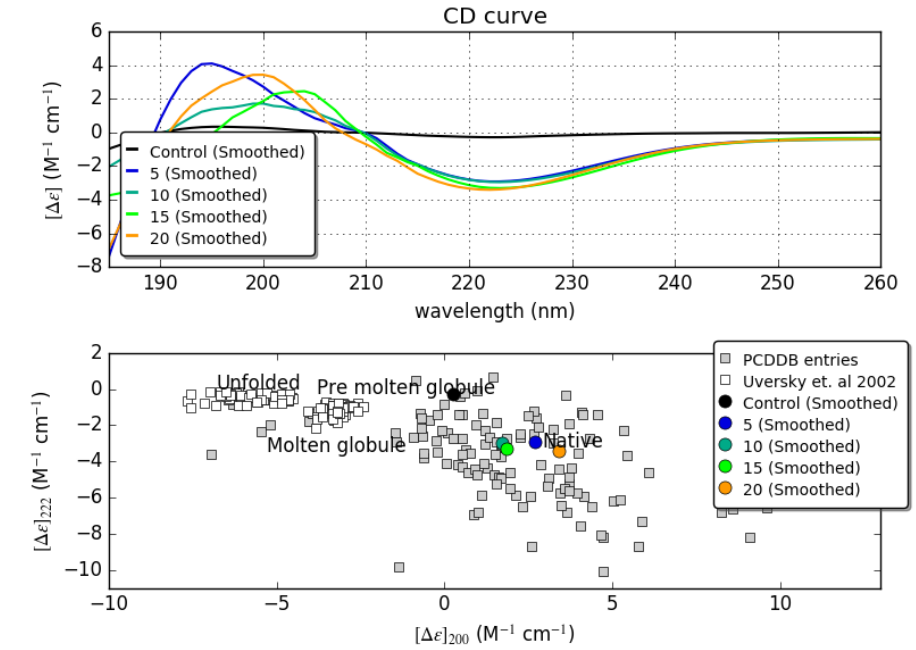

b. Na_2SeO_4

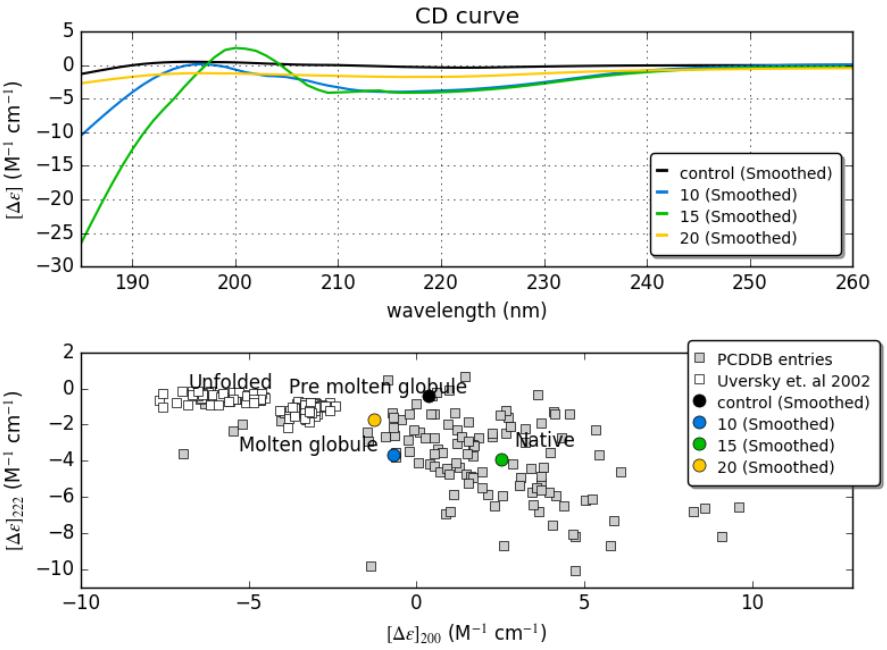

Figure 38: Effects of (**a**) Na_2SeO_3 and (**b**) Na_2SeO_4 on Aβ aggregation. Ten micromolar Aβ was incubated with each compound that were used at concentrations of 5, 10, 15, and 20 µM. Control represents Aβ alone.

Selenium compounds reduced the aggregation of Aβ at low concentrations.

4.1.4.6 Effects of organic compounds

Organic acids have also been used to measure their effects on the characteristics of Aβ's secondary structure. Figure 39 displays chemical structure of the selected compounds, and Table 30 lists these compounds' properties.

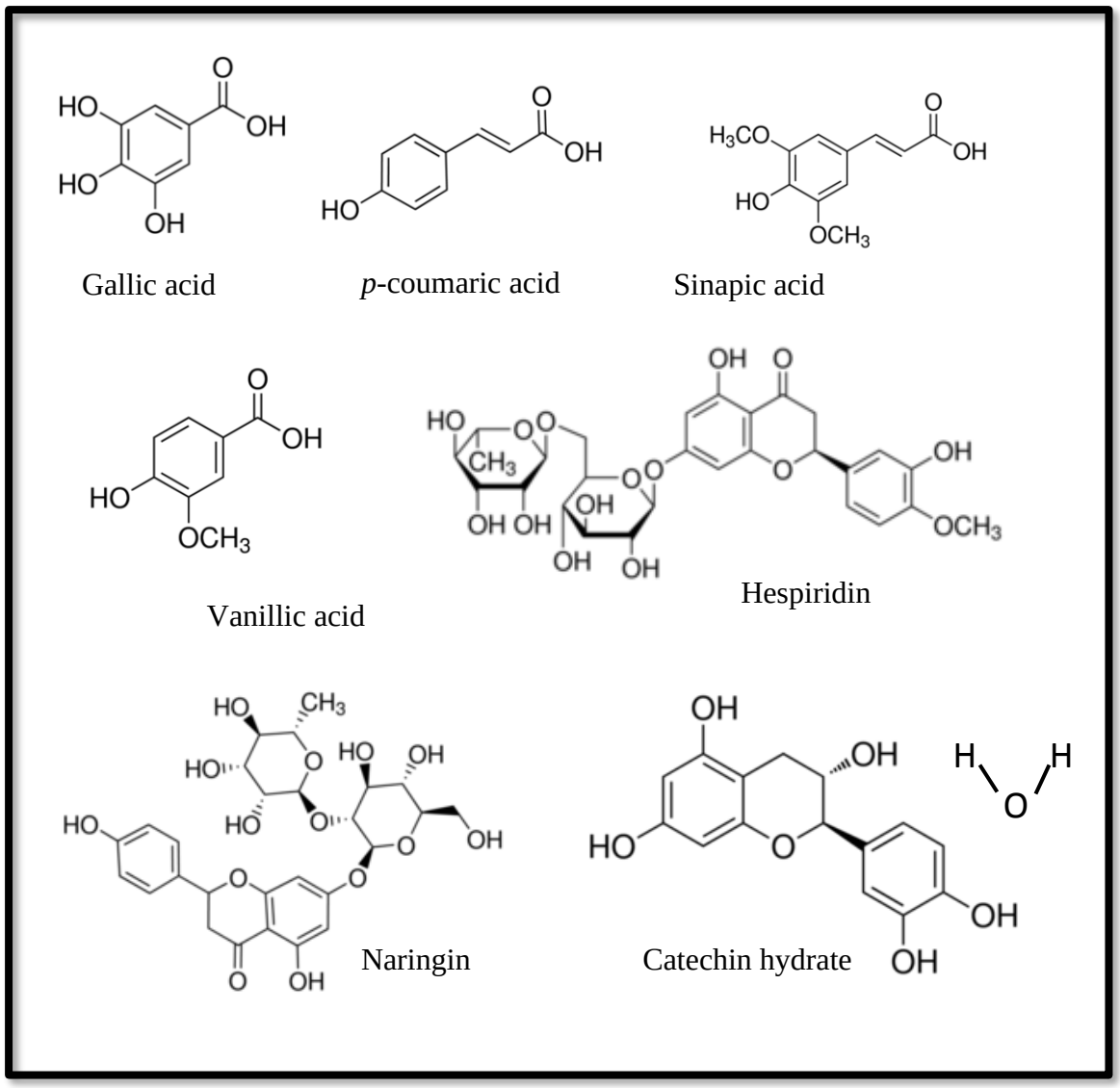

Figure 39: Chemical structure of organic acids.

Table 30: Properties of organic acids.

Compound name	Chemical name	CAS no.	Molecular formula	Molecular weight, g/mol
Gallic acid	3.4.5-Trihydroxybenzoic acid	149-91-7	$C_7H_6O_5$	170.12
***p*-coumaric acid**	4-Hydroxycinnamic acid	501-98-4	$C_9H_8O_3$	164.16
Sinapic acid	3,5-Dimethoxy-4-hydroxycinnamic acid	530-59-6	$C_{11}H_{12}O_5$	224.212
Vanilic acid	4-Hydroxy-3-methoxybenzoic acid	121-34-6	$C_8H_8O_4$	168.148
Hesperidin	Hesperidin	520-26-3	$C_{28}H_{34}O_{15}$	610.565
Naringin	Naringin	10236-47-2	$C_{27}H_{32}O_{14}$	580.539
(+)-Catechin hydrate	Catechuic acid	225937-10-0	$C_{15}H_{14}O_6.H_2O$	290.27

Figure 40 a–g shows CD signals at different concentration of each of the compounds used in the study.

a. Gallic acid

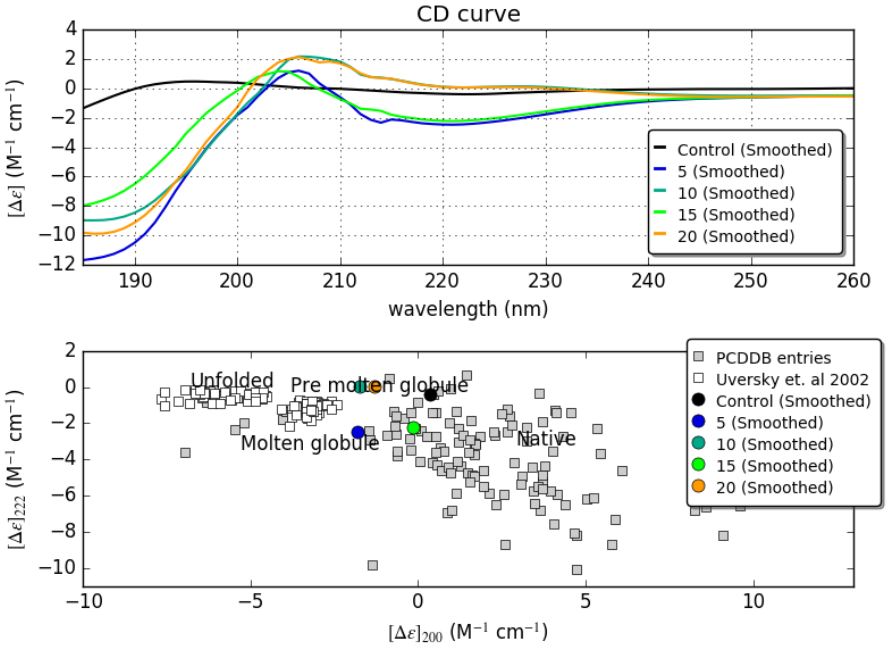

b. *p*-Coumaric acid

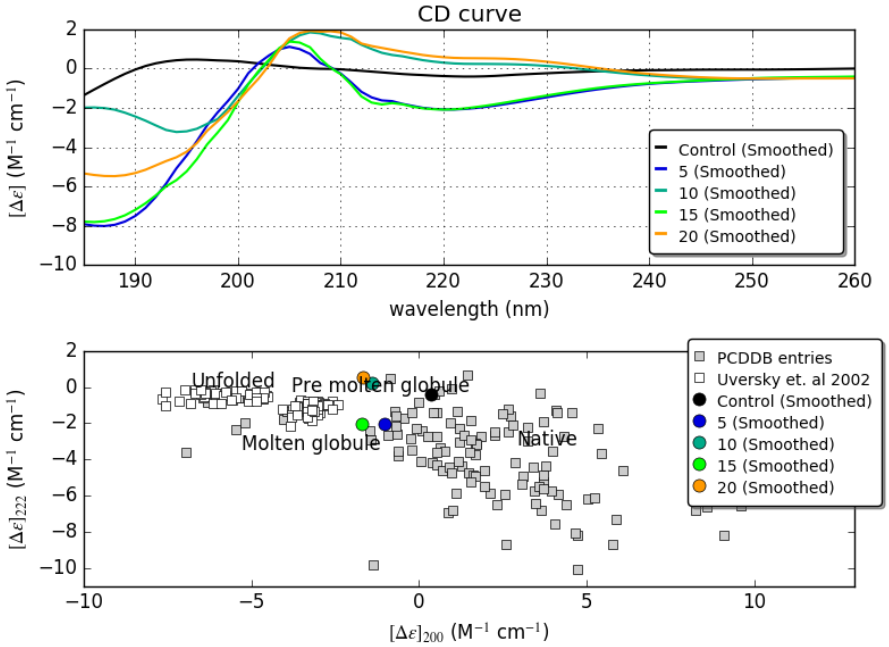

c. Sinapinic acid

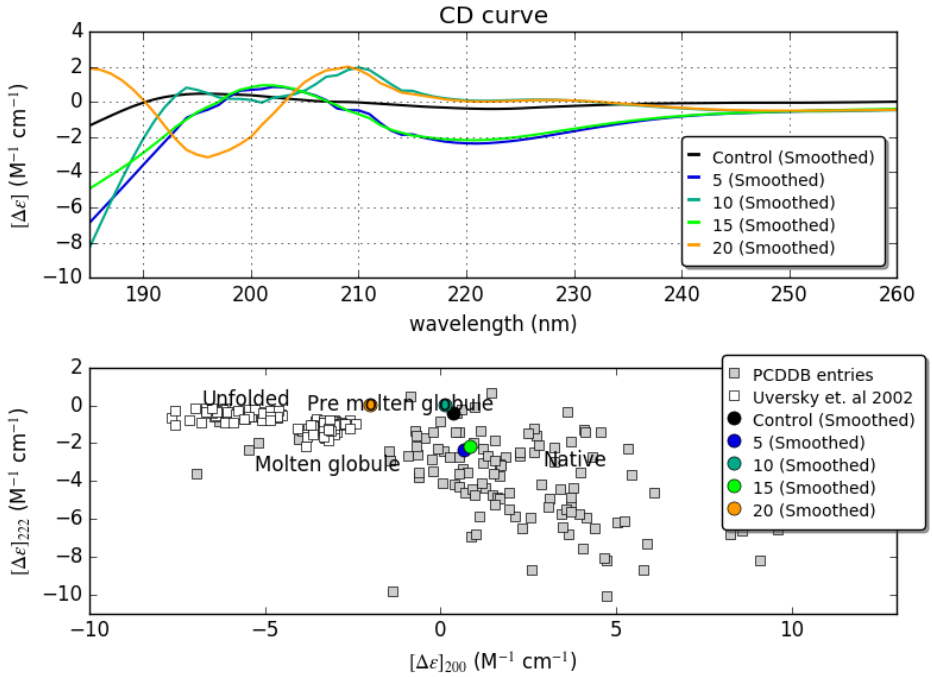

d. Vanillic acid

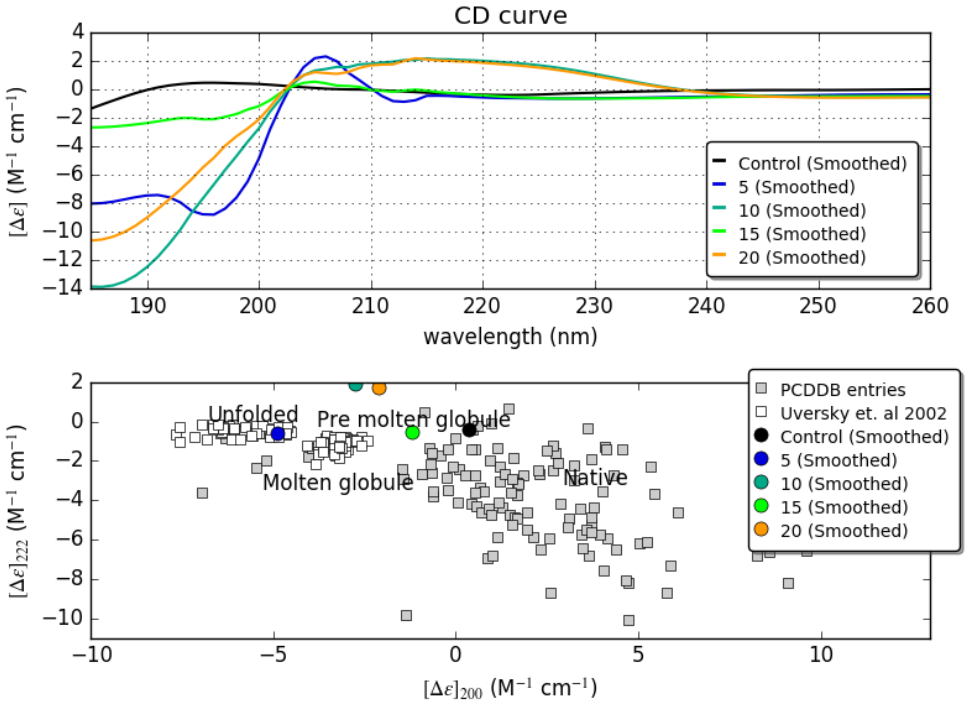

e. Hesperidin

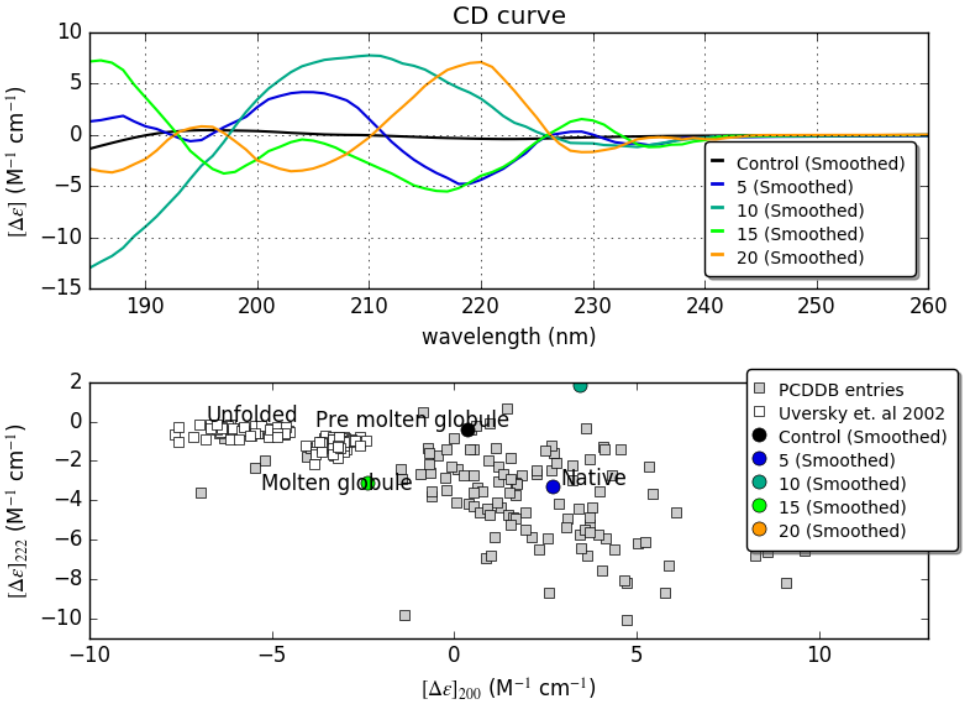

f. Naringin

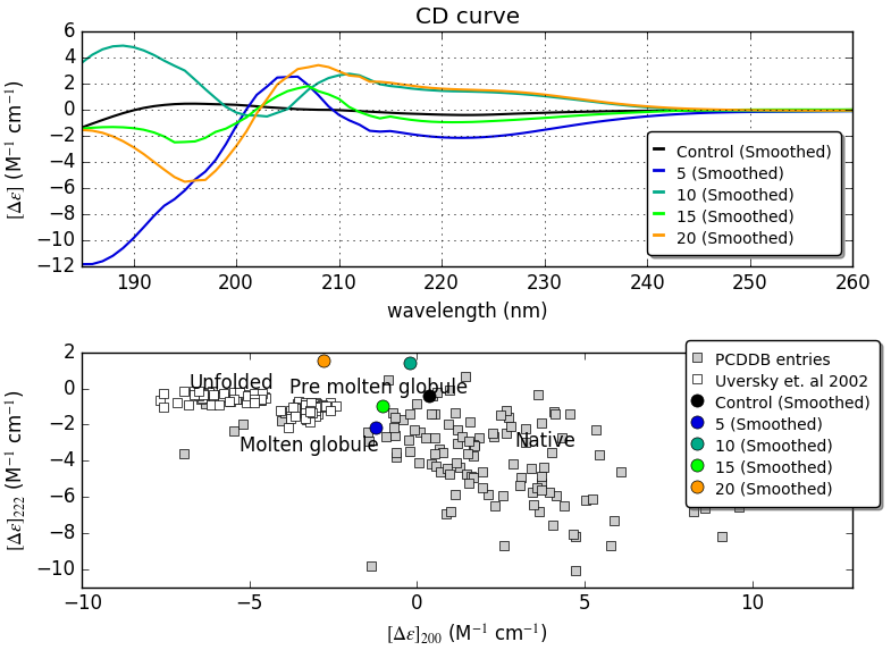

g. Catechin

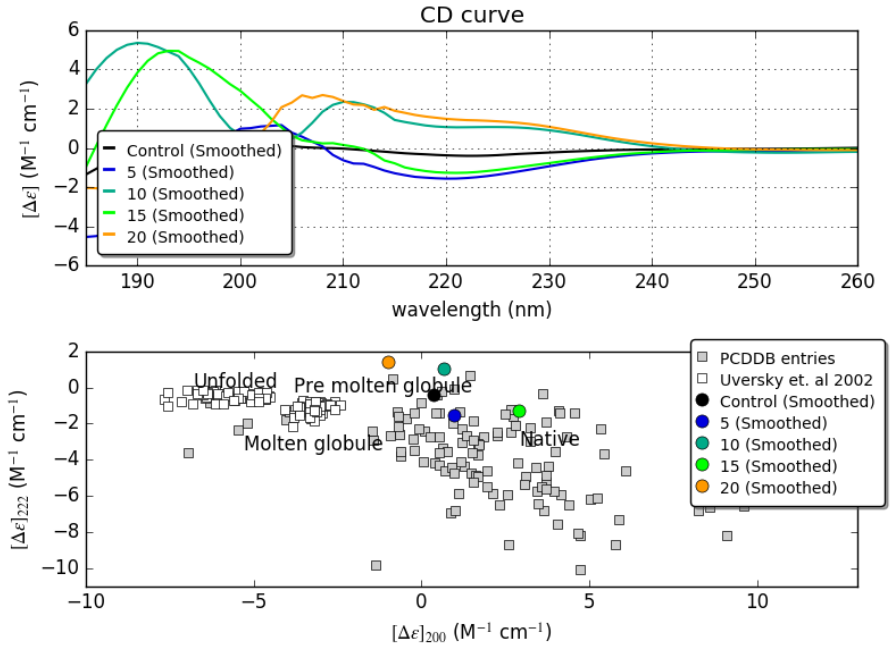

Figure 40: Effects of (**a**) gallic acid (**b**) *p*-coumaric acid, (**c**) sinapinic acid, (**d**) vanillic acid (**e**) hespiridin, (**f**) naringin and (**g.**) catechin on Aβ's aggregation. Ten micromolar Aβ was incubated with each compound that were used at concentrations of 5, 10, 15, and 20 µM. Control represents Aβ alone.

Aggregation of Aβ is achieved at only low concentrations, but not for vanilic acid and naringin, of these phytochemicals

4.1.4.7 Flavones and selenoflavones

Several flavones have been chosen and evaluated to study their impact on the secondary structure elements of Aβ (Figure 41)

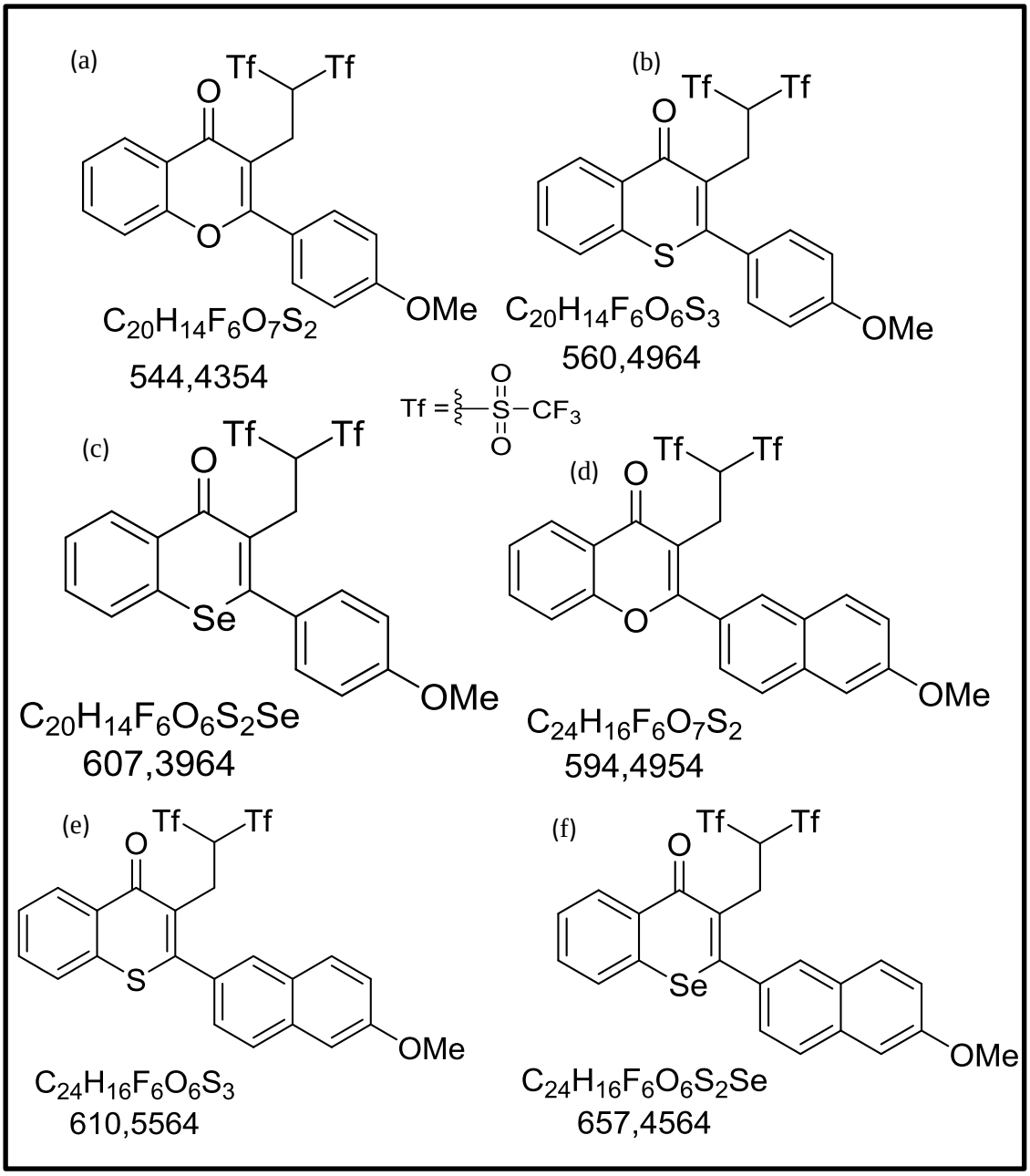

Figure 41: Chemical structure and molecular weight of the employed flavones in this study.

Analysis by circular dichroism spectrometry for these compounds in combination with Aβ at different concentrations showed limited effects on Aβ's secondary structural elements (α-helix, β-sheet, and random coil; Figure 42 a–f). Despite the role of flavonoids in protecting the brain from Aβ's toxicity, results showed that all flavonoids used in the analysis at all concentrations (5, 10, 15, and 20 µM) exhibited the same effects by preventing progressive Aβ accumulation rather than via changing secondary Aβ structural elements.

a.

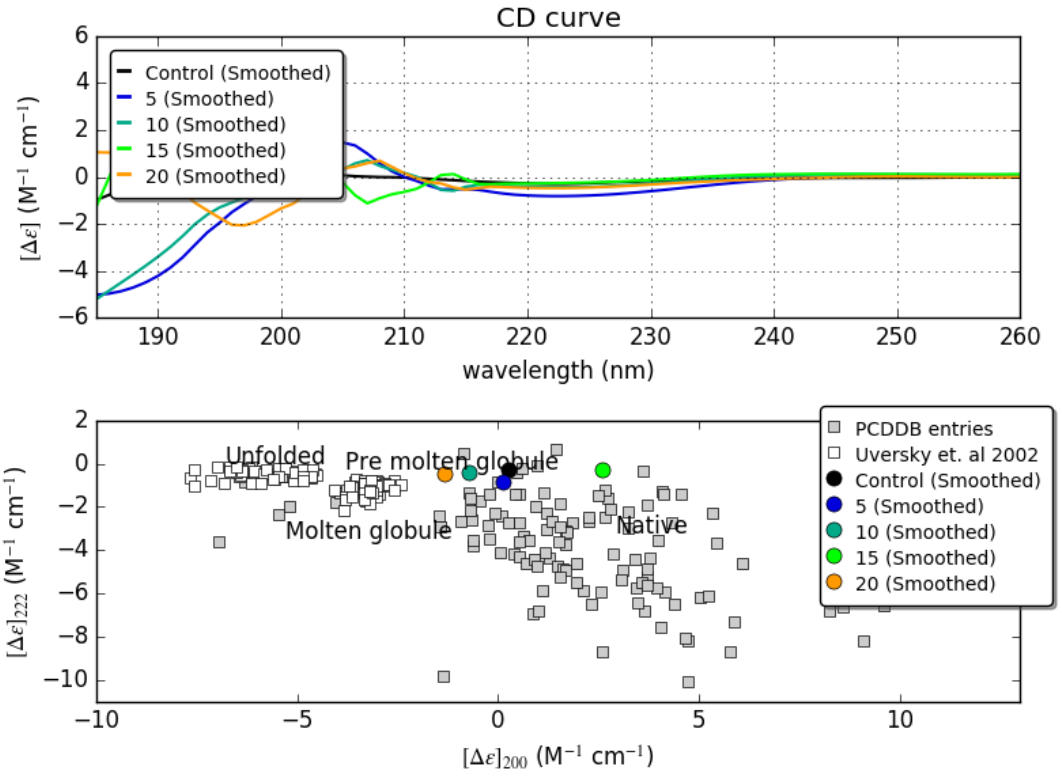

b.

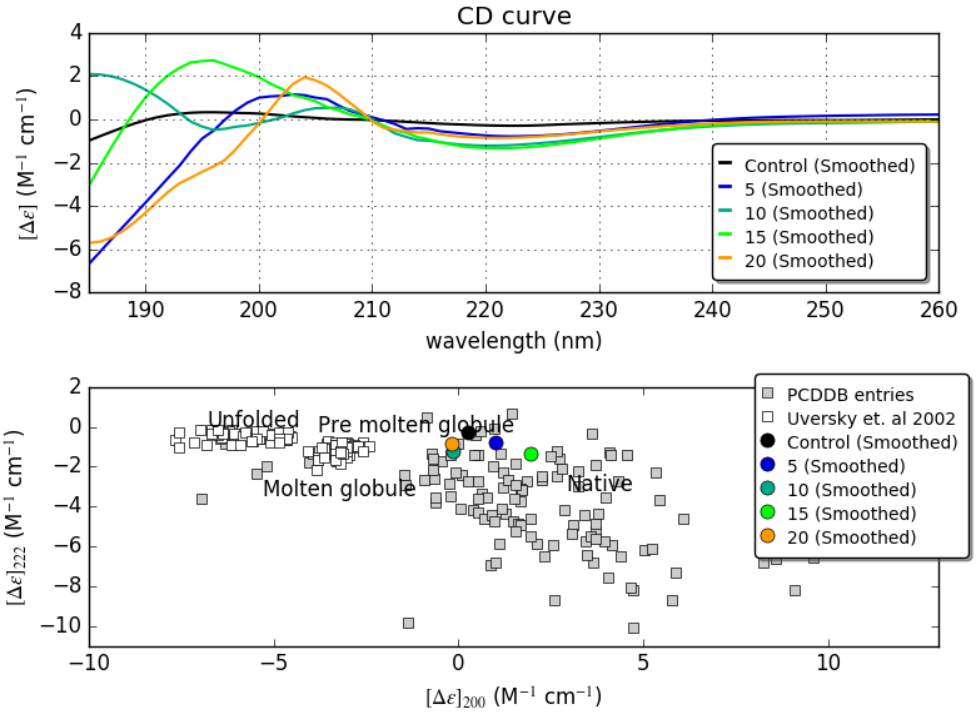
CD curve
[Δε] (M⁻¹ cm⁻¹)
wavelength (nm)
Control (Smoothed)
5 (Smoothed)
10 (Smoothed)
15 (Smoothed)
20 (Smoothed)
[Δε]222 (M⁻¹ cm⁻¹)
[Δε]200 (M⁻¹ cm⁻¹)
Unfolded
Pre molten globule
Molten globule
Native
PCDDB entries
Uversky et. al 2002

c.

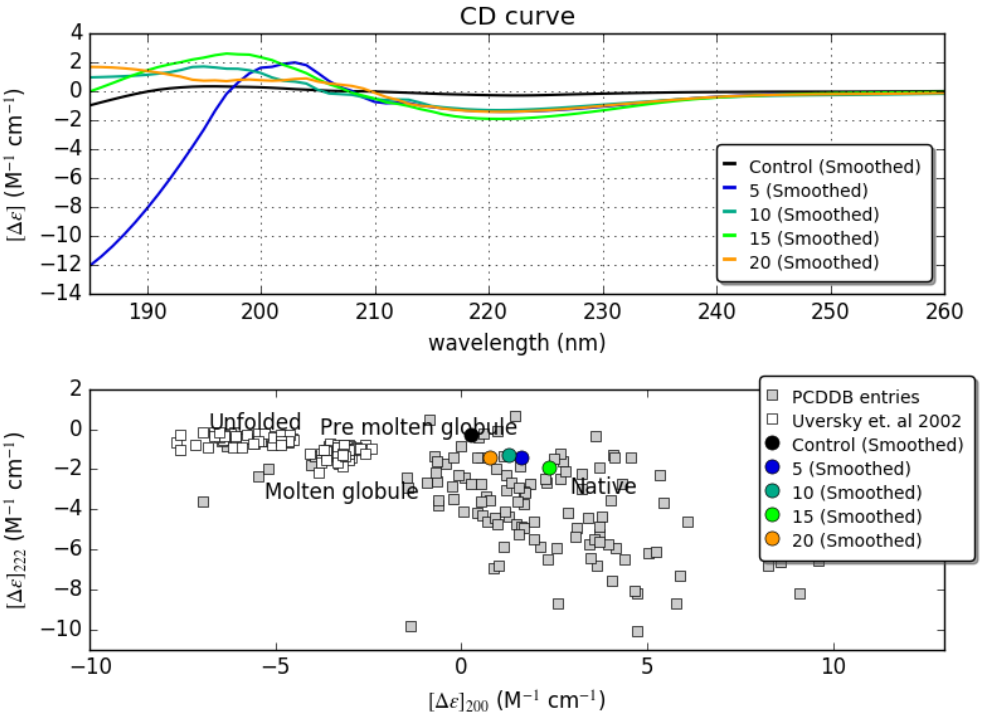
CD curve
[Δε] (M⁻¹ cm⁻¹)
wavelength (nm)
Control (Smoothed)
5 (Smoothed)
10 (Smoothed)
15 (Smoothed)
20 (Smoothed)
[Δε]222 (M⁻¹ cm⁻¹)
[Δε]200 (M⁻¹ cm⁻¹)
Unfolded
Pre molten globule
Molten globule
Native
PCDDB entries
Uversky et. al 2002

d.

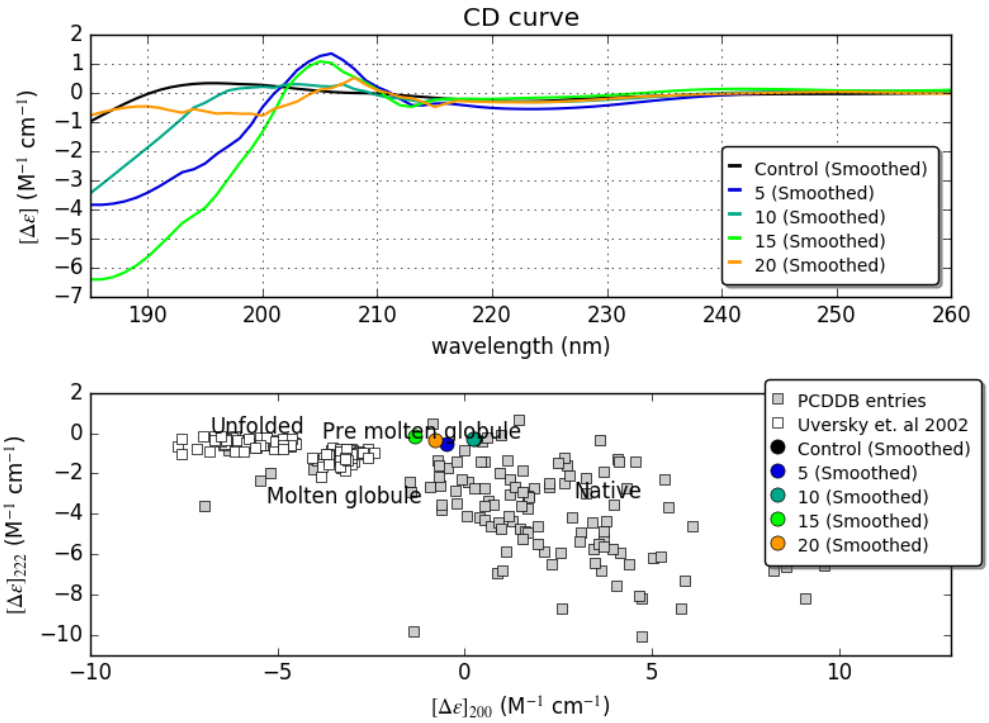
CD curve
[Δε] (M⁻¹ cm⁻¹)
wavelength (nm)
Control (Smoothed)
5 (Smoothed)
10 (Smoothed)
15 (Smoothed)
20 (Smoothed)
[Δε]222 (M⁻¹ cm⁻¹)
[Δε]200 (M⁻¹ cm⁻¹)
Unfolded
Pre molten globule
Molten globule
Native
PCDDB entries
Uversky et. al 2002

e.

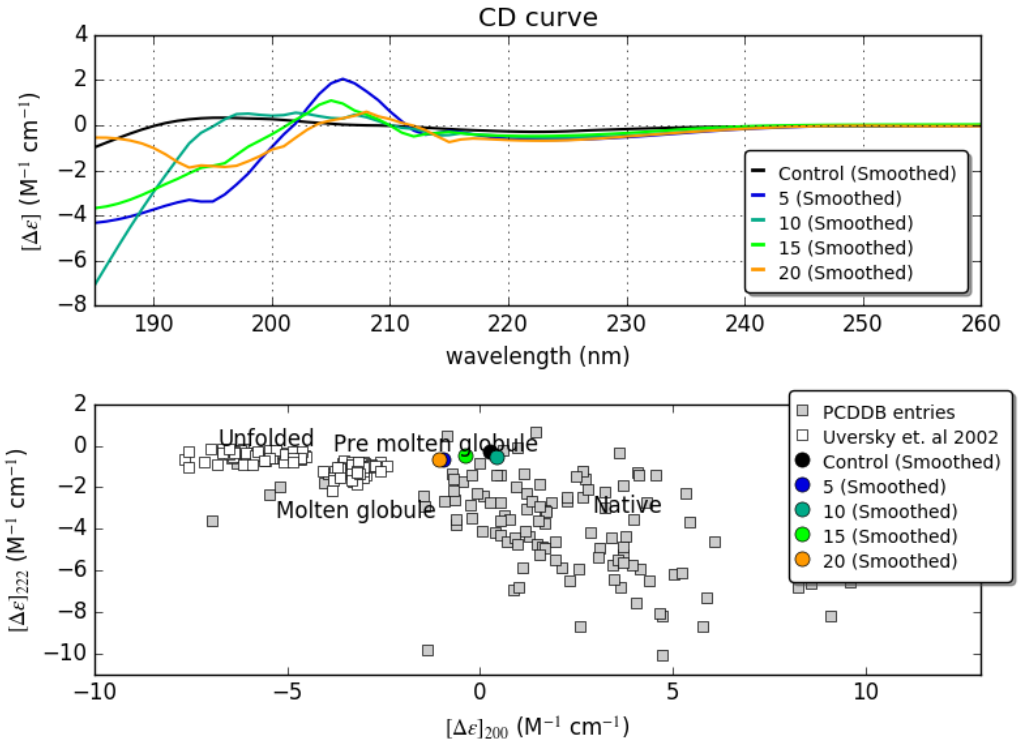
CD curve
[Δε] (M⁻¹ cm⁻¹)
wavelength (nm)
Control (Smoothed)
5 (Smoothed)
10 (Smoothed)
15 (Smoothed)
20 (Smoothed)
[Δε]222 (M⁻¹ cm⁻¹)
[Δε]200 (M⁻¹ cm⁻¹)
Unfolded
Pre molten globule
Molten globule
Native
PCDDB entries
Uversky et. al 2002

f.

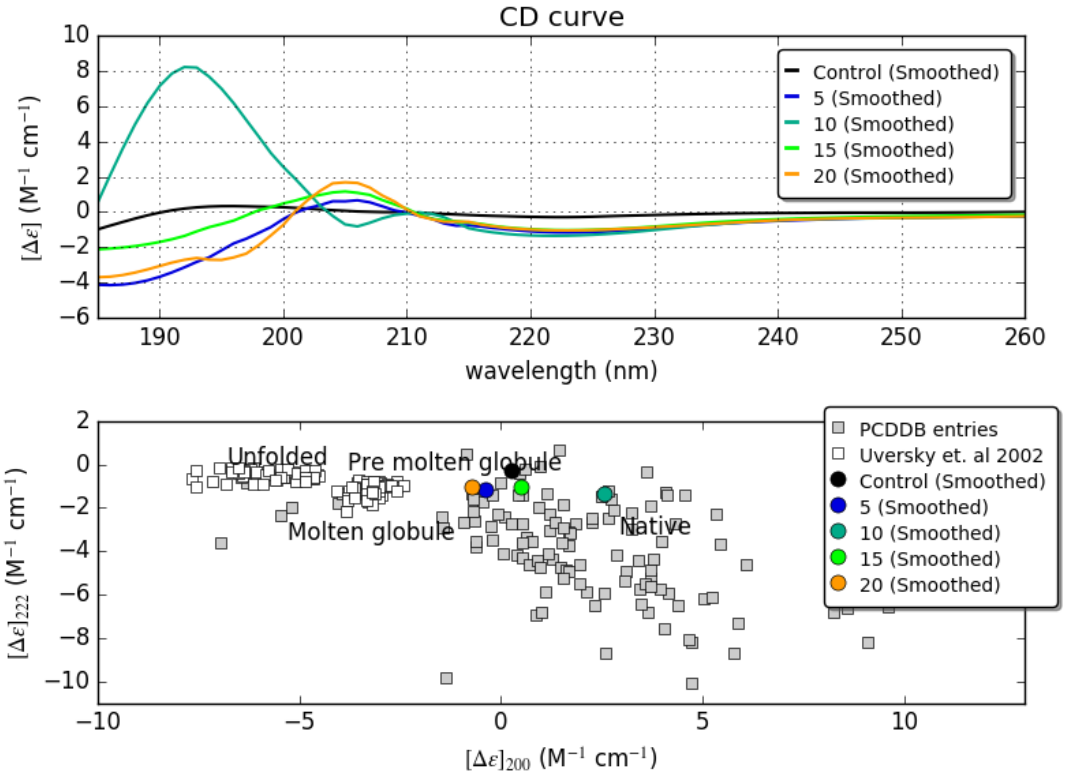

Figure 42: Effects of flavones and selenoflavones on Aβ aggregation. Ten micromolar Aβ was incubated with each compound that were used at concentrations of 5, 10, 15, and 20 µM. Control represents Aβ alone.

Negligible or no effect was detected for the flavones used in the study.

4.1.4.8 Effects of organic and inorganic compounds on AICD

Intracellular AICD accumulation was described as a regulator of γ-secretase transcription, hence increasing the production of Aβ by APP cleavage. Therefore, the effects of chemicals and phytochemicals were investigated for the first time in the current study by using the CD technique. Results are shown in Figure 43 a–j.

a. $C_{29}H_{44}O_2$

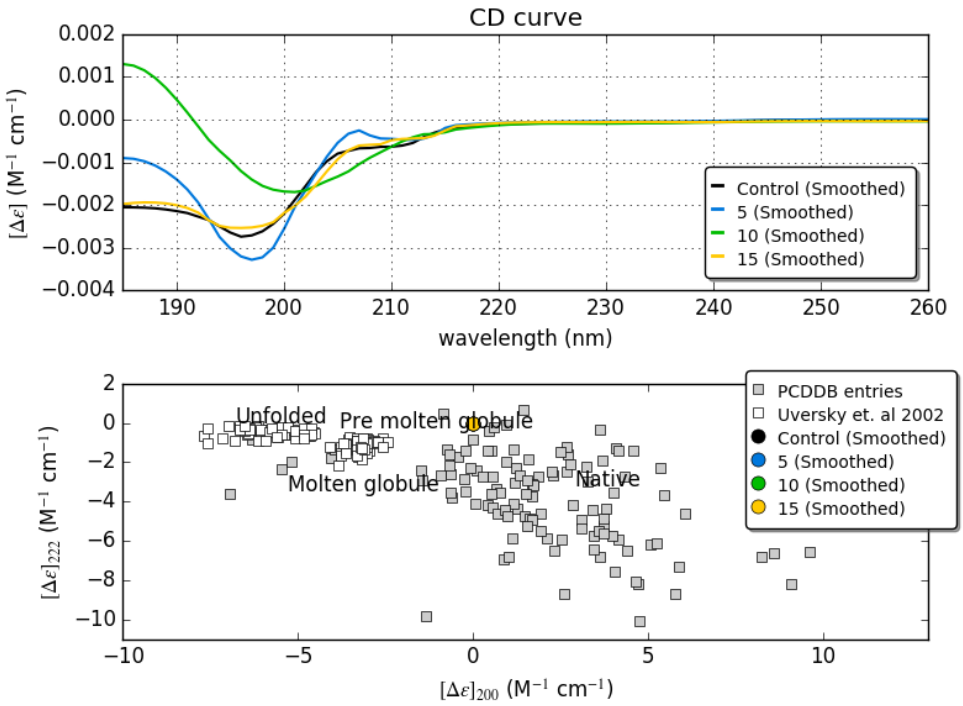

b. NaCl

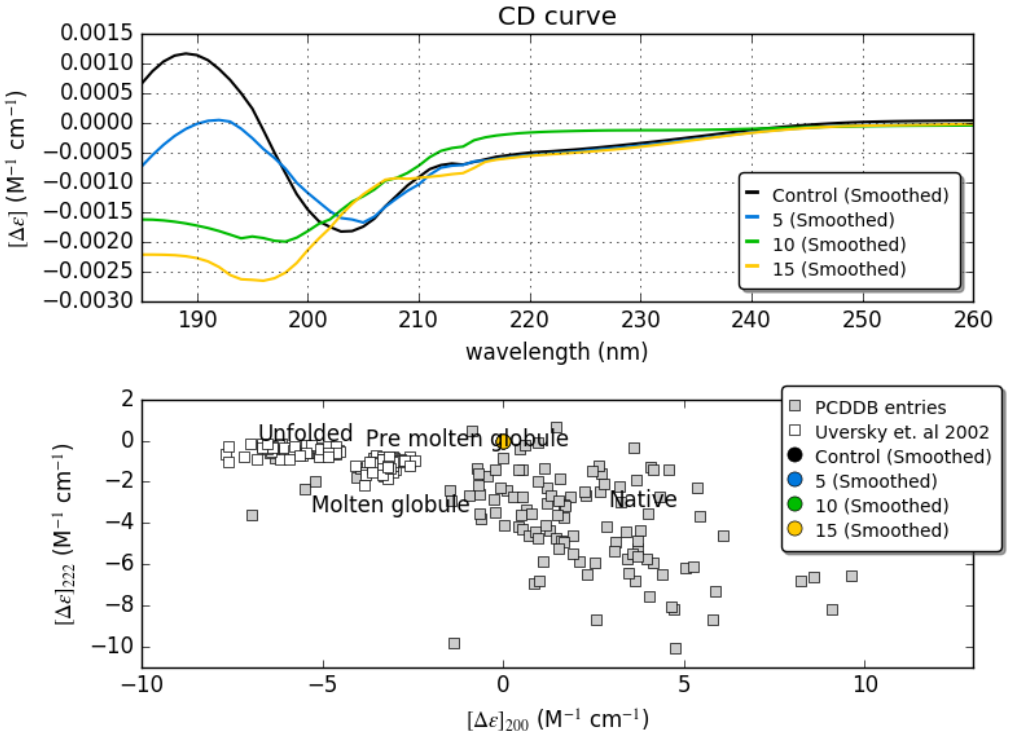

c. RbCl

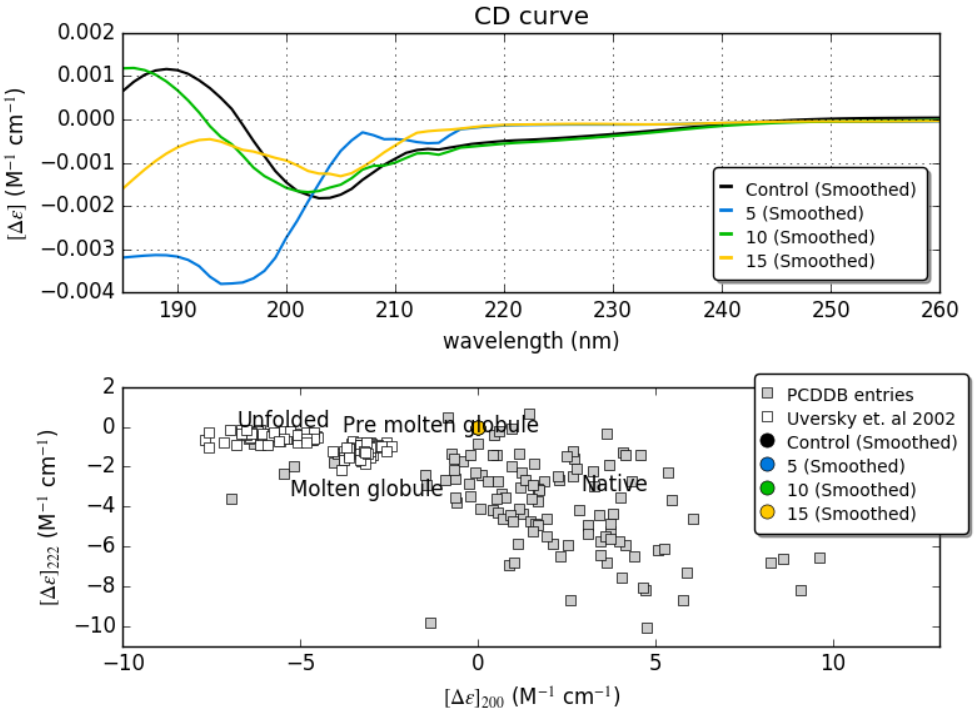

d. $CuCl_2$

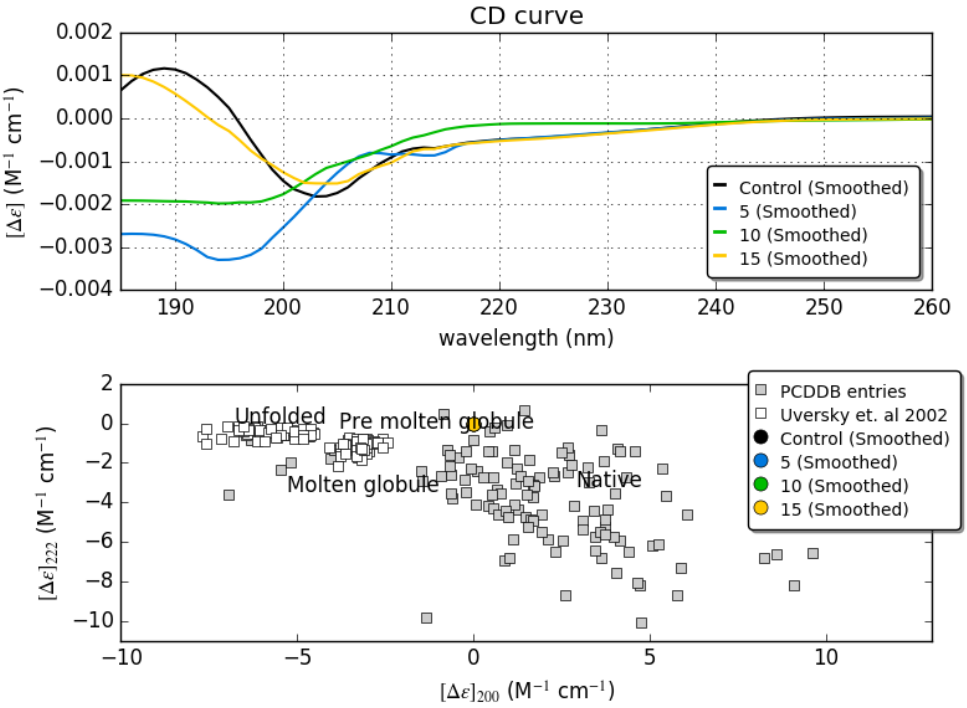

e. Na_2SO_3

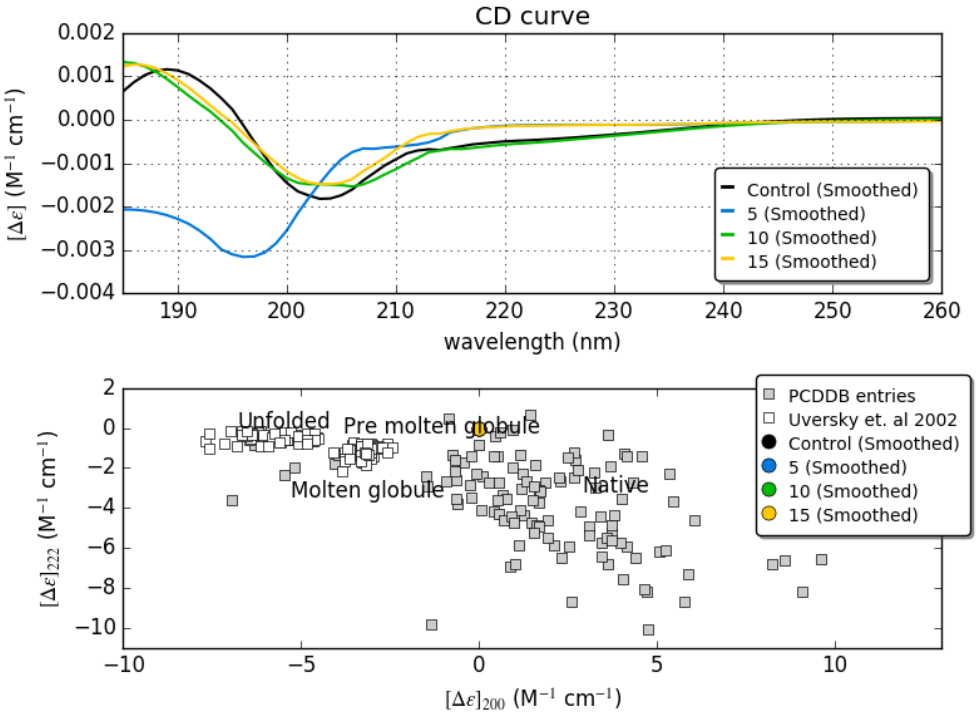

f. Na_2SO_4

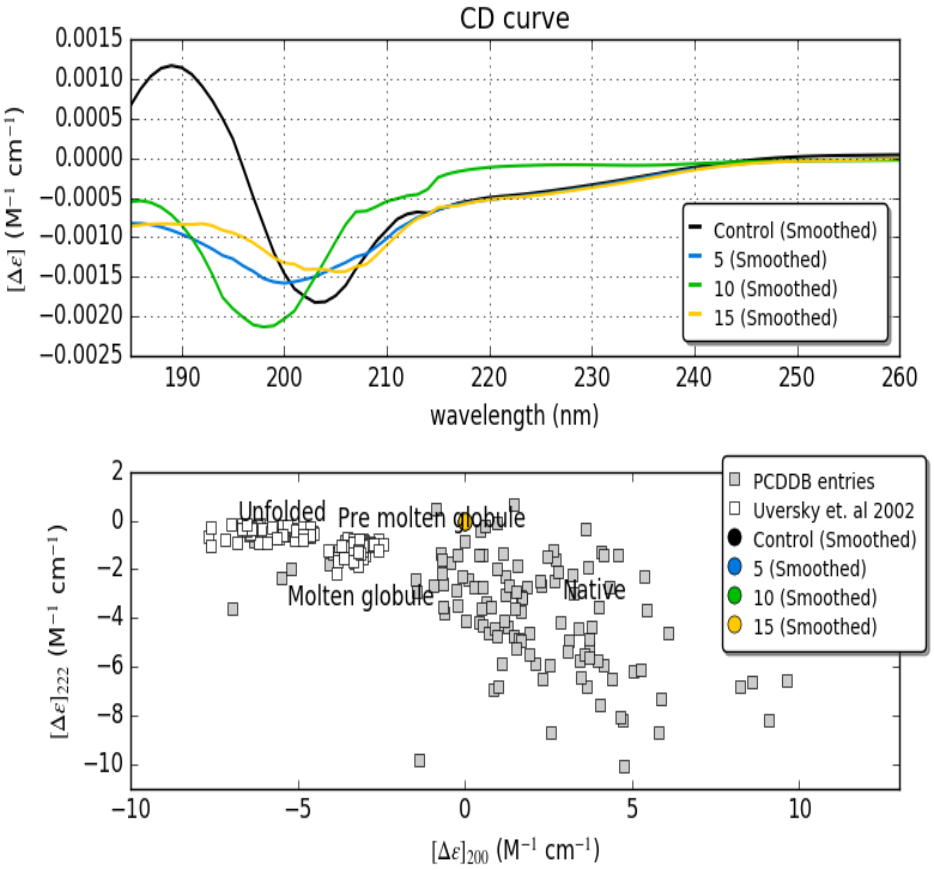

g. Gallic acid

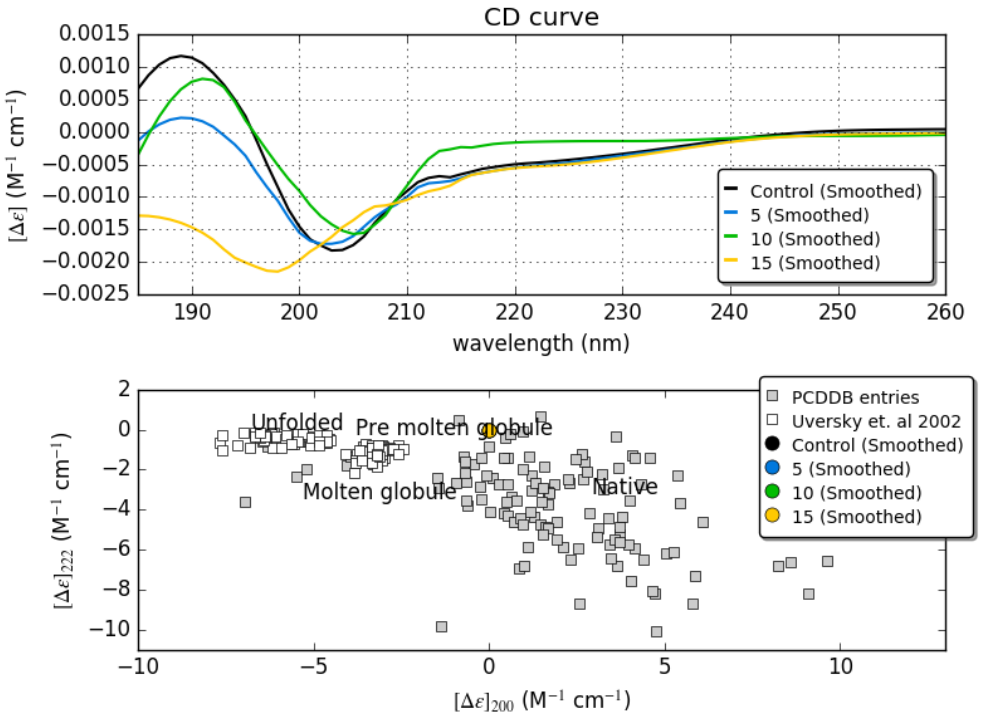

h. *P*-coumaric acid

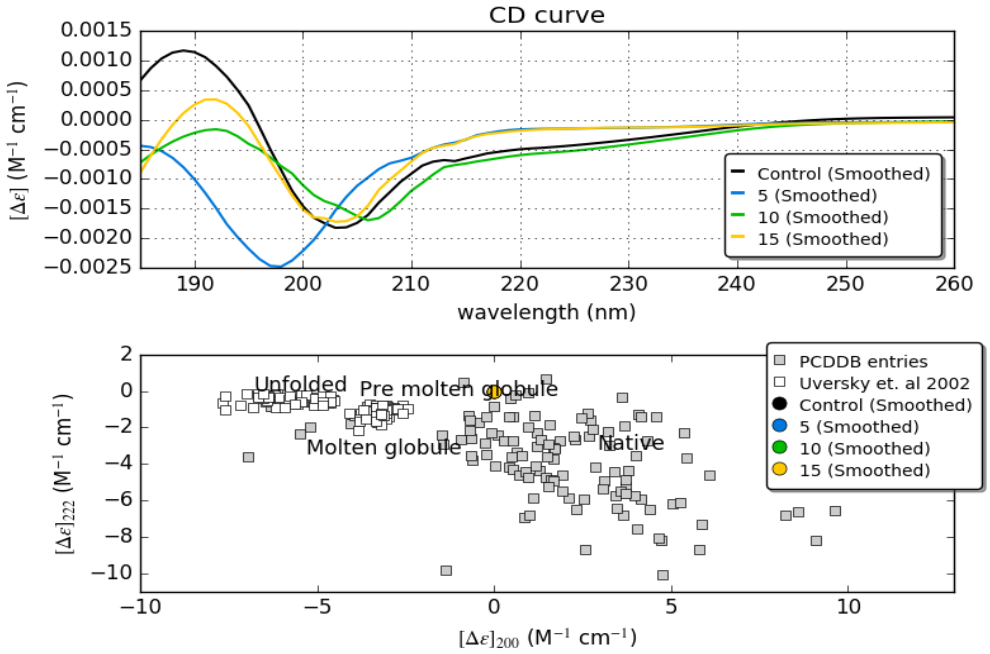

i. Sinapinic acid

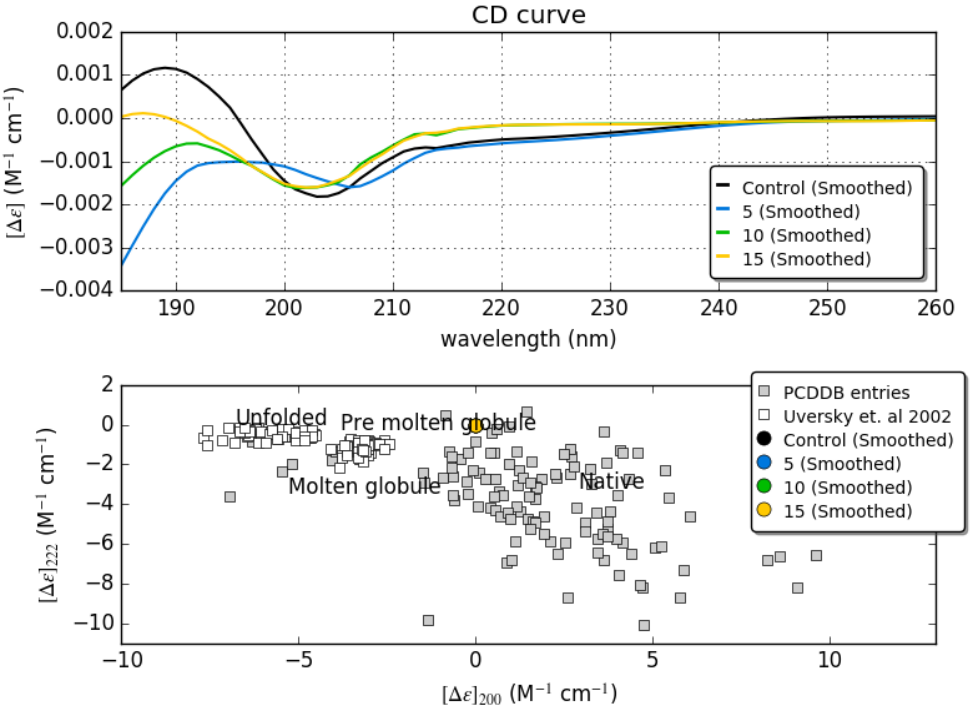

j. Vanillic acid

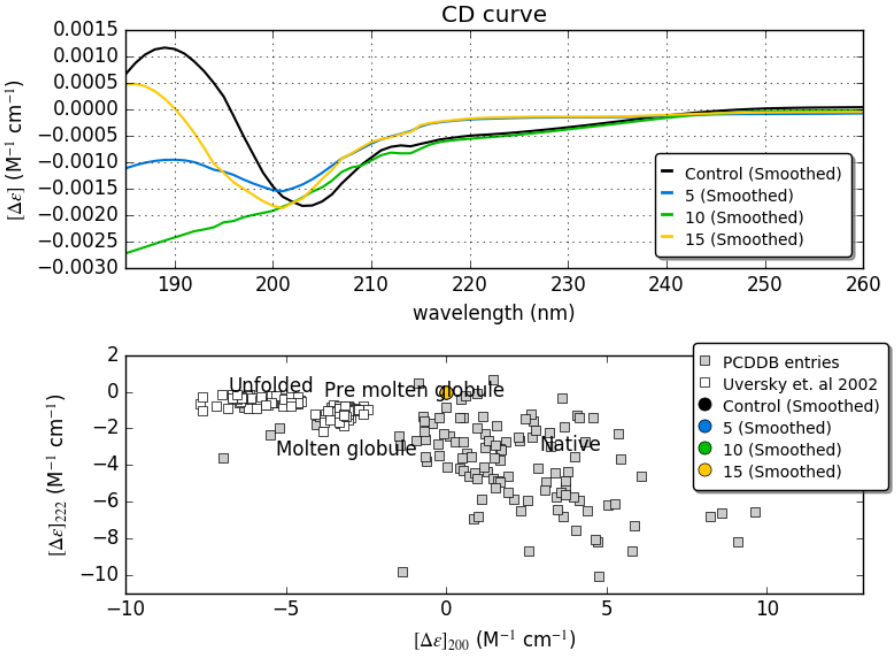

Figure 43: Effects of (**a**) $C_{29}H_{44}O_2$, (**b**) RbCl, (**c**) NaCl, (**d**) $CuCl_2$, (**e**) Na_2SO_3, (**f**) Na_2SO_4, (**g**) gallic acid, (**h**) *p*-coumaric acid, (**i**) sinapinic acid, and (**j**) vanillic acid on the aggregation of AICD. Ten micromolar AICD was incubated with each compound that were used at concentrations of 5, 10, and 15 µM. Control represents AICD alone.

Obviously, the investigated compounds at different concentrations produced minimal effects on AICD's secondary structural elements. Furthermore, there are undetected changes in the peptide's folding state as can be noted in the second panel of the above figure.

4.2 Discussion

4.2.1 Transcriptional regulation of cholesterol by APP

Although the impact of cholesterol homeostasis on the progression of AD due to the accumuleation of Aβ peptides in the amyloidogenic processing of APP and its deleterious impact has been investigated by several lines of studies. However, the influence of APP or its intracellular domain (AICD) or Aβ have not been studied which are targeted in the current study. Physiological role of APP, AICD and Aβ on lipids homeostasis and alterations has been investigated in AD brains (Grimm et al, 2017) while, the transcriptional function of these proteins was the one of the interests of this investigation. Moreover, some transcriptional and physiological studies reported the bidirectional influences of APP and its fragments, AICD and Aβ, on APOE ε4 allele, cholesterol and other lipids transporter in the central nervous system (CNS), because it has been suggested as a causative factor in AD (Grimm et al, 2017; Lee et al, 2017; Liu et al, 2013).

Cholesterol undergoes *de novo* biosynthesis in the astrocytes (Orth and Bellosta, 2012) because BBB impermeability does not allow its transport into the brain. *De novo* biosynthesis of cholesterol is a multistage process (Liscum, 2002) in which transcriptional regulation of the cholesterol pathway is mediated by the sterol-regulatory element binding protein type-2 (SREBP-2) (Horton et al., 2002; Ferris et al., 2017). This isoform of the protein and other isoforms (SREBP-1a and SREBP-1c) are a family of transcription factors that regulate cholesterol and fatty acid homeostasis (Accad and Frresse Jr, 1998). After synthesis, precursor (P)SREBP-2, is introduced into the endoplasmic reticulum (ER) as inactive protein (Ye et al., 2011). Precursor protein contains two transmembrane helices with N- and C- terminals facing the cytosol (Waterham, 2006). An interaction is occurring betwee C-terminus of (P)SREBP-2 with the C-terminus of the SREBP cleavage-activating protein (SCAP) which is an escort

protein regulated by sterol level. Detection of sterol level is achieved by sterol sensing domains (SSD) in five transmembrane helices (2-6) of the eight transmembrane helices of SCAP (Okamoto et al., 2006). The combination of (P)SREBP-2/SCAP is localized into coat protein complex II (COPII) which are vesicles bud from ER, and transport to the Golgi complex by budding process (Horton et al., 2002; Camargo et al., 2009). Precursor protein is cleaved sequentially at the Golgi by two proteases, site-1-protease (S1P) and site-2- protease (S2P). The result of sequential proteolytic processing is the release of the N-terminal of SREBP-2 to form the mature protein ((M)SREBP-2) which enters the nucleus to regulate gene transcription (Mohamed, et al., 2015). The process of cholesterol synthesis starts by forming acetoacetyl Co-A from two moles of acetyl Co-A in the presence of acetoacetyl Co-A thiolase (Zhang and Liu, 2014). 3-hydroxy-3-methylglutaryl (HMG) Co-A is formed from one mole of acetyl Co-A and acetoacetyl Co-A in the presence of (HMG) Co-A synthase (HMGS) (Sapir et al., 2014). HMGCR converts HMG Co-A to mevalonic acid. The product of HMGCR, mevalonic acid, is sequentially phosphorylated to 5-phosphomevalonate by the enzyme mevalonate kinase (MK) and to 5-pyrophosphomevalonate by phosphomevalonate kinase (PMK). 5-pyrophosphomevalonate is converted to isopentenylpyrophosphate (IPP) by mevalonate diphosphate decarboxylase (Nes, 2011). IPP is isomerized to dimethylallyl pyrophosphate (DMPP) in the presence of IPP isomerase (IPPI). IPP combines with DMPP to form geranyl pyrophosphate (GPP) after which GPP is condensed with another molecule of IPP to yield farnesylpyrophosphate (FPP) (Nes, 2011). GPP and FPP syntheses are both catalyzed by farnesylpyrophosphate synthase (FPPS), a prenyltranferase. FPP initiates the branches of the pathway that generates cholesterol and non-cholesterol isoprenoids (Mohamed et al., 2015; Lu et al., 2010; Song et al., 2005; Jo Y et al., 2011; Zelcer et al., 2014). Figure 44 shows a flowchart of cholesterol bio-synthesis steps.

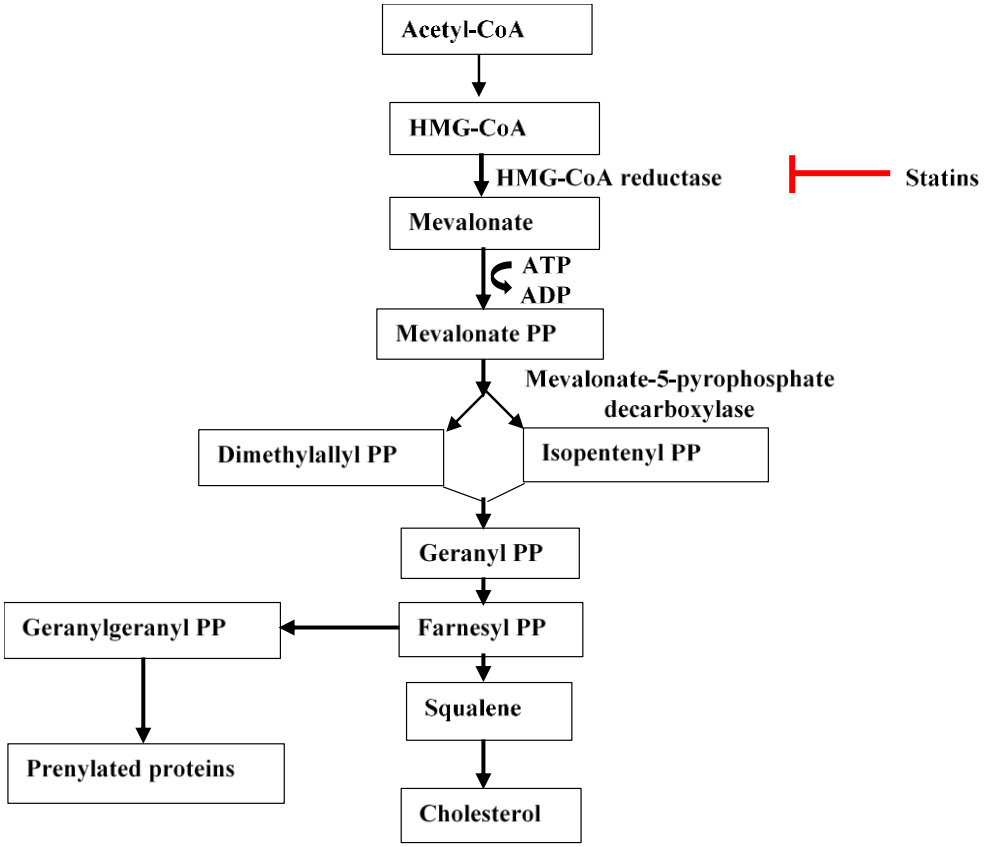

Figure 44: Cholesterol synthesis in the mevalonate pathway. The precursor acetyl Co A is converted first to 3-hydroxy-3- methylglutaryl-CoA (HMG-CoA) and then to mevalonate. The rate-limiting step of cholesterol biosynthesis is the conversion of HMG-CoA to mevalonate catalyzed by the HMG-CoA reductase (HMGCR), which is the target of statins (Checa 2014).

Cholesterol is essential for cell growth and function and a key constituent in maintaining functioning cell membrane (Hussain et. al., 2019 and Yeagle, 1991). However, hypercholesterolemia is proposed as a risk factor in developing AD (Pan et. al., 2018 and Howland et. al., 1998). Cholesterol levels has been proven to be associated with enhanced amyloid precursor protein (APP) level (Wood et. al., 2014). Aβ peptide, a hallmark of AD, which produced in the amyloidogenic pathway of APP by β- and γ-secretases sequential cleavage, has been shown to obstruct the activity of Hydroxymethylglutaryl-CoA reductase HMGCR, a rate-limit enzyme in cholesterol bio-synthesis, and subsequently diminishing cholesterol *de novo* bio-synthesis from a side and cholesterol levels regulate Aβ's production rate (Grimm et. al., 2005 and Bodovitz and Klein, 1996) from the other side. Amyloid intracellular domain (AICD), a product of γ-secretase cleavage of transmembrane terminal of APP (C99), is likely

participate in transcriptional events that reducing cholesterol bio-synthesis (Beel et. al., 2010). Epidemiological surveys in patients taking statin, cholesterol lowering drug, demonstrated a reduction in AD popularity (Wood et. al., 2014). Nonetheless, some studies demonstrated that enhancing dietary cholesterol of mouse models that expressing Swedish familial AD mutations and human Aβ has lowered Aβ40 and Aβ42 significantly but with no impact on C-terminal APP products (Goldman et al., 2018; Wood et. al, 2014; and Halford and Russel, 2008). Such controversial results suggesting that cholesterol homeostasis or distribution within the brain may have a role in APP processing and/or Aβ accumulation (Wood et. al., 2014) because brain is a cholesterol-rich organ which produces its own cholesterol and, blood brain barrier (BBB) maintains this homeostasis. Dysfunction of BBB because of ischemic stroke, for example, may affect this homeostasis due to the cholesterol gradient between the brain and the blood resulting in a turbulence in the brain cholesterol (Nation et al., 2019; Montagne et al., 2017; Roh et al., 2017, and Li et al., 2015).

In the current study, genes involved in the *de novo* cholesterol biosynthetic pathway have been studied in order to detect the influence of APP or one of its fragments (AICD and Aβ) on the expression of these genes by utilizing mouse embryonic fibroblasts lacking APP/APLP2 (MEF APP/APLP2-/-). Furthermore, MEF WT cells were used as the control for comparison and normalization purposes because such cells are expressing APP (Figure 13). Quantitative detection of relevant genes showed that all gene expressions, except the 3-hydroxy-3-methylglutaryl-CoA synthase-2 (HMGCS2) gene, were reduced in the absence of APP. As it is shown by the results, the rate-limit enzyme (HMGCR) is down-regulated significantly ($p \leq 0.001$) in MEF cells which are devoid of APP referring to a possible association to some extent between the expression of APP and cholesterol de novo bio-synthesis. These results are consistent with the results obtained some researches (Grimm et al, 2017; Mohamed et al, 2015 and, Pierrot et al, 2013). Likewise, mevalonate pathway genes; mevalonate kinase (MVK), phosphomevalonate kinase (PMVK), and mevalonate (diphospho) decarboxylase (MVD) exhibited a reduced expression and this is likely attributed to the impact of reduced upstream enzyme (HMGCR) or direct regulation by APP which is supported by findings of other researchers (Mohamed et al, 2015). This achievement is analogous to the results obtained when differentiating APP-knockout (APP KO) human induced pluripotent stem cells (hiPSCs) into human astrocytes where, a reduction in HMGCR expression was achieved (Fong et. al, 2018). Correspondingly, the SREBP-1 and related

genes (genes of proteins involved in escorting and delivering SREBP-1 from the endoplasmic reticulum [ER] to the nucleus) were studied by using the same cells for control and sample because this protein is responsible for transcription regulation of cholesterol biosynthesis as described in chapter II of this study. Results showed a reduction in SREBP-1 gene expression, except for the Sterol Regulatory Element Binding transcription Factor 1 (SREBF1) gene. Correspondingly, an identical achievements were obtained but by utilizing SREBP-2 protien (Mohamed et al, 2015). These results indicate that APP may participate in transcriptional regulation of cholesterol and there is a possibility of a link between higher cholesterol levels and increased APP expression. However, limited studies considered the transcriptional impact of APP on cholesterol biosynthesis while it has been studied thoroughly in this study.

Additionally, in order to study AICD's transcriptional role in cholesterol homeostasis, MEF APPΔCT15 was used. This cell line does not have functional AICD, which was achieved by deletion of last 15 amino acids of the APP C-terminal, MEF WT was used as control cells. Results showed a significant reduction in gene expression of HMGCR ($p \leq 0.001$) in cases in which the AICD function is eliminated when compared with control cells that have normal AICD expression. Identical impact is observed of APP and AICD in regulating cholesterol homeostasis (Wood et al, 2014). While, results of SREBP-1 gene expression revealed a marginal impact of AICD in regulating target genes compared to control cells. The impact of AICD on cholesterol bio-synthesis was first studied because no or little is known about its role in controlling cholesterol biosynthesis.

Finally, the influence of Aβ on gene expression of the cholesterol biosynthetic pathway was accomplished using MEF PS1res as a control cell line in which these cells were stably transfected with human PS1, but not human PS2, and deficient mouse PS1 and PS2. PS1 and PS2 proteins are the catalytic site of γ-secretase in which, in the amyloidogenic pathway, the product of γ-secretase is Aβ and AICD. MEF PS1/2-/- cells were used as sample cells. These cells were deficient in mouse PS1 and PS2 proteins by double knockdown genes of these proteins so as to prevent the production of endogenous Aβ. Results from the gene expression test showed an obvious increase in the cholesterol synthesis gene expressions in addition to SREBP-1 genes in the absence of Aβ. The rate of increase in these genes expressions was not equal. While HMGCS1

and HMGCR was significantly upregulated ($p \leq 0.001$), HMGCS2 exhibited insignificant increase illustrating that the difference between control and sample may occurred by chance. Most studies were investigated the impact of cholesterol or HMGCR inhibitors on the progression of AD (Zou et al, 2019; Mohamed et al, 2015 and, Wood et al, 2014) while in this novel study, the impact of Aβ on cholesterol biosynthesis pathway was studies. Aβ down-regulation was associated with an increase in cholesterol gene transcription, indicating that the amyloidogenic APP processing pathway is not the preferred pathway for maintaining cell functionality and may demonstrate the toxic impact of such peptide. Aβ's role in cell apoptosis in AD patients that is due to the loss of cell integrity may be explained as a result of Aβ over-expression and a lower rate of cholesterol production.

4.2.2 Influence of cholesterol in Aβ degradation

Cholesterol's effects on total Aβ degradation by enzymes involved in this process were examined. A reduction in Aβ of about 20% was determined for aggregated β amyloid peptides (Figure 19). Identical findings have been obtained elsewhere (Mett, 2017). The decrease in amyloid aggregation may result from the multiple proteases that have been shown to degrade the Aβ peptide, including IDE, NEP, endothelin-converting enzymes, and plasmin in the cytosol or cell membrane, and IDE in the extracellular (Weller et al., 2000). As is shown in Figure 20, a reduction in the remaining β-amyloid peptide of about 52%, 58%, 65% and 69% for incubation time intervals 8, 12, 24, and 30 h, respectively can be seen in the extracellular Aβ because of the enzymatic activity of IDE, which is secreted through unconventional pathway (Zhao et al., 2009) or because of the loss of cell integrity (Song et al., 2018). Results shown in Figure 21 support an important physiological role for extracellular IDE in Aβ catabolism and homeostasis in the presence of cholesterol, in which a decrease of about 20% was determined as can be seen in the same figure. According to the latter achievement, reduced cholesterol levels is likely to cause a decrease in the amount of IDE in detergent-resistant membranes (DRMs) the point in which co-localization of IDE and Aβ was shown to occur (Bulloj et al., 2008). This change in lipid compositions also has an impact on secreted IDE, leaving extracellular Aβ in a non-degraded form. For this reason, IDE considered as a therapeutic target for AD and type 2 diabetes mellitus (T2DM) because it degrades insulin and Aβ. In addition to these targets, IDE degrades glucagon and atrial natriuretic peptide (Shen et. al 2006). The multifaceted function of

IDE arises some concerns about its role as a therapeutic target and needs to be studied thoroughly. To confirm the hypothesis that IDE is the major Aβ degrading enzyme in the extracellular space, the same experiment was then repeated but with the use of N2a IDE knockdown cells. Tests were carried out with living cells and with culture medium to compare the results as shown in Figure 22 and 23, respectively. Both graphs are showing the important role of IDE as a degrading enzyme of the Aβ peptide. In living cells as presented in Figure 22, only 5% of the added synthetic human sequence Aβ was catabolized by multiple membrane proteases such as NEP, endothelin converting enzyme-1, plasmin, and matrix metalloproteinases (MMP9) in the absence of IDE. Thus, it can be concluded that IDE is responsible for degrading 15% of Aβ, whereas in N2a WT cells, the degradation was around 20% as shown previously in Figure 19. While in N2a IDE knockdown cells, the degradation was reduced to 5%. On the other hand, deleting the effects of IDE in the extracellular space resulted in an increase in Aβ aggregation. This increase proved the importance of IDE in the process of extracellular catabolism of Aβ. The increase in quantified Aβ is likely to the interaction with murine Aβ peptide (Steffen et. al, 2017; Bright et. al, 2014; and Fung et. al, 2004)

Two mechanisms have been developed to explain the secretion of IDE from the cytosol, one of which is by unconventional pathway, where IDE still secreted although secretion inhibitor had been used (Zhao et al., 2009), while in the second mechanism, IDE secreted due to the loss of cell integrity, and verified by the release of cytosolic enzymes (Song et al., 2018). Results obtained in this investigation supports the first mechanism because, cholesterol presence maintains cell membrane integrity thus the hypothesis of IDE secretion by the loss of cell integrity is eliminated (Dios et. al, 2019). However, the second secretion pathway can be explained when Aβ accumulation increases, due to impaired clearance or catabolism, and hence diminish cholesterol homeostasis and leading to the loss of cell integrity which releases the cell content including IDE.

Results in Figure 24 show that high cholesterol levels caused an increase in IDE gene expression of about 18% and 13% as compared with control (housekeeping) genes, β-actin and Polr2, respectively, which reflects cholesterol's impact on IDE transcription. Figure 25 summarizes the normalized results of cholesterol's impact on the IDE promoter in which results of cholesterol's influence on IDE gene expression was confirmed by an increase in IDE promoter activity. A significant increase of about 24%

was obtained for the IDE promoter as compared to control sample. Cholesterol's effects on IDE levels in the membrane and extracellular space was considered and evaluated by quantifying IDE protein with western blotting and N2a cells. Obviously, as shown in Figure 26, there was an effect of cholesterol on IDE protein demonstrated as an enhancement in the protein level by 22% for both intracellular and extracellular IDE. Results of IDE gene expression detection, promoter assays, and protein levels confirmed cholesterol's role on IDE at both transcription and regulatory levels, and the dual impact of high cholesterol levels on increasing Aβ deposits via APP processing from one side and up-regulation of IDE that degrades Aβ from the opposite side. Protein stability is a measure of a protein's capability to remain in its natural state (folded) because it is important to keep a protein's function. Therefore, the stability of the IDE protein has been measured in the presence of cholesterol in order to study the effects of high cholesterol levels on IDE protein stability. The results obtained from this experiment showed that there was an increase of about 47% in intracellular IDE and around 50% in extracellular IDE.

With respect to IDE activity, Figure 30b shows that there is no activity for IDE without cholesterol, whereas incubation with 100 μM cholesterol resulted in a steep increase in the first 400 s of the test followed by a gradual increase between the intervals of 400 to 1000 sec. After 1000 sec, there was no detected increase. In order to verify the role of phospholipids on the IDE activity, 150 μM of PC 18:0 was incubated with both control and sample wells in which fluorescence intensity was measured as shown in Figure 30d. The effects of PC 18:0 on the enzyme activity is obvious by the increase in both the control sample and cholesterol-containing sample curves. Identical impact was investigated for cholesterol, phospholipids. The rate of the increase was different, in which in the first 400 sec of the test, it was steep for cholesterol and phospholipid, while steepness was limited for the extracted lipid at the same time interval. The final steady state rate of fluorescence (after 1000 s from the beginning of the test) showed that the increase in activity was double compared to the starting point of the test; this finding confirmed the role of lipids in IDE's enzymatic activity.

4.2.3 Anti-microbial activity of Aβ peptide

Despite the deleterious impact of Aβ accumulation as shown previously and its enrollment in AD onset and progression, various studies have suggested a role for this

peptide in the innate immune system as an AMP (Kumar et al, 2016; Soscia et al. 2010). The mechanism of Aβ activity as an antimicrobial peptide can be explained by the interaction between the heparin-binding domains of soluble Aβ oligomers with microbial cell wall carbohydrates. Adhesion of pathogen to infected cells is inhibited thanks to protofibrils developed in such interaction. Propagation of Aβ fibrils mediates agglutination and eventual entrapment of unattached microbes (Washicosky et al. 2016). It is unclear yet whether Aβ production and accumulation could increase a response of the innate immune system to infections (Aryal et al., 2014; Spitzer et al., 2016, Regitz and Wenzel, 2014). Antimicrobial peptides or host defense peptides are targeting a broad spectrum of microorganisms (viruses, bacteria, fungus, and parasites) and can be found in prokaryotes and eukaryotes (Bahar and Ren, 2013). The role of Aβ in the innate immune system has been presented by some researchers (Cosztyla et. al, 2018; Kumar et al, 2016; and Soscia et al. 2010). Its effects have been proposed to be due to Aβ's agglutination characteristic that is considered to trap microbes (Cosztyla et. al., 2018 and Washicosky et al., 2016) and explained according to pathogen hypothesis for AD, in which bacterial infection mediates the aggregation of Aβ (Cosztyla et. al., 2018). In this study, although higher and toxic doses of Aβ have been utilized, the obtained results of the nematode viability test showed that the impact of Aβ as AMP is negligible at all doses of peptide that were used. Correspondingly, results with *E. coli* showed the same impact in which the density of viable cells at a higher dose of Aβ were >50 % as shown in Figure 32 a., and the growth increased in a dose-dependent manner to reach 80% as Aβ concentration decreased, indicating a marginal inhibitory effect of the peptide on *E. coli* growth. Similarly, the AlamarBlue assay demonstrated that there was a limited effect of Aβ as an antimicrobial peptide in inhibiting the growth of *C. albicans* at different Aβ concentrations. Interestingly, *S. cerevisiae* results revealed a slight enhancement in cell proliferation depending on the Aβ concentration as shown in Figure 32 c. Results obtained in this study revealed that there was no or only limited impact of Aβ on nematodal, fungal, and bacterial viability. Therefore, its role is still controversial, and more research is required in order to determine whether Aβ behaves as an AMP or a mere extrinsic influence due may be to the interaction of Aβ with cholesterol in lipopolysaccharide (LPS) molecules in the microorganisms (Bahar and Ren, 2013).

4.2.4 Regulation of Aβ aggregation by phytochemicals

It is well-accepted that the consumption of sufficient amounts of phytochemicals on a regular basis is as essential as the use of synthesized medications with respect to people's state of health or perhaps they provide an alternative solution to conventional medications in some cases. For example, omega 3 has been proven to enhance Aβ degradation and clearance through up-regulation of IDE enzymatic activity (Grimm et al, 2016). Additionally, brain is protected by blood brain barrier which strictly regulate the uptake of medications by efflux pumps. For these reasons, a broad array of phytochemicals has been studied here *in vitro* and applied at different doses in order to recognize and differentiate their influences regarding inhibition of Aβ aggregation through studying changes in its secondary structure.

4.2.4.1 Vitamins

Ascorbic acid (AA) or vitamin C which is a water soluble vitamin available in citrus fruits such as orange or grapefruit in addition to kiwi, mango, watermelon, strawberries, pineapple, and papaya as well as in vegetables such as green pepper, spinach, leafy greens, tomato, broccoli, and cabbage. It is known for its antioxidant features, reducing the free radicals induced damage, by reducing oxidative stress cytokine release due to deposited Aβ in hippocampus of rats (Harrison and May, 2009) and diminished cell apoptosis induced by the accumulation of Aβ in SH-SY5Y human neuroblastoma cells (Harrison and May, 2009) and suppressing fibrillogenesis of Aβ (Monacelli et. al., 2017). In the same context of the obtained results by previous studies, the role of ascorbic acid is shown in Figure 34a (first panel), where an increase in the α-helix secondary structural element can be noted at 222 nm (Greenfield, 2006), and in (second panel) the direction to native form of peptide can be seen as concentration of L-ascorbic acid increases. These results support the importance of ascorbic acid supplementation in maintaining the brain functionality (Hagel et. al., 2018). Vitamin E is known for its antioxidant characteristics as well as strengthen the immune system and supports cell functions. Main sources of this vitamin is, vegetable oils, nuts, and seeds. Some studies showed that α-tocopherol and α-tocotrienol participated in events related to Aβ disaggregation and clearance from the brain including enhancing the expression of IDE and LRP1 (Desrumaux et. al., 2018; La Fata et. al., 2014; and Nishida et. al, 2009). In line with these findings, results of the current study showed that CD spectrum measurements of α-tocotrienol revealed that the spectra at 193 and 197 nm for α-helix

and random coil, respectively (Greenfield, 2006), enhanced in a dose dependent rate of the compound concentrations, which indicates that α-tocotrienol was capable of maintaining Aβ in its native state. This finding is shown in Figure 34b for the CD spectra and peptide conformation prediction in which the shift was obvious from pre-molten globules to native peptides (folded), indicating a reduction in Aβ toxicity.

4.2.4.2 Tellurite

Similar observations of tellurite compounds were detected in which it was shown that at increasing K_2O_4Te hydrate concentrations, the α-helix was enhanced slightly at 200 nm, and the β-sheet at 195 nm increased more as shown in Figure 35a. The impact of increasing Na_2TeO_3 concentrations on the peptide's aggregation can be seen in Figure 35b as indicated by the α-helix spectra increase at 222 nm, which indicates that the peptide is conserved in its folded state. Moreover, in the same figure, there is a distinct shift in the peptide's pre-molten to native state.

4.2.4.3 Chlorides, sulfur, and selenium compounds

Lithium chloride salt can be found in grains and vegetables as well as in some sources of tap water. Dietary intake of Li has been determined in a range of 610-3100 μg of daily intake and prescribed for patients with bipolar disorder (Schrauzer et. al., 2002). Epidemiological studies evidenced the impact of lithium chloride in attenuating Aβ levels and around 31% enhancement in the clearance of the toxic peptide by increasing the expression of LRP-1 which is correlated with the clearance across BBB (Forlenza et. al., 2014). Contrarily, results from CD show that lithium chloride is considered an agent that may increase Aβ production (Feyt, et al., 2005). Along with this result, the CD spectrum of lithium chloride showed a limited effect on Aβ aggregation as shown in Figure 36a in which an increase in its concentration had limited effects at a wavelength of 222 nm, indicating that the α-helix secondary structure unaltered even with an increase in lithium chloride concentrations. There is an increasing in spectral signal around 215 nm wavelength, indicating an increase in β-sheet formation. Such increase in the β-sheet is unfavorable because it leads plaque formation. Analogous results have been obtained by treating Aβ with rubidium chloride (Figure 36b). Also, sodium chloride was found to have a role in Aβ accumulation in cultured cells resulting from abolished peptide clearance (Cheng et al., 2015). CD analysis of different concentrations of sodium chloride showed a sharp increase in the α-helix spectrum at

222 nm as shown in Figure 36c. Although all concentrations had a similar effect, the minimum concentration is preferred in order to avoid the side-effects caused by the higher doses of this salt. Oxidative stress induced by $CuCl_2$ has been characterized in AD via the interaction between copper and Aβ (Atwood et al., 2000 and Hu et al., 2016). Figure 36d shows the CD spectrum of $CuCl_2$ at different concentrations in which a considerable increase in the α-helix secondary structure was detected at a wavelength of 222 nm for all concentrations. Identical results were obtained with $ZnCl_2$ as shown in Figure 36e. The destructive impact of these two compounds in inducing oxidative stress is during metabolism due to releasing of free radicals. This effect can be minimized through reducing the intake to the minimum rate.

Sodium sulfite is one of the preservatives used in canned vegetables, potato chips, soup mixes, and vegetable juices. Acceptable daily intake (ADI) of 0.7 mg / kg of body weight / day was considered as a safe dose of sulfite (Lien et. al., 2016, and Zhang et al., 2004) to prevent the increase in reactive oxygen species (ROS) in the brain which is induced by increasing intake of such salt (Zhang et. al, 2004). Na_2SO_3 exhibited a significant effect in maintaining Aβ in its native conformation as shown in Figure 37b with a huge increase in the α-helix spectrum at 222 nm at the four concentrations used for the analysis. Correspondingly, Na_2SO_3 affected Aβ aggregation at a concentration of 5 µM as shown in Figure 37b, in which the highest increase in the α-helix secondary structural element spectra was obtained. This effect decreased as the concentration of Na_2SO_3 was increased. While, Na_2SO_4 which is used as a source of sodium in supplemented nutrients at a maximum of 200 mg sodium / day for adults (EFSA, 2010). The current results showed less impact on Aβ accumulation at 5 µM and 222 nm, but random coils increased at this concentration (Figure 37c) in the spectrum at 205 nm. For concentrations >5 µM, a large increase in the α-helix spectra was detected. These results suggest that the optimum Na_2SO_3 and Na_2SO_4 concentrations are 5 and 20 µM, respectively, for preservation of the Aβ secondary structural elements within the native or folded state. Otherwise, β-sheets may be formed and then form stacks that lead to insoluble senile plaques. Sulfites are used in packaged foods as preservatives to improve flavor or appearance, therefore AD patients should avoid processed food or minimize the intake of such foods to avoid burden of these compounds.

European medicines agency has determined the total food and supplementation) intake of sodium selenite and sodium selenite to a maximum of 300 µg / person / day (EPMAR, 2015). Na_2SeO_3 affected Aβ secondary structure as detected by an intense

signal at 193 nm, which corresponds to the α-helix. $Na2SeO_3$'s effects are dose-dependent as shown in Figure 38a. Na_2SeO_4's effects were characterized by a large increase in the CD spectra at 208 and 222 nm, both of which indicate an increase in the α-helix component of the Aβ secondary structure, except at higher concentration of Na_2SeO_4 (20 µM) in which no effects were detected as shown in Figure 38b. The detected role of selenium compounds supports the evidenced role of these compounds as antioxidants. Diets-enriched with selenium are essential for the clearance of Aβ because it is shown to prevent the accumulation *in vitro*, in this study, and *in vivo* as shown in section 2.8.2 of chapter two. However, to avoid the toxic impact and sensitivity by higher doses of selenium, ≥ 20 µM (EPMAR, 2015), it is highly recommended to use selenite and selenite at lower concentrations.

4.2.4.4 Organic acids

Gallic acid is the most active component of grape seed extract, which inhibits Aβ aggregation by stabilizing kappa-casein (a milk protein that forms amyloid fibrils immediately under physiological conditions) to prevent its aggregation (Liu et al., 2013). In line with this, gallic acid showed inhibition of Aβ deposition at lower concentrations (5 µM) as shown in Figure 40a, in which the CD signal increased at a wavelength of 222 nm. Nonetheless, higher concentrations had an adverse effect by decreasing α-helix formation. Besides that, *p*-coumaric acid has been shown to attenuate Aβ (25-35)-induced toxicity by regulating nuclear factor (NF)-κB signaling pathway. NF-κB is a transcription factor that plays a key role in the gene regulation associated with inflammation and its activation is one of the signaling pathways through which Aβ exerts its neurotoxicity (Yoon et al., 2014). Analysis of CD spectra of *p*-coumaric acid-treated Aβ at different concentrations emphasized that at concentrations <15 µM, α-helix formation increased significantly, while an adverse effect was obtained at 20 µM as shown in Figure 40b, indicating a limitation in the use of this compound in human diet. Sinapinic acid is a phenolic antioxidant and free radical scavenger (Chen, 2016) and has been suggested as a source of nutraceuticals in brain disorders such as AD (Bais et al., 2017). Analysis of the CD spectra of this compound displayed a role in α-helix formation at a concentration of 5 µM in which the signal at a wavelength of 222 nm increased at this concentration. A higher concentration of sinapinic acid had a negative role on Aβ deposition as shown by reduced spectra at a wavelength of 222 nm (Figure 40c.). Vanillic acid is an antioxidant that attenuated Aβ1-

42-induced oxidative stress and cognitive impairment in mice (Ul-Amin. et al., 2017). However, CD spectra of Aβ with different concentrations of vanillic acid showed limited effects on the secondary structural elements of Aβ at low concentrations (5 µM and 10 µM), there was no enhancement in α-helix formation, whereas at higher vanillic acid concentrations (15 and 20 µM), there were negative effects suggesting that an increase in concentration is not preferable (Figure 40d). Hesperidin produced downregulatory autophagy characteristics that controlled the impairment of energy metabolism which leading to neuronal injury in AD (Huang et al, 2012; Cho, 2006, and Wang et al., 2013). Only at lower concentration (5 µM) did hesperidin cause an enhancement in α-helix formation (Figure 40e), whereas, higher concentrations produced random responses. Naringin has been shown to have a role in improving the long-term memory of AD patients by inhibition of calcium/calmodulin-dependent protein kinase II (CaMKII) auto-phosphorylation (an enzyme that plays an important role in long-term memory (Wang et al., 2013). Limited enhancement in α-helix formation at a wavelength of 222 nm accompanied by the formation of β-sheets at a wavelength 218 nm (Figure 40f), at lower concentrations (5 µM). Other concentrations had no or opposite effects. Catechin hydrate has been shown to prevent Aβ-induced neurotoxicity (Heo and Lee, 2005). The CD spectrum of catechin hydrate showed that at a lower concentration of 5 µM, an enhanced signal obtained at wavelength 222 nm indicating the formation of an α-helix (Figure 40g), while higher concentrations had less effects on α-helix formation.

Flavonoids (Figure 42) are potent antioxidants and metal chelators. However, the used flavonoids are not suggested to act as impairment factors of Aβ deposition due to the weak signals obtained for α-helix formation at all concentrations of compounds that were used in the experiments. The unanticipated results can be explained as polyphenols cross blood-brain barrier and inhibit amyloidogenic pathway (Teles et al., 2018) rather than preventing the accumulation of Aβ.

Secondary structure elements of AICD seems unaffected by chemicals used in the CD study as shown in Figure 43, indicating that the aggregation could be attributed to other factors such as Fe65 which translocate this fragment to the nucleus.

Despite that CD investigation is a fast and accurate method for studying the state of specific protein or peptide. However, such method is an *in vitro* study, and this type of study could be a limitation because change in secondary structure of Aβ or AICD is a

multifactorial process which involves various signaling pathways that's still need to be studied.

Table 31 summarizes the effect of each compound on Aβ aggregation according to its concentration in the solution.

Table 31: Detected impact of phytochemicals and inorganic compounds on the resistance of Aβ to aggregation.

Compound	Concentration of compound, µM			
	5	10	15	20
L-ascorbic acid		-	+	++
α-tocotrienol		+	++	++
$K_2TeO_4.H_2O$		+	++	++
Na_2TeO_3		+	++	++
LiCl	-	-	-	-
RbCl	-	-	-	-
NaCl	+	+	+	+
$CuCl_2$	+	+	+	+
$ZnCl_2$	+	+	+	+
Na_2S	++	++	++	++
Na_2SO_3	+	+	+	-
Na_2SO_4	-	+	+	++
Na_2SeO_3	-	+	+	+
Na_2SeO_4		+	+	-
Gallic acid	+	+	-	-
p-coumaric acid	+	+	-	-
Sinapic acid	+	+	-	-
Vanilic acid	-	-	- -	- -
Hesperidin	+	-	-	-
Naringin	-	-	-	-
Catechin hydrate	+	-	-	-

++: High impact
+: moderate impact
-: low impact
--: very low impact

Chapter V
Conclusions

According to the results obtained, tests performed, materials used, equipment employed, literature cited and laboratory conditions, the following can be concluded:

1) APP and its fragment (AICD) deletion from MEF cells down-regulated gene expression of cholesterol, SREBP-1, and related gene expressions, indicating a role for these proteins in cholesterol homeostasis in the lipid raft microdomain of a cell membrane.

2) Aβ peptide affected the cholesterol bio-synthetic pathway at a transcriptional level in mouse embryogenic fibroblasts by up-regulating cholesterol gene expression significantly, and in the absence of Aβ affected genes involved in the cholesterol synthetic pathway, SREBP-1 and related genes. These effects may be related to cell apoptosis in AD patients due to the loss of cell wall integrity upon the reduced levels of cholesterol.

3) The presence of cholesterol in N2a living cells (intracellular) and in culture medium (extracellular) caused a reduction in recombinant human Aβ to (81%) in both compartments, possibly due to the effects of degrading enzymes such as IDE, NEP, ECE-1, and MMP.

4) Mouse neuroblastoma cells that do not express insulin-degrading enzyme (N2a IDE kd) showed significant degradation of Aβ after incubation with cholesterol in living cells (95%), whereas an enhancement in Aβ aggregation occurred in these cells' culture medium (130%). Both results indicate that IDE is the most important enzyme involved in Aβ peptide degradation in addition to its activity not only at the cell membrane but also in the extracellular space as a result of exosomal secretion. These results support the mechanism of un-conventional secretion pathway of IDE. However, the mechanism of IDE secretion due to the loss of cell integrity supports the role of Aβ in losing the cell of its integrity due to Aβ's impact

on cholesterol bio-synthesis, which is essential to the cell membrane and integrity.

5) Cholesterol's effects on IDE appear to be up-regulation of IDE gene expression as compared to housekeeping genes β-actin (118%) and Pol2 (113%). IDE gene promoter activity also increased in the presence of cholesterol (124%), indicating that cholesterol has an impact on IDE transcription and thus increasing IDE synthesis and association intracellularly (122%) and secretion extracellularly (123%). In line with these findings, the enzymatic activity of IDE significantly increased three times (for example, a three time increase in activity when incubated with cholesterol in N2a cells was observed). Furthermore, cholesterol caused an increase in IDE stability (maintaining the folded state of protein) in the cytosol (147%) and extracellular space (150%). Due to these effects, the interaction between cholesterol and the enzyme needs to be studied to determine whether such effects occurred of this interaction or because of other factors related to the increased proportion of cholesterol.

6) There may be no specific role for Aβ in the innate immune system as an AMP in nematodes. Also, according to the limited effects of Aβ in inhibiting the growth of different fungi and bacteria used in the study, its role as an AMP may not be a substantially characteristic but could be an extrinsic effect due to Aβ's agglutination features.

7) A study of L-ascorbic acid and α-tocotrienol effects showed a reduction in Aβ accumulation at a concentration of 20 μM for both agents as evaluated using the CD technique to detect changes in this peptide's secondary structural elements. This concentration for both vitamins is recommended as it relates to prevention of Aβ peptides aggregation.

8) $K_2TeO_4.H_2O$ and Na_2TeO_3 caused an increase in α-helix formation at a wavelength of 222 nm when its concentration was increased to 20 μM in the Aβ solution, indicating a reliable role in preventing peptide aggregation.

9) Chlorides, which have been used in this study, affected Aβ's secondary structure in which LiCl, NaCl, $CuCl_2$, and $ZnCl_2$ enhanced formation of α-helices at a lower concentration of 5 µM, indicating that the use of chlorides should be used at minimum doses in the human diet or as supplements to suppress the undesirable impact of these compounds.

10) Na_2S at a concentration of 5 µM, affected Aβ's α-helix formation as indicated by the intense spectra at a wavelength of 222 nm, whereas Na_2SO_3 and Na_2SO_4 had the same effects at concentrations of 20 µM and 15 µM, respectively.

11) Nutrients containing Na_2SeO_3, and Na_2SeO_4 are recommended because both of these compounds produced an increase in α-helix formation at concentrations of 20 µM and 10 µM, respectively.

12) Organic compounds at different concentrations that have been employed in this study showed an increase in maintenance of Aβ in its folded form and thus prevents the peptide aggregation. Gallic, *p*-coumaric, sinapinic, and vanillic acids, hesperidin, naringenin, catechin, and the group of flavones at a concentration of 5 µM for every one of the above-mentioned compounds that were used in the study produced an improvement regarding Aβ secondary structure by maintaining the peptide in its native form (folded) and preventing formation of β-sheets

13) CD spectrometry is a method that has been used for *in vitro* structural element detection of peptides. However, utilizing this method in the study of aggregation of Aβ peptide can be regarded as a one-dimensional study because the impact of a specified compound was studied on the peptide's secondary structural elements regardless of the effects caused by other factors (such as proteins and enzymes). Peptide accumulation is a complex and multifactorial process.

Bibliography

1. Aaseth, J., Alexander, J., Bjorklund, G., Hestad, K., Dusek, P., Roos, P. M., Alehagen, U. (2016). *Treatment strategies in Alzheimer's disease: a review with focus on selenium supplementation.* Biometals **29**: 12 827-839.
2. Abbott, N.J., Ronnback, L., Hansson, E. (2006). *Astrocyte-endothelial interactions at the blood-brain barrier*. Nat. Rev. Neurosci. **7**: 12 41-5f
3. Accad, M. and Farese Jr. R.V. (1998). *Cholesterol homeostasis: a role for oxysterols. Current Biology* **8**: 3 R601-R604.
4. Adessi and Soto. (2002). *Beta-sheet breaker strategy for the treatment of Alzheimer's disease*. Drug development research **56**: 9 184-193.
5. Anand, P. and Singh, B. (2013). *Flavonoids as lead compounds modulating the enzyme targets in Alzheimer's disease*. Med Chem Res. **22**: 14 3061-3075.
6. Andrew B., Mitchel, J.W., Cole, P.F., McArdle, Yu-Ching C., Kathleen A. Ryan, Mary J. Sparks, Braxton D. Mitchell and Steven J. Kittner. (2015). *Obesity increases risk of ischemic stroke in young adults*. Stroke, **46**(6): 1690-1692.
7. Arbor, S.C., Mike L., and Medhane C. (2016). *Amyloid-beta Alzheimer targets- protein processing, lipid rafts, and amyloid-beta pores*. Yale journal of biology and medicine 89, pp. 5-21.
8. Arenas, F., Garcia-Ruiz, C., and Fernandez-Checa, J. C. (2017). *Intracellular cholesterol trafficking and impact in neurodegeneration*. Front. Mol. Neurosci. 10:382. doi: 10.3389/fnmol.2017.00382.
9. Aryal, R.J.J., Woods, J.C., Hovart, D., Johnstone, M. (2014). *Is the A-beta peptide of Alzheimer's disease an antimicrobial peptide?* Gerontol Geriatr Res, 3:4.
10. Awood, C., Richard, S., Scarpa, C., Xudong, H., Moir, D., Jones, W., Fairlie, D., Tanzi, R. and Bush, A. (2000). *Characterization of copper interactions with Alzheimer amyloid β peptides: identification of an attomolar-affinity copper binding site on amyloid β1-42*. Journal of neurochemistry. **75**, 1219-1233.
11. Backstrom J.R., Lim, G., Cullen, M. and Tokes, Z. (1996). *Matrix Metalloproteinase-9 (MMP-9) is synthesized in neurons of the human hippocampus and is capable of degrading the Amyloid-β peptide (1-40)*. The journal of neuroscience, **16**(24): 7910-7919.
12. Bahar, A. A., and Ren, D., (2013). *Antimicrobial peptides.* Pharmaceuticals, 6, 1543-1575; doi: 10.3390/ph6121543.
13. Bais, S., kumari, R. and Prashar, Y. (2017). *Therapeutic effect of sinapic acid in aluminium chloride induced dementia of Alzheimer's type in rats*. J Acute Dis; **6**(4): 154-162.
14. Ballatore, C., Virginia M., Lee, Y. and Trojanowski, J. (2007). *Tau-mediated neurodegeneration in Alzheimer's disease and related disorders*. Nature publishing group, nature reviews, neuroscience, 663.
15. Balouiri M., Sadiki, M. and Ibnsouda, S. (2016). *Methods for in vitro evaluating antimicrobial activity: A review.* Journal of Pharmaceutical analysis **6**, 71-79.

16. Baptista, F.I., Henriques, A.G., Silva, A.M., Jens, W. and Odete A. B. (2013). *Flavonoids as therapeutic compounds targeting key proteins involved in Alzheimer's disease.* ACS chem. Neurosci. **5**, 83-92.

17. Baranello, R.J., Bharani, K.L., Vasudevaraju P., Chopra, N., Lahiri, D.K., Greig, N.H., Miguel, A.P. and Kumar, S. (2015*). Amyloid-beta protein clearance and degradation (ABCD) pathways and their role in Alzheimer's disease*. Cur. Alzheimer Res. **12**(1):32-46.

18. Barnes, D.E. and Yaffe, K. (2005). *Vitamin E and donepezil for the treatment of mild cognitive impairment*. N. Engl. J. Med., 353, 951-952.

19. Barnes, K., Anthony, J.T. and Kenny, A.J. (1992). *Membrane localization of endopeptidase-24.11 and peptidyl dipeptidase A (angiotensin converting enzyme) in the pig brain: a study using subcellular fractionation and electron microscopic immunocytochemistry*. J. neurochem. 58, 2088-2096.

20. Bauer, H.C., Taraweger, A., Zweimuller-Mayer, J., Lehner, C., Tempfer, H., Krizbai, I. and Wilhelm I. (2011). *New aspects of the molecular constituents of tissue barriers*. J. Neural Transm.;118:7-21.

21. Beel, A. J., Sakakura, M., Barrett, P. J., and Sanders, C. R., (2010). *Direct binding of cholesterol to the amyloid precursor protein: An important interaction in lipid-Alzheimer's disease relationships?.* Biochim biophys acta. August; 1801(8): 975-982. Doi: 10.1016/j.bbalip.2010.03.008.

22. Beel, A.J., Sakakura, M., Barrett, P. J., and Sanders, C. R. (2010). *Direct binding of cholesterol to the amyloid precursor protein: An important interaction in lipid-Alzheimer's disease relationship?.* Biochim Biophys Acta; 1801(8): 975-982. doi:10.1016/j.bbalip.2010.03.008.

23. Behl, C. (1997). *Amyloid β-protein toxicity and oxidative stress in Alzheimer's disease.* Cell tissue res. 290, 471-480.

24. Bjorkhem, I. (2006). *Crossing the barrier: oxysterols as cholesterol transporters and metabolic modulators in the brain*. J. of Internal Med. 260 :493-508.

25. Bodovitz, S., and Klein, W. L., (1996). *Cholesterol modulates α-secretase cleavage of amyloid precursor protein.* The journal of biological chemistry, Vol. 271, No. 8, issue of February 23, pp. 4436-4440.

26. Brigelius-Flohe, R. and Traber, M.G. (1999). *Vitamin E: function and metabolism*. FASEB J. **13** 1145-1155.

27. Bright, J., Hussain, S., Dang, V., Wright, S., Cooper, B., Byun, T., Ramos, C., Singh, A., Parry, G., Stagliano, N., and Prenner, I. G., (2015). *Human secreted tau increases amyloid-beta production.* Neurobiology of aging 36, 693-709.

28. Bulloj, A., Maria C. Leal, Surace, E.I., Zhang, X., Huaxi, X., Maria D. Ledesma, Castano, E.M., and Laura Morelli. (2008). *Detergent resistant membrane-associated IDE in brain tissue and cultured cells: relevance to Aβ and insulin degradation.* Molecular neurodegeneration, 3:22.

29. Bush, A.I., and Tanzi, R.E. (2000). *The galvanization of β-amyloid in Alzheimer's disease*. PNAS vol.99, **11**, 7317-7319.

30. Camargo, N.S. and Verheijen, M.H.G. (2009). *SREBPs: SREBP function in glia-neuron interactions.* FEBS journal 276, 628-636.

31. Cao, X. and Thomas C.S. (2000). *A transcriptively active complex of APP with Fe65 and histone acetyltransferase tip60*. Science vol. 293.

32. Caseli, L., Rafael, G.O., Douglas, C.M., Furriel, R.P., Francisco, A.L., Bruno, M. and Zaniquelli, E.D. (2005). *Effects of molecular surface packing on the enzymatic activity modulation of an anchord protein on phospholipid Langmuir monolayers*. Langmuir, **21**, 4090-4095.

33. Chang, T. Y., Yamauchi, Y., Hasan, M. T., and Chang, C. (2017). *Cellular cholesterol homeostasis and Alzheimer's disease*. J. Lipid Res. 58(12):2239-2254. doi: 10.119/jlr.R075630.

34. Chang, T.Y., Catherine C.Y., Chang, E.B., Maximillian, A.R. and Murphy, S. (2010*). Neuronal cholesterol esterification by ACAT1 in Alzheimer's disease*. IUBMB Life, **62**(4): 261-267.

35. Checa, J. and Fernandez, C. (2015). *Free cholesterol – a double-edge sword in Alzheimer*. Chapter 6 from the book, Alzheimer's disease – challenges for the future.

36. Cheignon, C., Tomas, M., Bonnefont-Rousselot, P., Faller, C., and Hureau, F. (2018). *Oxidative stress and he amyloid beta peptide in Alzheimer's disease*. Redox bilogy **14** 450-464.

37. Chen, C. (2016). *Sinapic acid and its derivatives as medicine in oxidative stress-induced diseases and aging*. Hidawi Publishing Corporation, Oxidative Medicine and Cellular Longevity vol. 2016, Article ID 3571614, **10**.

38. Cheng, X.J., Gao, Y., Zhao, Y.W. and Cheng, X.D. (2015). *Sodium chloride increases Aβ levels by suppressing Aβ clearance in cultured cells*. PLOS One.

39. Cho, J. (2006). *Antioxidant and neuroprotective effects of hesperidin and its aglycone hesperidin.* Arch Pharm Res, Vol 29, No. **8**, 699-706.

40. Christ, K,. Imke, W., Bakowsky, U., Hans-Georg S., and Gerd, B. (2007). *The role of lipid II in membrane binding of and pore formation by nisin analyzed by two combined biosensor techniques*. Biochemica et Biophysica Acta 1768, **10** 694-704.

41. Craft, N. E., Haitema, T.B., Garnett, K.M., Fitch, K.A., Dorey, C.K. (2004). *Carotenoid, tocopherol, and retinol concentration in elderly human brain*. J. Nutr. Health Aging. **8** 156-162.

42. Daneman, R. and Alexandre, P. (2015). *The blood-brain barrier*. Cold spring harb perspect boil.**7**: a020412.

43. Desrumaux, C. M., Mansuy, M., Lemaire, S., Przybilski, J., Guren, N. L., Givalois, L., and Lagrost, L., (2018). *Brain vitamin E deficiency during development is associated with increased glutamate levels and anxiety in adult mice.* Frontiers in behavioral neuroscience, brief research report, doi: 10.3389/fnbeh.2018.00310.

44. Dietschy J.M. and Stephen D.T. (2004). *Cholesterol metabolism in the central nervous system during development and in the mature animal*. Journal of lipid research Volume 45.

45. Dietschy, J.M. (2009). *Central nervous system: cholesterol turnover, brain development and neurodegeneration*. Biol. Chem; **390**(4): 287-293.

46. Dios, C., Bartolessis, I., Agujetas, V. R., Camps, E. B., Mari, M., Morales, A., and Colell, A., (2019). *Oxidative inactivation of amyloid beta-degrading proteases by cholesteol-enhanced mitochondrial.* Redox biology 26, 101283, https://doi.org/10.1016/j.redox.2019.101283.

47. Du, X., Chao, W. and Qiong, L. (2016). *Potential roles of selenium and selenoproteins in the prevention of Alzheimer's disease*. Current topics in medicinal chemistry, vol. 16, issue 8.

48. Duering, M., Grimm, M.O., Grimm, H.S., Schroder, J., Hartmann, T. (2005). *Mean age of onset in familial Alzheimer's disease is determined by amyloid ββ*. Neurobiol. βging **26** 785-788.

49. Dyrks, T., Dyrks, E., Monning, U., Urmoneit, B., Jonathan, T., and Beyreuther, K. *Generation of Aβ4 from the amyloid protein precursor and fragments thereof*. Federation of European Biochemical Societies Vol. 335, no. **1**, 89-93.

50. Eckman, E.A., Reed, D.K. and Christopher B.E. (2000). *Degradation of the Alzheimer's amyloid β peptide by endothelin-converting enzyme*. JBC vol. 276, No. 27 Issue of July 6, pp.8 24540-24548.

51. EFSA, European Food Safety Authority, (2010). *Scientific opinion on the use of potassium sulphate and sodium sulphate as sources of respectively potassium and sodium added for nutritional purposes to food supplements.* EFSA Journal 2010;8(12):1940.

52. EPMAR, European public MRL assessment report, (2015). *Potassium selenite (all food producing species), Sodium selenite (all food producing species), Sodium selenite (all food producing species).* European Medicines Agency, EMA/CVMP/187590/2015, Committee for medicinal products for veterinary use.

53. Evin, G., and Andreas W. (2002). *Biogenesis and metabolism of Alzheimer's disease Aβ amyloid peptides.* Peptides, **23** 1285-1297.

54. Fairus, S., Rosnah, M.N., Hwee, M.C. and Kalyana, S. (2012). *Alpha-tocotrienol is the most abundant tocotrienol isomer circulated in plasma and lipoprotein after postprabdial tocotrienol-rich vitamin E supplementation*. Nutrition journal 11:5.

55. Farina, N., Isaac, M.G., Clark, A.R. Rusted, J. and Tabet, N. (2012). *Vitamin E Alzheimer's dementia and mild cognitive impairment.* Cohrane Database Syst. Rev. 11.

56. Fassbender, K., Simons, M., Bergmann, C., Stroick, M., Lutjohann, D., Keller, P. Runz, H., Kuhl, S., Bertsch, T., Bergmann, K., et al. (2001). *Simvastatin strongly reduces levels of Alzheimer's disease β-amyloid peptides Aβ 42 and Aβ 40 in vitro and in vivo.* Proc. Natl. Acad. Sci. USA, **98** 5856-5861.

57. Fath, T., Jochen, E. and Roland, B. (2002). *Tau-mediated cytotoxicity in a pseudo hyperphosphorylation model of Alzheimer's disease*. The journal of neuroscience, **22** (922):9733-9741.

58. Ferri, C.P., Martin, P., Brayne, C., Henry, B., Fratiglioni, L., Ganguli, M., Hall, K., Hasegawa, K., Hendrie, H., Huang, Y., Jorm, A., Mathers, C., Menezes, P.R., Rimmer, E., Scazufca, M. (2005). *Global prevalence of dementia: a delphi consensus study*. Lancet. **366** (9503): 5 2112-2117.

59. Ferris, H.A., Perry, R.J., Moreira G.V., Shulman, G.I., Horton, J.D. and Kahn, R. (2017). *Loss of astrocyte cholesterol synthesis disrupts neuronal function and alters whole-body metabolism*. PNAS, vol. 114 no. **5** 1189-1194.

60. Feyt, C., Campard, K.C., Leory, K. Kuli, F., Courtoy, P.J., Brion, J.P. and Octave, J.N. (2005). *Lithium chloride increases the production of amyloid-β peptide independently from its inhibition of Glycon Synthase Kinase 3*. The journal of Biological chemistry vol. 280, no. **39**, pp 7 33220-33227.

61. Fong, L. K., Yang, M. M., Chaves, R. S., Reyna, S. M., Langness V. F., Woodruff, G., Robertes, E. A., Young, J. E., and Goldstein, L. S. B. (2018). *Full-length amyloid precursor protein regulates lipoprotein metabolism and amyloid-β clearance in human astrocytes.* J. Biol. Chem. 293(29) 11341-11357.

62. Fong, L. K., Yang, M. M., Chaves, R. S., Reyna, S. M., Langness, V. F., Woodruff, G., Roberts, E. A., Young, J. E., and Goldstein, L. S. B., (2018). *Ful-length amyloid precursor protein regulates lipoprotein metabolism and amyloid-β clearance in human astrocytes.* JBC papers in press, June 1.

63. Forlenza, O. V., De-Paula, V. J. R., and Diniz, B. S. O., (2014). *Neuroprotective effects of Lithium: Implications for the treatment of Alzheimer's disease and related neurodegenerative disorders.* American chemical society, dx.doi.org/10.1021/cn5000309, ACS Chem. Neurosci, 5, 443-450.

64. Frautschy, S.A., Fusheng, Y., Michael, I., Brad, H., Saido, T.C., Karen, H. and Greg M.C. (1998). *Microglial response to amyloid plaques in APPsw transgenic mice*. American journal of pathology, Vol. 152, No. 1.

65. Fung, J., Frost, D., Chakrabartty, A., and McLaurin, J., (2004). *Interaction of human and mouse Aβ peptides.* Journal of neurochemistry, doi: 10.1111/j.1471-4159.2004.02828.x.

66. Funke, S.A. and Dieter, W. (2012). *Peptides for therapy and diagnosis of Alzheimer's disease*. Current Pharmaceutical Design, **18** 755-767.

67. G-Biosceinces protocol. (2016). *AlamarBlue cell viability assay reagent*. G-Biosciences 1-800-628-7730, 1-314-991-6034.

68. Ghasemi, E., Nazanin, G.A., Mahdi, T., Parsa, P. and Aval, S.F. (2015). *Tracking the footprint of pesticides in Alzheimer's disease.* J Integr Syst Neurosci, Vol. **1**(1): 14-19.

69. Goerke, J. (1998). *Review Pulmonary surfactant: functions and molecular composition*. Biochemica et biophysica acta 1408, **10** 79-89.

70. Goldman, S. E., Goez, D., Last, D., Naor, S., Zaltsman, S. L., Ginon, I. S., Baranes, D. A., Shemesh, C., Greenberg, R. T., Tsach, S., Lotan, R., Frenkel, A. L., Shish, A., Mardor, Y., Beeri, M. S., and Cooper, I., (2018). *High-fat diet protects the blood-brain barrier in an Alzheimer's disease mouse model.* Aging cell, doi. 10.1111/acel.12818.

71. Gopalan, Y., Shuaib, I.L., Magosso, E., Ansari, M.A., Abu Bakar, M.R., Wong, J.W., Khan, N.A., Liong, W.C., Sundram, K., Ng, B.H., et al. (2001). *Clinical investigation of the protective effects of palm vitamin E tocotrienols on, brain white matter*. Stroke **45** 1422-1428.

72. Gorelick, P.B., Angelo, S., Black, S.E., Charles, D., Greenberg, S.M., Ladecola, C., Launer, L.J., Launert, S., Lopez, O.L., Nyenhuis, D., Peterson, R.C., Schneider, J.A., Tzourio, C., Arnett, D.K., Bennett, D.A., Chui, H.C., Higashida, R.T., Lindquist, R., Nilsson, P.M., Roman, G.C., Sellke, F.W. and Seshadri, S. (2011). *Vascular contributions to cognitive impairment and dementia.* Stroke. **42**(9): 2672-2713.

73. Gosselet, F. (2011). *The mysterious link between cholesterol and Alzheimer's disease: is the blood-brain barrier a suspect?* J Alzheimer's Dis Res.1:1.

74. Gosztyla, M. L., Brother, H. M., and Robinson, S. R., (2018). *Alzheimer's amyloid-β is an antimicrobial peptide: A review of the evidence.* Journal of Alzheimer's disease, 64(4), 1495-1506.

75. Greenfield, N.J. (2006). *Using circular dichroism spectra to estimate protein secondary structure.* Nat. Protocol, **1**(6): 2876-2890.

76. Grimm M.O., Kuchenbecker, J., Grosgen, S., Burg, V.K., Hundsdorfer, B., Rothhaar, T.L., Friess, P., de Wilde, M.C., Broersen, L.M., Penke, B., et al. (2011). *Docosahexaenoic acid reduces amyloid β production via multiple pleitropic mechanisms*. J. Biol. Chem 286, 11 14028-14039.

77. Grimm, H.S., Beher, D., Lichtenhaler, S.F., Shearman, M.S., Beyreuther, K., Hartmann, T. (2003). *γ-secretase cleavage site specifity differs for intracellular and secretory amyloid β*. J. Biol. Chem. **278**, 8 13077-13085.

78. Grimm, M. O. W., Grimm, H. S., Paetzold, A. J., Zinser, E. G., Halonen, R., Duering, M., Tschaepe, J. A., Strooper, B. D., Mueller, U., Shen, J., and Hartmann, T., (2005). *Regulation of cholesterol and sphingomyelin metabolism by amyloid-β and presenilin.* Nature cell biology, Vol. 7 No. 11, November.

79. Grimm, M. O. W., Mett, J., Grimm, H. S. and Hartmann, T. (2017). *APP function and lipids: bidirectional link.* Front. Mol. Neurosci. 10:63. Doi: 10.3389/fnmol.2017.00063.

80. Grimm, M.O., Grimm, H.S., Tomic, I., Beyreuther, K., Hartmann, T., Bergmann, C. (2008). *Independent inhibition of Alzheimer's disease β- and γ-secretase cleavage by lowered cholesterol-rich membrane microdomains*. J. Biol. Chem. **283**, 9 11302-11311.

81. Grimm, M.O., Haupenthal, V.J., Rothhaar, T.L., Zimmer, V.C., Grosgen, S., Hudsdorfer, B., Lehmann, J., Grimm, H.S., and Hartmann, T. (2013). *Effect of different phospholipids on alphs-secretase activity in the non-amyloidogenic pathway of Alzheimer's disease*. International journal of molecular sciences **14**, 5879-5898.

82. Grimm, M.O., Mett, J., Stahlmann, C.P., Grosgen, S., Haupenthal, V.J., Blumel, T., Hundsdorfer, B., Zimmer, V.C., Mylonas, N.T., Tanila, H., et al. (2015). *APP intracellular domain derived from amyloidogenic β- and γ-secretase cleavage regulates neprilysin expression.* Front. Aging Neurosci. **7**, 77-94.

83. Grimm, M.O., Zinser, E.G., Grosgen, S., Hundsdorfer, B., Rothhaar, T.L., Burg, V.K., Kaestner, L., Bayer, T.A., Lipp, P., Muller, U., et al. (2012). *Amyloid precursor protein (APP) mediated regulation of ganglioside homeostasis linking Alzheimer's disease pathology with ganglioside metabolism*. Plos ONE **7**, e34095.

84. Grimm, M.O.W., Hartmann, T. (2012). *Recent understanding of the molecular mechanisms of Alzheimer's disease*. J. Addict. Res. Ther. **5**, 1-27.

85. Grimm, M.O.W., Stahlmann, C.P., Mett, J., Haupenthal, V.J., Zimmer, V.C., Lehmann, J., Hundsdorfer, B., Ebdres, K., Grimm H.S. and Hartmann., T. (2015). *Vitamin E: curse or benefit in Alzheimer's disease? A systematic investigation of the impact of α-, γ- and δ-tocopherol on Aβ generation and degradation in neuroblastoma cells*. J Nutr Health Aging, Vol. 19, No. **6**.

86. Hagel, A. F., Albrecht, H., Dauth, W. Hagel, W., Vitali, F., Ganzleben, I., Schultis, H. W., Konturek, P. C., Stein, J., Neurath, M. F., and Raithel, M. (2018). *Plasma concentrations of ascorbic acid in a cross section of the German population.* Journal of international medical research, Vol. 46(1) 168-174.

87. Halford, R. W., and Russell, D. W. (2008). *Reduction of cholesterol synthesis in the mouse brain does not affect amyloid formation in Alzheimer's disease, but does*

extend lifespan. The national academy of sciences of the USA, PNAS, 3502-3506, Vol. 106, No. 9, March 3.

88. Harrison, F. E., and May, J. M. (2009). *Vitamin C function in the brain: vital role of the ascorbate transporter (SVCT2).* Free radic. Boil. Med. March 15; 46(6): 719-730. Doi:10.1016/j.freeradbiomed.2008.12.018.
89. Haupentthal, V.j. (2016). *Die Bedeutung von phospholipiden und oxidierten lipiden fur die prozessierung des amyloid-vorlaufer proteins (APP) und die Alzheimer krankheit.* Doktorin Dissertation, der Universitat des Saarlandes.
90. Heber, S., Herms, J., Gajic, V., Hainfellner, J., Aguzzi, A., Rulicke, H.K., von Koch, C., Sisodia, S., Tremml, P., Lipp, H.P., Wolfer, D.P. and Muller, U. (2000). *Mice with combined gene knock-outs reveal essential and partially redundant functions of amyloid precursor protein family members.* The journal of neuroscience, November 1, **20**(21):7951-7963.
91. Hensley, K., Carney, J.M., Mattson, M.P., Aksenova, M., Harris, M., Wu, J.F., Floyd, R.A. and Butterfield, D.A. (1994). *A model for β-amyloid aggregation and neurotoxicity based on free radical generation by the peptide: relevance to Alzheimer disease*. Proc. Natl. Acad. Sci. USA, Vol. 91, pp. 3270-3274, Medical sciences.
92. Heo, H.J. and Lee, C.Y. (2005). *Epicatechin and catechin in cocoa inhibit amyloid β protein induced apoptosis*. J. Agric. Food Chem. **53**, 1445-1448.
93. Herreman, A., Serneels, L., Annaert, W., Collen, D., Schoonjanst, L. and Strooper, B.D. (2000). *Total inactivation of α-secretase activity in presenilin-deficient embryogenic stem cells*. Nature Cell Biology vol. 2, **2** 461-462.
94. Hollmann, P.C.H. and Katan, M.B. (1999). *Dietary flavonoids: intake, health effects and bioavailability*. Food and chemical toxicology **37** 937-942.
95. Horton, J.D., Goldstein J.L. and Brown, M.S. (2002). *SREBPs: activators of the complete program of cholesterol and fatty acid synthesis in the liver*. J. Clin. Invest. 109: **6** 1125-1131.
96. Howland, D. S., Trusko, S. P., Savage, M. J., Reaume, A. G., Lang, D. M., Hirsch, J. D., Maeda, N., Siman, R., Greenberg, B. D., Scott, R. W., and Flood, D.G. (1998). *Modulation of secreted β-amyloid precursor protein and amyloid β-peptide in brain by cholesterol.* The journal of biological chemistry, Vol, 273, No, 26, Issue of June 26, pp. 16576-16576.
97. Hu, H.L., Ni, X.S., Canning, S.D. and Wang, X.P. (2016). *Oxidative damage of Copper chloride overload to the cultured rat astrocytes.* Am J Transl Res **8** (2): 1273-1280.
98. Hu, J., Igarashi, A., Kamata, M. and Nakagawa, M. (2001). *Angiotensin-converting enzyme degrades Alzheimer amyloid β-peptide (Aβ); retards Aβ aggregation, deposition, fibril formation; and inhibits cytotoxicity*. The journal of biological chemistry vol. 276, No. 51, Issue of December 21, pp. **5** 47863-47868.
99. Huang, S.M., Tsai, S.Y., Lin, J.A., Wu, C.H. and Yen, G.C. (2012). *Cytoprotective effects of hesperetin and hesperidin against amyloid β-induced impairment of glucose transport through downregulation of neuronal autophagy*. Mol. Nutr. Food Res. **56**, 8 601-609.
100. Hung, Y. H., Bush, A. I., and Fontaine, S. L. (2013). *Links between Copper and cholesterol in Alzheimer's disease.* Frontiers in Physiology, doi: 10.3389/fphys.2013.00111.

101. Hussain, G., Wang, J., Rasul, A., Anwar, H., Imran, A., Qasim, M., Zafar, S., Kamran, S. K. S., Razzaq, A., Aziz, N., Ahmad, W., Shabbir, A., Iqbal, J., Baig, S. M., and Sun, T. (2019). Role of cholesterol and sphingolipids in brain development and neurological diseases. Lipids in health and disease, 18:26, https://doi.org/10.1186/s12944-019-0965-z.

102. Ida, N., Hartmann, T., Pantel, J., Schroder, J., Zerfass, R., Forstl, H., Sandbrink, R., Masters, C.L., Beyreuther, K. (1996). *Analysis of heterogeneous A4 peptides in human cerebrospinal fluid and blood by a newly developed sensitive western blot assay*. J. Biol. Chem. **271**, 6 22908-22914.

103. Jiang, Q. (2014). *Natural forms of vitamin E: metabolism, antioxidant and anti-inflammatory activities and the role in disease prevention and therapy*. Free Radic Biol Med. **14** 76-90.

104. Jo, Y., Peter C., Lee, W., Sguigna, V. and Russel A.D.B. (2001). *Sterol-induced degradation of HMG CoA reductase depends on interplay of two insigs and two ubiquitin ligases, gp78 and Trc8*. PNAS, vol. 108 no. 51, **5** 20503-20508.

105. Juan, C., Liu, L., Li, M.S., Wang, L.J., Liu, Y.Q., Liu, M., and Ji, B.S. (2013). *Alteration in p-glycoprotein at the blood-brain barrier in the early period of MCAO in rats*. Journal of pharmacy and pharmacology, **65**, pp. 7 665-672.

106. Kadowaki, H., Nishitoh, H., Urano, F., Sadamitsu, C., Matsuzawa, A., Takeda, K., Masutani, H., Yodoi, J., Urano, Y., Nagano, T. and Ichijo, H. (2005). *Amyloid β induces neuronal cell death through ROS-mediated ASK1 activation*. Cell death and differentiation **12**, 5 19-24.

107. Kant, R., Langness, V. F., Herrera, C. M., Wagner, S. L., Bang, A. G., and Goldstein, L. S. B. (2019). *Cholesterol metabolism is a druggable axis that independently regulates tau and amyloid-β in iPSC- derived Alzheimer's disease neurons*. Cell Stem Cell, 24, 363-375, doi.org/10.1016/j.stem.2018.12.013.

108. Kent, C., Schimmel, S.D. and Vagelos, P.R. (1974). *Lipid composition of plasma membranes from developing chick muscle cells in culture*. Biochemica et Biophysica Acta, 360, **9** 312-321.

109. Khan, A., Kalaria, R.N., Corbett, A., and Ballard, C. (2016). *Update on vascular dementia*. Journal of geriatric psychiatry and neurology. vol. **29**(5) 281-301.

110. Kim S.I., Yi, J.S. and Ko, Y.G. (2006). *Amyloid β oligomerization is induced by brain lipid rafts*. J. of Cellular Biochemistry **99**:878-889.

111. Kim, J., Basak, J.M. and Holtzman, D.M. (2009). *The role of apolipoprotein E in Alzheimer's disease.* Neuron. **63**(3): 287-303.

112. Kimberly, W., Taylor, J.B., Zheng, S., Guenette, Y. and Dennis, J.S. (2001). *The intracellular domain of the β-amyloid precursor protein is stabilized by Fe65 and translocates to the nucleus in a notch-like manner*. The journal of biological chemistry vol. 276, No. **43**, pp. 4 40288-40292.

113. Kitazawa, M., Heng-Wei H. and Rodrigo, M. (2016). *Copper exposure perturbs brain inflammatory responses and impairs clearance of amyloid-beta.* Toxicological sciences, 152, **10** 194-204.

114. Kivipelto, M., Helkala, E.L., Laakso, M.P., Hanninen, T., Hallikainen, M., Alhainen, K., Soininen, H., Tuomilehto, J., Nissinen, A. (2001). *Midlife vascular risk factor and Alzheimer's disease in later life: longitudinal, population-based study*. Br. Med. J. 322, **4** 1447-1451.

115. Klebe, R.J., Chen, T. and Tuddle, F.H. (1970). *Controlled production of proliferating somatic cell hybrids*. The journal of cell biology, vol. **45**, pages, 8 74-82.

116. Knobler. Charles M. (1992). *Phase transitions in monolayers*. Annu. Rev. Chem. **43**: 207-36.

117. Krycer, J.R., Phan, L. and Brwon, A.J. (2012). *A key regulator of cholesterol homeostasis, SREBP-2, can be targeted in prostate cancer cell with natural products*. Biochem. J. 446, **10** 191-201.

118. Kumar, D.K., Vijaya, S., Hoon, C., Kevin J., Washicosky, W., Eimer, A., Tucker, S., Ghofrani, J., Leftkowitz, A., McColl, G., Goldstein, L.E., Tanzi, R.E. and Moir, R.D. (2016). *Amyloid-β peptide protects against microbial infection in mouse and worm models of Alzheimer's disease*. Science translational medicine, vol. **8** issue 340 340ra72.

119. Kumar, N. and Pruthi, V. (2014). *Potential applications od ferulic acid from natural sources*. Biotechnology Reports 4, **7,** 86-93.

120. La Fata, G., Weber, P. and Mohajeri, M.H. (2014). *Effects of vitamin E on cognitive performance during ageing and Alzheimer's disease*. Nutrients, **6**, 5453-5472

121. La Fata, G., Weber, P., and Mohajeri, M. H., (2014). *Effects of Vitamin E on cognitive performance during ageing and Alzheimer's disease.* Nutrients, 6, 5453-5472; doi: 10.3390/nu6125453.

122. Lauridsen, C., Leonard, S.W., Griffen, D.A., Liebler, D.C., McClure, T.D. and Traber, M.G. (2001). *Quantitative analysis by liquid chromatography-tandem mass spectrometry of deuterium-labeled and unlabeled vitamin E in biological samples*. Analytical Biochem. 289, **6**, 89-95.

123. Laurie, C.D. (2010). *Protocols for neuronal cell culture*. Fourth edition, Humana press.

124. Ledesma, M.D., da Silva, J.S., Crassaerts, K., Delacourte, A., de Strooper, B. and Dotti, C.G. (2000). *Brain plasmin enhances APP α-cleavage and Aβ degradation and is reduced in Alzheimer's disease brains*. EMBO reports vol. 1, no. **6**, pp 5 530-535.

125. Li, C., Jiang, Z., Lu, W., Arrick, D., McCarter, K., and Sun, H. (2015). *Effect of obesity on early blood-brain barrier disruption following transient focal cerebral ischemia.* Obesity science & practice, doi: 10.1002/osp4.30.

126. Lien, K. W., Hsieh, D. P.H., Huang, H. Y., Wu, C. H., Ni, S. P. and Ling, M. P. (2016). *Food safety risk assessment for estimating dietary intake of sulfites in the Taiwanese population.* Toxicology reports, 3, 544-551.

127. Liscum, L. (2002). *Cholesterol biosynthesis*. D.E. Vance and J.E. Vance (Eds.) Biochemistry of lipids, Lipoproteins and Membranes (4^{th} Ed.), ch. 15.

128. Liu, W.Y., Wang, Z.B., Zhang, L.C., Xin, W. and Ling Li. (2012). *Tight junction in blood brain barrier: an overview of structure regulation, and regulator substances*. CNS neurosciences & therapeutics **18** 609-615.

129. Livak, K.J. and Thomas D.S. (2001). *Analysis of relative gene expression data using real-time quantitative PCR and the* $2^{-\Delta\Delta C}{}_T$ *method*. Elsevier science, 1046-2023/01.

130. Lu, J., Dong, W., Yuan-lin, Z., Bin, H., Zi-feng, Z., Qun, S., Zi-hui, Z., Chan-min, L. and Yong-jian W. (2010). *Quercetin activates AMP-activated protein kinase by reducing PP2C expression protecting old mouse brain against high cholesterol-induced neurotoxicity*. J. Pathol; 222: **13** 199-212.

131. Luissint, A.C., Cedric, A., Fabianne, G., Kayathiri, G. and Pierre P.C. (2012). *Tight junctions at the blood brain barrier: physiological architecture and disease-associated dysregulation*. CNS ,**14** 9:23.

132. Ma, L., Zhengyi, Y., Chenjing, L., Zhiyuan, Z., Xu, S. and Lihong H. (2005). *Design, synthesis and SAR study of hydroxychalcone inhibitors of human β- secretase (BACE1)*. Journal of enzyme inhibition and medicinal chemistry, 26:5, 643-648.

133. Mangialasche, F., Polidori, M.C., Monastero, R., Ercolani, S., Camarda, C., Cecchetti, R., Mecocci, P. (2009). *Biomarkers of oxidative and nitrosative damage in Alzheimer's disease and mild cognitive impairment*. Ageing Res. Rev. **8**, 285-305.

134. Mangialasche, F., Solomon, A., Kareholt, I., Hooshmand, B., Cecchetti, R., Fratiglioni, L., Soininen, H., Laatikainen, T., Mecocci, P., Kivipelto, M. (2013*). Serum levels of vitamin E forms and risk of cognitive impairment in a finnish cohort of older adults.* Exp. Gerontol. 48, **7** 1428-1435.

135. Mangialasche, F., Westman, E., Kivipelto, M., Muehlboeck, J.S., Cecchetti, R., Baglioni, M., Tarducci, R., Gobbi, G., Floridi, P., Soininen, H., et al. (2013a). *Classification and prediction of clinical diagnosis of Alzheimer's disease based on MRI and plasma measures of α-/γ-tocotrienol and γ-tocopherol*. J. Intern. Med. 273, **19** 602-621.

136. Mangialashe, F., Kivipelto, M., Mecocci, P., Rizzuto, D., Palmer, K., Winblad, B., Fratiglioni, L. (2010). *High plasma levels of vitamin E forms and reduced Alzheimer's disease risk in advanced age*. J. Alzheimer's Dis. **20**, 1029-1037.

137. Massaad, C. A. (2011). *Neuronal and vascular oxidative stress in Alzheimer's disease*. Current neuropharmacology, **9**, 662-673.

138. Matsuyama, K., Yamamoto, Y. and Sakai, K. (2017*). A clinical research of the effect of ferulic acid and angelica archangelica extract on amyloid beta deposition in mild cognitive impairment patients.* International conference of Alzheimer's disease.

139. Maynard, C.J., Bush, A.I., Masters, C.L., Roberto, C. and Qiao-Xin, L. (2005). *Metals and amyloid -β in Alzheimer's disease*. Int. J. Exp. Path. 86, **12** 147-159.

140. McConnell, H.M. (1991). *Structures and transitions in lipid monolayers at the air-water interface.* Annu. Rev. Phys. Chem. **42**: 171-95.

141. Mett, Janine. (2017). *Die regulation Aβ-degradierender enzyme durch die interazellulare domane von APP (AICD) und die lipidhomoostase*. Ph.D. thesis, University of Saarland, College of Medicine.

142. Micsonai, A., Frank, W., Linda, K., Young-Ho, L., Yuji, G., Matthieu, R. and Kardos, J. (2015). *Accurate secondary structure prediction and fold recognition for circular dichroism spectroscopy*. PNAS, **8** E3095-E3103.

143. Miller, E.R. 3rd, Pastor-Barriuso, R., Dalal, D., Riemersma, R.A., Appel, L.J., Gullar, E. (2005). *Meta-analysis: high-dosage vitamin E supplementation may increase all-cause mortality*. Am. Intern. Med. 142, **9** 37-46.

144. Mohamed, A., Keven, S. and de Chaves, E.P. (2015). *The mevalonate pathway in Alzheimer's disease-cholesterol and non-sterol isoprenoids*. Alzheimer disease-challenges for the future book, chapter 7.

145. Mohamed, A., Smith, K., and de Chaves, E. P. (2015). *The mevalonate pathway in Alzheimer's disease – cholesterol and non-sterol isoprenoids*. Intech, http://dx.doi.org/10.5772/59904. Chapter 7

146. Mohwald, H. (1990). *Phospholipid and phospholipid-protein monolayers at the air/water interface*. Annu. Rev. Chem. **41**:441-76.

147. Mold, M., Ouro-Gano, L., Wieckowski B.M. and Exley, C. (2013). *Copper prevents amyloid-β1-42 from forming amyloid fibrils under near-physiological conditions in vitro*. Scientific reports, **3**:1256.

148. Monacelli, F., Acquarone, E., Giannnotti, C., Borghi, R., and Nenciono, A., (2017). Vitamin C, aging and Alzheimer's disease. Nutrients, 9, 670; doi:10.3390/nu9070670.

149. Montagne, A., Zhao, Z., and Zlokovic, B. V. (2017). *Alzheimer's disease: A matter of blood-brain barrier dysfunction?*. J. Exp. Med. Vol. 214 No. 11, 3151-3169.

150. Montagne, A., Zhen, Z. and Zlokovic, B.V. (2017). *Alzheimer's disease: a matter of blood-brain barrier dysfunction.* Exp. Med.

151. Morris, M.C., Evans, D.A., Tangney, C.C., Bienias, L.L., Wilson, R.S., Aggarwal, N.T., Scherr, P.A. (2005). *Relation of the tocopherol forms to incident Alzheimer disease and to cognitive change*. A. J. Clin. Nutr. 81, **6** 508-514.

152. Muid, S., Froemming, G.R.A., Rahman, T., Ali, A.M. and Nawawi, H.M. (2016). *Delta- and gamma-tocotrienol isomers are potent in inhibiting inflammation and endothelial activation in stimulated human endothelial cells.* Food & Nutrition Research **60** 31526.

153. Munden, J.W., Blois, D.W. and Swarbrick, J. (1968). *Surface pressure relaxation and hysteresis in stearic acid monolayers at the air-water interface*. Journal of pharmaceutical sciences, j. appl. Microbiol., **16**, 1102.

154. Murphy, M.P. and LeVine III, H. (2010). *Alzheimer's disease and the β-amyloid peptide.* J Alzheimer's Dis. **19**(1): 311.

155. Nagai, N., Kotani, S., Mano, Y., Ueno, A., Ito, Y., Kitaba, T., Takata, T. and Fuji, N. (2017). *Ferulic acid suppresses amyloid β production in the human lens epithelial cell stimulated with hydrogen peroxide*. Hindawi, BioMed Research International, Article ID 5343010, 9 pages.

156. Nation, D. A., Sweeney, M. D., Montagne, A., Sagare, A., D'Orazio, L. M., Pachicano, M., Sepehrband, F., Nelson, A. R., Buennagel, D. P., Harrington, M. G., Benzinger, T. L. S., Fagan, A. M., Ringman, J. M., Schneider, L. S., Morris, J. C., Chui, H. C., Law, M., Toga, A. W., and Zlokovic, B. V. (2019). *Blood-brain barrier breakdown is an early biomarker of human cognitive dysfunction.* Nature Medicine, Vol, 25, February, 270-276.

157. Nes, W.D. (2011). *Biosynthesis of cholesterol and other sterols*. Chem Rev. 111, **28** 6423-6451.

158. Nie, Q., Xiao-Guang, D.U. and Mei-Yu, G. (2011). *Small molecule inhibitors of amyloid β peptide aggregation as a potential therapeutic strategy for Alzheimer's disease*. Acta Pharmacologica Sinica 32: **6** 545-551.

159. Nino, M.R., Rodrigues, A.L. and Rodrigues J.M.P. (2008). *Relaxation phenomena in phospholipid monolayers at the air-water interface*. Colloids and surface A: physicochemical and engineering aspects 320.1, **10** 260-270.

160. Nishida, M.; Bir, A.; Banerjee, A.; Bhowmick, P.; Chakrabarti, S. (2016). *Multiple mechanisms of age-dependent accumulation of amyloid β protein in rat brain: prevention by dietary supplementation with N-acetylcysteine, α-lipoic acid and α-tocopherol*. Neurochem. Int. 95, **39** 62-99.

161. Nishida, Y., Ito, S., Ohtsuki, S., Yamamoto, N., Takahashi, T., Iwata, N., Jishage, K., Yamada, H., Sasaguri, H., Yokota, S., Piao, W., Tomimitsu, H., Saido, T. C., Yanagisawa, K., Terasaki, T., Mizusawa, H., and Yokota, T. (2009). *Depletion of vitamin E increases amyloid β accumulation by decreasing its clearances from brain and blood in a mouse model of Alzheimer's disease.* The journal of biological chemistry vol. 284, No, 48, pp. 33400-33408, November, 27.

162. Nishida, Y., Shingo, I., Sumio, O., Naoki, Y., Tsubura, T., Nobuhisa, I., Kou-ichi, J., Hiromi, Y., Hiroki, S., Shigefumi, Y., Wenying, P., Hiroyuki, T., Takaomi, C.S., Katsuhiko, Y., Tetsuya, T., Hidehiro, M. and Takanori, Y. (2009). *Depletion of Vitamin E increases amyloid β accumulation by decreasing its clearances from brain and blood in a mouse model of Alzheimer disease*. The journal of biological chemistry vol. 284, No. 48, pp. **8** 33400-33408.

163. Nohturfft, A., Daisuke, Y., Goldstein, J.L., Brown, M.S. and Espenshade, P.J. (2000). *Regulated step in cholesterol feedback localized to budding of SCAP from ER Membranes*. Cell, vol. 102, **8** 315-323.

164. O'Brien, J.S. and Sampsom, E.L. (1965). *Lipid composition of the normal human brain: gray matter, white matter, and myelin*. Journal of lipid Research Vol. **6**.

165. Obele, V., Bakowsky, U., Zuhorn, I.S. and Hoekstr, D. (2000). *Lipoplex formation under equilibrium conditions reveals a three- step mechanism*. Biophysical journal vol. 79, **7** 1447-1454.

166. Okamoto, K., Kakuma, T., Fukuchi, S., Masaki, T., Sakata, T. and Yoshimatsu, H. (2006). *Sterol regulatory element binding protein (SREBP)-1 expression in brain is affected by age but not by hormones or metabolic changes*. Brain Research 1081, **8** 19-27.

167. Orth, M. and Bellosta, S. (2012). *Cholesterol: Its regulation and role in central nervous system disorders.* Hindawi Pub. Corp. Cholesterol, Art. ID 292598, 19 pages.

168. Pan, Y., Xu, J., Chen, C., Chen, F., Jin, P., Zhu, K., Hu, C. W., You, M. Chen, M., and Hu, F. (2018). *Royal jelly reduces cholesterol levels, ameliorates Aβ pathology and enhances neuronal metabolic activities in a rabbit model of Alzheimer's disease.* Front. Aging neurosci. 10:50. Doi: 10.3389/fnagi.2018.00050.

169. Parker, R.A., Pearce, B.C., Clark, R.W., Gordon, D.A., and Wright, J.J. (1993). *Tocotrienols regulate cholesterol production in mammalian cells by post-transcriptional suppression of 3-hydroxy-3-methylglutaryl-coenzyme a reductase*. J. Biol. Chem. 268, **8** 11230-11238.

170. Pearce, B.C., Parker, P.A., Deason, M.E., Qureshi, A.A. and Wright, J.J.K. (1992). *Hypocholesterolemic activity of synthetic and natural Tocotrienols*. J. Med. Chem. 35, **11** 3595-3606.

171. Petrov, A. M., Kasimov, M. R., and Zefirov, A. L. (2016). *Brain cholesterol metabolism and its defects: Linkage to neurodegenerative diseases and synaptic dysfunction*. Park- media Ltd. ACTA nature, Vol. 8, No. 1 (28).

172. Pierrot, N., Tyteca, D., D'auria, L., Dewachter, I., Gailly, P., Hendrickx, A., Tasiaux, B., El haylani, L., Muls, N., N'kuli, F., Laquerriere, A., Demoulin, J. B., Campion, D., Brion, J. P., Courtoy, P. J., Campard, P. K., and Octave, J. N. (2013). *Amyloid precursor protein controls cholesterol turnover needed for neuronal activity*. EMBO Mol Med 5, 608-625.

173. Pike, L.J. (2003) *Lipid rafts: bringing order to chaos*. Journal of Lipid Research, Vol. **44**.

174. Pillai, R., Uyehara-Lock, J.H. and Bellinger, F.P. (2014). *Selenium and selenoprotein function in brain disorders*. International Union of Biochemistry and Molecular Biology Vol. 66, No. **4**, pages 10 229-239.

175. Qiu, W.Q., Walsh, D.M., Zhen, Y., Vekrellis, K., Jimin, Z., Podlisny, M.P., Rosner, M.R., Afshin, S. and Hersh. L.B. (1998). *Insulin-degrading enzyme regulate extracellular levels of amyloid β-protein by degradation*. The journal of Biological Chemistry, vol. 273, No. **49**, pp. 8 32730-32738.

176. Rampersad, S.N. (2012). *Multiple applications of Alamar Blue as an indicator of metabolic function and cellular health in cell viability bioassays*. Sensors **12**, 12347-12360.

177. Rao, X., Xuelin, H., Zhicheng, Z. and Xin, L. *An improvement of the 2^(-delta delta CT) method for quantitative real-time polymerase chain reaction data analysis.* Biostatistics, Bioinformatics and Biomathematics, **3**(3), 71–85.

178. Ravishankar, D., Corona, G., Hogan, S.M., Spencer, J.P.E., Greco, F. and Osboen, H.M.I. (2016). *Thioflavones as novel neuroprotective agents*. Bioorganic and medicinal chemistry, **24** (21). pp. 7 5513-5520.

179. Redzic, Z. (2011). *Molecular biology of the blood-brain barrier and the blood-cerebrospinal fluid barriers: similarities and differences*. CNS, **5** 8:3.

180. Regitz, C. and Uwe, W. (2014) *Amyloid-beta (Aβ1-42)-induced paralysis in Caenorhabditis elegans is reduced by restricted cholesterol supply*. Neuroscience letters 576, **3** 93-96.

181. Reiter, E., Qing, J., and Stephan, C. (2007). *Anti-inflammatory properties of α- and γ-tocopherol*. Mol. Aspects Med. **28**(5-6): 668-691.

182. Ricciarelli, R., Argellati, F., Pronzato, M.A., Domenicotti, C. (2007). *Vitamin E and neurodegenerative diseases.* Mol. Asp, Med. 28, **15** 591-606.

183. Robinson, S.R. and Bishop, G.M. (2002). *Aβ as a bio flocculant: implications for the amyloid hypothesis of Alzheimer's disease*. Neurobiology of aging, **23** 1051-1072.

184. Roh, H. T., Cho, S. Y., and So, W. Y. (2017). *Obesity promotes oxidative stress and exacerbates blood-brain barrier disruption after high-intensity exercise.* Journal of sport and health science 6 225-230.

185. Rohan, S.H.A., Angela, j., Wickenden, C., Ling-Sun, J., Wilkinson, S.L. (1997). *Cell-specific expression of β-amyloid precursor protein isoform mRNAs and proteins in neurons and astrocytes*. Molecular Brain Research 47, **9** 147-156.

186. Roher, A.E., Kasunic, T.C., Woods, A.S., Cotter, R.J., Ball, M.J. and Fridman, R. (1994). *Proteolysis of Aβ peptide from Alzheimer disease brain by gelatinase A*. Biochmical and biophysical research communications pages Vol. 205, No. 3, **6** 1755-1761.

187. Rondanelli, M., Faliva, M.A., Peroni, G., Moncaglieri, F., Infantino, V., Naso, M. and Perna, S. (2015). *Focus on pivotal role of dietary intake (diet and supplement) and blood levels of tocopherols and tocotrienols in obtaining successful aging*. It. J. Mol. Sci. **16**, 22 23227-23249.

188. Ross. C.A. and Poirier, M.A. (2004). *Protein aggregation and neurodegenerative disease*. Nat. Med. 10 suppl S 10-7.

189. Rushworth, J.V. and Hooper N.M. (2011). *Lipid rafts: linking Alzheimer's amyloid-β production, aggregation, and toxicity at neuronal membranes*. Int. j. of Alzheimer's Disease, Article ID 603052, 14 pages.

190. Saido, T. and Leissring, M.A. (2012). *Proteolytic degradation of amyloid β-protein*. Cold Spring Harb Perspect Mec **2**: a006379.

191. Saito, Y., Matsushima, T. and Suzuki, T. (2013). *Mechanism of Alzheimer amyloid β-protein precursor localization to membrane lipid rafts*. Understanding Alzheimer disease, Chapter 2.

192. Sakai, J., Duncan, E.A., Rawson, R.B., Xianxin, H., Brown, M.S. and Goldstein, J.L. (1996). *Sterol-regulated release of SREBP-2 from cell membranes requires two sequential cleavages, one within a transmembrane segment*. Cell, vol. 85, **9** 1037-1046.

193. Salustri, C., Mariacristina, S., Bucossi, S. and Squitti, R. (2015). *Metals involvement in Alzheimer's disease- a patho-genetic view.* Alzheimer's disease – challenges for the future book, Chapter 4.

194. Sandoval, K.E. and Witt, K.A. (2008). *Blood-brain barrier tight junction permeability and ischemic stroke.* Neurobiology of disease, vol. 32, issue 2, **19** 200-219.

195. Santos, J.R., Gois, A.M., Mendoca, D.M.F. and Freire, M.A. (2014). *Nutritional status, oxidative stress and dementia: the role of selenium in Alzheimer's disease*. Frontiers in neuroscience, Vol. **6** Article 206.

196. Sapir, A., Assaf, T., Thijs, K., Kaitlin, C., Prashant, M., Bardenheier, A., Podolsky, L., Bening-Abu-Shach, U., Boxem, M., Tsui-fen, C., Broday, L. and Sternberg, P.W. (2014). *Controlled sumoylation of the mevalonate pathway enzyme HMGS-1 regulates metabolism during aging*. PNAS **9** E3880-E3889.

197. Schrauzer, G. N. (2002). *Lithium: occurrence, dietary intakes, nutritional essentiality.* Journal of the American college of nutrition, Vol, 21, No. 1, 14-21.

198. Seghezza, S., Diaspro, A., Canale, C. and Dante S. (2014). *Cholesterol drives Aβ(1-42) interaction with lipid rafts in model membranes*. American Chemical Scociety, Langmuir 30, **7** 13934-13941.

199. Selkoe, D.J., American college of physicians, and American physological society. (2004). *Alzheimer disease: mechanistic understanding predicts novel therapies*. Ann. Intern. Med. 140, **9** 627-638.

200. Sen, C.K., Khanna, S., and Roy, S. (2006). *Tocotrienols: vitamin E beyond tocopherols*. Life Sci. 78, **10** 2088-2098.

201. Serpel, L.C. (2000). *Alzheimer's amyloid fibrils: structure and assembly*. Biochimica et Biophysica Acta 1502, **14** 16-30.

202. Setsukinai, K., Yasuteru, U., Katsuko, K., Hideyuki, J.M. And Tetsuo, N. (2003). *Development of Novel fluorescence probes that can reliably detect reactive oxygen species and distinguish specific species*. The journal of Biological Chemistry vol. 278, no. **5**, issue of January 31, pp. 5 3170-3175.

203. Sgarbossa, A., Giacomazza, D. and di Carlo, M. (2015). *Ferulic acid: a hope for Alzheimer's disease therapy from plants.* Nutrients **7**, 18 5764-5782.

204. Shen, Y., Andrzej, J., Rosner, M.R. and Wei-Jen, T. (2006). *Structures of human insulin-degrading enzyme reveal a new substrate recognition mechanism*. Nature, **443**(7113), 870–874. http://doi.org/10.1038/nature05143

205. Shen, Y., Joachimiak, A., Rosner, M.R., and Tang, W. J. (2006). *Structures of human insulin-degrading enzyme reveal a new substrate recognition mechanism.* Nature, 443(7113): 870-874.

206. Shibata, M., Yamada, S., Kumar, S.R., Calero, M., Bading, J., Frangione, B., Holtzman, D.M., Miller, C.A., Strickland, D.K., Ghiso, J. and Zlokovic, B.V. (2000). *Clearance of Alzheimer's amyloid-β1-40 peptide from brain by LDL receptor-related protein-1 at the blood-brain barrier*. J. Clin Invest. 106:**10** 1489-1499.

207. Shirotani, K., Tsubuki, S., Iwata, N., Takaki, Y, Harigaya, W., Maruyama, K., Kiryu-Seo, S., Kiyama, H., Iwata, H., Tomita, T., Iwatsubo, T. and Saido, T.C. (2001). *Neprilysin degrades both amyloid β peptides 1-40 and 1-42 most rapidly and efficiently among thiorphan- and phosphoramidon- sensitive endopeptidases.* The journal of Biological Chemistry vol. 276, no. 24, issue of June 15, pp. **6** 21895-21901.

208. Simons, M., Keller, P., DeStrooper, B., Beyreuther, K., Dotti, C.G., Simons, K. (1998). *Cholesterol depletion inhibits the generation of β-amyloid in hippocampal neurons*. Proc. Natl. Acad. Sci. USA 95, **4** 6460-6464.

209. Slomnicki, L.P. and Wieslawa L. (2008). *A putative role of the amyloid precursor protein intracellular domain (AICD) in transcription*. Acta neurobiol Exp 68: **9** 219-228.

210. Smith, P.K., Krohn, P.I., Hermanson, G.T., Mallia, A.K., Gartner, F.H., Provenzano, M.D., Fujimoto, E.K., Goeke, N.M., Olson, B.J. and Klenk, D.C. (1985). *Measurement of protein using Bicinchoninic acid*. Analytical biochemistry 150, **9** 76-85.

211. Song, B.L., and Russell A.D.B. (2006). *Insig-dependent ubiquitination and degradation of 3-hydroxy-3-methylglutaryl Coenzyme A reductase stimulated by δ- and γ-tocotrienols*. The journal of Biological Chemistry vol. 281, no. 35, pp. **7** 25054-25061.

212. Song, B.L., Navdar, S. and Russel A. (2005). *DeBose-Boyd. Gp78, a membrane-anchored ubiquitin ligase, associate with insig-1 and couples' sterol-regulated ubiquitination to degradation of HNG CoA reductase*. Molecular Cell, Vol. 19, **11** 829-840.

213. Song, E.S., Rodgers, D.W. and Hersh, L.B. (2018). *Insulin-degrading enzyme is not secreted from cultured cells.* Scientific Reports, 8:2335, doi:10.10:38/s41598-018-20597-6.

214. Soscia, S.J., Kirby, J.E., Washicosky, K.J., Tucker, S.M., Ingelsson, M., Hyman, B., Burton, M.A., Goldstein, L.E., Duong, S., Tanzi, R.E., and Moir, R.D. (2010). *The Alzheimer's disease-associated amyloid β-protein is an antimicrobial peptide*. Plos one, Vol. **5**, issue 3, e9505.

215. Spitzer, P., Condic, M., Herrmann, M., Oberstein, T.J., Scharin-Mehlmann, M., Gilbert, D.F., Friedrich, O., Gromer, T., Kornhuber, J., Lang, R. and Maler, J.M. (2016). *Amyloidogenic amyloid -β-peptide variants induce microbial agglutination and exert antimicrobial activity*. Scientific reports, **6**:32228.

216. Sriyudthsak, M. (1987). *Enzyme-immobilized Langmuir-blodgett film for a biosensor*. Third int. conference on Langmuir-Blodgett films, Gottingen, F.R.G., **5** 26-31.

217. Steffen, J., Krohn, M., Schwitlick, C., Btuening, T., Paarmann, K., Pietrzik, C. U., Biverstal, H., Jansone, B., Langer, O., and Pahnke, J. (2017). *Expression of endogenous mouse APP modulates β-amyloid deposition in hAPP-transgenic mice.* Acta neuropathological communications 5:49

218. Stine, W.B., Jungbauer, L., Chunjiang, Y., and Mary J.L. (2011). *Preparing synthetic Aβ in different aggregation states.* Methods Mol Biol. 670: **18** 13-32.

219. Suk, S.H., Sacco, R.L., Boden-Albala, B., Cheun, J.F., Pittman, J.G., Elkind, M.S. (2003). *Abdominal obesity and risk of ischemic stroke the northern Manhattan stroke study*. Stroke pp. **6** 1586-1592.

220. Sultana, R., Ravagna, A., Mohmmad-Abdul, H., Calabrese, V. and Butterfield, D.A. (2005). *Ferulic acid ethyl ester protects neurons against amyloid β-peptide (1-42)-induced oxidative stree and neurotoxicity: relationship to antioxidant activity*. Journal of Neurochemistry, 92, **9** 749-758.

221. Sung, S., Yuemang, Y., Kuunihiro, U., Hengxuan, Y., Virginia M., Lee, -y., Trojanowski, J.Q. and Pratico, D.. (2003). *Early Vitamin E supplementation in young but not aged mice reduces Aβ levels and amyloid deposition in a transgenic model of Alzheimer's disease*. The FASEB journal Vol. 18, No. 2, pp. **2** 323-325.

222. Swomley, A.M., Forster, S., Keeney, J.T., Triplett, J., Zhaoshu, Z., Rukhsana S., Butterfield, A. (2014). *Abeta, oxidative stress in Alzheimer disease: Evidence based on proteomics studies*. Biochmicha et bioophysica acta 1842, **9** 1248-1257.

223. Takaki, Y., Iwata, N., Tsubuki, S., Taniguchi, S., Toyoshima, S., Lu, B., Gerard, N.P., Gerard, C., Hahn-Jun, L., Shirotani, K. and Takaomi C.S. (2000). *Biochemical identification of the neutral endopeptidase family member responsible for the catabolism of amyloid β peptide in the brain.* J. Biochem 128, **5** 897-902.

224. Teles, R.B.A., Diniz, T.C., Pinto, T.C.C., Oliveira R.G., Silva, M.G., Lavor, E.M., Fernandes, A.W.C., Oliveira, A.P., Ribeiro, F.P.R.A., Silva, A.A.M., Cavalcante, T.C.F., Quintans, L.J., and Almeida, J.R.G.S. (2018). *Flavonoids as therapeutic agents in Alzheimer's and Parkinson's diseases: A systematic review of preclinical evidences.* Oxidative medicine and cellular longevity, Article ID 7043213, 21 pages, Hindawi.

225. Thakurta, I.G., Banerjee, P., Bagh, M.B., Ghosh, A., Sahoo, A., and Chattopadhyay, S. (2014). *Combination of N-acetylcysteine, α-lipoic acid and α-tocopherol substantially prevents the brain synaptosomal alterations and memory and learning deficits of aged rats*. Exp. Gerontol., 50, **6** 19-25.

226. Tietz, S. and Engelhardt, B. (2015). *Brain barriers: crosstalk between complex tight junctions and adherents' junctions.* J. Cell Biol. 209: **13** 493-506.

227. Ulamin, F., Shah, S.A. and Kim, M.O. (2010). *Vanilic acid attenuates Aβ1-42-induced oxidative stress and cognitive impairment in mice*. Scientific reports, **7**:40753.

228. Usoro, O.B., and Mousa, S.A. (2010). *Vitamin E forms in Alzheimer's disease: a review of controversial and clinical experiences*. Critical Reviews in Food Science and Nutrition, 50:5, 414-419, DOI: 10.1080/10408390802304222

229. Valastyan, S., Thakur, V., Johnson, A., Kumar, K. and Manor, D. (2008). *Novel transcriptional activities of vitamin E: inhibition of cholesterol biosynthesis*. Biochemistry. 15; 47(2): **8** 744-752.

230. Vekrellis, K., Zhen, Y., Wei, Q.Q., Walsh, D., Hartley, D., Chesneau, V., Rosner, M.R. and Selkoe, D.J. (2000). *Neurons regulate extracellular levels of amyloid β-protein via proteolysis by insulin-degrading enzyme.* The journal of Neuroscience, March 1, 20(5): **8** 1657-1665.

231. Vetrivel, K.S. and Thinakaran, G. (2010). *Membrane rafts in Alzheimer's didsease beta-amyloid production.* Biochim. Biophys. Acta. **1801**(8): 7 860-867.

232. Wallez, Y. and Huber P. (2008). *Endothelial adherens and tight junctions in vascular homeostasis.* Inflammation and angiogenesis. Biochmica. et Biophysica. Acta 1778, **15** 794-809.

233. Wang, D.M., Li, S.Q., Zhu, X.Y., Wang, Y., Wu, W.L. and Zhang. X.J. (2013) *Protective effects of hesperidin against amyloid-β (Aβ) induced neurotoxicity through the voltage dependent anion channel 1 (VDAC1)-mediated mitochondrial apoptotic pathway in PC12 cells*. Neurochem. Res 38: **10** 1034-1044.

234. Wang, D.M., Yang, Y.J., Shang, L., Guan F.F. and Zhang, L.F. (2013). *Naringin enhances CaMKII activity and improves long-term memory in a mouse model of Alzheimer's disease.* Int. L. Mol. Sci. 14, **10** 5576-5586.

235. Wang, D.S., Dickson, D.W. and Malter, J.S. (2006). *B-amyloid degradation and Alzheimer's disease.* Journal of biomedicine and biotechnology Article ID 58406, pages 12.

236. Waterham, H.R. (2006). *Defects of cholesterol biosynthesis*. FEBS letters 580, **7** 5442-5449.

237. Wei, Q.Q., Walsh, D.M., Zhen, Y., Vekrelli, K., Zhang, J., Podlisny, M.B., Rosner, M.R., Safavi, A., Hersh, L.B. (1998). *Insulin -degrading enzyme regulates extracellular levels of amyloid β-protein degradation*. The journal of Biological chemistry, vol. 273, no. 49, issue of December 4, pp. **8** 32730-32738.

238. Weller, R.O., Massey, A., Yu-Min, K. and Roher, A.E. (2000). *Cerebral amyloid angiopathy: accumulation of Aβ in interstitial fluid drainage pathways in Alzheimer's disease*. Cerebral amyloid angiopathy, 903:110-7.

239. Wiedemann, C., Bellstedt, P. and Gorlach, M. (2013). *CAPITO- a web server-based analysis and plotting tool for circular dichroism data*. Bioinformatics, vol. 29 no. **14**, **7** 1750-1757.

240. Wiedemann, C., Bellstedt, P., and Goerlach, M. (2013). *CAPITO – a web server-based analysis and plotting tool for circular dichroism data*. Bioinformatics, Vol. 29 no. 14, pages 1750-1757.

241. Wong, B.X., Hung, Y.H., Bush, A.I. and Duce, J.A. (2014). *Metals and cholesterol: two sides of the same coin in Alzheimer's disease pathology*. Frontiers in aging neurosciences. vol. **6** Article 91, 12.

242. Wong, W.Y., Ward, L.C., Fong, C.W., Yap, W.N. and Brown, L. (2017). *Anti-inflammatory γ- and δ-tocotrienols improve cardiovascular, liver and metabolic function in diet-induced obese rats*. Eur J Nautr 56: **17** 133-150.

243. Wood, W. G., Li, L., Mueller, W. E., and Eckert, G. P. (2014). *Cholesterol as a causative factor in Alzheimer disease: a debatable hypothesis.* J. Neurochem, 2014 May; 129(4): 559-572.

244. World Health Program. (2000). *Obesity: preventing and managing the global epidemic*. Technical report series, 894.

245. Wu, S.J., Liu, P.L. and Lean-Teik, N. (2008). *Tocotrienol-rich fraction of palm oil exhibits anti-inflammatory property by suppressing the expression of inflammatory mediators in human monocytic cells*. Mol Nautr. Food Res. 52, **8** 921-929.

246. Xia, W. and Huanbiao, M. (2016). *Potential of tocotrienols in the prevention and therapy of Alzheimer's disease*. Journal of nutritional biochemistry 31, **8** 1-9.

247. Xu, W., Ferrari, C. and Wang, H.X. (2013). *Epidemiology of Alzheimer's disease*. Understanding Alzeimer's disease book, chapter 13.

248. Xu, Z. (2008). *Comparison of extraction methods for quantifying vitamin E from animal tissues*. Bioresour. Technol. 99, **4** 8705-8709.

249. Ye, J. and DeBose-Boyd, R.A. (2011). *Regulation of cholesterol and fatty acid synthesis.* Cold spring harb pespect boil **3**: a004754.

250. Ye, J., and DeBose-Boyd, R. A. (2011). *Regulation of cholesterol and fatty acid synthesis.* Cold Spring Harb Perspect Biol ;3:a004754.

251. Yeagle, P.L. (1991). *Modulation of membrane function by cholesterol.* Department of biochemistry, University at Buffalo (SUNY), School of medicine.

252. Yoon, J.H., Youn, K., Ho, C.T., Karwe, M.V., Jeong, W.S. and Jun, M. (2014). *p-coumaric acid and ursolic acid from corni fructus attenuated β-amyloid(25-35)-induced toxicity through regulation of the NF-κB signaling pathway in PC12 cells*. ACS pubs. J. Agric. Food Chem. 62, **5** 4911-4916.

253. Younkin, S.G. (1998). *The role of Aβ42 in Alzheimer's disease*. J. Physiology (Paris) 92, **3** 289-292.

254. Zelcer, N., Sharpe, L.J., Loregger, A., Ika, K., Cook, E.C.L., Phan, L., Stevenson, J., and Brown, A.J. (2014). *The E3 ubiquitin ligase MARCH6 degrades squalene monooxygenase and affects 3-hydroxy-3-methyl-glutaryl coenzyme A reductase and the cholesterol synthesis pathway*. Molecular and cell biology. vol. 34, no. 7 pp. **8** 1262-1270.

255. Zhang, J. and Liu, Q. (2015). *Cholesterol metabolism and homeostasis in the brain*. Protein cell, 6(4): **10** 254-264.

256. Zhang, J., and Liu, Q. (2015). *Cholesterol metabolism and homeostasis in the brain*. Protein cell, 6(4):254-264, doi: 10.1007/s 13238-014-0131-3.

257. Zhang, Xin., Vincent, A. S., Halliwell, B., and wong, K. P. (2004). *A mechanism of Sulfite neurotoxicity.* The journal of biological chemistry, by the American society for biochemistry and molecular biology, Inc.

258. Zhao, J., Li, L., and Leissring, M.A. (2009). *Insulin-degrading enzyme is exported via an unconventional protein secretion pathway.* BioMed Central, Molecular Neurodegeneration, 4:4 doi:10.1186/1750-1326-4-4.

259. Zhao, Z., Nelson, A.R., Betsholtz, C. and Zlokovic, B.V. (2015). *Establishment and dysfunction of the blood-brain barrier*. Cell 163, 7.

260. Zlokovic, B.V. (2008). *The blood-brain barrier in health and chronic neurodegenerative disorders.* Neuron 57, **6** 25-31.

261. Zou, T., Duan, Y., Zhou, X., Chen, W., Ying, X., Liu, G., Zhao, Y., Zhu, M., Pari, A., Alimo, K., Miao, H., Kabinur, K., Zhang, L., Wang, Q., and Duan, S. (2019). *Significant association of 3-hydroxy-3-methylglutaryl-CoA reductase (HMGCR) rs3846662 and sirtuin 1 (SIRT1) rs7895833 and apolipoprotein E (APOE) hypermethylation with mild cognitive impairment (MCI).* Medicine. 98(28):e16405, DOI: 10.1097/MD.0000000000016405 PMID: 31305452

Appendix

Appendix A:

List of apparatus, chemicals and disposables

Table A-1: Apparatus and related accessories

Name	**Manufacturer**
Analytical balance	Multiple
CanoScan LiDE 50	Canon
Centrifuges	Multiple
Electronic pipette, 8-channel	Eppendorf
Fluorometer / Luminometer Infinite M1000 pro	Tecan
Fluorometer Safire II	Tecan
Freezer -20°C Premium	Liebherr
Freezer -80°C Hera Freeze	Thermo Electron
Freezer box Cryo container	Nalgene
Gel chamber Novex Mini-cell	Life Technologies
Hamilton capillary	Hamilton
Heating block thermo shaker	Universal Laboratory
Incubator	Different
Incubator Heracell 150	Heraeus
Incubator, 37°C	Heraeus
Light microscope Nikon	Nikon
Magnetic heating stirrer	Heidolph instruments
Mass Spectrometer 4000 QTRAP	AB Sciex
Microwaves	Multiple
MINILYS homogenizer	Peqlab
NanoDrop 8000 UV -Vis spectrophotometer	Thermo Scientific
Nitrogen tank -196°C	Air Liquide
PCR cycler PRIMUS 25 Advanced	Peqlab
pH meter 766	Calimatic kink
PikoReal PCR	Thermo Scientific

Name	Manufacturer
Pipette boy Comfort	Integra Biosciences AG
Pipette set	Eppendorf
Potter tube	B. brown
Precision balance	Different
Precision balance EW	Core
Rotor TLA-55	Beckman Coulter
Single multi pipette M4	Eppendorf
Trans blot gel holder + sponge	BioRad
Transfer chamber	BioRad
Ultracentrifuge Optima LE-80K	Beckman Coulter
Vortex Genie2	Bender & Hobein
Water bath	Multiple
Wheaton shaker multi reax	Heidolph instrument

Table A-2: List of chemical materials used in the study

Name	Supplier
1-Step PNPP	Thermo Scientific
3'-(p-aminophenyl) fluorescein (APF)	Invitrogen
3'-(p-hydrophenyl) fluorescein (HPF)	Invitrogen
Ampicillin	Roth
Aβ1-40 peptide	GenScript
Aβ1-42 peptide	GenScript
Aβ1-42 peptide	Innovagen
Bicinchoninic acid	Sigma Aldrich
BSA	Roth
BSA fatty acid free	Sigma Aldrich
$CaCl_2$.$2H_2O$	Merck Millipore
Chloroform, HPLC grade	Merck Millipore
Complete protease inhibitor cocktail EDTA	Roche
Complete protease inhibitor without EDTA	Roche

Name	Supplier
CuSo4 .5H_2O	Roth
Cycloheximide from Streptomyces	Sigma Aldrich
DMEM	Sigma Aldrich
DMSO	Roth
ECL hyper film	Amersham
ECL solutions	Perkin Elmer
EDTA	Roth
Ethanol HPLC grade	Sigma Aldrich
Fast SYBR green master mix	Life technologies
FCS	PAN Biotech
Fixer	Kodak
GBX developer solutions	Kodak
Glycerin	Roth
HBS buffer	Synvolux theraputics
HEPES	Sigma Aldrich
Isopropanol HPLC grade	VWR
KCl	Merck Millipore
Lipofectamine 2000	Life technologies
MEM amino acid solution	Sigma Aldrich
Methanol HPLC grade	VWR
$MgCl_2$	Roth
Milk powder blotting grade	Roth
NaCl	Applichem
NaCl	Sigma Aldrich
NEM	Santa Cruz technologies
Opti-MEM	Life technologies
Penicillin / Streptomycin solution	Sigma Aldrich
Protein G Sepharose	Sigma Aldrich
Recombinant human IDE	R&D Systems
SDS	Sigma Aldrich
Sodium pyrovate	Sigma Aldrich

Name	Supplier
Sucrose	Sigma Aldrich
Tricine	Biomol
Tris	Sigma Aldrich
Triton X-100	Merch Millipore
TRIzol	Life technologies
Trypsin / EDTA solution	Sigma Aldrich
Tween-20	Sigma Aldrich
Water HPLC grade	VWR
Water RNase-free	Qiagen
$ZnCl_2$	Sigma Aldrich
β-mercapto ethanol	Sigma Aldrich
β-secretase inhibitor II	Calbiochem
β-secretase inhibitor IV	Calbiochem
β-secretase inhibitor X	Calbiochem
γ-secretase substrate	Calbiochem

Table A-3: Disposable materials used in the research

Name	Supplier
10 cm dishes for cell culture	Sarstedt
12-well plate for cell culture	Falcon
24-well plate for cell culture	Falcon
6-well plate for cell culture	Falcon
96 well Maxi-sorp plate, black	VWR
96 well plate for cell culture	Falcon
96 well plate for RT-PCR	Thermo Scientific
96 well plate, black	Costar
96 well plate, transparent	Greiner
96 well plate, white	Nunc
96-deep well plate	Nunc
Amicon Ultra 0.5 ml filter tube 30K	Merck Millipore

Name	Supplier
Filter paper	Whatman
Freezing tubes 1.8 ml	Nunc
Glass beads for MINILYS homogenizer 0.55 mm	Peqlab
Glass bottles, 2 ml	Neolab
Glass pipette	Neolab
Glass tubes	Wheaton
Needels 23G x1”, 0.6 mm x 25 mm	Becton Dickinson & Co.
Needels 24G x 1”, 0.55 mm x 25 mm	Becton Dickinson & Co.
Nitrocellulose membrane, 0.2 µm pore size	Whatman
Nitrocellulose membrane, 0.45 µm pore size	Whatman
Pasteur pipette	VWR
Petri dishes	Sarstedt
Photo copying films	Xerox
Reaction tubes, 1.5 ml	Eppendorf
Reaction tubes. 2 ml	Eppendorf
Rubber scraper	Hartenstein
Sealing film for 96 well plate	Peqlab
Sealing film for RT-PCR plate	Thermo scientific
Silicon mat	Nunc
Syringe, 1 ml	Becton Dickinson & Co.
Tris-Tricine gel, 10-20 %	Anamed gel elctrophoresis
Ultra-centrifuge tubes	Beckman Coulter

Appendix B:

qRT-PCR results of cholesterol, SREBP-1, and IDE genes

Table B-1: Quantification of gene expression for MEF WT, MEF APP Δ CT 15 (MEF dd), and MEF APP/APLP2 -/- (MEF 10.6), first experiment, part one.

Data step:	4		Show channel:	Thresholds:
Sample Group:	Default	Ch 1	No	
Method:	Threshold	Ch 2	No	
Smoothing:	ON	Ch 3	No	
Smoothing window:	5	Ch 4	No	
Baseline:	Trend	Ch 5	Yes	1731.05
Baseline range start:	3			
Baseline range end:	7			

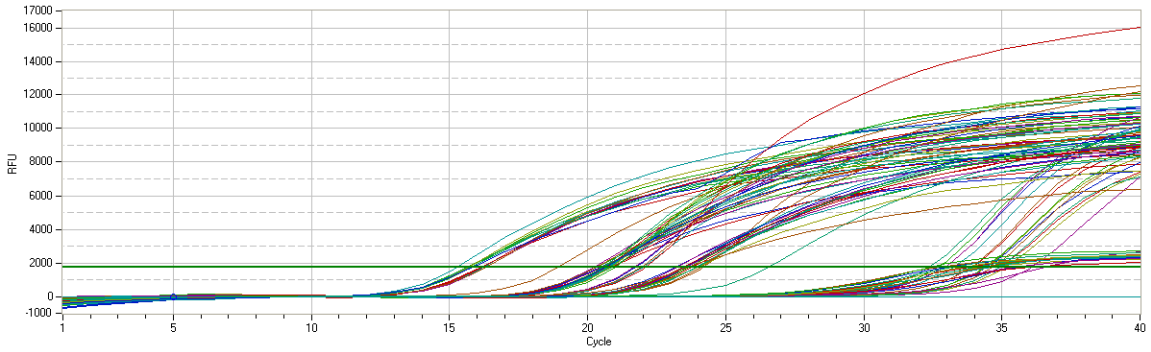

Well	Fluorophore	Sample Type	Sample Name	Target	Cq
A01-Ch5	SYBR	Empty	mef wt 13	Actin Beta	16.14
A02-Ch5	SYBR	Empty	mef wt 15	Actin Beta	18.93
A03-Ch5	SYBR	Empty	mef wt 16	Actin Beta	15.64
A04-Ch5	SYBR	Empty	mef wt 17	Actin Beta	15.64
A05-Ch5	SYBR	Empty	mef wt 18	Actin Beta	15.66
A06-Ch5	SYBR	Empty	mef dd 19	Actin Beta	16.22
A07-Ch5	SYBR	Empty	mef dd 20	Actin Beta	16.19
A08-Ch5	SYBR	Empty	mef dd 22	Actin Beta	16.28
A09-Ch5	SYBR	Empty	mef dd 23	Actin Beta	16.19
A10-Ch5	SYBR	Empty	mef dd24	Actin Beta	16.27
A11-Ch5	SYBR	Empty	mef 10.6 26	Actin Beta	15.67
A12-Ch5	SYBR	Empty	mef 10.6 27	Actin Beta	15.8

A13-Ch5	SYBR	Empty	mef 10.6 28	Actin Beta	15.8
A14-Ch5	SYBR	Empty	mef 10.6 29	Actin Beta	15.25
A15-Ch5	SYBR	Empty	mef 10.6 30	Actin Beta	15.82
A16-Ch5	[none]	[none]			n. def.
B01-Ch5	SYBR	Empty	mef wt 13	hmgcs_1	20.32
B02-Ch5	SYBR	Empty	mef wt 15	hmgcs_1	23.98
B03-Ch5	SYBR	Empty	mef wt 16	hmgcs_1	20.46
B04-Ch5	SYBR	Empty	mef wt 17	hmgcs_1	20.45
B05-Ch5	SYBR	Empty	mef wt 18	hmgcs_1	20.49
B06-Ch5	SYBR	Empty	mef dd 19	hmgcs_1	20.84
B07-Ch5	SYBR	Empty	mef dd 20	hmgcs_1	20.62
B08-Ch5	SYBR	Empty	mef dd 22	hmgcs_1	20.54
B09-Ch5	SYBR	Empty	mef dd 23	hmgcs_1	20.55
B10-Ch5	SYBR	Empty	mef dd24	hmgcs_1	20.85
B11-Ch5	SYBR	Empty	mef 10.6 26	hmgcs_1	20.65
B12-Ch5	SYBR	Empty	mef 10.6 27	hmgcs_1	20.72
B13-Ch5	SYBR	Empty	mef 10.6 28	hmgcs_1	20.2
B14-Ch5	SYBR	Empty	mef 10.6 29	hmgcs_1	20.84
B15-Ch5	SYBR	Empty	mef 10.6 30	hmgcs_1	20.29
B16-Ch5	[none]	[none]			n. def.
C01-Ch5	SYBR	Empty	mef wt 13	hmgcs_2	34.4
C02-Ch5	SYBR	Empty	mef wt 15	hmgcs_2	36.07
C03-Ch5	SYBR	Empty	mef wt 16	hmgcs_2	34.93
C04-Ch5	SYBR	Empty	mef wt 17	hmgcs_2	34.64
C05-Ch5	SYBR	Empty	mef wt 18	hmgcs_2	34.39
C06-Ch5	SYBR	Empty	mef dd 19	hmgcs_2	32.63
C07-Ch5	SYBR	Empty	mef dd 20	hmgcs_2	32.34
C08-Ch5	SYBR	Empty	mef dd 22	hmgcs_2	33.22
C09-Ch5	SYBR	Empty	mef dd 23	hmgcs_2	32.89
C10-Ch5	SYBR	Empty	mef dd24	hmgcs_2	32.92
C11-Ch5	SYBR	Empty	mef 10.6 26	hmgcs_2	33.93
C12-Ch5	SYBR	Empty	mef 10.6 27	hmgcs_2	33.88
C13-Ch5	SYBR	Empty	mef 10.6 28	hmgcs_2	35.15
C14-Ch5	SYBR	Empty	mef 10.6 29	hmgcs_2	34.36
C15-Ch5	SYBR	Empty	mef 10.6 30	hmgcs_2	34.9
C16-Ch5	[none]	[none]			n. def.
D01-Ch5	SYBR	Empty	mef wt 13	hmgcr	20.65
D02-Ch5	SYBR	Empty	mef wt 15	hmgcr	24.19
D03-Ch5	SYBR	Empty	mef wt 16	hmgcr	20.79
D04-Ch5	SYBR	Empty	mef wt 17	hmgcr	20.52
D05-Ch5	SYBR	Empty	mef wt 18	hmgcr	20.74
D06-Ch5	SYBR	Empty	mef dd 19	hmgcr	22
D07-Ch5	SYBR	Empty	mef dd 20	hmgcr	21.73
D08-Ch5	SYBR	Empty	mef dd 22	hmgcr	21.68

D09-Ch5	SYBR	Empty	mef dd 23	hmgcr	22.1
D10-Ch5	SYBR	Empty	mef dd24	hmgcr	21.93
D11-Ch5	SYBR	Empty	mef 10.6 26	hmgcr	20.98
D12-Ch5	SYBR	Empty	mef 10.6 27	hmgcr	21.01
D13-Ch5	SYBR	Empty	mef 10.6 28	hmgcr	20.54
D14-Ch5	SYBR	Empty	mef 10.6 29	hmgcr	20.7
D15-Ch5	SYBR	Empty	mef 10.6 30	hmgcr	20.64
D16-Ch5	[none]	[none]			n. def.
E01-Ch5	SYBR	Empty	mef wt 13	mvk	23.49
E02-Ch5	SYBR	Empty	mef wt 15	mvk	26.54
E03-Ch5	SYBR	Empty	mef wt 16	mvk	23.56
E04-Ch5	SYBR	Empty	mef wt 17	mvk	23.18
E05-Ch5	SYBR	Empty	mef wt 18	mvk	23.26
E06-Ch5	SYBR	Empty	mef dd 19	mvk	23.74
E07-Ch5	SYBR	Empty	mef dd 20	mvk	24.1
E08-Ch5	SYBR	Empty	mef dd 22	mvk	23.98
E09-Ch5	SYBR	Empty	mef dd 23	mvk	23.66
E10-Ch5	SYBR	Empty	mef dd24	mvk	23.94
E11-Ch5	SYBR	Empty	mef 10.6 26	mvk	23.51
E12-Ch5	SYBR	Empty	mef 10.6 27	mvk	23.55
E13-Ch5	SYBR	Empty	mef 10.6 28	mvk	23.54
E14-Ch5	SYBR	Empty	mef 10.6 29	mvk	23.44
E15-Ch5	SYBR	Empty	mef 10.6 30	mvk	23.63
E16-Ch5	[none]	[none]			n. def.
F01-Ch5	SYBR	Empty	mef wt 13	pmvk	32.97
F02-Ch5	SYBR	Empty	mef wt 15	pmvk	36.5
F03-Ch5	SYBR	Empty	mef wt 16	pmvk	33.7
F04-Ch5	SYBR	Empty	mef wt 17	pmvk	32.64
F05-Ch5	SYBR	Empty	mef wt 18	pmvk	34.35
F06-Ch5	SYBR	Empty	mef dd 19	pmvk	34.42
F07-Ch5	SYBR	Empty	mef dd 20	pmvk	33.94
F08-Ch5	SYBR	Empty	mef dd 22	pmvk	34.49
F09-Ch5	SYBR	Empty	mef dd 23	pmvk	35.6
F10-Ch5	SYBR	Empty	mef dd24	pmvk	35.38
F11-Ch5	SYBR	Empty	mef 10.6 26	pmvk	35.93
F12-Ch5	SYBR	Empty	mef 10.6 27	pmvk	34.28
F13-Ch5	SYBR	Empty	mef 10.6 28	pmvk	33.61
F14-Ch5	SYBR	Empty	mef 10.6 29	pmvk	32.39
F15-Ch5	SYBR	Empty	mef 10.6 30	pmvk	33.17
F16-Ch5	[none]	[none]			n. def.

Table B-2 Quantification of gene expression for MEF WT, MEF APP Δ CT 15 (MEF dd), and MEF APP/APLP2 -/- (MEF 10.6), first experiment, part two.

Data step:	4		Show channel:	Thresholds:
Sample Group:	Default	Ch 1	No	
Method:	Threshold	Ch 2	No	
Smoothing:	ON	Ch 3	No	
Smoothing window:	5	Ch 4	No	
Baseline:	Trend	Ch 5	Yes	2403.18
Baseline range start:	3			
Baseline range end:	7			

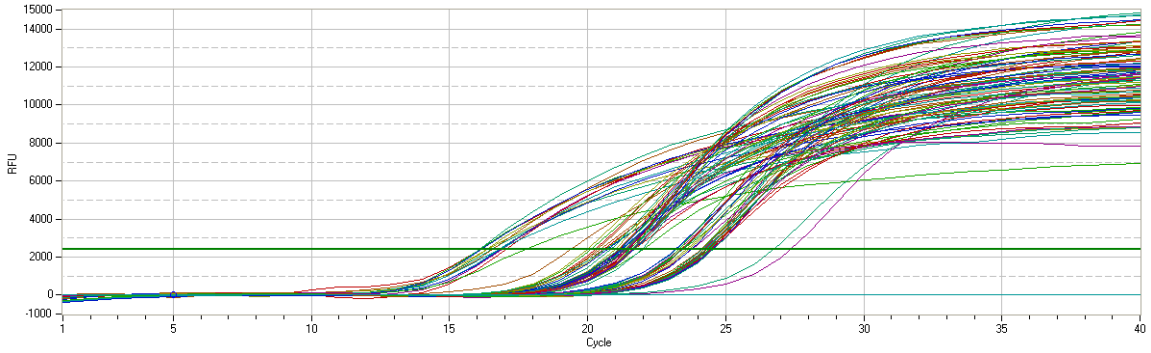

Well	Fluorophore	Sample Type	Sample Name	Target	Cq
A01-Ch5	SYBR	Empty	mef wt 13	Actin Beta	16.11
A02-Ch5	SYBR	Empty	mef wt 15	Actin Beta	19.41
A03-Ch5	SYBR	Empty	mef wt 16	Actin Beta	16.38
A04-Ch5	SYBR	Empty	mef wt 17	Actin Beta	16.09
A05-Ch5	SYBR	Empty	mef wt 18	Actin Beta	16.53
A06-Ch5	SYBR	Empty	mef dd 19	Actin Beta	16.78
A07-Ch5	SYBR	Empty	mef dd 20	Actin Beta	16.84
A08-Ch5	SYBR	Empty	mef dd 22	Actin Beta	16.88
A09-Ch5	SYBR	Empty	mef dd 23	Actin Beta	17.04
A10-Ch5	SYBR	Empty	mef dd 24	Actin Beta	16.56
A11-Ch5	SYBR	Empty	mef 10.6 26	Actin Beta	16.33
A12-Ch5	SYBR	Empty	mef 10.6 27	Actin Beta	17.74
A13-Ch5	SYBR	Empty	mef 10.6 28	Actin Beta	16.08
A14-Ch5	SYBR	Empty	mef 10.6 29	Actin Beta	16.79
A15-Ch5	SYBR	Empty	mef 10.6 30	Actin Beta	16.14
A16-Ch5	[none]	[none]			n. def.
B01-Ch5	SYBR	Empty	mef wt 13	mvd	23.45
B02-Ch5	SYBR	Empty	mef wt 15	mvd	26.74
B03-Ch5	SYBR	Empty	mef wt 16	mvd	23.21

B04-Ch5	SYBR	Empty	mef wt 17	mvd	23.18
B05-Ch5	SYBR	Empty	mef wt 18	mvd	23.31
B06-Ch5	SYBR	Empty	mef dd 19	mvd	24.46
B07-Ch5	SYBR	Empty	mef dd 20	mvd	24.29
B08-Ch5	SYBR	Empty	mef dd 22	mvd	24.19
B09-Ch5	SYBR	Empty	mef dd 23	mvd	24.13
B10-Ch5	SYBR	Empty	mef dd 24	mvd	24.53
B11-Ch5	SYBR	Empty	mef 10.6 26	mvd	24.3
B12-Ch5	SYBR	Empty	mef 10.6 27	mvd	24.51
B13-Ch5	SYBR	Empty	mef 10.6 28	mvd	24.19
B14-Ch5	SYBR	Empty	mef 10.6 29	mvd	24.44
B15-Ch5	SYBR	Empty	mef 10.6 30	mvd	24.23
B16-Ch5	[none]	[none]			n. def.
C01-Ch5	SYBR	Empty	mef wt 13	fdps	20.72
C02-Ch5	SYBR	Empty	mef wt 15	fdps	23.78
C03-Ch5	SYBR	Empty	mef wt 16	fdps	20.59
C04-Ch5	SYBR	Empty	mef wt 17	fdps	20.46
C05-Ch5	SYBR	Empty	mef wt 18	fdps	20.64
C06-Ch5	SYBR	Empty	mef dd 19	fdps	22
C07-Ch5	SYBR	Empty	mef dd 20	fdps	21.48
C08-Ch5	SYBR	Empty	mef dd 22	fdps	21.28
C09-Ch5	SYBR	Empty	mef dd 23	fdps	21.32
C10-Ch5	SYBR	Empty	mef dd 24	fdps	21.47
C11-Ch5	SYBR	Empty	mef 10.6 26	fdps	20.28
C12-Ch5	SYBR	Empty	mef 10.6 27	fdps	20.35
C13-Ch5	SYBR	Empty	mef 10.6 28	fdps	19.98
C14-Ch5	SYBR	Empty	mef 10.6 29	fdps	20.13
C15-Ch5	SYBR	Empty	mef 10.6 30	fdps	20.63
C16-Ch5	[none]	[none]			n. def.
D01-Ch5	SYBR	Empty	mef wt 13	fdtf1	21.66
D02-Ch5	SYBR	Empty	mef wt 15	fdtf1	24.39
D03-Ch5	SYBR	Empty	mef wt 16	fdtf1	21.12
D04-Ch5	SYBR	Empty	mef wt 17	fdtf1	21.36
D05-Ch5	SYBR	Empty	mef wt 18	fdtf1	21.13
D06-Ch5	SYBR	Empty	mef dd 19	fdtf1	21.36
D07-Ch5	SYBR	Empty	mef dd 20	fdtf1	21.33
D08-Ch5	SYBR	Empty	mef dd 22	fdtf1	21.23
D09-Ch5	SYBR	Empty	mef dd 23	fdtf1	21.12
D10-Ch5	SYBR	Empty	mef dd 24	fdtf1	21.34
D11-Ch5	SYBR	Empty	mef 10.6 26	fdtf1	21
D12-Ch5	SYBR	Empty	mef 10.6 27	fdtf1	21.17
D13-Ch5	SYBR	Empty	mef 10.6 28	fdtf1	20.82
D14-Ch5	SYBR	Empty	mef 10.6 29	fdtf1	21.21
D15-Ch5	SYBR	Empty	mef 10.6 30	fdtf1	21.21

D16-Ch5	[none]	[none]			n. def.
E01-Ch5	SYBR	Empty	mef wt 13	sqle	21.6
E02-Ch5	SYBR	Empty	mef wt 15	sqle	24.41
E03-Ch5	SYBR	Empty	mef wt 16	sqle	21.68
E04-Ch5	SYBR	Empty	mef wt 17	sqle	21.2
E05-Ch5	SYBR	Empty	mef wt 18	sqle	21.41
E06-Ch5	SYBR	Empty	mef dd 19	sqle	21.57
E07-Ch5	SYBR	Empty	mef dd 20	sqle	21.59
E08-Ch5	SYBR	Empty	mef dd 22	sqle	21.66
E09-Ch5	SYBR	Empty	mef dd 23	sqle	21.52
E10-Ch5	SYBR	Empty	mef dd 24	sqle	21.95
E11-Ch5	SYBR	Empty	mef 10.6 26	sqle	21.56
E12-Ch5	SYBR	Empty	mef 10.6 27	sqle	21.64
E13-Ch5	SYBR	Empty	mef 10.6 28	sqle	21.62
E14-Ch5	SYBR	Empty	mef 10.6 29	sqle	21.44
E15-Ch5	SYBR	Empty	mef 10.6 30	sqle	21.61
E16-Ch5	[none]	[none]			n. def.
F01-Ch5	SYBR	Empty	mef wt 13	lss	23.43
F02-Ch5	SYBR	Empty	mef wt 15	lss	27.35
F03-Ch5	SYBR	Empty	mef wt 16	lss	23.43
F04-Ch5	SYBR	Empty	mef wt 17	lss	23.39
F05-Ch5	SYBR	Empty	mef wt 18	lss	23.65
F06-Ch5	SYBR	Empty	mef dd 19	lss	24.37
F07-Ch5	SYBR	Empty	mef dd 20	lss	24.27
F08-Ch5	SYBR	Empty	mef dd 22	lss	24.13
F09-Ch5	SYBR	Empty	mef dd 23	lss	23.76
F10-Ch5	SYBR	Empty	mef dd 24	lss	24.46
F11-Ch5	SYBR	Empty	mef 10.6 26	lss	24.32
F12-Ch5	SYBR	Empty	mef 10.6 27	lss	24.1
F13-Ch5	SYBR	Empty	mef 10.6 28	lss	23.57
F14-Ch5	SYBR	Empty	mef 10.6 29	lss	23.3
F15-Ch5	SYBR	Empty	mef 10.6 30	lss	23.44
F16-Ch5	[none]	[none]			n. def.

Table B-3: Quantification of gene expression for MEF WT, MEF APP Δ CT 15 (MEF dd), and MEF APP/APLP2 -/- (MEF 10.6), second experiment, part one.

Data step:	4		Show channel:	Thresholds:
Sample Group:	Default	Ch 1	No	
Method:	Threshold	Ch 2	No	
Smoothing:	ON	Ch 3	No	
Smoothing window:	5	Ch 4	No	

Baseline:	Trend	Ch 5	Yes	727.05
Baseline range start:	3			
Baseline range end:	7			

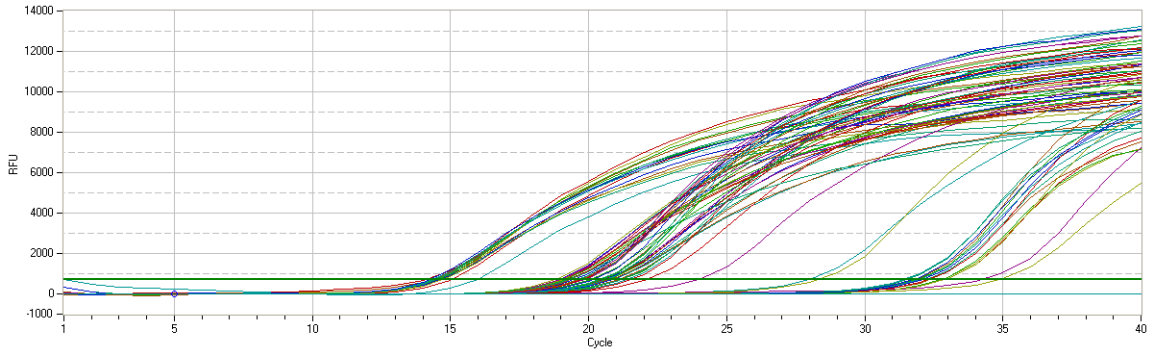

Well	Fluorophore	Sample Type	Sample Name	Target	Cq
A01-Ch5	SYBR	Empty	wT	actin beta	15.06
A02-Ch5	SYBR	Empty	wT	actin beta	14.51
A03-Ch5	SYBR	Empty	wT	actin beta	14.77
A04-Ch5	SYBR	Empty	wT	actin beta	14.42
A05-Ch5	SYBR	Empty	wT	actin beta	14.7
A06-Ch5	SYBR	Empty	DD	actin beta	15.98
A07-Ch5	SYBR	Empty	DD	actin beta	14.65
A08-Ch5	SYBR	Empty	DD	actin beta	24.03
A09-Ch5	SYBR	Empty	DD	actin beta	14.1
A10-Ch5	SYBR	Empty	DD	actin beta	14.34
A11-Ch5	SYBR	Empty	10.6	actin beta	14.72
A12-Ch5	SYBR	Empty	10.6	actin beta	14.53
A13-Ch5	SYBR	Empty	10.6	actin beta	14.49
A14-Ch5	SYBR	Empty	10.6	actin beta	14.39
A15-Ch5	SYBR	Empty	10.6	actin beta	14.24
A16-Ch5	[none]	[none]			n. def.
B01-Ch5	SYBR	Empty	wT	polr2	20.69
B02-Ch5	SYBR	Empty	wT	polr2	20.84
B03-Ch5	SYBR	Empty	wT	polr2	20.9
B04-Ch5	SYBR	Empty	wT	polr2	20.52
B05-Ch5	SYBR	Empty	wT	polr2	20.6
B06-Ch5	SYBR	Empty	DD	polr2	22.11
B07-Ch5	SYBR	Empty	DD	polr2	21.14
B08-Ch5	SYBR	Empty	DD	polr2	34.95
B09-Ch5	SYBR	Empty	DD	polr2	21.21

B10-Ch5	SYBR	Empty	DD	polr2	21.16
B11-Ch5	SYBR	Empty	10.6	polr2	21.39
B12-Ch5	SYBR	Empty	10.6	polr2	20.87
B13-Ch5	SYBR	Empty	10.6	polr2	20.59
B14-Ch5	SYBR	Empty	10.6	polr2	20.61
B15-Ch5	SYBR	Empty	10.6	polr2	20.8
B16-Ch5	[none]	[none]			n. def.
C01-Ch5	SYBR	Empty	wT	hmcs1	19.5
C02-Ch5	SYBR	Empty	wT	hmcs1	19.06
C03-Ch5	SYBR	Empty	wT	hmcs1	19.25
C04-Ch5	SYBR	Empty	wT	hmcs1	19.17
C05-Ch5	SYBR	Empty	wT	hmcs1	19.1
C06-Ch5	SYBR	Empty	DD	hmcs1	20.11
C07-Ch5	SYBR	Empty	DD	hmcs1	19.03
C08-Ch5	SYBR	Empty	DD	hmcs1	28.05
C09-Ch5	SYBR	Empty	DD	hmcs1	19.01
C10-Ch5	SYBR	Empty	DD	hmcs1	19.01
C11-Ch5	SYBR	Empty	10.6	hmcs1	19.13
C12-Ch5	SYBR	Empty	10.6	hmcs1	19.34
C13-Ch5	SYBR	Empty	10.6	hmcs1	18.82
C14-Ch5	SYBR	Empty	10.6	hmcs1	19.19
C15-Ch5	SYBR	Empty	10.6	hmcs1	19.28
C16-Ch5	[none]	[none]			n. def.
D01-Ch5	SYBR	Empty	wT	hmgcs2	32.94
D02-Ch5	SYBR	Empty	wT	hmgcs2	32.34
D03-Ch5	SYBR	Empty	wT	hmgcs2	32.81
D04-Ch5	SYBR	Empty	wT	hmgcs2	32.75
D05-Ch5	SYBR	Empty	wT	hmgcs2	32.27
D06-Ch5	SYBR	Empty	DD	hmgcs2	31.45
D07-Ch5	SYBR	Empty	DD	hmgcs2	32.13
D08-Ch5	SYBR	Empty	DD	hmgcs2	34.24
D09-Ch5	SYBR	Empty	DD	hmgcs2	32.3
D10-Ch5	SYBR	Empty	DD	hmgcs2	31.8
D11-Ch5	SYBR	Empty	10.6	hmgcs2	32.96
D12-Ch5	SYBR	Empty	10.6	hmgcs2	31.96
D13-Ch5	SYBR	Empty	10.6	hmgcs2	31.53
D14-Ch5	SYBR	Empty	10.6	hmgcs2	32.02
D15-Ch5	SYBR	Empty	10.6	hmgcs2	31.75
D16-Ch5	[none]	[none]			n. def.
E01-Ch5	SYBR	Empty	wT	hmgcr	20.44
E02-Ch5	SYBR	Empty	wT	hmgcr	19.6
E03-Ch5	SYBR	Empty	wT	hmgcr	19.84
E04-Ch5	SYBR	Empty	wT	hmgcr	19.78
E05-Ch5	SYBR	Empty	wT	hmgcr	19.7

E06-Ch5	SYBR	Empty	DD	hmgcr	21.56
E07-Ch5	SYBR	Empty	DD	hmgcr	20.37
E08-Ch5	SYBR	Empty	DD	hmgcr	28.34
E09-Ch5	SYBR	Empty	DD	hmgcr	20.64
E10-Ch5	SYBR	Empty	DD	hmgcr	20.41
E11-Ch5	SYBR	Empty	10.6	hmgcr	20.58
E12-Ch5	SYBR	Empty	10.6	hmgcr	20.19
E13-Ch5	SYBR	Empty	10.6	hmgcr	19.87
E14-Ch5	SYBR	Empty	10.6	hmgcr	19.77
E15-Ch5	SYBR	Empty	10.6	hmgcr	19.73

Table B-4: Quantification of gene expression for MEF WT, MEF APP Δ CT 15 (MEF dd), and MEF APP/APLP2 -/- (MEF 10.6), second experiment, part two.

Data step:	4		Show channel:	Thresholds:
Sample Group:	Default	Ch 1	No	
Method:	Threshold	Ch 2	No	
Smoothing:	ON	Ch 3	No	
Smoothing window:	5	Ch 4	No	
Baseline:	Trend	Ch 5	Yes	764.99
Baseline range start:	3			
Baseline range end:	7			

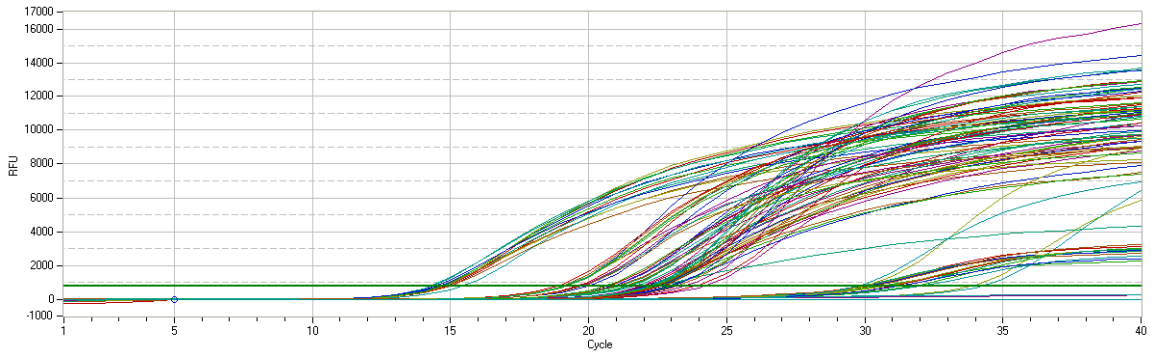

Well	Fluorophore	Sample Type	Sample Name	Target	Cq
A01-Ch5	SYBR	Empty	WT	actin beta	14.94
A02-Ch5	SYBR	Empty	WT	actin beta	14.78
A03-Ch5	SYBR	Empty	WT	actin beta	14.69
A04-Ch5	SYBR	Empty	WT	actin beta	14.56
A05-Ch5	SYBR	Empty	WT	actin beta	14.68

A06-Ch5	SYBR	Empty	DD	actin beta	15.38
A07-Ch5	SYBR	Empty	DD	actin beta	14.57
A08-Ch5	SYBR	Empty	DD	actin beta	24.15
A09-Ch5	SYBR	Empty	DD	actin beta	14.84
A10-Ch5	SYBR	Empty	DD	actin beta	14.99
A11-Ch5	SYBR	Empty	10.6	actin beta	14.74
A12-Ch5	SYBR	Empty	10.6	actin beta	14.62
A13-Ch5	SYBR	Empty	10.6	actin beta	14.27
A14-Ch5	SYBR	Empty	10.6	actin beta	14.22
A15-Ch5	SYBR	Empty	10.6	actin beta	14.38
A16-Ch5	[none]	[none]			n. def.
B01-Ch5	SYBR	Empty	WT	polr2	20.87
B02-Ch5	SYBR	Empty	WT	polr2	21.1
B03-Ch5	SYBR	Empty	WT	polr2	20.88
B04-Ch5	SYBR	Empty	WT	polr2	20.63
B05-Ch5	SYBR	Empty	WT	polr2	20.8
B06-Ch5	SYBR	Empty	DD	polr2	22.24
B07-Ch5	SYBR	Empty	DD	polr2	21.3
B08-Ch5	SYBR	Empty	DD	polr2	33.85
B09-Ch5	SYBR	Empty	DD	polr2	21.33
B10-Ch5	SYBR	Empty	DD	polr2	21.59
B11-Ch5	SYBR	Empty	10.6	polr2	21.39
B12-Ch5	SYBR	Empty	10.6	polr2	20.83
B13-Ch5	SYBR	Empty	10.6	polr2	21.01
B14-Ch5	SYBR	Empty	10.6	polr2	20.64
B15-Ch5	SYBR	Empty	10.6	polr2	21
B16-Ch5	[none]	[none]			n. def.
C01-Ch5	SYBR	Empty	WT	mvk	22.88
C02-Ch5	SYBR	Empty	WT	mvk	22.43
C03-Ch5	SYBR	Empty	WT	mvk	22.44
C04-Ch5	SYBR	Empty	WT	mvk	22.34
C05-Ch5	SYBR	Empty	WT	mvk	22.4
C06-Ch5	SYBR	Empty	DD	mvk	23.03
C07-Ch5	SYBR	Empty	DD	mvk	22.03
C08-Ch5	SYBR	Empty	DD	mvk	34.19
C09-Ch5	SYBR	Empty	DD	mvk	22.12
C10-Ch5	SYBR	Empty	DD	mvk	21.87
C11-Ch5	SYBR	Empty	10.6	mvk	22.02
C12-Ch5	SYBR	Empty	10.6	mvk	22.27
C13-Ch5	SYBR	Empty	10.6	mvk	22.3
C14-Ch5	SYBR	Empty	10.6	mvk	22.47
C15-Ch5	SYBR	Empty	10.6	mvk	22.48
C16-Ch5	[none]	[none]			n. def.
D01-Ch5	SYBR	Empty	WT	pmvk	30.01

D02-Ch5	SYBR	Empty	WT	pmvk	29.85
D03-Ch5	SYBR	Empty	WT	pmvk	29.85
D04-Ch5	SYBR	Empty	WT	pmvk	30.44
D05-Ch5	SYBR	Empty	WT	pmvk	29.75
D06-Ch5	SYBR	Empty	DD	pmvk	32.05
D07-Ch5	SYBR	Empty	DD	pmvk	30.06
D08-Ch5	SYBR	Empty	DD	pmvk	n. def.
D09-Ch5	SYBR	Empty	DD	pmvk	31
D10-Ch5	SYBR	Empty	DD	pmvk	30.09
D11-Ch5	SYBR	Empty	10.6	pmvk	30.74
D12-Ch5	SYBR	Empty	10.6	pmvk	31.68
D13-Ch5	SYBR	Empty	10.6	pmvk	31.15
D14-Ch5	SYBR	Empty	10.6	pmvk	n. def.
D15-Ch5	SYBR	Empty	10.6	pmvk	31.24
D16-Ch5	[none]	[none]			n. def.
E01-Ch5	SYBR	Empty	WT	mvd	22.55
E02-Ch5	SYBR	Empty	WT	mvd	22.21
E03-Ch5	SYBR	Empty	WT	mvd	22.13
E04-Ch5	SYBR	Empty	WT	mvd	22.45
E05-Ch5	SYBR	Empty	WT	mvd	21.9
E06-Ch5	SYBR	Empty	DD	mvd	22.64
E07-Ch5	SYBR	Empty	DD	mvd	22.37
E08-Ch5	SYBR	Empty	DD	mvd	30
E09-Ch5	SYBR	Empty	DD	mvd	22.28
E10-Ch5	SYBR	Empty	DD	mvd	22.16
E11-Ch5	SYBR	Empty	10.6	mvd	22.15
E12-Ch5	SYBR	Empty	10.6	mvd	23.04
E13-Ch5	SYBR	Empty	10.6	mvd	23.48
E14-Ch5	SYBR	Empty	10.6	mvd	23.87
E15-Ch5	SYBR	Empty	10.6	mvd	23.13
E16-Ch5	[none]	[none]			n. def.
F01-Ch5	SYBR	Empty	WT	fdps	19.12
F02-Ch5	SYBR	Empty	WT	fdps	19.08
F03-Ch5	SYBR	Empty	WT	fdps	18.82
F04-Ch5	SYBR	Empty	WT	fdps	19.03
F05-Ch5	SYBR	Empty	WT	fdps	19.06
F06-Ch5	SYBR	Empty	DD	fdps	20.52
F07-Ch5	SYBR	Empty	DD	fdps	19.65
F08-Ch5	SYBR	Empty	DD	fdps	29.7
F09-Ch5	SYBR	Empty	DD	fdps	19.97
F10-Ch5	SYBR	Empty	DD	fdps	19.65
F11-Ch5	SYBR	Empty	10.6	fdps	19.52
F12-Ch5	SYBR	Empty	10.6	fdps	19.73
F13-Ch5	SYBR	Empty	10.6	fdps	19.11

F14-Ch5	SYBR	Empty	10.6	fdps	19.16
F15-Ch5	SYBR	Empty	10.6	fdps	19.12
F16-Ch5	[none]	[none]			n. def.

Table B-5: Quantification of gene expression for MEF WT, MEF APP Δ CT 15 (MEF dd), and MEF APP/APLP2 -/- (MEF 10.6), second experiment, part three.

Data step:	4		Show channel:	Thresholds:
Sample Group:	Default	Ch 1	No	
Method:	Threshold	Ch 2	No	
Smoothing:	ON	Ch 3	No	
Smoothing window:	5	Ch 4	No	
Baseline:	Trend	Ch 5	Yes	1026.33
Baseline range start:	3			
Baseline range end:	7			

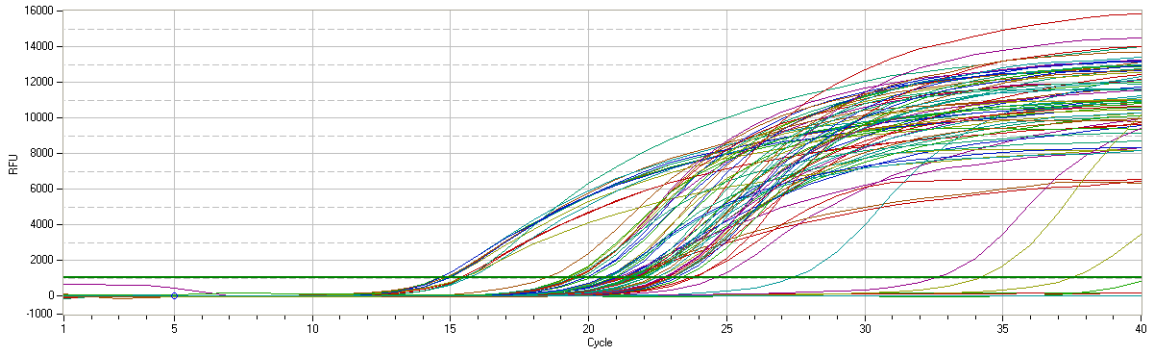

Well	Fluorophore	Sample Type	Sample Name	Target	Cq
A01-Ch5	SYBR	Empty	WT	actin beta	15.3
A02-Ch5	SYBR	Empty	WT	actin beta	14.83
A03-Ch5	SYBR	Empty	WT	actin beta	14.93
A04-Ch5	SYBR	Empty	WT	actin beta	14.55
A05-Ch5	SYBR	Empty	WT	actin beta	14.86
A06-Ch5	SYBR	Empty	DD	actin beta	15.6
A07-Ch5	SYBR	Empty	DD	actin beta	14.96
A08-Ch5	SYBR	Empty	DD	actin beta	24.55
A09-Ch5	SYBR	Empty	DD	actin beta	15.42
A10-Ch5	SYBR	Empty	DD	actin beta	14.78
A11-Ch5	SYBR	Empty	10.6	actin beta	15.41
A12-Ch5	SYBR	Empty	10.6	actin beta	n. def.
A13-Ch5	SYBR	Empty	10.6	actin beta	15.46
A14-Ch5	SYBR	Empty	10.6	actin beta	14.6

A15-Ch5	SYBR	Empty	10.6	actin beta	14.56
A16-Ch5	[none]	[none]			n. def.
B01-Ch5	SYBR	Empty	WT	polr2	21.67
B02-Ch5	SYBR	Empty	WT	polr2	21.86
B03-Ch5	SYBR	Empty	WT	polr2	21.83
B04-Ch5	SYBR	Empty	WT	polr2	21.17
B05-Ch5	SYBR	Empty	WT	polr2	21.54
B06-Ch5	SYBR	Empty	DD	polr2	22.9
B07-Ch5	SYBR	Empty	DD	polr2	21.73
B08-Ch5	SYBR	Empty	DD	polr2	37.39
B09-Ch5	SYBR	Empty	DD	polr2	21.8
B10-Ch5	SYBR	Empty	DD	polr2	21.64
B11-Ch5	SYBR	Empty	10.6	polr2	21.45
B12-Ch5	SYBR	Empty	10.6	polr2	21.2
B13-Ch5	SYBR	Empty	10.6	polr2	21.02
B14-Ch5	SYBR	Empty	10.6	polr2	21.24
B15-Ch5	SYBR	Empty	10.6	polr2	21.16
B16-Ch5	[none]	[none]			n. def.
C01-Ch5	SYBR	Empty	WT	fdft	19.88
C02-Ch5	SYBR	Empty	WT	fdft	19.33
C03-Ch5	SYBR	Empty	WT	fdft	n. def.
C04-Ch5	SYBR	Empty	WT	fdft	18.4
C05-Ch5	SYBR	Empty	WT	fdft	19.33
C06-Ch5	SYBR	Empty	DD	fdft	20.05
C07-Ch5	SYBR	Empty	DD	fdft	19.59
C08-Ch5	SYBR	Empty	DD	fdft	27.32
C09-Ch5	SYBR	Empty	DD	fdft	19.86
C10-Ch5	SYBR	Empty	DD	fdft	19.45
C11-Ch5	SYBR	Empty	10.6	fdft	19.41
C12-Ch5	SYBR	Empty	10.6	fdft	19.48
C13-Ch5	SYBR	Empty	10.6	fdft	19.22
C14-Ch5	SYBR	Empty	10.6	fdft	19.19
C15-Ch5	SYBR	Empty	10.6	fdft	19.31
C16-Ch5	[none]	[none]			n. def.
D01-Ch5	SYBR	Empty	WT	sqle	23.68
D02-Ch5	SYBR	Empty	WT	sqle	21.43
D03-Ch5	SYBR	Empty	WT	sqle	22.38
D04-Ch5	SYBR	Empty	WT	sqle	21.43
D05-Ch5	SYBR	Empty	WT	sqle	21.37
D06-Ch5	SYBR	Empty	DD	sqle	22.01
D07-Ch5	SYBR	Empty	DD	sqle	20.98
D08-Ch5	SYBR	Empty	DD	sqle	32.56
D09-Ch5	SYBR	Empty	DD	sqle	21.63
D10-Ch5	SYBR	Empty	DD	sqle	20.63

D11-Ch5	SYBR	Empty	10.6	sqle	20.52
D12-Ch5	SYBR	Empty	10.6	sqle	20.84
D13-Ch5	SYBR	Empty	10.6	sqle	20.59
D14-Ch5	SYBR	Empty	10.6	sqle	20.62
D15-Ch5	SYBR	Empty	10.6	sqle	20.47
D16-Ch5	[none]	[none]			n. def.
E01-Ch5	SYBR	Empty	WT	lss	23.31
E02-Ch5	SYBR	Empty	WT	lss	22.93
E03-Ch5	SYBR	Empty	WT	lss	23.01
E04-Ch5	SYBR	Empty	WT	lss	22.63
E05-Ch5	SYBR	Empty	WT	lss	22.72
E06-Ch5	SYBR	Empty	DD	lss	23.76
E07-Ch5	SYBR	Empty	DD	lss	22.24
E08-Ch5	SYBR	Empty	DD	lss	34.11
E09-Ch5	SYBR	Empty	DD	lss	n. def.
E10-Ch5	SYBR	Empty	DD	lss	22.01
E11-Ch5	SYBR	Empty	10.6	lss	22.38
E12-Ch5	SYBR	Empty	10.6	lss	23.15
E13-Ch5	SYBR	Empty	10.6	lss	22.63
E14-Ch5	SYBR	Empty	10.6	lss	22.78
E15-Ch5	SYBR	Empty	10.6	lss	22.93

Table B-6: Quantification of gene expression for MEF WT and MEF APP Δ CT 15 (MEF dd), third experiment, part one.

Data step:	4		Show channel:	Thresholds:
Sample Group:	Default	Ch 1	No	
Method:	Threshold	Ch 2	No	
Smoothing:	ON	Ch 3	No	
Smoothing window:	5	Ch 4	No	
Baseline:	Trend	Ch 5	Yes	1501,66
Baseline range start:	3			
Baseline range end:	7			

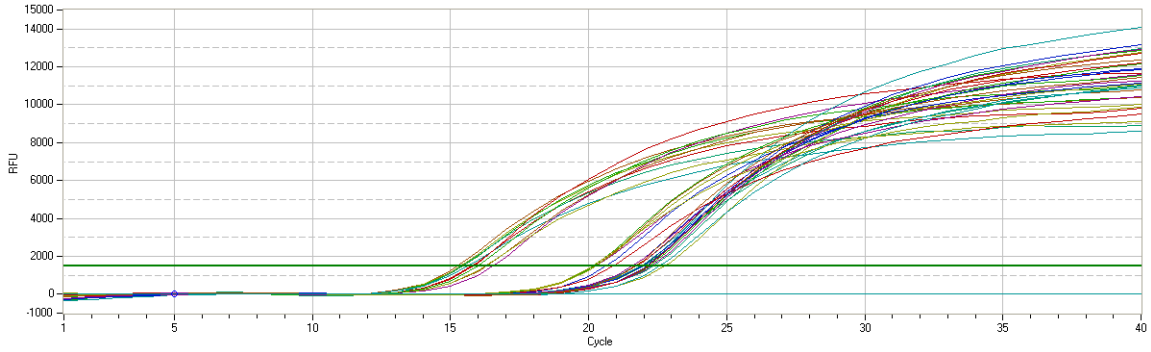

Well	Fluorophore	Sample Type	Sample Name	Target	Cq
A01-Ch5	SYBR	Empty	wT	actin beta	15,77
A02-Ch5	SYBR	Empty	wT	actin beta	15,26
A03-Ch5	SYBR	Empty	wT	actin beta	15,36
A04-Ch5	SYBR	Empty	wT	actin beta	15,46
A05-Ch5	SYBR	Empty	wT	actin beta	15,44
A06-Ch5	SYBR	Empty	wT	actin beta	15,65
A07-Ch5	[none]	[none]			n. def.
A08-Ch5	SYBR	Empty	wt 3	actin beta	16,54
A09-Ch5	SYBR	Empty	DD	actin beta	15,85
A10-Ch5	SYBR	Empty	DD	actin beta	16,31
A11-Ch5	SYBR	Empty	DD	actin beta	16,28
A12-Ch5	SYBR	Empty	DD	actin beta	16,01
A13-Ch5	[none]	[none]			n. def.
A14-Ch5	[none]	[none]			n. def.
A15-Ch5	[none]	[none]			n. def.
A16-Ch5	[none]	[none]			n. def.
B01-Ch5	SYBR	Empty	wT	polr2	22
B02-Ch5	SYBR	Empty	wT	polr2	21,91
B03-Ch5	SYBR	Empty	wT	polr2	21,71
B04-Ch5	SYBR	Empty	wT	polr2	21,58
B05-Ch5	SYBR	Empty	wT	polr2	21,57
B06-Ch5	SYBR	Empty	wT	polr2	21,73
B07-Ch5	[none]	[none]			n. def.
B08-Ch5	SYBR	Empty	DD	polr2	22,75
B09-Ch5	SYBR	Empty	DD	polr2	22,18
B10-Ch5	SYBR	Empty	DD	polr2	22,31
B11-Ch5	SYBR	Empty	DD	polr2	21,99
B12-Ch5	SYBR	Empty	DD	polr2	21,98
B13-Ch5	[none]	[none]			n. def.
B14-Ch5	[none]	[none]			n. def.
B15-Ch5	[none]	[none]			n. def.
B16-Ch5	[none]	[none]			n. def.

C01-Ch5	SYBR	Empty	wT	hmgcr	20,62
C02-Ch5	SYBR	Empty	wT	hmgcr	20,28
C03-Ch5	SYBR	Empty	wT	hmgcr	20,91
C04-Ch5	SYBR	Empty	wT	hmgcr	20,24
C05-Ch5	SYBR	Empty	wT	hmgcr	20,28
C06-Ch5	SYBR	Empty	wT	hmgcr	20,19
C07-Ch5	[none]	[none]			n. def.
C08-Ch5	SYBR	Empty	DD	hmgcr	22,59
C09-Ch5	SYBR	Empty	DD	hmgcr	22,11
C10-Ch5	SYBR	Empty	DD	hmgcr	22,28
C11-Ch5	SYBR	Empty	DD	hmgcr	22,15
C12-Ch5	SYBR	Empty	DD	hmgcr	21,68
C13-Ch5	SYBR	Empty	wt 3	hmgcr	20,17

Table B-7: Quantification of gene expression for MEF WT and MEF APP Δ CT 15 (DD), third experiment, part two.

Data step:	4		Show channel:	Thresholds:
Sample Group:	Default	Ch 1	No	
Method:	Threshold	Ch 2	No	
Smoothing:	ON	Ch 3	No	
Smoothing window:	5	Ch 4	No	
Baseline:	Trend	Ch 5	Yes	1696,96
Baseline range start:	3			
Baseline range end:	7			

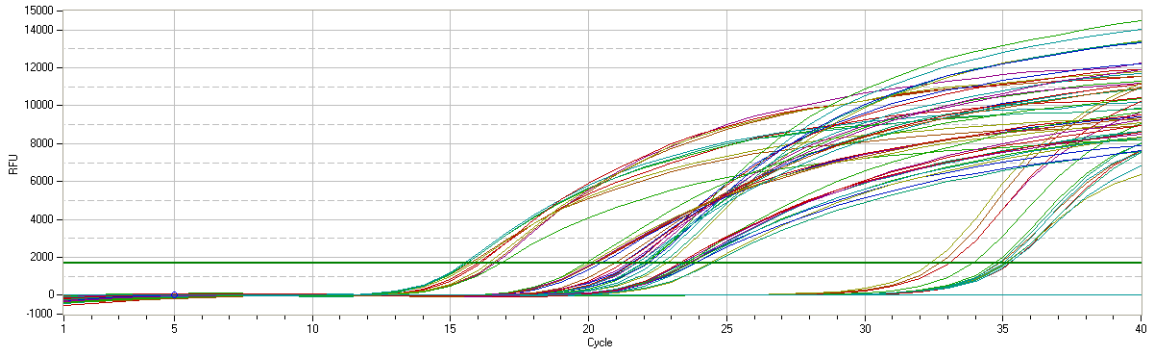

Well	Fluorophore	Sample Type	Sample Name	Target	Cq
A01-Ch5	SYBR	Empty	wt	actin beta	16,01
A02-Ch5	SYBR	Empty	wt	actin beta	15,7
A03-Ch5	SYBR	Empty	wt	actin beta	15,82
A04-Ch5	SYBR	Empty	wt	actin beta	15,61
A05-Ch5	SYBR	Empty	wt	actin beta	15,56

A06-Ch5	SYBR	Empty	wt	actin beta	15,5
A07-Ch5	[none]	[none]			n. def.
A08-Ch5	SYBR	Empty	DD	actin beta	16,61
A09-Ch5	SYBR	Empty	DD	actin beta	16,1
A10-Ch5	SYBR	Empty	DD	actin beta	16,52
A11-Ch5	SYBR	Empty	DD	actin beta	16,37
A12-Ch5	SYBR	Empty	DD	actin beta	16,81
A13-Ch5	[none]	[none]			n. def.
A14-Ch5	[none]	[none]			n. def.
A15-Ch5	[none]	[none]			n. def.
A16-Ch5	[none]	[none]			n. def.
B01-Ch5	SYBR	Empty	wt	polr2	22,08
B02-Ch5	SYBR	Empty	wt	polr2	22
B03-Ch5	SYBR	Empty	wt	polr2	21,95
B04-Ch5	SYBR	Empty	wt	polr2	21,52
B05-Ch5	SYBR	Empty	wt	polr2	21,73
B06-Ch5	SYBR	Empty	wt	polr2	21,59
B07-Ch5	[none]	[none]			n. def.
B08-Ch5	SYBR	Empty	DD	polr2	22,81
B09-Ch5	SYBR	Empty	DD	polr2	22,07
B10-Ch5	SYBR	Empty	DD	polr2	22,65
B11-Ch5	SYBR	Empty	DD	polr2	22,34
B12-Ch5	SYBR	Empty	DD	polr2	22,14
B13-Ch5	[none]	[none]			n. def.
B14-Ch5	[none]	[none]			n. def.
B15-Ch5	[none]	[none]			n. def.
B16-Ch5	[none]	[none]			n. def.
C01-Ch5	SYBR	Empty	wt	hmgcs1	20,43
C02-Ch5	SYBR	Empty	wt	hmgcs1	20,18
C03-Ch5	SYBR	Empty	wt	hmgcs1	20,26
C04-Ch5	SYBR	Empty	wt	hmgcs1	20,26
C05-Ch5	SYBR	Empty	wt	hmgcs1	20,05
C06-Ch5	SYBR	Empty	wt	hmgcs1	19,91
C07-Ch5	[none]	[none]			n. def.
C08-Ch5	SYBR	Empty	DD	hmgcs1	21,72
C09-Ch5	SYBR	Empty	DD	hmgcs1	21,19
C10-Ch5	SYBR	Empty	DD	hmgcs1	21,42
C11-Ch5	SYBR	Empty	DD	hmgcs1	21,22
C12-Ch5	SYBR	Empty	DD	hmgcs1	20,96
C13-Ch5	[none]	[none]			n. def.
C14-Ch5	[none]	[none]			n. def.
C15-Ch5	[none]	[none]			n. def.
C16-Ch5	[none]	[none]			n. def.
D01-Ch5	SYBR	Empty	wt	hmgcs2	35,24

D02-Ch5	SYBR	Empty	wt	hmgcs2	34,9
D03-Ch5	SYBR	Empty	wt	hmgcs2	35,1
D04-Ch5	SYBR	Empty	wt	hmgcs2	34,68
D05-Ch5	SYBR	Empty	wt	hmgcs2	34,83
D06-Ch5	SYBR	Empty	wt	hmgcs2	35,03
D07-Ch5	[none]	[none]			n. def.
D08-Ch5	SYBR	Empty	DD	hmgcs2	33,06
D09-Ch5	SYBR	Empty	DD	hmgcs2	33,06
D10-Ch5	SYBR	Empty	DD	hmgcs2	32,69
D11-Ch5	SYBR	Empty	DD	hmgcs2	32,37
D12-Ch5	SYBR	Empty	DD	hmgcs2	33,91
D13-Ch5	SYBR	Empty	wt	hmgcs2	35,13
D14-Ch5	SYBR	Empty	wt	hmgcs2	35,24
D15-Ch5	[none]	[none]			n. def.
D16-Ch5	[none]	[none]			n. def.
E01-Ch5	SYBR	Empty	wt	mvk	23,7
E02-Ch5	SYBR	Empty	wt	mvk	23,41
E03-Ch5	SYBR	Empty	wt	mvk	23,47
E04-Ch5	SYBR	Empty	wt	mvk	23,64
E05-Ch5	SYBR	Empty	wt	mvk	23,39
E06-Ch5	SYBR	Empty	wt	mvk	23,3
E07-Ch5	[none]	[none]			n. def.
E08-Ch5	SYBR	Empty	DD	mvk	24,39
E09-Ch5	SYBR	Empty	DD	mvk	23,53
E10-Ch5	SYBR	Empty	DD	mvk	24,47
E11-Ch5	SYBR	Empty	DD	mvk	23,85
E12-Ch5	SYBR	Empty	DD	mvk	23,83
E13-Ch5	SYBR	Empty	wt	mvk	23,62
E14-Ch5	SYBR	Empty	wt	mvk	23,31

Table B-8: Quantification of gene expression for MEF WT and MEF APP Δ CT 15 (DD), third experiment, part three.

Data step:	4		Show channel:	Thresholds:
Sample Group:	Default	Ch 1	No	
Method:	Threshold	Ch 2	No	
Smoothing:	ON	Ch 3	No	
Smoothing window:	5	Ch 4	No	
Baseline:	Trend	Ch 5	Yes	2069,06
Baseline range start:	3			
Baseline range end:	7			

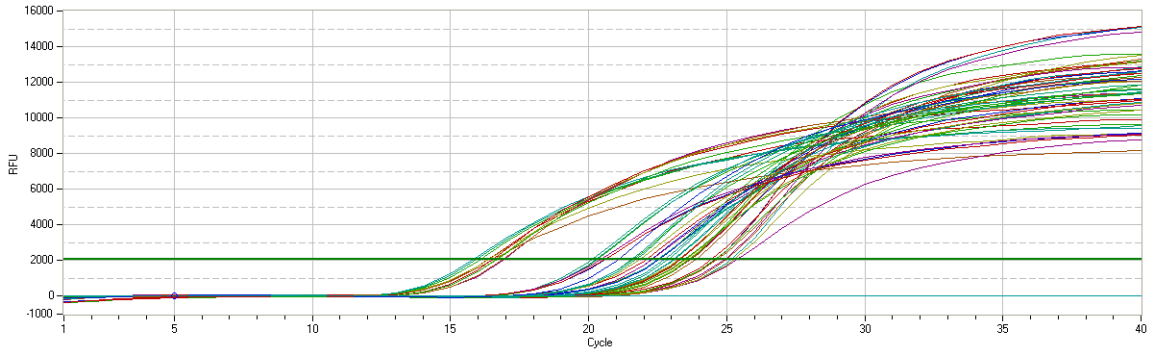

Well	Fluorophore	Sample Type	Sample Name	Target	Cq
A01-Ch5	SYBR	Empty	wt	actin beta	16,36
A02-Ch5	SYBR	Empty	wt	actin beta	16,53
A03-Ch5	SYBR	Empty	wt	actin beta	16,37
A04-Ch5	SYBR	Empty	wt	actin beta	16,08
A05-Ch5	SYBR	Empty	wt	actin beta	15,95
A06-Ch5	SYBR	Empty	wt	actin beta	15,83
A07-Ch5	[none]	[none]			n. def.
A08-Ch5	SYBR	Empty	DD	actin beta	16,93
A09-Ch5	SYBR	Empty	DD	actin beta	16,49
A10-Ch5	SYBR	Empty	DD	actin beta	16,9
A11-Ch5	SYBR	Empty	DD	actin beta	16,66
A12-Ch5	SYBR	Empty	DD	actin beta	16,66
A13-Ch5	[none]	[none]			n. def.
A14-Ch5	[none]	[none]			n. def.
A15-Ch5	[none]	[none]			n. def.
A16-Ch5	[none]	[none]			n. def.
B01-Ch5	SYBR	Empty	wt	polr2	22,5
B02-Ch5	SYBR	Empty	wt	polr2	22,5
B03-Ch5	SYBR	Empty	wt	polr2	22,5
B04-Ch5	SYBR	Empty	wt	polr2	22,28
B05-Ch5	SYBR	Empty	wt	polr2	22,28
B06-Ch5	SYBR	Empty	wt	polr2	22,07
B07-Ch5	[none]	[none]			n. def.
B08-Ch5	SYBR	Empty	DD	polr2	23,25
B09-Ch5	SYBR	Empty	DD	polr2	22,55
B10-Ch5	SYBR	Empty	DD	polr2	23,11
B11-Ch5	SYBR	Empty	DD	polr2	22,73
B12-Ch5	SYBR	Empty	DD	polr2	22,55
B13-Ch5	[none]	[none]			n. def.
B14-Ch5	[none]	[none]			n. def.
B15-Ch5	[none]	[none]			n. def.
B16-Ch5	[none]	[none]			n. def.

C01-Ch5	SYBR	Empty	wt	pmvk	23,91
C02-Ch5	SYBR	Empty	wt	pmvk	23,66
C03-Ch5	SYBR	Empty	wt	pmvk	23,71
C04-Ch5	SYBR	Empty	wt	pmvk	23,89
C05-Ch5	SYBR	Empty	wt	pmvk	23,62
C06-Ch5	SYBR	Empty	wt	pmvk	23,65
C07-Ch5	[none]	[none]			n. def.
C08-Ch5	SYBR	Empty	DD	pmvk	25,16
C09-Ch5	SYBR	Empty	DD	pmvk	24,57
C10-Ch5	SYBR	Empty	DD	pmvk	24,93
C11-Ch5	SYBR	Empty	DD	pmvk	24,58
C12-Ch5	SYBR	Empty	DD	pmvk	24,66
C13-Ch5	[none]	[none]			n. def.
C14-Ch5	[none]	[none]			n. def.
C15-Ch5	[none]	[none]			n. def.
C16-Ch5	[none]	[none]			n. def.
D01-Ch5	SYBR	Empty	wt	mvd	23,31
D02-Ch5	SYBR	Empty	wt	mvd	23,28
D03-Ch5	SYBR	Empty	wt	mvd	23,51
D04-Ch5	SYBR	Empty	wt	mvd	23,47
D05-Ch5	SYBR	Empty	wt	mvd	22,9
D06-Ch5	SYBR	Empty	wt	mvd	23,09
D07-Ch5	[none]	[none]			n. def.
D08-Ch5	SYBR	Empty	DD	mvd	25,38
D09-Ch5	SYBR	Empty	DD	mvd	24,43
D10-Ch5	SYBR	Empty	DD	mvd	24,99
D11-Ch5	SYBR	Empty	DD	mvd	25,24
D12-Ch5	SYBR	Empty	DD	mvd	24,57
D13-Ch5	[none]	[none]			n. def.
D14-Ch5	[none]	[none]			n. def.
D15-Ch5	[none]	[none]			n. def.
D16-Ch5	[none]	[none]			n. def.
E01-Ch5	SYBR	Empty	wt	fdps	20,29
E02-Ch5	SYBR	Empty	wt	fdps	20,12
E03-Ch5	SYBR	Empty	wt	fdps	20,27
E04-Ch5	SYBR	Empty	wt	fdps	20,61
E05-Ch5	SYBR	Empty	wt	fdps	20,43
E06-Ch5	SYBR	Empty	wt	fdps	20,57
E07-Ch5	[none]	[none]			n. def.
E08-Ch5	SYBR	Empty	DD	fdps	21,83
E09-Ch5	SYBR	Empty	DD	fdps	21,59
E10-Ch5	SYBR	Empty	DD	fdps	21,68
E11-Ch5	SYBR	Empty	DD	fdps	21,54
E12-Ch5	SYBR	Empty	DD	fdps	21,08

Table B-9: Quantification of gene expression for MEF WT and MEF APP Δ CT 15 (DD), third experiment, part four.

Data step:	4		Show channel:	Thresholds:
Sample Group:	Default	Ch 1	No	
Method:	Threshold	Ch 2	No	
Smoothing:	ON	Ch 3	No	
Smoothing window:	5	Ch 4	No	
Baseline:	Trend	Ch 5	Yes	2081,28
Baseline range start:	3			
Baseline range end:	7			

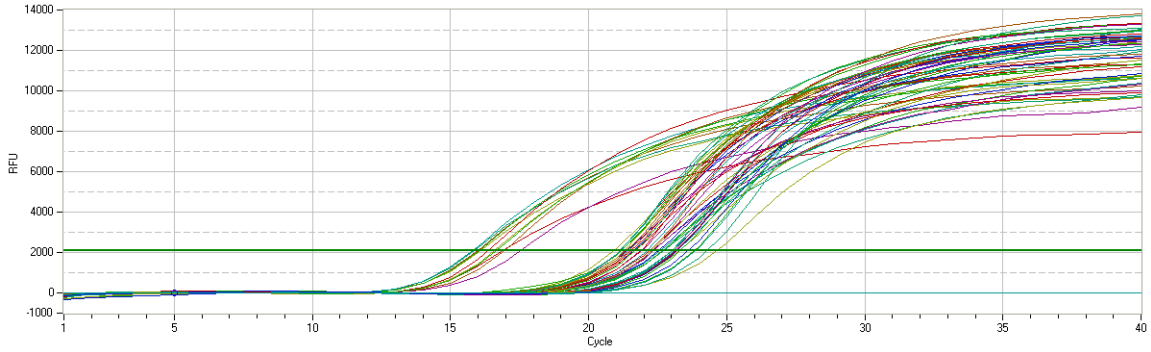

Well	Fluorophore	Sample Type	Sample Name	Target	Cq
A01-Ch5	SYBR	Empty	WT	actin beta	16,88
A02-Ch5	SYBR	Empty	WT	actin beta	15,97
A03-Ch5	SYBR	Empty	WT	actin beta	16,09
A04-Ch5	SYBR	Empty	WT	actin beta	16,02
A05-Ch5	SYBR	Empty	WT	actin beta	15,84
A06-Ch5	SYBR	Empty	WT	actin beta	15,78
A07-Ch5	[none]	[none]			n. def.
A08-Ch5	SYBR	Empty	DD	actin beta	17,51
A09-Ch5	SYBR	Empty	DD	actin beta	16,34
A10-Ch5	SYBR	Empty	DD	actin beta	16,92
A11-Ch5	SYBR	Empty	DD	actin beta	16,57
A12-Ch5	SYBR	Empty	DD	actin beta	16,64
A13-Ch5	[none]	[none]			n. def.
A14-Ch5	[none]	[none]			n. def.
A15-Ch5	[none]	[none]			n. def.
A16-Ch5	[none]	[none]			n. def.
B01-Ch5	SYBR	Empty	WT	polr2	22,65
B02-Ch5	SYBR	Empty	WT	polr2	22,7
B03-Ch5	SYBR	Empty	WT	polr2	22,57
B04-Ch5	SYBR	Empty	WT	polr2	22,31

B05-Ch5	SYBR	Empty	WT	polr2	22,32
B06-Ch5	SYBR	Empty	WT	polr2	22,17
B07-Ch5	[none]	[none]			n. def.
B08-Ch5	SYBR	Empty	DD	polr2	23,29
B09-Ch5	SYBR	Empty	DD	polr2	22,66
B10-Ch5	SYBR	Empty	DD	polr2	23,17
B11-Ch5	SYBR	Empty	DD	polr2	23,03
B12-Ch5	SYBR	Empty	DD	polr2	22,51
B13-Ch5	[none]	[none]			n. def.
B14-Ch5	[none]	[none]			n. def.
B15-Ch5	[none]	[none]			n. def.
B16-Ch5	[none]	[none]			n. def.
C01-Ch5	SYBR	Empty	WT	fdft	21,39
C02-Ch5	SYBR	Empty	WT	fdft	21,32
C03-Ch5	SYBR	Empty	WT	fdft	20,91
C04-Ch5	SYBR	Empty	WT	fdft	21,17
C05-Ch5	SYBR	Empty	WT	fdft	20,91
C06-Ch5	SYBR	Empty	WT	fdft	21,16
C07-Ch5	[none]	[none]			n. def.
C08-Ch5	SYBR	Empty	DD	fdft	22,08
C09-Ch5	SYBR	Empty	DD	fdft	21,6
C10-Ch5	SYBR	Empty	DD	fdft	21,91
C11-Ch5	SYBR	Empty	DD	fdft	21,51
C12-Ch5	SYBR	Empty	DD	fdft	21,44
C13-Ch5	[none]	[none]			n. def.
C14-Ch5	[none]	[none]			n. def.
C15-Ch5	[none]	[none]			n. def.
C16-Ch5	[none]	[none]			n. def.
D01-Ch5	SYBR	Empty	WT	sqle	21,63
D02-Ch5	SYBR	Empty	WT	sqle	21,36
D03-Ch5	SYBR	Empty	WT	sqle	21,25
D04-Ch5	SYBR	Empty	WT	sqle	21,16
D05-Ch5	SYBR	Empty	WT	sqle	21,11
D06-Ch5	SYBR	Empty	WT	sqle	21,13
D07-Ch5	[none]	[none]			n. def.
D08-Ch5	SYBR	Empty	DD	sqle	22,31
D09-Ch5	SYBR	Empty	DD	sqle	21,85
D10-Ch5	SYBR	Empty	DD	sqle	22,24
D11-Ch5	SYBR	Empty	DD	sqle	22,27
D12-Ch5	SYBR	Empty	DD	sqle	21,65
D13-Ch5	[none]	[none]			n. def.
D14-Ch5	[none]	[none]			n. def.
D15-Ch5	[none]	[none]			n. def.
D16-Ch5	[none]	[none]			n. def.

E01-Ch5	SYBR	Empty	WT	lss	23,3
E02-Ch5	SYBR	Empty	WT	lss	23,03
E03-Ch5	SYBR	Empty	WT	lss	23,08
E04-Ch5	SYBR	Empty	WT	lss	23,2
E05-Ch5	SYBR	Empty	WT	lss	23,12
E06-Ch5	SYBR	Empty	WT	lss	23,16
E07-Ch5	[none]	[none]			n. def.
E08-Ch5	SYBR	Empty	DD	lss	24,63
E09-Ch5	SYBR	Empty	DD	lss	23,8
E10-Ch5	SYBR	Empty	DD	lss	24,28
E11-Ch5	SYBR	Empty	DD	lss	23,87
E12-Ch5	SYBR	Empty	DD	lss	23,57

Table B-10: Quantification of gene expression for MEF WT and MEF APP/APLP2 -/- (MEF 10.6), third experiment, part one.

Data step:	4		Show channel:	Thresholds:
Sample Group:	Default	Ch 1	No	
Method:	Threshold	Ch 2	No	
Smoothing:	ON	Ch 3	No	
Smoothing window:	5	Ch 4	No	
Baseline:	Trend	Ch 5	Yes	1868,34
Baseline range start:	3			
Baseline range end:	7			

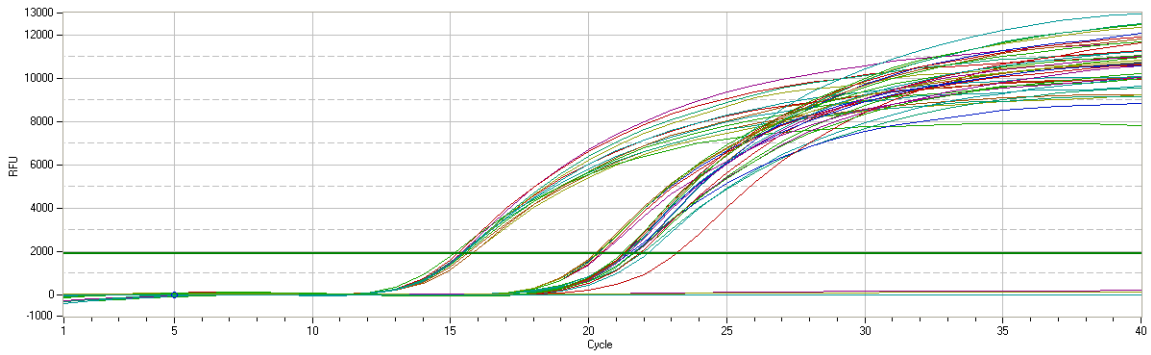

Well	Fluorophore	Sample Type	Sample Name	Target	Cq
A01-Ch5	SYBR	Empty	WT	actin beta	15,36
A02-Ch5	SYBR	Empty	WT	actin beta	15,59
A03-Ch5	SYBR	Empty	WT	actin beta	15,76

A04-Ch5	SYBR	Empty	WT	actin beta	15,1
A05-Ch5	SYBR	Empty	WT	actin beta	15,37
A06-Ch5	SYBR	Empty	WT	actin beta	15,37
A07-Ch5	[none]	[none]			n. def.
A08-Ch5	SYBR	Empty	10,6	actin beta	15,35
A09-Ch5	SYBR	Empty	10,6	actin beta	15,23
A10-Ch5	SYBR	Empty	10,6	actin beta	15,74
A11-Ch5	SYBR	Empty	10,6	actin beta	15,47
A12-Ch5	SYBR	Empty	10,6 (11)	actin beta	15,49
A13-Ch5	SYBR	Empty	WT	actin beta	15,42
A14-Ch5	SYBR	Empty	10,6 (12)	actin beta	15,44
A15-Ch5	[none]	[none]			n. def.
A16-Ch5	[none]	[none]			n. def.
B01-Ch5	SYBR	Empty	WT	polr2	21,77
B02-Ch5	SYBR	Empty	WT	polr2	21,88
B03-Ch5	SYBR	Empty	WT	polr2	22,08
B04-Ch5	SYBR	Empty	WT	polr2	21,43
B05-Ch5	SYBR	Empty	WT	polr2	21,59
B06-Ch5	SYBR	Empty	WT	polr2	21,79
B07-Ch5	[none]	[none]			n. def.
B08-Ch5	SYBR	Empty	10,6	polr2	21,61
B09-Ch5	SYBR	Empty	10,6	polr2	21,27
B10-Ch5	SYBR	Empty	10,6	polr2	21,55
B11-Ch5	SYBR	Empty	10,6	polr2	21,31
B12-Ch5	SYBR	Empty	10,6 (10)	polr2	21,55
B13-Ch5	SYBR	Empty	10,6	polr2	n. def.
B14-Ch5	SYBR	Empty	10,6 (12)	polr2	23,15
B15-Ch5	[none]	[none]			n. def.
B16-Ch5	[none]	[none]			n. def.
C01-Ch5	SYBR	Empty	WT	hmgcr	20,27
C02-Ch5	SYBR	Empty	WT	hmgcr	20,46
C03-Ch5	SYBR	Empty	WT	hmgcr	20,39
C04-Ch5	SYBR	Empty	WT	hmgcr	20,2
C05-Ch5	SYBR	Empty	WT	hmgcr	20,25
C06-Ch5	SYBR	Empty	WT	hmgcr	20,33
C07-Ch5	[none]	[none]			n. def.
C08-Ch5	SYBR	Empty	10,6	hmgcr	21,31
C09-Ch5	SYBR	Empty	10,6	hmgcr	21,25
C10-Ch5	SYBR	Empty	10,6	hmgcr	21,37
C11-Ch5	SYBR	Empty	10,6	hmgcr	21,22
C12-Ch5	SYBR	Empty	10,6 (11)	hmgcr	21,27
C13-Ch5	SYBR	Empty	10,6	hmgcr	n. def.
C14-Ch5	SYBR	Empty	10,6 (12)	hmgcr	21,17

Table B-11: Quantification of gene expression for MEF WT and MEF APP/APLP2 -/- (MEF clone 10.6), third experiment, part two.

Data step:	4		Show channel:	Thresholds:
Sample Group:	Default	Ch 1	No	
Method:	Threshold	Ch 2	No	
Smoothing:	ON	Ch 3	No	
Smoothing window:	5	Ch 4	No	
Baseline:	Trend	Ch 5	Yes	1717,82
Baseline range start:	3			
Baseline range end:	7			

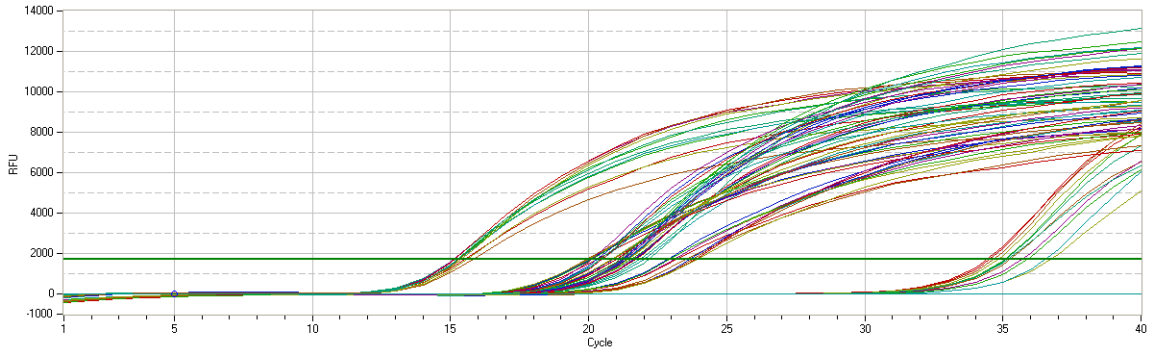

Well	Fluorophore	Sample Type	Sample Name	Target	Cq
A01-Ch5	SYBR	Empty	WT	actin beta	15,55
A02-Ch5	SYBR	Empty	WT	actin beta	15,83
A03-Ch5	SYBR	Empty	WT	actin beta	15,59
A04-Ch5	SYBR	Empty	WT	actin beta	15,31
A05-Ch5	SYBR	Empty	WT	actin beta	15,13
A06-Ch5	SYBR	Empty	WT	actin beta	15,33
A07-Ch5	[none]	[none]			n. def.
A08-Ch5	SYBR	Empty	10,6	actin beta	15,14
A09-Ch5	SYBR	Empty	10,6	actin beta	15,16
A10-Ch5	SYBR	Empty	10,6	actin beta	15,32
A11-Ch5	SYBR	Empty	10,6	actin beta	15,39
A12-Ch5	SYBR	Empty	10,6	actin beta	15,28
A13-Ch5	SYBR	Empty	10,6	actin beta	15,25
A14-Ch5	[none]	[none]			n. def.
A15-Ch5	[none]	[none]			n. def.
A16-Ch5	[none]	[none]			n. def.
B01-Ch5	SYBR	Empty	WT	polr2	21,54

B02-Ch5	SYBR	Empty	WT	polr2	21,85
B03-Ch5	SYBR	Empty	WT	polr2	21,99
B04-Ch5	SYBR	Empty	WT	polr2	21,64
B05-Ch5	SYBR	Empty	WT	polr2	21,6
B06-Ch5	SYBR	Empty	WT	polr2	21,68
B07-Ch5	[none]	[none]			n. def.
B08-Ch5	SYBR	Empty	10,6	polr2	21,42
B09-Ch5	SYBR	Empty	10,6	polr2	21,24
B10-Ch5	SYBR	Empty	10,6	polr2	22,16
B11-Ch5	SYBR	Empty	10,6	polr2	21,36
B12-Ch5	SYBR	Empty	10,6	polr2	21,36
B13-Ch5	SYBR	Empty	10,6	polr2	21,18
B14-Ch5	[none]	[none]			n. def.
B15-Ch5	[none]	[none]			n. def.
B16-Ch5	[none]	[none]			n. def.
C01-Ch5	SYBR	Empty	WT	hmgcs1	20,06
C02-Ch5	SYBR	Empty	WT	hmgcs1	20,32
C03-Ch5	SYBR	Empty	WT	hmgcs1	20,33
C04-Ch5	SYBR	Empty	WT	hmgcs1	19,97
C05-Ch5	SYBR	Empty	WT	hmgcs1	19,98
C06-Ch5	SYBR	Empty	WT	hmgcs1	20,12
C07-Ch5	[none]	[none]			n. def.
C08-Ch5	SYBR	Empty	10,6	hmgcs1	20,83
C09-Ch5	SYBR	Empty	10,6	hmgcs1	20,9
C10-Ch5	SYBR	Empty	10,6	hmgcs1	21,01
C11-Ch5	SYBR	Empty	10,6	hmgcs1	21,01
C12-Ch5	SYBR	Empty	10,6	hmgcs1	20,86
C13-Ch5	SYBR	Empty	10,6	hmgcs1	20,82
C14-Ch5	[none]	[none]			n. def.
C15-Ch5	[none]	[none]			n. def.
C16-Ch5	[none]	[none]			n. def.
D01-Ch5	SYBR	Empty	WT	hmgcs2	34,4
D02-Ch5	SYBR	Empty	WT	hmgcs2	35,25
D03-Ch5	SYBR	Empty	WT	hmgcs2	36,72
D04-Ch5	SYBR	Empty	WT	hmgcs2	35,92
D05-Ch5	SYBR	Empty	WT	hmgcs2	35,12
D06-Ch5	SYBR	Empty	WT	hmgcs2	36,53
D07-Ch5	[none]	[none]			n. def.
D08-Ch5	SYBR	Empty	10,6	hmgcs2	35,69
D09-Ch5	SYBR	Empty	10,6	hmgcs2	34,51
D10-Ch5	SYBR	Empty	10,6	hmgcs2	34,67
D11-Ch5	SYBR	Empty	10,6	hmgcs2	34,82
D12-Ch5	SYBR	Empty	10,6	hmgcs2	35,08
D13-Ch5	SYBR	Empty	10,6	hmgcs2	35,19

D14-Ch5	[none]	[none]			n. def.
D15-Ch5	[none]	[none]			n. def.
D16-Ch5	[none]	[none]			n. def.
E01-Ch5	SYBR	Empty	WT	hmgcr	20,32
E02-Ch5	SYBR	Empty	WT	hmgcr	20,41
E03-Ch5	SYBR	Empty	WT	hmgcr	20,49
E04-Ch5	SYBR	Empty	WT	hmgcr	20,3
E05-Ch5	SYBR	Empty	WT	hmgcr	20,13
E06-Ch5	SYBR	Empty	WT	hmgcr	20,49
E07-Ch5	[none]	[none]			n. def.
E08-Ch5	SYBR	Empty	10,6	hmgcr	21,42
E09-Ch5	SYBR	Empty	10,6	hmgcr	21,13
E10-Ch5	SYBR	Empty	10,6	hmgcr	21,23
E11-Ch5	SYBR	Empty	10,6	hmgcr	21,27
E12-Ch5	SYBR	Empty	10,6	hmgcr	21,26
E13-Ch5	SYBR	Empty	10,6	hmgcr	21,29
E14-Ch5	[none]	[none]			n. def.
E15-Ch5	[none]	[none]			n. def.
E16-Ch5	[none]	[none]			n. def.
F01-Ch5	SYBR	Empty	WT	mvk	22,86
F02-Ch5	SYBR	Empty	WT	mvk	23,14
F03-Ch5	SYBR	Empty	WT	mvk	23,21
F04-Ch5	SYBR	Empty	WT	mvk	23,56
F05-Ch5	SYBR	Empty	WT	mvk	22,95
F06-Ch5	SYBR	Empty	WT	mvk	22,96
F07-Ch5	[none]	[none]			n. def.
F08-Ch5	SYBR	Empty	10,6	mvk	23,68
F09-Ch5	SYBR	Empty	10,6	mvk	23,67
F10-Ch5	SYBR	Empty	10,6	mvk	23,75
F11-Ch5	SYBR	Empty	10,6	mvk	23,86
F12-Ch5	SYBR	Empty	10,6	mvk	23,76
F13-Ch5	SYBR	Empty	10,6	mvk	23,92

Table B-12: Quantification of gene expression for MEF WT and MEF APP/APLP2 -/- (MEF clone 10.6), third experiment, part three.

Data step:	4		Show channel:	Thresholds:
Sample Group:	Default	Ch 1	No	
Method:	Threshold	Ch 2	No	
Smoothing:	ON	Ch 3	No	
Smoothing window:	5	Ch 4	No	
Baseline:	Trend	Ch 5	Yes	1739,97
Baseline range start:	3			
Baseline range end:	7			

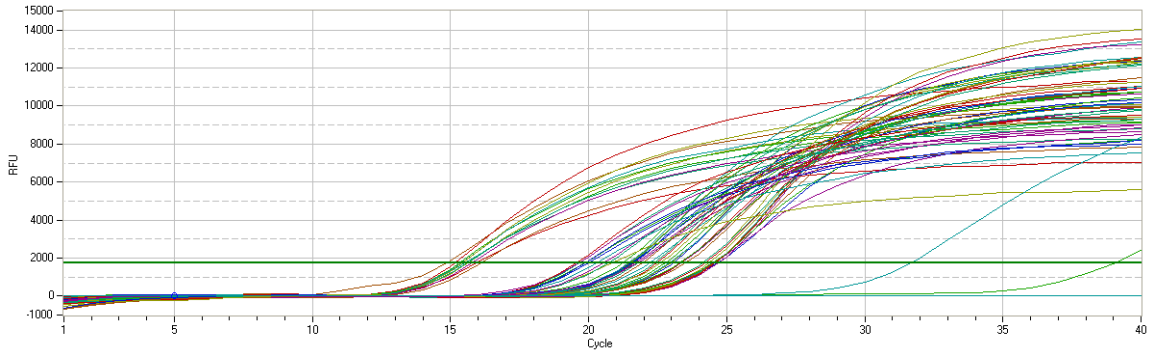

Well	Fluorophore	Sample Type	Sample Name	Target	Cq
A01-Ch5	SYBR	Empty	WT	actin beta	15,96
A02-Ch5	SYBR	Empty	WT	actin beta	14,88
A03-Ch5	SYBR	Empty	WT	actin beta	15,62
A04-Ch5	SYBR	Empty	WT	actin beta	15,32
A05-Ch5	SYBR	Empty	WT	actin beta	15,53
A06-Ch5	SYBR	Empty	WT	actin beta	15,4
A07-Ch5	[none]	[none]			n. def.
A08-Ch5	SYBR	Empty	10,6	actin beta	15,76
A09-Ch5	SYBR	Empty	10,6	actin beta	15,17
A10-Ch5	SYBR	Empty	10,6	actin beta	16,1
A11-Ch5	SYBR	Empty	10,6	actin beta	15,41
A12-Ch5	SYBR	Empty	10,6	actin beta	15,6
A13-Ch5	SYBR	Empty	10,6	actin beta	15,61
A14-Ch5	[none]	[none]			n. def.
A15-Ch5	[none]	[none]			n. def.
A16-Ch5	[none]	[none]			n. def.
B01-Ch5	SYBR	Empty	WT	polr2	21,6
B02-Ch5	SYBR	Empty	WT	polr2	21,76
B03-Ch5	SYBR	Empty	WT	polr2	22,21
B04-Ch5	SYBR	Empty	WT	polr2	21,58
B05-Ch5	SYBR	Empty	WT	polr2	21,75
B06-Ch5	SYBR	Empty	WT	polr2	21,67
B07-Ch5	[none]	[none]			n. def.
B08-Ch5	SYBR	Empty	10,6	polr2	21,48
B09-Ch5	SYBR	Empty	10,6	polr2	21,21
B10-Ch5	SYBR	Empty	10,6	polr2	21,52
B11-Ch5	SYBR	Empty	10,6	polr2	21,42
B12-Ch5	SYBR	Empty	10,6	polr2	21,53
B13-Ch5	SYBR	Empty	10,6	polr2	21,67
B14-Ch5	[none]	[none]			n. def.
B15-Ch5	[none]	[none]			n. def.

B16-Ch5	[none]	[none]			n. def.
C01-Ch5	SYBR	Empty	WT	pmvk	23,08
C02-Ch5	SYBR	Empty	WT	pmvk	23,37
C03-Ch5	SYBR	Empty	WT	pmvk	23,34
C04-Ch5	SYBR	Empty	WT	pmvk	23,5
C05-Ch5	SYBR	Empty	WT	pmvk	23,01
C06-Ch5	SYBR	Empty	WT	pmvk	23,31
C07-Ch5	[none]	[none]			n. def.
C08-Ch5	SYBR	Empty	10,6	pmvk	24,49
C09-Ch5	SYBR	Empty	10,6	pmvk	24,66
C10-Ch5	SYBR	Empty	10,6	pmvk	24,67
C11-Ch5	SYBR	Empty	10,6	pmvk	24,57
C12-Ch5	SYBR	Empty	10,6	pmvk	24,49
C13-Ch5	SYBR	Empty	10,6	pmvk	24,14
C14-Ch5	[none]	[none]			n. def.
C15-Ch5	[none]	[none]			n. def.
C16-Ch5	[none]	[none]			n. def.
D01-Ch5	SYBR	Empty	WT	mvd	22,46
D02-Ch5	SYBR	Empty	WT	mvd	21,96
D03-Ch5	SYBR	Empty	WT	mvd	22,56
D04-Ch5	SYBR	Empty	WT	mvd	22,78
D05-Ch5	SYBR	Empty	WT	mvd	22,38
D06-Ch5	SYBR	Empty	WT	mvd	22,96
D07-Ch5	[none]	[none]			n. def.
D08-Ch5	SYBR	Empty	10,6	mvd	24,51
D09-Ch5	SYBR	Empty	10,6	mvd	24,21
D10-Ch5	SYBR	Empty	10,6	mvd	24,51
D11-Ch5	SYBR	Empty	10,6	mvd	24,36
D12-Ch5	SYBR	Empty	10,6	mvd	24,48
D13-Ch5	SYBR	Empty	10,6	mvd	24,14
D14-Ch5	[none]	[none]			n. def.
D15-Ch5	[none]	[none]			n. def.
D16-Ch5	[none]	[none]			n. def.
E01-Ch5	SYBR	Empty	WT	fdps	19,89
E02-Ch5	SYBR	Empty	WT	fdps	19,65
E03-Ch5	SYBR	Empty	WT	fdps	20,29
E04-Ch5	SYBR	Empty	WT	fdps	20,01
E05-Ch5	SYBR	Empty	WT	fdps	19,63
E06-Ch5	SYBR	Empty	WT	fdps	19,55
E07-Ch5	[none]	[none]			n. def.
E08-Ch5	SYBR	Empty	10,6	fdps	20,83
E09-Ch5	SYBR	Empty	10,6	fdps	39,04
E10-Ch5	SYBR	Empty	10,6	fdps	20,7
E11-Ch5	SYBR	Empty	10,6	fdps	31,65

E12-Ch5	SYBR	Empty	10,6	fdps	19,87
E13-Ch5	SYBR	Empty	10,6	fdps	20,53

Table B-13: Quantification of gene expression for MEF WT and MEF APP/APLP2 -/- (MEF clone 10.6), third experiment, part four.

Data step:	4		Show channel:	Thresholds:
Sample Group:	Default	Ch 1	No	
Method:	Threshold	Ch 2	No	
Smoothing:	ON	Ch 3	No	
Smoothing window:	5	Ch 4	No	
Baseline:	Trend	Ch 5	Yes	1907,14
Baseline range start:	3			
Baseline range end:	7			

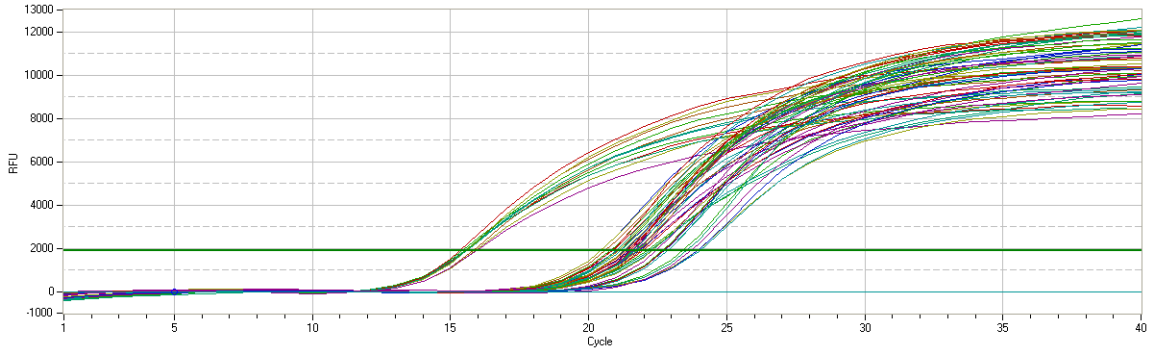

Well	Fluorophore	Sample Type	Sample Name	Target	Cq
A01-Ch5	SYBR	Empty	WT	actin beta	15,58
A02-Ch5	SYBR	Empty	WT	actin beta	15,82
A03-Ch5	SYBR	Empty	WT	actin beta	15,94
A04-Ch5	SYBR	Empty	WT	actin beta	15,46
A05-Ch5	SYBR	Empty	WT	actin beta	15,54
A06-Ch5	SYBR	Empty	WT	actin beta	15,57
A07-Ch5	[none]	[none]			n. def.
A08-Ch5	SYBR	Empty	10,6	actin beta	15,98
A09-Ch5	SYBR	Empty	10,6	actin beta	15,37
A10-Ch5	SYBR	Empty	10,6	actin beta	15,56
A11-Ch5	SYBR	Empty	10,6	actin beta	15,59
A12-Ch5	SYBR	Empty	10,6	actin beta	15,56
A13-Ch5	SYBR	Empty	10,6	actin beta	15,59
A14-Ch5	[none]	[none]			n. def.
A15-Ch5	[none]	[none]			n. def.
A16-Ch5	[none]	[none]			n. def.

B01-Ch5	SYBR	Empty	WT	polr2	22,12
B02-Ch5	SYBR	Empty	WT	polr2	22,21
B03-Ch5	SYBR	Empty	WT	polr2	22,29
B04-Ch5	SYBR	Empty	WT	polr2	21,84
B05-Ch5	SYBR	Empty	WT	polr2	21,78
B06-Ch5	SYBR	Empty	WT	polr2	21,98
B07-Ch5	[none]	[none]			n. def.
B08-Ch5	SYBR	Empty	10,6	polr2	22,29
B09-Ch5	SYBR	Empty	10,6	polr2	21,35
B10-Ch5	SYBR	Empty	10,6	polr2	21,71
B11-Ch5	SYBR	Empty	10,6	polr2	21,68
B12-Ch5	SYBR	Empty	10,6	polr2	21,48
B13-Ch5	SYBR	Empty	10,6	polr2	21,63
B14-Ch5	[none]	[none]			n. def.
B15-Ch5	[none]	[none]			n. def.
B16-Ch5	[none]	[none]			n. def.
C01-Ch5	SYBR	Empty	WT	fdft	20,43
C02-Ch5	SYBR	Empty	WT	fdft	21,06
C03-Ch5	SYBR	Empty	WT	fdft	20,88
C04-Ch5	SYBR	Empty	WT	fdft	20,61
C05-Ch5	SYBR	Empty	WT	fdft	20,43
C06-Ch5	SYBR	Empty	WT	fdft	20,78
C07-Ch5	[none]	[none]			n. def.
C08-Ch5	SYBR	Empty	10,6	fdft	21,02
C09-Ch5	SYBR	Empty	10,6	fdft	21,3
C10-Ch5	SYBR	Empty	10,6	fdft	21,43
C11-Ch5	SYBR	Empty	10,6	fdft	21,4
C12-Ch5	SYBR	Empty	10,6	fdft	21,28
C13-Ch5	SYBR	Empty	10,6	fdft	21,28
C14-Ch5	[none]	[none]			n. def.
C15-Ch5	[none]	[none]			n. def.
C16-Ch5	[none]	[none]			n. def.
D01-Ch5	SYBR	Empty	WT	sqle	20,85
D02-Ch5	SYBR	Empty	WT	sqle	21,35
D03-Ch5	SYBR	Empty	WT	sqle	21,07
D04-Ch5	SYBR	Empty	WT	sqle	21,15
D05-Ch5	SYBR	Empty	WT	sqle	21,03
D06-Ch5	SYBR	Empty	WT	sqle	21,15
D07-Ch5	[none]	[none]			n. def.
D08-Ch5	SYBR	Empty	10,6	sqle	21,57
D09-Ch5	SYBR	Empty	10,6	sqle	21,49
D10-Ch5	SYBR	Empty	10,6	sqle	21,88
D11-Ch5	SYBR	Empty	10,6	sqle	21,76
D12-Ch5	SYBR	Empty	10,6	sqle	21,6

D13-Ch5	SYBR	Empty	10,6	sqle	21,62
D14-Ch5	[none]	[none]			n. def.
D15-Ch5	[none]	[none]			n. def.
D16-Ch5	[none]	[none]			n. def.
E01-Ch5	SYBR	Empty	WT	lss	22,68
E02-Ch5	SYBR	Empty	WT	lss	22,88
E03-Ch5	SYBR	Empty	WT	lss	22,87
E04-Ch5	SYBR	Empty	WT	lss	22,76
E05-Ch5	SYBR	Empty	WT	lss	22,45
E06-Ch5	SYBR	Empty	WT	lss	22,72
E07-Ch5	[none]	[none]			n. def.
E08-Ch5	SYBR	Empty	10,6	lss	23,96
E09-Ch5	SYBR	Empty	10,6	lss	23,43
E10-Ch5	SYBR	Empty	10,6	lss	23,57
E11-Ch5	SYBR	Empty	10,6	lss	24,04
E12-Ch5	SYBR	Empty	10,6	lss	23,96
E13-Ch5	SYBR	Empty	10,6	lss	23,72

Table B-14: Quantification of gene expression for MEF PS1 rescue (MEF 26), and MEF PS1/2 -/- (MEF DK), first experiment, part one.

Data step:	4		Show channel:	Thresholds:
Sample Group:	Default	Ch 1	No	
Method:	Threshold	Ch 2	No	
Smoothing:	ON	Ch 3	No	
Smoothing window:	5	Ch 4	No	
Baseline:	Trend	Ch 5	Yes	1281.52
Baseline range start:	3			
Baseline range end:	7			

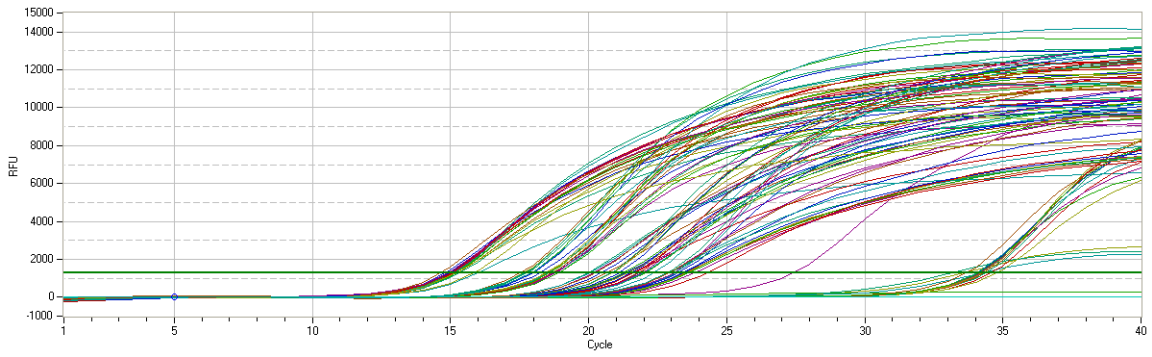

Well	Fluorophore	Sample Type	Sample Name	Target	Cq
A01-Ch5	SYBR	Empty	#26 1	actin beta	15.09
A02-Ch5	SYBR	Empty	#26 2	actin beta	15.29
A03-Ch5	SYBR	Empty	#26 3	actin beta	15.27
A04-Ch5	SYBR	Empty	#26 4	actin beta	15.19
A05-Ch5	SYBR	Empty	#26 5	actin beta	15.31
A06-Ch5	SYBR	Empty	#26 6	actin beta	15.99
A07-Ch5	SYBR	Empty	DK 1	actin beta	14.79
A08-Ch5	SYBR	Empty	DK 2	actin beta	27.41
A09-Ch5	SYBR	Empty	DK 3	actin beta	15.06
A10-Ch5	SYBR	Empty	DK 4	actin beta	15.05
A11-Ch5	SYBR	Empty	DK 5	actin beta	15.88
A12-Ch5	SYBR	Empty	DK 6	actin beta	15.14
A13-Ch5	SYBR	Empty	#26 1	actin beta	15.06
A14-Ch5	SYBR	Empty	#26 2	actin beta	15.15
A15-Ch5	SYBR	Empty	#26 3	actin beta	14.98
A16-Ch5	SYBR	Empty	#26 4	actin beta	14.93
B01-Ch5	SYBR	Empty	#26 1	ATP	18.54
B02-Ch5	SYBR	Empty	#26 2	ATP	18.88
B03-Ch5	SYBR	Empty	#26 3	ATP	18.51
B04-Ch5	SYBR	Empty	#26 4	ATP	18.21
B05-Ch5	SYBR	Empty	#26 5	ATP	18.73
B06-Ch5	SYBR	Empty	#26 6	ATP	18.42
B07-Ch5	SYBR	Empty	DK 1	ATP	17.5
B08-Ch5	SYBR	Empty	DK 2	ATP	17.64
B09-Ch5	SYBR	Empty	DK 3	ATP	17.92
B10-Ch5	SYBR	Empty	DK 4	ATP	17.64
B11-Ch5	SYBR	Empty	DK 5	ATP	18.77
B12-Ch5	SYBR	Empty	DK 6	ATP	18
B13-Ch5	SYBR	Empty	#26 1	ATP	18.8
B14-Ch5	SYBR	Empty	#26 2	ATP	18.67
B15-Ch5	SYBR	Empty	#26 3	ATP	18.66
B16-Ch5	SYBR	Empty	#26 4	ATP	18.48
C01-Ch5	SYBR	Empty	#26 1	hmgcs_1	21.34
C02-Ch5	SYBR	Empty	#26 2	hmgcs_1	21.59
C03-Ch5	SYBR	Empty	#26 3	hmgcs_1	21.59
C04-Ch5	SYBR	Empty	#26 4	hmgcs_1	20.63
C05-Ch5	SYBR	Empty	#26 5	hmgcs_1	21.39
C06-Ch5	SYBR	Empty	#26 6	hmgcs_1	21.27
C07-Ch5	SYBR	Empty	DK 1	hmgcs_1	19.99
C08-Ch5	SYBR	Empty	DK 2	hmgcs_1	20.04
C09-Ch5	SYBR	Empty	DK 3	hmgcs_1	20.42
C10-Ch5	SYBR	Empty	DK 4	hmgcs_1	20.19
C11-Ch5	SYBR	Empty	DK 5	hmgcs_1	21.61

C12-Ch5	SYBR	Empty	DK 6	hmgcs_1	20.24
C13-Ch5	SYBR	Empty	#26 1	pmvk	33.6
C14-Ch5	SYBR	Empty	#26 2	pmvk	n. def.
C15-Ch5	SYBR	Empty	#26 3	pmvk	33.12
C16-Ch5	SYBR	Empty	#26 4	pmvk	34.27
D01-Ch5	SYBR	Empty	#26 1	hmgcs_2	34.54
D02-Ch5	SYBR	Empty	#26 2	hmgcs_2	33.65
D03-Ch5	SYBR	Empty	#26 3	hmgcs_2	34.75
D04-Ch5	SYBR	Empty	#26 4	hmgcs_2	34.06
D05-Ch5	SYBR	Empty	#26 5	hmgcs_2	34.33
D06-Ch5	SYBR	Empty	#26 6	hmgcs_2	34.05
D07-Ch5	SYBR	Empty	DK 1	hmgcs_2	34.12
D08-Ch5	SYBR	Empty	DK 2	hmgcs_2	34.15
D09-Ch5	SYBR	Empty	DK 3	hmgcs_2	34.26
D10-Ch5	SYBR	Empty	DK 4	hmgcs_2	34.27
D11-Ch5	SYBR	Empty	DK 5	hmgcs_2	34.22
D12-Ch5	SYBR	Empty	DK 6	hmgcs_2	34.12
D13-Ch5	SYBR	Empty	#26 1	mvd	22.87
D14-Ch5	SYBR	Empty	#26 2	mvd	23.17
D15-Ch5	SYBR	Empty	#26 3	mvd	23.24
D16-Ch5	SYBR	Empty	#26 4	mvd	23.08
E01-Ch5	SYBR	Empty	#26 1	hmgcr	22.04
E02-Ch5	SYBR	Empty	#26 2	hmgcr	21.81
E03-Ch5	SYBR	Empty	#26 3	hmgcr	22
E04-Ch5	SYBR	Empty	#26 4	hmgcr	21.48
E05-Ch5	SYBR	Empty	#26 5	hmgcr	21.92
E06-Ch5	SYBR	Empty	#26 6	hmgcr	21.81
E07-Ch5	SYBR	Empty	DK 1	hmgcr	20.81
E08-Ch5	SYBR	Empty	DK 2	hmgcr	20.83
E09-Ch5	SYBR	Empty	DK 3	hmgcr	21.09
E10-Ch5	SYBR	Empty	DK 4	hmgcr	20.81
E11-Ch5	SYBR	Empty	DK 5	hmgcr	22.32
E12-Ch5	SYBR	Empty	DK 6	hmgcr	21.09
E13-Ch5	SYBR	Empty	#26 5	actin beta	15.04
E14-Ch5	SYBR	Empty	#26 6	actin beta	15.04
E15-Ch5	SYBR	Empty	DK 7	actin beta	14.64
E16-Ch5	SYBR	Empty	DK 8	actin beta	15.18
F01-Ch5	SYBR	Empty	#26 1	mvk	23.4
F02-Ch5	SYBR	Empty	#26 2	mvk	23.86
F03-Ch5	SYBR	Empty	#26 3	mvk	23.58
F04-Ch5	SYBR	Empty	#26 4	mvk	23.44
F05-Ch5	SYBR	Empty	#26 5	mvk	23.52
F06-Ch5	SYBR	Empty	#26 6	mvk	23.63
F07-Ch5	SYBR	Empty	DK 1	mvk	22.89

F08-Ch5	SYBR	Empty	DK 2	mvk	22.87
F09-Ch5	SYBR	Empty	DK 3	mvk	23.43
F10-Ch5	SYBR	Empty	DK 4	mvk	22.9
F11-Ch5	SYBR	Empty	DK 5	mvk	24.27
F12-Ch5	SYBR	Empty	DK 6	mvk	22.93
F13-Ch5	SYBR	Empty	#26 5	ATP	18.43
F14-Ch5	SYBR	Empty	#26 6	ATP	18.93
F15-Ch5	SYBR	Empty	DK 7	ATP	17.74
F16-Ch5	SYBR	Empty	DK 8	ATP	17.94

Table B-15: Quantification of gene expression for MEF PS1 rescue (MEF 26), and MEF PS1/2 -/- (MEF DK), first experiment, part two.

Data step:	4		Show channel:	Thresholds:
Sample Group:	Default	Ch 1	No	
Method:	Threshold	Ch 2	No	
Smoothing:	ON	Ch 3	No	
Smoothing window:	5	Ch 4	No	
Baseline:	Trend	Ch 5	Yes	1201.06
Baseline range start:	3			
Baseline range end:	7			

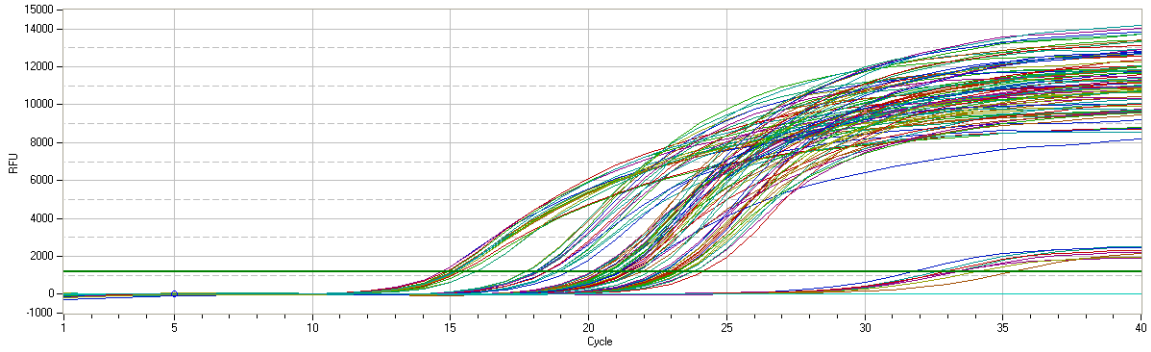

Well	Fluorophore	Sample Type	Sample Name	Target	Cq
A01-Ch5	SYBR	Empty	#26 1	actin beta	15.37
A02-Ch5	SYBR	Empty	#26 2	actin beta	15.25
A03-Ch5	SYBR	Empty	#26 3	actin beta	15.16
A04-Ch5	SYBR	Empty	#26 4	actin beta	15.52
A05-Ch5	SYBR	Empty	#26 5	actin beta	15.14
A06-Ch5	SYBR	Empty	#26 6	actin beta	15.17
A07-Ch5	SYBR	Empty	DK 1	actin beta	14.64
A08-Ch5	SYBR	Empty	DK 2	actin beta	14.69

A09-Ch5	SYBR	Empty	DK 3	actin beta	14.86
A10-Ch5	SYBR	Empty	Dk 4	actin beta	15.06
A11-Ch5	SYBR	Empty	Dk 5	actin beta	15.98
A12-Ch5	SYBR	Empty	Dk 6	actin beta	15.26
A13-Ch5	SYBR	Empty	#26 5	pmvk	33.3
A14-Ch5	SYBR	Empty	#26 6	pmvk	32.68
A15-Ch5	SYBR	Empty	DK 7	pmvk	31.76
A16-Ch5	SYBR	Empty	DK 8	pmvk	33.23
B01-Ch5	SYBR	Empty	#26 1	ATP	18.83
B02-Ch5	SYBR	Empty	#26 2	ATP	18.94
B03-Ch5	SYBR	Empty	#26 3	ATP	18.96
B04-Ch5	SYBR	Empty	#26 4	ATP	18.44
B05-Ch5	SYBR	Empty	#26 5	ATP	18.5
B06-Ch5	SYBR	Empty	#26 6	ATP	18.44
B07-Ch5	SYBR	Empty	DK 1	ATP	17.69
B08-Ch5	SYBR	Empty	DK 2	ATP	17.71
B09-Ch5	SYBR	Empty	DK 3	ATP	18.05
B10-Ch5	SYBR	Empty	Dk 4	ATP	17.72
B11-Ch5	SYBR	Empty	Dk 5	ATP	18.83
B12-Ch5	SYBR	Empty	Dk 6	ATP	18.09
B13-Ch5	SYBR	Empty	#26 5	mvd	22.77
B14-Ch5	SYBR	Empty	#26 6	mvd	22.94
B15-Ch5	SYBR	Empty	DK 7	mvd	22.8
B16-Ch5	SYBR	Empty	DK 8	mvd	22.77
C01-Ch5	SYBR	Empty	#26 1	fdps	21.41
C02-Ch5	SYBR	Empty	#26 2	fdps	21.66
C03-Ch5	SYBR	Empty	#26 3	fdps	21.2
C04-Ch5	SYBR	Empty	#26 4	fdps	20.64
C05-Ch5	SYBR	Empty	#26 5	fdps	21.09
C06-Ch5	SYBR	Empty	#26 6	fdps	20.95
C07-Ch5	SYBR	Empty	DK 1	fdps	20.16
C08-Ch5	SYBR	Empty	DK 2	fdps	20.2
C09-Ch5	SYBR	Empty	DK 3	fdps	20.67
C10-Ch5	SYBR	Empty	Dk 4	fdps	20.14
C11-Ch5	SYBR	Empty	Dk 5	fdps	21.51
C12-Ch5	SYBR	Empty	Dk 6	fdps	20.33
C13-Ch5	SYBR	Empty	DK 9	actin beta	15.28
C14-Ch5	SYBR	Empty	DK 10	actin beta	14.94
C15-Ch5	SYBR	Empty	DK 11	actin beta	15.98
C16-Ch5	SYBR	Empty	DK 12	actin beta	15.13
D01-Ch5	SYBR	Empty	#26 1	fdft1	21.14
D02-Ch5	SYBR	Empty	#26 2	fdft1	21.92
D03-Ch5	SYBR	Empty	#26 3	fdft1	21.1
D04-Ch5	SYBR	Empty	#26 4	fdft1	20.6

D05-Ch5	SYBR	Empty	#26 5	fdft1	20.76
D06-Ch5	SYBR	Empty	#26 6	fdft1	20.98
D07-Ch5	SYBR	Empty	DK 1	fdft1	20.46
D08-Ch5	SYBR	Empty	DK 2	fdft1	20.51
D09-Ch5	SYBR	Empty	DK 3	fdft1	20.7
D10-Ch5	SYBR	Empty	Dk 4	fdft1	20.28
D11-Ch5	SYBR	Empty	Dk 5	fdft1	21.3
D12-Ch5	SYBR	Empty	Dk 6	fdft1	20.67
D13-Ch5	SYBR	Empty	DK 9	ATP	18.19
D14-Ch5	SYBR	Empty	DK 10	ATP	18.11
D15-Ch5	SYBR	Empty	DK 11	ATP	19.27
D16-Ch5	SYBR	Empty	DK 12	ATP	18.17
E01-Ch5	SYBR	Empty	#26 1	fdft1	21.6
E02-Ch5	SYBR	Empty	#26 2	fdft1	21.73
E03-Ch5	SYBR	Empty	#26 3	fdft1	21.71
E04-Ch5	SYBR	Empty	#26 4	fdft1	21.15
E05-Ch5	SYBR	Empty	#26 5	fdft1	21.34
E06-Ch5	SYBR	Empty	#26 6	fdft1	21.41
E07-Ch5	SYBR	Empty	DK 1	fdft1	20.51
E08-Ch5	SYBR	Empty	DK 2	fdft1	20.74
E09-Ch5	SYBR	Empty	DK 3	fdft1	21.06
E10-Ch5	SYBR	Empty	Dk 4	fdft1	20.76
E11-Ch5	SYBR	Empty	Dk 5	fdft1	22.19
E12-Ch5	SYBR	Empty	Dk 6	fdft1	21.11
E13-Ch5	SYBR	Empty	DK 9	pmvk	33.46
E14-Ch5	SYBR	Empty	DK 10	pmvk	32.9
E15-Ch5	SYBR	Empty	DK 11	pmvk	35.42
E16-Ch5	SYBR	Empty	DK 12	pmvk	34.04
F01-Ch5	SYBR	Empty	#26 1	fdft1	23.16
F02-Ch5	SYBR	Empty	#26 2	fdft1	23.77
F03-Ch5	SYBR	Empty	#26 3	fdft1	23.09
F04-Ch5	SYBR	Empty	#26 4	fdft1	23.01
F05-Ch5	SYBR	Empty	#26 5	fdft1	23.37
F06-Ch5	SYBR	Empty	#26 6	fdft1	23.24
F07-Ch5	SYBR	Empty	DK 1	fdft1	22.19
F08-Ch5	SYBR	Empty	DK 2	fdft1	22.6
F09-Ch5	SYBR	Empty	DK 3	fdft1	22.65
F10-Ch5	SYBR	Empty	Dk 4	fdft1	22.51
F11-Ch5	SYBR	Empty	Dk 5	fdft1	24.15
F12-Ch5	SYBR	Empty	Dk 6	fdft1	23.13
F13-Ch5	SYBR	Empty	DK 9	mvd	23.43
F14-Ch5	SYBR	Empty	DK 10	mvd	23.21
F15-Ch5	SYBR	Empty	DK 11	mvd	23.81
F16-Ch5	SYBR	Empty	DK 12	mvd	23.48

Table B-16: Quantification of gene expression for MEF PS1 rescue (MEF 26), and MEF PS1/2 -/- (MEF DK), first experiment, part three.

Data step:	4		Show channel:	Thresholds:
Sample Group:	Default	Ch 1	No	
Method:	Threshold	Ch 2	No	
Smoothing:	ON	Ch 3	No	
Smoothing window:	5	Ch 4	No	
Baseline:	Trend	Ch 5	Yes	1201,06
Baseline range start:	3			
Baseline range end:	7			

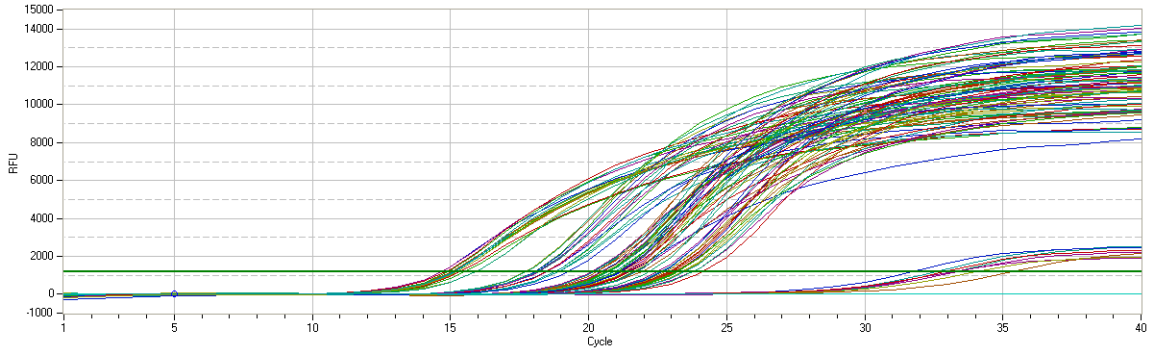

Well	Fluorophore	Sample Type	Sample Name	Target	Cq
A01-Ch5	SYBR	Empty	1	Actin	15,37
A02-Ch5	SYBR	Empty	2	Actin	15,25
A03-Ch5	SYBR	Empty	3	Actin	15,16
A04-Ch5	SYBR	Empty	4	Actin	15,52
A05-Ch5	SYBR	Empty	5	Actin	15,14
A06-Ch5	SYBR	Empty	6	Actin	15,17
A07-Ch5	SYBR	Empty	7	Actin	14,64
A08-Ch5	SYBR	Empty	8	Actin	14,69
A09-Ch5	SYBR	Empty	9	Actin	14,86
A10-Ch5	SYBR	Empty	10	Actin	15,06
A11-Ch5	SYBR	Empty	11	Actin	15,98
A12-Ch5	SYBR	Empty	12	Actin	15,26
A13-Ch5	SYBR	Empty	5	pmvk	33,3
A14-Ch5	SYBR	Empty	6	pmvk	32,68
A15-Ch5	SYBR	Empty	7	pmvk	31,76
A16-Ch5	SYBR	Empty	8	pmvk	33,23
B01-Ch5	SYBR	Empty	1	ATP	18,83
B02-Ch5	SYBR	Empty	2	ATP	18,94
B03-Ch5	SYBR	Empty	3	ATP	18,96
B04-Ch5	SYBR	Empty	4	ATP	18,44

B05-Ch5	SYBR	Empty	5	ATP	18,5
B06-Ch5	SYBR	Empty	6	ATP	18,44
B07-Ch5	SYBR	Empty	7	ATP	17,69
B08-Ch5	SYBR	Empty	8	ATP	17,71
B09-Ch5	SYBR	Empty	9	ATP	18,05
B10-Ch5	SYBR	Empty	10	ATP	17,72
B11-Ch5	SYBR	Empty	11	ATP	18,83
B12-Ch5	SYBR	Empty	12	ATP	18,09
B13-Ch5	SYBR	Empty	5	mvd	22,77
B14-Ch5	SYBR	Empty	6	mvd	22,94
B15-Ch5	SYBR	Empty	7	mvd	22,8
B16-Ch5	SYBR	Empty	8	mvd	22,77
C01-Ch5	SYBR	Empty	1	fdps	21,41
C02-Ch5	SYBR	Empty	2	fdps	21,66
C03-Ch5	SYBR	Empty	3	fdps	21,2
C04-Ch5	SYBR	Empty	4	fdps	20,64
C05-Ch5	SYBR	Empty	5	fdps	21,09
C06-Ch5	SYBR	Empty	6	fdps	20,95
C07-Ch5	SYBR	Empty	7	fdps	20,16
C08-Ch5	SYBR	Empty	8	fdps	20,2
C09-Ch5	SYBR	Empty	9	fdps	20,67
C10-Ch5	SYBR	Empty	10	fdps	20,14
C11-Ch5	SYBR	Empty	11	fdps	21,51
C12-Ch5	SYBR	Empty	12	fdps	20,33
C13-Ch5	SYBR	Empty	9	act	15,28
C14-Ch5	SYBR	Empty	10	act	14,94
C15-Ch5	SYBR	Empty	11	act	15,98
C16-Ch5	SYBR	Empty		act	15,13
D01-Ch5	SYBR	Empty	1	fdft1	21,14
D02-Ch5	SYBR	Empty	2	fdft1	21,92
D03-Ch5	SYBR	Empty	3	fdft1	21,1
D04-Ch5	SYBR	Empty	4	fdft1	20,6
D05-Ch5	SYBR	Empty	5	fdft1	20,76
D06-Ch5	SYBR	Empty	6	fdft1	20,98
D07-Ch5	SYBR	Empty	7	fdft1	20,46
D08-Ch5	SYBR	Empty	8	fdft1	20,51
D09-Ch5	SYBR	Empty	9	fdft1	20,7
D10-Ch5	SYBR	Empty	10	fdft1	20,28
D11-Ch5	SYBR	Empty	11	fdft1	21,3
D12-Ch5	SYBR	Empty	12	fdft1	20,67
D13-Ch5	SYBR	Empty	9	Atp	18,19
D14-Ch5	SYBR	Empty	10	Atp	18,11
D15-Ch5	SYBR	Empty	11	Atp	19,27
D16-Ch5	SYBR	Empty		Atp	18,17

E01-Ch5	SYBR	Empty	1	sqle	21,6
E02-Ch5	SYBR	Empty	2	sqle	21,73
E03-Ch5	SYBR	Empty	3	sqle	21,71
E04-Ch5	SYBR	Empty	4	sqle	21,15
E05-Ch5	SYBR	Empty	5	sqle	21,34
E06-Ch5	SYBR	Empty	6	sqle	21,41
E07-Ch5	SYBR	Empty	7	sqle	20,51
E08-Ch5	SYBR	Empty	8	sqle	20,74
E09-Ch5	SYBR	Empty	9	sqle	21,06
E10-Ch5	SYBR	Empty	10	sqle	20,76
E11-Ch5	SYBR	Empty	11	sqle	22,19
E12-Ch5	SYBR	Empty	12	sqle	21,11
E13-Ch5	SYBR	Empty	9	pmvk	33,46
E14-Ch5	SYBR	Empty	10	pmvk	32,9
E15-Ch5	SYBR	Empty	11	pmvk	35,42
E16-Ch5	SYBR	Empty		pmvk	34,04
F01-Ch5	SYBR	Empty	1	lss	23,16
F02-Ch5	SYBR	Empty	2	lss	23,77
F03-Ch5	SYBR	Empty	3	lss	23,09
F04-Ch5	SYBR	Empty	4	lss	23,01
F05-Ch5	SYBR	Empty	5	lss	23,37
F06-Ch5	SYBR	Empty	6	lss	23,24
F07-Ch5	SYBR	Empty	7	lss	22,19
F08-Ch5	SYBR	Empty	8	lss	22,6
F09-Ch5	SYBR	Empty	9	lss	22,65
F10-Ch5	SYBR	Empty	10	lss	22,51
F11-Ch5	SYBR	Empty	11	lss	24,15
F12-Ch5	SYBR	Empty	12	lss	23,13
F13-Ch5	SYBR	Empty	9	mvd	23,43
F14-Ch5	SYBR	Empty	10	mvd	23,21
F15-Ch5	SYBR	Empty	11	mvd	23,81
F16-Ch5	SYBR	Empty		mvd	23,48

Table B-17: Quantification of gene expression for MEF PS1 rescue (MEF 26), and MEF PS1/2 -/- (MEF DK), second experiment, part one.

Data step:	4		Show channel:	Thresholds:
Sample Group:	Default	Ch 1	No	
Method:	Threshold	Ch 2	No	
Smoothing:	ON	Ch 3	No	
Smoothing window:	5	Ch 4	No	
Baseline:	Trend	Ch 5	Yes	1343,37

Baseline range start:	3			
Baseline range end:	7			

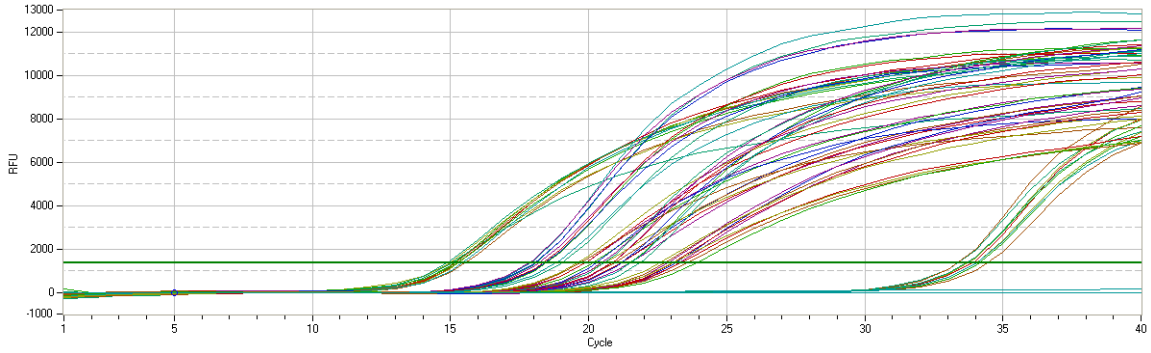

Well	Fluorophore	Sample Type	Sample Name	Target	Cq
A01-Ch5	SYBR	Empty	#26 1	actin beta	15,26
A02-Ch5	SYBR	Empty	#26 2	actin beta	15,5
A03-Ch5	SYBR	Empty	#26 3	actin beta	15,27
A04-Ch5	SYBR	Empty	#26 4	actin beta	15,11
A05-Ch5	SYBR	Empty	#26 5	actin beta	15,01
A06-Ch5	[none]	[none]			n. def.
A07-Ch5	[none]	[none]			n. def.
A08-Ch5	[none]	[none]			n. def.
A09-Ch5	[none]	[none]			n. def.
A10-Ch5	SYBR	Empty	DK 8	actin beta	15,16
A11-Ch5	SYBR	Empty	DK 9	actin beta	14,96
A12-Ch5	SYBR	Empty	DK10	actin beta	15,22
A13-Ch5	SYBR	Empty	DK 11	actin beta	14,88
A14-Ch5	SYBR	Empty	DK 12	actin beta	15,42
A15-Ch5	[none]	[none]			n. def.
A16-Ch5	[none]	[none]			n. def.
B01-Ch5	SYBR	Empty	#1	ATP	18,44
B02-Ch5	SYBR	Empty		ATP	19,02
B03-Ch5	SYBR	Empty		ATP	18,79
B04-Ch5	SYBR	Empty		ATP	18,38
B05-Ch5	SYBR	Empty		ATP	18,18
B06-Ch5	[none]	[none]			n. def.
B07-Ch5	[none]	[none]			n. def.
B08-Ch5	[none]	[none]			n. def.
B09-Ch5	[none]	[none]			n. def.
B10-Ch5	SYBR	Empty		ATP	18,06
B11-Ch5	SYBR	Empty		ATP	17,87
B12-Ch5	SYBR	Empty		ATP	18,04
B13-Ch5	SYBR	Empty		ATP	17,79

B14-Ch5	SYBR	Empty		ATP	18,32
B15-Ch5	[none]	[none]			n. def.
B16-Ch5	[none]	[none]			n. def.
C01-Ch5	SYBR	Empty	#1	hmgcs1	21,16
C02-Ch5	SYBR	Empty		hmgcs1	21,45
C03-Ch5	SYBR	Empty		hmgcs1	21,16
C04-Ch5	SYBR	Empty		hmgcs1	20,9
C05-Ch5	SYBR	Empty		hmgcs1	20,54
C06-Ch5	[none]	[none]			n. def.
C07-Ch5	[none]	[none]			n. def.
C08-Ch5	[none]	[none]			n. def.
C09-Ch5	[none]	[none]			n. def.
C10-Ch5	SYBR	Empty		hmgcs1	19,88
C11-Ch5	SYBR	Empty		hmgcs1	19,88
C12-Ch5	SYBR	Empty		hmgcs1	19,69
C13-Ch5	SYBR	Empty		hmgcs1	19,58
C14-Ch5	SYBR	Empty		hmgcs1	20,15
C15-Ch5	[none]	[none]			n. def.
C16-Ch5	[none]	[none]			n. def.
D01-Ch5	SYBR	Empty	#1	hmgcs2	33,84
D02-Ch5	SYBR	Empty		hmgcs2	34,42
D03-Ch5	SYBR	Empty		hmgcs2	34,04
D04-Ch5	SYBR	Empty		hmgcs2	33,67
D05-Ch5	SYBR	Empty		hmgcs2	33,33
D06-Ch5	[none]	[none]			n. def.
D07-Ch5	[none]	[none]			n. def.
D08-Ch5	[none]	[none]			n. def.
D09-Ch5	[none]	[none]			n. def.
D10-Ch5	SYBR	Empty		hmgcs2	33,32
D11-Ch5	SYBR	Empty		hmgcs2	33,68
D12-Ch5	SYBR	Empty		hmgcs2	34,13
D13-Ch5	SYBR	Empty		hmgcs2	33,64
D14-Ch5	SYBR	Empty		hmgcs2	34,04
D15-Ch5	[none]	[none]			n. def.
D16-Ch5	[none]	[none]			n. def.
E01-Ch5	SYBR	Empty	#1	hmgcr	21,47
E02-Ch5	SYBR	Empty		hmgcr	21,82
E03-Ch5	SYBR	Empty		hmgcr	21,49
E04-Ch5	SYBR	Empty		hmgcr	21,18
E05-Ch5	SYBR	Empty		hmgcr	20,81
E06-Ch5	[none]	[none]			n. def.
E07-Ch5	[none]	[none]			n. def.
E08-Ch5	[none]	[none]			n. def.
E09-Ch5	[none]	[none]			n. def.

E10-Ch5	SYBR	Empty		hmgcr	20,52
E11-Ch5	SYBR	Empty		hmgcr	n. def.
E12-Ch5	SYBR	Empty		hmgcr	20,25
E13-Ch5	SYBR	Empty		hmgcr	20,43
E14-Ch5	SYBR	Empty		hmgcr	20,8
E15-Ch5	[none]	[none]			n. def.
E16-Ch5	[none]	[none]			n. def.
F01-Ch5	SYBR	Empty	#1	MVK	23,13
F02-Ch5	SYBR	Empty		MVK	23,25
F03-Ch5	SYBR	Empty		MVK	23,05
F04-Ch5	SYBR	Empty		MVK	22,74
F05-Ch5	SYBR	Empty		MVK	22,52
F06-Ch5	[none]	[none]			n. def.
F07-Ch5	[none]	[none]			n. def.
F08-Ch5	[none]	[none]			n. def.
F09-Ch5	[none]	[none]			n. def.
F10-Ch5	SYBR	Empty		MVK	22,86
F11-Ch5	SYBR	Empty		MVK	23,33
F12-Ch5	SYBR	Empty		MVK	23,55
F13-Ch5	SYBR	Empty		MVK	23,05
F14-Ch5	SYBR	Empty		MVK	23,89

Table B-18: Quantification of gene expression for MEF PS1 rescue (MEF 26), and MEF PS1/2 -/- (MEF DK), second experiment, part two.

Data step:	4		Show channel:	Thresholds:
Sample Group:	Default	Ch 1	No	
Method:	Threshold	Ch 2	No	
Smoothing:	ON	Ch 3	No	
Smoothing window:	5	Ch 4	No	
Baseline:	Trend	Ch 5	Yes	1330.82
Baseline range start:	3			
Baseline range end:	7			

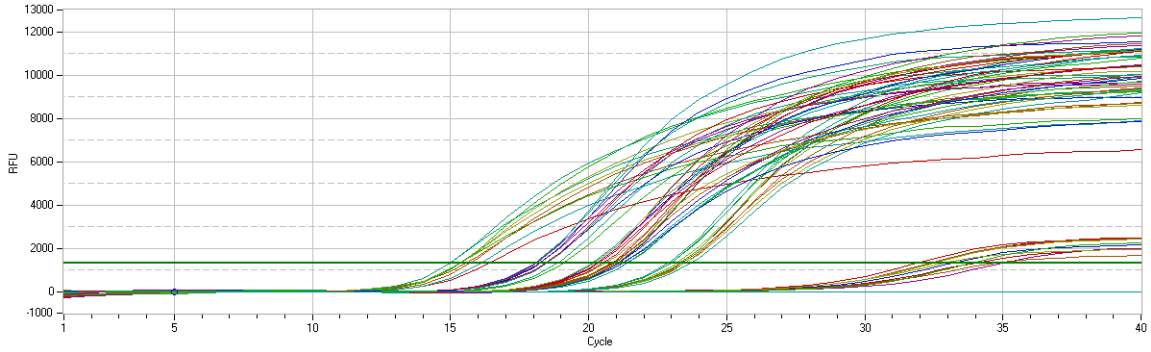

Well	Fluorophore	Sample Type	Sample Name	Target	Cq
A01-Ch5	SYBR	Empty	#26 1	actin beta	16.41
A02-Ch5	SYBR	Empty	#26 2	actin beta	15.71
A03-Ch5	SYBR	Empty	#26 3	actin beta	15.41
A04-Ch5	SYBR	Empty	#26 4	actin beta	15.4
A05-Ch5	SYBR	Empty	#26 5	actin beta	15.02
A06-Ch5	[none]	[none]			n. def.
A07-Ch5	[none]	[none]			n. def.
A08-Ch5	[none]	[none]			n. def.
A09-Ch5	[none]	[none]			n. def.
A10-Ch5	SYBR	Empty	DK 8	actin beta	15.57
A11-Ch5	SYBR	Empty	DK 9	actin beta	15.39
A12-Ch5	SYBR	Empty	Dk 10	actin beta	15.37
A13-Ch5	SYBR	Empty	Dk 11	actin beta	15.04
A14-Ch5	SYBR	Empty	Dk 12	actin beta	16.12
A15-Ch5	[none]	[none]			n. def.
A16-Ch5	[none]	[none]			n. def.
B01-Ch5	SYBR	Empty	#26 1	ATP	19.1
B02-Ch5	SYBR	Empty	#26 2	ATP	18.9
B03-Ch5	SYBR	Empty	#26 3	ATP	18.5
B04-Ch5	SYBR	Empty	#26 4	ATP	18.44
B05-Ch5	SYBR	Empty	#26 5	ATP	18.23
B06-Ch5	[none]	[none]			n. def.
B07-Ch5	[none]	[none]			n. def.
B08-Ch5	[none]	[none]			n. def.
B09-Ch5	[none]	[none]			n. def.
B10-Ch5	SYBR	Empty	DK 8	ATP	18.08
B11-Ch5	SYBR	Empty	DK 9	ATP	18.12
B12-Ch5	SYBR	Empty	Dk 10	ATP	18.23
B13-Ch5	SYBR	Empty	Dk 11	ATP	18.1
B14-Ch5	SYBR	Empty	Dk 12	ATP	18.43
B15-Ch5	[none]	[none]			n. def.

B16-Ch5	[none]	[none]			n. def.
C01-Ch5	SYBR	Empty	#26 1	PMVK	33.25
C02-Ch5	SYBR	Empty	#26 2	PMVK	35.05
C03-Ch5	SYBR	Empty	#26 3	PMVK	33.99
C04-Ch5	SYBR	Empty	#26 4	PMVK	34.94
C05-Ch5	SYBR	Empty	#26 5	PMVK	32.97
C06-Ch5	[none]	[none]			n. def.
C07-Ch5	[none]	[none]			n. def.
C08-Ch5	[none]	[none]			n. def.
C09-Ch5	[none]	[none]			n. def.
C10-Ch5	SYBR	Empty	DK 8	PMVK	32.47
C11-Ch5	SYBR	Empty	DK 9	PMVK	31.99
C12-Ch5	SYBR	Empty	Dk 10	PMVK	32.4
C13-Ch5	SYBR	Empty	Dk 11	PMVK	32.56
C14-Ch5	SYBR	Empty	Dk 12	PMVK	33.95
C15-Ch5	[none]	[none]			n. def.
C16-Ch5	[none]	[none]			n. def.
D01-Ch5	SYBR	Empty	#26 1	MVD	23.34
D02-Ch5	SYBR	Empty	#26 2	MVD	23.49
D03-Ch5	SYBR	Empty	#26 3	MVD	23.23
D04-Ch5	SYBR	Empty	#26 4	MVD	23.02
D05-Ch5	SYBR	Empty	#26 5	MVD	22.92
D06-Ch5	[none]	[none]			n. def.
D07-Ch5	[none]	[none]			n. def.
D08-Ch5	[none]	[none]			n. def.
D09-Ch5	[none]	[none]			n. def.
D10-Ch5	SYBR	Empty	DK 8	MVD	23.41
D11-Ch5	SYBR	Empty	DK 9	MVD	23.51
D12-Ch5	SYBR	Empty	Dk 10	MVD	23.32
D13-Ch5	SYBR	Empty	Dk 11	MVD	23.04
D14-Ch5	SYBR	Empty	Dk 12	MVD	23.72
D15-Ch5	[none]	[none]			n. def.
D16-Ch5	[none]	[none]			n. def.
E01-Ch5	SYBR	Empty	#26 1	Fdps	21.4
E02-Ch5	SYBR	Empty	#26 2	Fdps	21.42
E03-Ch5	SYBR	Empty	#26 3	Fdps	21.24
E04-Ch5	SYBR	Empty	#26 4	Fdps	21.11
E05-Ch5	SYBR	Empty	#26 5	Fdps	20.88
E06-Ch5	[none]	[none]			n. def.
E07-Ch5	[none]	[none]			n. def.
E08-Ch5	[none]	[none]			n. def.
E09-Ch5	[none]	[none]			n. def.
E10-Ch5	SYBR	Empty	DK 8	Fdps	20.16
E11-Ch5	SYBR	Empty	DK 9	Fdps	20.2

E12-Ch5	SYBR	Empty	Dk 10	Fdps	20.23
E13-Ch5	SYBR	Empty	Dk 11	Fdps	20.19
E14-Ch5	SYBR	Empty	Dk 12	Fdps	20.36

Table B-19: Quantification of gene expression for MEF PS1 rescue (MEF 26), and MEF PS1/2 -/- (MEF DK), second experiment, part three.

Data step:	4		Show channel:	Thresholds:
Sample Group:	Default	Ch 1	No	
Method:	Threshold	Ch 2	No	
Smoothing:	ON	Ch 3	No	
Smoothing window:	5	Ch 4	No	
Baseline:	Trend	Ch 5	Yes	0
Baseline range start:	3			
Baseline range end:	7			

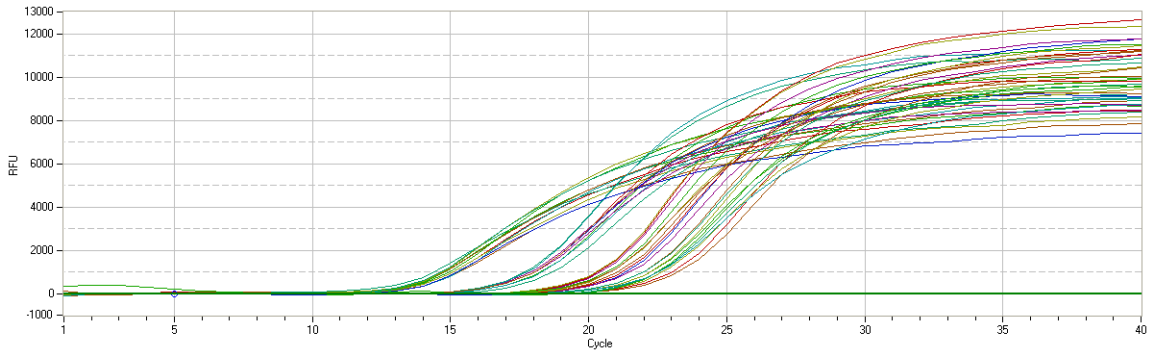

Well	Fluorophore	Sample Type	Sample Name	Target	Cq
A01-Ch5	SYBR	Empty	#26 1	actin beta	11.3
A02-Ch5	SYBR	Empty	#26 2	actin beta	10.87
A03-Ch5	SYBR	Empty	#26 3	actin beta	10.95
A04-Ch5	SYBR	Empty	#26 4	actin beta	11.23
A05-Ch5	SYBR	Empty	#26 5	actin beta	5.46
A06-Ch5	[none]	[none]			n. def.
A07-Ch5	[none]	[none]			n. def.
A08-Ch5	[none]	[none]			n. def.
A09-Ch5	[none]	[none]			n. def.
A10-Ch5	SYBR	Empty	DK 1	actin beta	6.32
A11-Ch5	SYBR	Empty	Dk 2	actin beta	9.42
A12-Ch5	SYBR	Empty	Dk 3	actin beta	10.9
A13-Ch5	SYBR	Empty	Dk 4	actin beta	11.01
A14-Ch5	SYBR	Empty	Dk 5	actin beta	11.29

A15-Ch5	[none]	[none]			n. def.
A16-Ch5	[none]	[none]			n. def.
B01-Ch5	SYBR	Empty	#26 1	ATP	14.14
B02-Ch5	SYBR	Empty	#26 2	ATP	14.87
B03-Ch5	SYBR	Empty	#26 3	ATP	14.08
B04-Ch5	SYBR	Empty	#26 4	ATP	14.02
B05-Ch5	SYBR	Empty	#26 5	ATP	14.01
B06-Ch5	[none]	[none]			n. def.
B07-Ch5	[none]	[none]			n. def.
B08-Ch5	[none]	[none]			n. def.
B09-Ch5	[none]	[none]			n. def.
B10-Ch5	SYBR	Empty	DK 1	ATP	13.88
B11-Ch5	SYBR	Empty	Dk 2	ATP	14.03
B12-Ch5	SYBR	Empty	Dk 3	actin beta	12.03
B13-Ch5	SYBR	Empty	Dk 4	ATP	13.21
B14-Ch5	SYBR	Empty	Dk 5	ATP	13.93
B15-Ch5	SYBR	Empty	DK 3	ATP	13.93
B16-Ch5	[none]	[none]			n. def.
C01-Ch5	SYBR	Empty	#26 1	sqle	17.79
C02-Ch5	SYBR	Empty	#26 2	sqle	17.13
C03-Ch5	SYBR	Empty	#26 3	sqle	17.25
C04-Ch5	SYBR	Empty	#26 4	sqle	17.22
C05-Ch5	SYBR	Empty	#26 5	sqle	17.05
C06-Ch5	[none]	[none]			5.06
C07-Ch5	[none]	[none]			n. def.
C08-Ch5	[none]	[none]			n. def.
C09-Ch5	[none]	[none]			19.49
C10-Ch5	SYBR	Empty	DK 1	sqle	16.73
C11-Ch5	SYBR	Empty	Dk 2	sqle	16.51
C12-Ch5	SYBR	Empty	Dk 3	sqle	16.2
C13-Ch5	SYBR	Empty	Dk 4	sqle	16.23
C14-Ch5	SYBR	Empty	Dk 5	sqle	16.48
C15-Ch5	[none]	[none]			15.63
C16-Ch5	[none]	[none]			n. def.
D01-Ch5	SYBR	Empty	#26 1	lss	19.18
D02-Ch5	SYBR	Empty	#26 2	lss	19.1
D03-Ch5	SYBR	Empty	#26 3	lss	19.12
D04-Ch5	SYBR	Empty	#26 4	lss	18.27
D05-Ch5	SYBR	Empty	#26 5	lss	19
D06-Ch5	[none]	[none]			n. def.
D07-Ch5	[none]	[none]			n. def.
D08-Ch5	[none]	[none]			n. def.
D09-Ch5	[none]	[none]			n. def.
D10-Ch5	SYBR	Empty	DK 1	lss	18.15

D11-Ch5	SYBR	Empty	Dk 2	lss	17.76
D12-Ch5	SYBR	Empty	Dk 3	lss	19.49
D13-Ch5	SYBR	Empty	Dk 4	lss	17.84
D14-Ch5	SYBR	Empty	Dk 5	lss	17.68
D15-Ch5	[none]	[none]			21.2

Table B-20: Quantification of gene expression for MEF PS1 rescue (MEF 26), and MEF PS1/2 -/- (MEF DK), three experiment, part one.

Data step:	4		Show channel:	Thresholds:
Sample Group:	Default	Ch 1	No	
Method:	Threshold	Ch 2	No	
Smoothing:	ON	Ch 3	No	
Smoothing window:	5	Ch 4	No	
Baseline:	Trend	Ch 5	Yes	1269,81
Baseline range start:	3			
Baseline range end:	7			

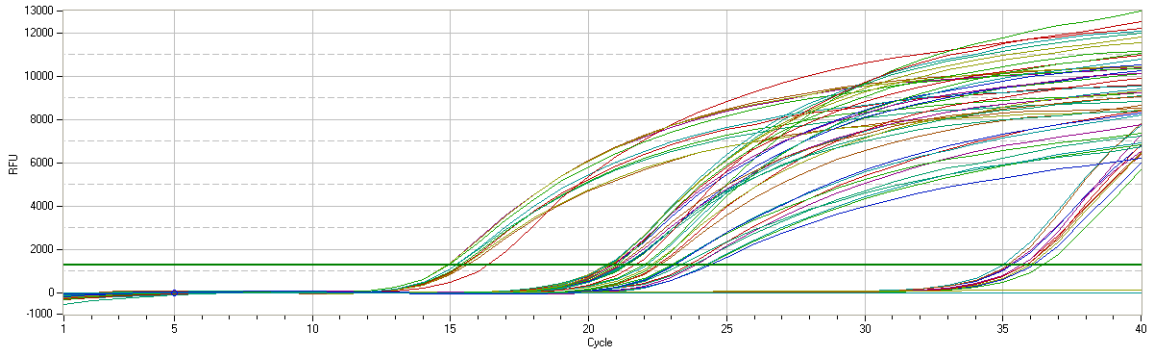

Well	Fluorophore	Sample Type	Sample Name	Target	Cq
A01-Ch5	SYBR	Empty	#26	actin beta	15.45
A02-Ch5	SYBR	Empty	#26	actin beta	15.59
A03-Ch5	SYBR	Empty	#26	actin beta	15.48
A04-Ch5	SYBR	Empty	#26	actin beta	15.35
A05-Ch5	SYBR	Empty	#26	actin beta	15.22
A06-Ch5	SYBR	Empty	#26	actin beta	15.19
A07-Ch5	[none]	[none]			n. def.
A08-Ch5	SYBR	Empty	DK	actin beta	14.86
A09-Ch5	SYBR	Empty	DK	actin beta	16.34
A10-Ch5	SYBR	Empty	DK	actin beta	14.9

A11-Ch5	SYBR	Empty	DK	actin beta	14.87
A12-Ch5	SYBR	Empty	DK	actin beta	14.96
A13-Ch5	[none]	[none]			n. def.
A14-Ch5	[none]	[none]			n. def.
A15-Ch5	[none]	[none]			n. def.
A16-Ch5	[none]	[none]			n. def.
B01-Ch5	SYBR	Empty	#26	polr2	21.35
B02-Ch5	SYBR	Empty	#26	polr2	21.25
B03-Ch5	SYBR	Empty	#26	polr2	21.27
B04-Ch5	SYBR	Empty	#26	polr2	21.31
B05-Ch5	SYBR	Empty	#26	polr2	21.16
B06-Ch5	SYBR	Empty	#26	polr2	20.8
B07-Ch5	[none]	[none]			n. def.
B08-Ch5	SYBR	Empty	DK	polr2	20.65
B09-Ch5	SYBR	Empty	DK	polr2	22
B10-Ch5	SYBR	Empty	DK	polr2	20.68
B11-Ch5	SYBR	Empty	DK	polr2	20.66
B12-Ch5	SYBR	Empty	DK	polr2	20.88
B13-Ch5	[none]	[none]			n. def.
B14-Ch5	[none]	[none]			n. def.
B15-Ch5	[none]	[none]			n. def.
B16-Ch5	[none]	[none]			n. def.
C01-Ch5	SYBR	Empty	#26	hmgcs2	36.09
C02-Ch5	SYBR	Empty	#26	hmgcs2	35.25
C03-Ch5	SYBR	Empty	#26	hmgcs2	35.66
C04-Ch5	SYBR	Empty	#26	hmgcs2	35.82
C05-Ch5	SYBR	Empty	#26	hmgcs2	36.01
C06-Ch5	SYBR	Empty	#26	hmgcs2	36.44
C07-Ch5	[none]	[none]			n. def.
C08-Ch5	SYBR	Empty	DK	hmgcs2	35.01
C09-Ch5	SYBR	Empty	DK	hmgcs2	35.33
C10-Ch5	SYBR	Empty	DK	hmgcs2	35.63
C11-Ch5	SYBR	Empty	DK	hmgcs2	35.81
C12-Ch5	SYBR	Empty	DK	hmgcs2	35.16
C13-Ch5	[none]	[none]			n. def.
C14-Ch5	[none]	[none]			n. def.
C15-Ch5	[none]	[none]			n. def.
C16-Ch5	[none]	[none]			n. def.
D01-Ch5	SYBR	Empty	#26	hmgcr	22.5
D02-Ch5	SYBR	Empty	#26	hmgcr	22.55
D03-Ch5	SYBR	Empty	#26	hmgcr	22.23
D04-Ch5	SYBR	Empty	#26	hmgcr	22.33
D05-Ch5	SYBR	Empty	#26	hmgcr	21.3
D06-Ch5	SYBR	Empty	#26	hmgcr	22.08

D07-Ch5	[none]	[none]			n. def.
D08-Ch5	SYBR	Empty	DK	hmgcr	20.86
D09-Ch5	SYBR	Empty	DK	hmgcr	21.65
D10-Ch5	SYBR	Empty	DK	hmgcr	21.09
D11-Ch5	SYBR	Empty	DK	hmgcr	20.77
D12-Ch5	SYBR	Empty	DK	hmgcr	20.98
D13-Ch5	[none]	[none]			n. def.
D14-Ch5	[none]	[none]			n. def.
D15-Ch5	[none]	[none]			n. def.
D16-Ch5	[none]	[none]			n. def.
E01-Ch5	SYBR	Empty	#26	Mvk	24.29
E02-Ch5	SYBR	Empty	#26	Mvk	23.78
E03-Ch5	SYBR	Empty	#26	Mvk	24.24
E04-Ch5	SYBR	Empty	#26	Mvk	24.39
E05-Ch5	SYBR	Empty	#26	Mvk	23.86
E06-Ch5	SYBR	Empty	#26	Mvk	23.65
E07-Ch5	[none]	[none]			n. def.
E08-Ch5	SYBR	Empty	DK	Mvk	n. def.
E09-Ch5	SYBR	Empty	DK	Mvk	23
E10-Ch5	SYBR	Empty	DK	Mvk	23.34
E11-Ch5	SYBR	Empty	DK	Mvk	23.05
E12-Ch5	SYBR	Empty	DK	Mvk	23.11

Table B-21: Quantification of gene expression for MEF PS1 rescue (MEF 26), and MEF PS1/2 -/- (MEF DK), third experiment, part two.

Data step:	4		Show channel:	Thresholds:
Sample Group:	Default	Ch 1	No	
Method:	Threshold	Ch 2	No	
Smoothing:	ON	Ch 3	No	
Smoothing window:	5	Ch 4	No	
Baseline:	Trend	Ch 5	Yes	1819.42
Baseline range start:	3			
Baseline range end:	7			

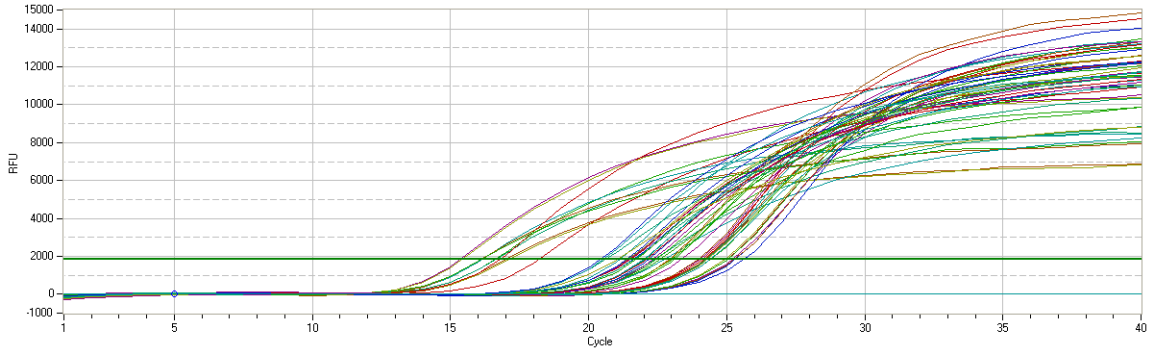

Well	Fluorophore	Sample Type	Sample Name	Target	Cq
A01-Ch5	SYBR	Empty	#26	actin beta	18.19
A02-Ch5	SYBR	Empty	#26	actin beta	16.96
A03-Ch5	SYBR	Empty	#26	actin beta	17.1
A04-Ch5	SYBR	Empty	#26	actin beta	16.57
A05-Ch5	SYBR	Empty	#26	actin beta	16.62
A06-Ch5	SYBR	Empty	#26	actin beta	16.14
A07-Ch5	[none]	[none]			n. def.
A08-Ch5	SYBR	Empty	DK	actin beta	15.34
A09-Ch5	SYBR	Empty	DK	actin beta	16.75
A10-Ch5	SYBR	Empty	DK	actin beta	16.08
A11-Ch5	SYBR	Empty	DK	actin beta	15.41
A12-Ch5	SYBR	Empty	DK	actin beta	16.12
A13-Ch5	[none]	[none]			n. def.
A14-Ch5	[none]	[none]			n. def.
A15-Ch5	[none]	[none]			n. def.
A16-Ch5	[none]	[none]			n. def.
B01-Ch5	SYBR	Empty	#26	polr2	22.55
B02-Ch5	SYBR	Empty	#26	polr2	22.35
B03-Ch5	SYBR	Empty	#26	polr2	22.7
B04-Ch5	SYBR	Empty	#26	polr2	21.57
B05-Ch5	SYBR	Empty	#26	polr2	21.41
B06-Ch5	SYBR	Empty	#26	polr2	21.46
B07-Ch5	[none]	[none]			n. def.
B08-Ch5	SYBR	Empty	DK	polr2	21.37
B09-Ch5	SYBR	Empty	DK	polr2	23.01
B10-Ch5	SYBR	Empty	DK	polr2	21.6
B11-Ch5	SYBR	Empty	DK	polr2	21.12
B12-Ch5	SYBR	Empty	DK	polr2	21.33
B13-Ch5	[none]	[none]			n. def.
B14-Ch5	[none]	[none]			n. def.
B15-Ch5	[none]	[none]			n. def.
B16-Ch5	[none]	[none]			n. def.

C01-Ch5	SYBR	Empty	#26	pmvk	25.25
C02-Ch5	SYBR	Empty	#26	pmvk	25.17
C03-Ch5	SYBR	Empty	#26	pmvk	25
C04-Ch5	SYBR	Empty	#26	pmvk	25.25
C05-Ch5	SYBR	Empty	#26	pmvk	24.93
C06-Ch5	SYBR	Empty	#26	pmvk	25.03
C07-Ch5	[none]	[none]			n. def.
C08-Ch5	SYBR	Empty	DK	pmvk	24.17
C09-Ch5	SYBR	Empty	DK	pmvk	25.58
C10-Ch5	SYBR	Empty	DK	pmvk	24.03
C11-Ch5	SYBR	Empty	DK	pmvk	24.16
C12-Ch5	SYBR	Empty	DK	pmvk	24
C13-Ch5	[none]	[none]			n. def.
C14-Ch5	[none]	[none]			n. def.
C15-Ch5	[none]	[none]			n. def.
C16-Ch5	[none]	[none]			n. def.
D01-Ch5	SYBR	Empty	#26	mvd	24.26
D02-Ch5	SYBR	Empty	#26	mvd	24.2
D03-Ch5	SYBR	Empty	#26	mvd	24.28
D04-Ch5	SYBR	Empty	#26	mvd	24.39
D05-Ch5	SYBR	Empty	#26	mvd	24.23
D06-Ch5	SYBR	Empty	#26	mvd	24.37
D07-Ch5	[none]	[none]			n. def.
D08-Ch5	SYBR	Empty	DK	mvd	23.34
D09-Ch5	SYBR	Empty	DK	mvd	24.08
D10-Ch5	SYBR	Empty	DK	mvd	22.93
D11-Ch5	SYBR	Empty	DK	mvd	22.96
D12-Ch5	SYBR	Empty	DK	mvd	23.08
D13-Ch5	[none]	[none]			n. def.
D14-Ch5	[none]	[none]			n. def.
D15-Ch5	[none]	[none]			n. def.
D16-Ch5	[none]	[none]			n. def.
E01-Ch5	SYBR	Empty	#26	fdps	22.4
E02-Ch5	SYBR	Empty	#26	fdps	22.01
E03-Ch5	SYBR	Empty	#26	fdps	21.97
E04-Ch5	SYBR	Empty	#26	fdps	22.15
E05-Ch5	SYBR	Empty	#26	fdps	22.31
E06-Ch5	SYBR	Empty	#26	fdps	22.08
E07-Ch5	[none]	[none]			n. def.
E08-Ch5	SYBR	Empty	DK	fdps	21.01
E09-Ch5	SYBR	Empty	DK	fdps	21.67
E10-Ch5	SYBR	Empty	DK	fdps	20.58
E11-Ch5	SYBR	Empty	DK	fdps	20.51
E12-Ch5	SYBR	Empty	DK	fdps	20.41

Table B-22: Quantification of gene expression for MEF PS1 rescue (MEF 26), and MEF PS1/2 -/- (MEF DK), third experiment, part three.

Data step:	4		Show channel:	Thresholds:
Sample Group:	Default	Ch 1	No	
Method:	Threshold	Ch 2	No	
Smoothing:	ON	Ch 3	No	
Smoothing window:	5	Ch 4	No	
Baseline:	Trend	Ch 5	Yes	1993,26
Baseline range start:	3			
Baseline range end:	7			

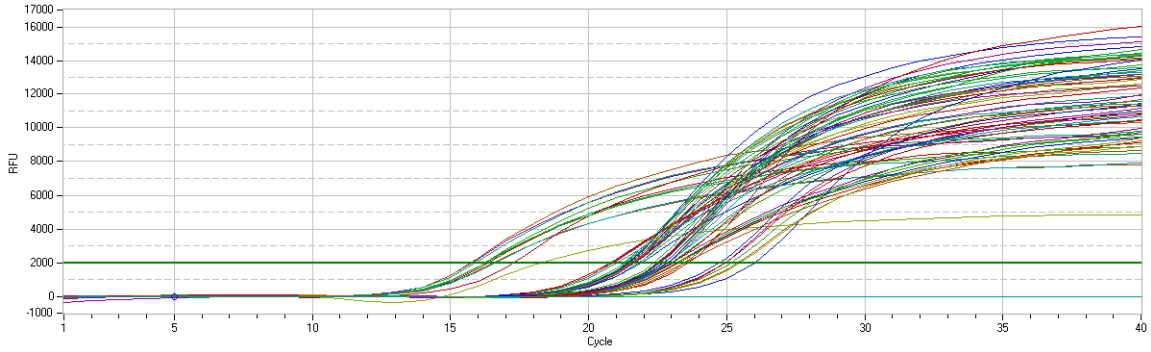

Well	Fluorophore	Sample Type	Sample Name	Target	Cq
A01-Ch5	SYBR	Empty	#26	actin beta	16.4
A02-Ch5	SYBR	Empty	#26	actin beta	16.57
A03-Ch5	[none]	[none]			16.89
A04-Ch5	SYBR	Empty	#26	actin beta	16.25
A05-Ch5	SYBR	Empty	#26	actin beta	16.27
A06-Ch5	SYBR	Empty	#26	actin beta	16.6
A07-Ch5	[none]	[none]			n. def.
A08-Ch5	SYBR	Empty	DK	actin beta	15.79
A09-Ch5	SYBR	Empty	DK	actin beta	17.26
A10-Ch5	SYBR	Empty	DK	actin beta	15.72
A11-Ch5	SYBR	Empty	DK	actin beta	18.31
A12-Ch5	SYBR	Empty	DK	actin beta	16.26
A13-Ch5	SYBR	Empty	#26 3	actin beta	15.9
A14-Ch5	[none]	[none]			n. def.
A15-Ch5	[none]	[none]			n. def.
A16-Ch5	[none]	[none]			n. def.
B01-Ch5	SYBR	Empty	#26	polr2	21.78
B02-Ch5	SYBR	Empty	#26	polr2	21.8
B03-Ch5	SYBR	Empty	#26	polr2	21.65
B04-Ch5	SYBR	Empty	#26	polr2	21.56

B05-Ch5	SYBR	Empty	#26	polr2	21.65
B06-Ch5	SYBR	Empty	#26	polr2	21.59
B07-Ch5	[none]	[none]			n. def.
B08-Ch5	SYBR	Empty	DK	polr2	21.43
B09-Ch5	SYBR	Empty	DK	polr2	23.02
B10-Ch5	SYBR	Empty	DK	polr2	21.43
B11-Ch5	SYBR	Empty	DK	polr2	21.29
B12-Ch5	SYBR	Empty	DK	polr2	21.43
B13-Ch5	[none]	[none]			n. def.
B14-Ch5	[none]	[none]			n. def.
B15-Ch5	[none]	[none]			n. def.
B16-Ch5	[none]	[none]			n. def.
C01-Ch5	SYBR	Empty	#26	hmgcs1	23.24
C02-Ch5	SYBR	Empty	#26	hmgcs1	23.02
C03-Ch5	SYBR	Empty	#26	hmgcs1	23.26
C04-Ch5	SYBR	Empty	#26	hmgcs1	23.51
C05-Ch5	SYBR	Empty	#26	hmgcs1	23.22
C06-Ch5	SYBR	Empty	#26	hmgcs1	23.18
C07-Ch5	[none]	[none]			n. def.
C08-Ch5	SYBR	Empty	DK	hmgcs1	21.05
C09-Ch5	SYBR	Empty	DK	hmgcs1	21.9
C10-Ch5	SYBR	Empty	DK	hmgcs1	20.83
C11-Ch5	SYBR	Empty	DK	hmgcs1	20.76
C12-Ch5	SYBR	Empty	DK	hmgcs1	20.9
C13-Ch5	[none]	[none]			n. def.
C14-Ch5	[none]	[none]			n. def.
C15-Ch5	[none]	[none]			n. def.
C16-Ch5	[none]	[none]			n. def.
D01-Ch5	SYBR	Empty	#26	fdft	22.48
D02-Ch5	SYBR	Empty	#26	fdft	22.52
D03-Ch5	SYBR	Empty	#26	fdft	22.54
D04-Ch5	SYBR	Empty	#26	fdft	22.55
D05-Ch5	SYBR	Empty	#26	fdft	22.47
D06-Ch5	SYBR	Empty	#26	fdft	22.85
D07-Ch5	[none]	[none]			n. def.
D08-Ch5	SYBR	Empty	DK	fdft	21.52
D09-Ch5	SYBR	Empty	DK	fdft	23.07
D10-Ch5	SYBR	Empty	DK	fdft	21.46
D11-Ch5	SYBR	Empty	DK	fdft	21.36
D12-Ch5	SYBR	Empty	DK	fdft	21.25
D13-Ch5	[none]	[none]			n. def.
D14-Ch5	[none]	[none]			n. def.
D15-Ch5	[none]	[none]			n. def.
D16-Ch5	[none]	[none]			n. def.

E01-Ch5	SYBR	Empty	#26	sqle	22.86
E02-Ch5	SYBR	Empty	#26	sqle	22.74
E03-Ch5	SYBR	Empty	#26	sqle	22.57
E04-Ch5	SYBR	Empty	#26	sqle	22.72
E05-Ch5	SYBR	Empty	#26	sqle	22.51
E06-Ch5	SYBR	Empty	#26	sqle	22.56
E07-Ch5	[none]	[none]			n. def.
E08-Ch5	SYBR	Empty	DK	sqle	21.57
E09-Ch5	SYBR	Empty	DK	sqle	22.35
E10-Ch5	SYBR	Empty	DK	sqle	21.35
E11-Ch5	SYBR	Empty	DK	sqle	21.38
E12-Ch5	SYBR	Empty	DK	sqle	21.39
E13-Ch5	[none]	[none]			n. def.
E14-Ch5	[none]	[none]			n. def.
E15-Ch5	[none]	[none]			n. def.
E16-Ch5	[none]	[none]			n. def.
F01-Ch5	SYBR	Empty	#26	lss	26.03
F02-Ch5	SYBR	Empty	#26	lss	24.94
F03-Ch5	SYBR	Empty	#26	lss	24.96
F04-Ch5	SYBR	Empty	#26	lss	25.4
F05-Ch5	SYBR	Empty	#26	lss	25.46
F06-Ch5	SYBR	Empty	#26	lss	25.16
F07-Ch5	[none]	[none]			n. def.
F08-Ch5	SYBR	Empty	DK	lss	22.93
F09-Ch5	SYBR	Empty	DK	lss	24.72
F10-Ch5	SYBR	Empty	DK	lss	22.84
F11-Ch5	SYBR	Empty	DK	lss	23.6
F12-Ch5	SYBR	Empty	DK	lss	23.48

Table B-23: Quantification of qRT-PCR test by $2^{-\Delta\Delta}$ method for MEF WT (control) and MEF Δ CT 15 cells.

No.	ΔCt control	ΔCt hmgcs1	Average, ΔCt control	ΔΔCt control	ΔΔCt hmgcs1	control	hmgcs1
1	5.05	4.43		0.312	-0.308	0.8055243	1.23799
2	4.82	4.26		0.082	-0.478	0.944747	1.392811
3	4.81	4.36		0.072	-0.378	0.9513183	1.299539
4	4.83	4.58	4.738	0.092	-0.158	0.9382212	1.115739
1	4.44	4.13		-0.084	-0.394	1.0599528	1.314032
2	4.55	4.38		0.026	-0.144	0.9821396	1.104964
3	4.48	4.02		-0.044	-0.504	1.0309683	1.41814
4	4.75	4.91		0.226	0.386	0.8550022	0.765248
5	4.4	4.67	4.524	-0.124	0.146	1.0897521	0.903753

1	4.42	5.11		-0.076	0.614	1.0540914	0.653383
2	4.48	5.09		-0.016	0.594	1.0111521	0.662504
3	4.44	4.9		-0.056	0.404	1.0395794	0.75576
4	4.65	4.85		0.154	0.354	0.8987551	0.782412
5	4.49	4.15	4.496	-0.006	-0.346	1.0041675	1.271032
					Average	0.976098	1.048379
					SD	0.082228	0.283473
					SE	0.0219764	0.075761
No.	ΔCt control	ΔCt hmgcs2	Average, ΔCt control	ΔΔCt control	ΔΔCt hmgcs2	control	hmgcs2
1	18.26	16.42		-0.224	-2.064	1.1679674	4.18144
2	17.14	16.15		-1.344	-2.334	2.5385418	5.042014
3	19.29	16.94		0.806	-1.544	0.5719655	2.916019
4	19	16.7		0.516	-1.784	0.699308	3.443797
5	18.73	16.65	18.484	0.246	-1.834	0.8432311	3.565242
1	17.88	15.47		-0.05	-2.46	1.0352649	5.502167
2	17.83	17.48		-0.1	-0.45	1.0717735	1.36604
3	18.33	18.2		0.4	0.27	0.7578583	0.82932
4	17.57	17.46	17.93	-0.36	-0.47	1.2834259	1.385109
1	19.23	16.45		0.02	-2.76	0.9862327	6.773962
2	19.2	16.96		-0.01	-2.25	1.0069556	4.756828
3	19.28	16.17		0.07	-3.04	0.952638	8.224911
4	19.07	16		-0.14	-3.21	1.1019051	9.253505
5	19.27	17.1	19.21	0.06	-2.11	0.9592641	4.316913
					Average	1.069738	4.396948
					SD	0.4628777	2.488258
					SE	0.1237093	0.665015
No.	ΔCt control	ΔCt hmgcr	Average, ΔCt control	ΔΔCt control	ΔΔCt hmgcr	control	hmgcr
1	4.51	5.78		-0.466	0.804	1.3812744	0.572759
2	5.26	5.54		0.284	0.564	0.8213107	0.676424
3	5.15	5.4		0.174	0.424	0.8863817	0.745355
4	4.88	5.91		-0.096	0.934	1.068806	0.523405
5	5.08	5.66	4.976	0.104	0.684	0.9304497	0.622437
1	5.38	5.58		0.2	0.4	0.8705506	0.757858
2	5.09	5.72		-0.09	0.54	1.0643702	0.687771
3	5.07	4.31		-0.11	-0.87	1.0792282	1.827663
4	5.36	6.54		0.18	1.36	0.882703	0.389582
5	5	6.07	5.18	-0.18	0.89	1.1328839	0.539614
1	4.85	6.05		-0.158	1.042	1.1157393	0.485654
2	5.02	6.26		0.012	1.252	0.9917167	0.419866
3	5.55	5.97		0.542	0.962	0.6868181	0.513345
4	4.78	5.87		-0.228	0.862	1.1712102	0.550189

5	4.84	5.67	5.008	-0.168	0.662	1.1234999	0.632002
					Average	1.0137962	0.662928
					SD	0.171471	0.340055
					SE	0.0442736	0.087802
No.	ΔCt control	ΔCt mvk	Average, ΔCt control	ΔΔCt control	ΔΔCt mvk	control	mvk
1	7.35	7.52		-0.254	-0.084	1.1925089	1.059953
2	7.61	7.91		0.006	0.306	0.9958498	0.808881
3	7.92	7.7		0.316	0.096	0.803294	0.935623
4	7.54	7.47		-0.064	-0.134	1.0453601	1.097332
5	7.6	7.67	7.604	-0.004	0.066	1.0027764	0.955283
1	7.94	7.65		0.172	-0.118	0.8876113	1.085229
2	7.65	7.46		-0.118	-0.308	1.0852294	1.23799
3	7.78	7.28		0.012	-0.488	0.9917167	1.402499
4	7.72	6.88	7.768	-0.048	-0.888	1.0338307	1.850609
1	7.69	7.78		-0.092	-0.002	1.0658467	1.001387
2	7.71	7.43		-0.072	-0.352	1.0511729	1.276329
3	7.65	7.95		-0.132	0.168	1.0958118	0.890076
4	8.03	7.48		0.248	-0.302	0.842063	1.232852
5	7.83	7.02	7.782	0.048	-0.762	0.9672763	1.69584
					Average	1.0043106	1.180706
					SD	0.1040832	0.300624
					SE	0.0278174	0.080345
No.	ΔCt control	ΔCt pmvk	Average, ΔCt control	ΔΔCt control	ΔΔCt pmvk	control	pmvk
1	16.83	18.2		-0.8	0.57	1.7411011	0.673617
2	17.57	17.75		-0.06	0.12	1.0424658	0.920188
3	18.06	18.21		0.43	0.58	0.7422618	0.668964
4	17	19.41		-0.63	1.78	1.547565	0.291183
5	18.69	19.11	17.63	1.06	1.48	0.4796321	0.358489
1	15.07	16.67		-0.18	1.42	1.1328839	0.373712
2	15.07	15.49		-0.18	0.24	1.1328839	0.846745
3	15.88	16.16		0.63	0.91	0.6461764	0.532185
4	15.07	15.1	15.25	-0.18	-0.15	1.1328839	1.109569
1	7.55	8.23		0.05	0.73	0.9659363	0.602904
2	7.13	8.08		-0.37	0.58	1.2923528	0.668964
3	7.34	8.03		-0.16	0.53	1.1172871	0.692555
4	7.81	7.92		0.31	0.42	0.8066418	0.747425
5	7.67	8	7.5	0.17	0.5	0.8888427	0.707107
					Average	1.0477796	0.656686
					SD	0.3379131	0.222623
					SE	0.0903111	0.059498

No.	ΔCt control	ΔCt mvd	Average, ΔCt control	ΔΔCt control	ΔΔCt mvd	control	mvd
1	7.34	7.68		0.266	0.606	0.8316221	0.657016
2	7.33	7.45		0.256	0.376	0.8374065	0.770571
3	6.83	7.31		-0.244	0.236	1.1842716	0.849096
4	7.09	7.09		0.016	0.016	0.9889709	0.988971
5	6.78	7.97	7.074	-0.294	0.896	1.2260349	0.537375
1	7.61	7.26		0.092	-0.258	0.9382212	1.19582
2	7.43	7.8		-0.088	0.282	1.0628957	0.82245
3	7.89	7.44		0.372	-0.078	0.7727105	1.055554
4	7.22	7.17	7.518	-0.298	-0.348	1.2294389	1.272795
1	6.95	8.45		-0.086	1.414	1.0614232	0.37527
2	6.75	7.94		-0.286	0.904	1.2192551	0.534403
3	7.14	8.09		0.104	1.054	0.9304497	0.481631
4	7.39	8.58		0.354	1.544	0.7824118	0.342933
5	6.95	7.91	7.036	-0.086	0.874	1.0614232	0.545632
					Average	1.0090382	0.744965
					SD	0.1661068	0.298448
					SE	0.0443939	0.079764
No.	ΔCt control	ΔCt fdps	Average, ΔCt control	ΔΔCt control	ΔΔCt fdps	control	fdps
1	4.61	5.22		0.276	0.886	0.8258777	0.541112
2	4.37	4.64		0.036	0.306	0.9753555	0.808881
3	4.21	4.4		-0.124	0.066	1.0897521	0.955283
4	4.37	4.28		0.036	-0.054	0.9753555	1.038139
5	4.11	4.91	4.334	-0.224	0.576	1.1679674	0.670821
1	4.18	5.14		-0.112	0.848	1.0807254	0.555554
2	4.3	5.08		0.008	0.788	0.9944702	0.579146
3	4.13	5.55		-0.162	1.258	1.1188371	0.418123
4	4.47	5.13		0.178	0.838	0.8839275	0.559419
5	4.38	4.66	4.292	0.088	0.368	0.9408261	0.774856
1	3.93	4.9		-0.256	0.714	1.1941632	0.609628
2	3.59	5.1		-0.596	0.914	1.5115199	0.530712
3	3.9	4.78		-0.286	0.594	1.2192551	0.662504
4	4.53	4.88		0.344	0.694	0.7878539	0.618138
5	4.98	4.42	4.186	0.794	0.234	0.5767428	0.850274
					Average	1.022842	0.678173
					SD	0.2186316	0.172817
					SE	0.0564504	0.044621
No.	ΔCt control	ΔCt fdft	Average, ΔCt control	ΔΔCt control	ΔΔCt fdft	control	fdft
1	5.55	4.58		0.522	-0.448	0.6964057	1.364148
2	4.98	4.49		-0.048	-0.538	1.0338307	1.451958

3	4.74	4.35		-0.288	-0.678	1.2209465	1.59992
4	5.27	4.08		0.242	-0.948	0.8455723	1.929196
5	4.6	4.78	5.028	-0.428	-0.248	1.3453672	1.18756
1	4.58	4.45		0.23	0.1	0.8526349	0.933033
2	4.5	3.63		0.15	-0.72	0.9012505	1.647182
3	4.47	4.67	4.35	0.12	0.32	0.9201877	0.80107
1	4.51	4.57		-0.47	-0.41	1.3851095	1.328686
2	5.35	5.26		0.37	0.28	0.7737825	0.823591
3	4.82	4.99		-0.16	0.01	1.1172871	0.993092
4	5.15	4.94		0.17	-0.04	0.8888427	1.028114
5	5.07	4.8	4.98	0.09	-0.18	0.9395227	1.132884
					Average	0.9939031	1.247726
					SD	0.21445	0.343769
					SE	0.0594777	0.095344
No.	ΔCt control	ΔCt sqle	Average, ΔCt control	ΔΔCt control	ΔΔCt sqle	control	sqle
1	5.49	4.79		0.334	-0.366	0.7933338	1.288775
2	5	4.75		-0.156	-0.406	1.1141937	1.325007
3	5.3	4.78		0.144	-0.376	0.9050065	1.297739
4	5.11	4.48		-0.046	-0.676	1.0323985	1.597704
5	4.88	5.39	5.156	-0.276	0.234	1.2108331	0.850274
1	8.38	6.41		1.216	-0.754	0.4304746	1.686462
2	6.6	6.02		-0.564	-1.144	1.4783624	2.209929
3	6.88	6.21		-0.284	-0.954	1.217566	1.937236
1	4.75	4.8		-0.392	-0.342	1.3122113	1.267513
2	5.39	5.51		0.248	0.368	0.842063	0.774856
3	5.16	5.32		0.018	0.178	0.9876009	0.883928
4	5.14	5.7		-0.002	0.558	1.0013873	0.679243
5	5.27	5.01	5.142	0.128	-0.132	0.9150992	1.095812
					Average	1.0185023	1.299575
					SD	0.2639655	0.461159
					SE	0.0732109	0.127902
No.	ΔCt control	ΔCt lss	Average, ΔCt control	ΔΔCt control	ΔΔCt lss	control	lss
1	7.32	7.59		-0.026	0.244	1.0181852	0.844401
2	7.94	7.43		0.594	0.084	0.6625035	0.943438
3	7.05	7.25		-0.296	-0.096	1.2277357	1.068806
4	7.3	6.72		-0.046	-0.626	1.0323985	1.54328
5	7.12	7.9	7.346	-0.226	0.554	1.1695877	0.681129
1	8.01	8.16		-0.016	0.134	1.0111521	0.911301
2	8.1	7.28		0.074	-0.746	0.9500004	1.677136
3	8.08	9.56		0.054	1.534	0.9632619	0.345319
4	7.86	7.23	8.026	-0.166	-0.796	1.1219435	1.73628

1	6.42	7.12		-0.566	0.134	1.4804133	0.911301
2	7.06	7.46		0.074	0.474	0.9500004	0.719966
3	6.99	7.36		0.004	0.374	0.9972313	0.77164
4	7.18	7.3		0.194	0.314	0.8741786	0.804408
5	7.28	6.93	6.986	0.294	-0.056	0.8156375	1.039579
					Average	1.0195878	0.999856
					SD	0.1946408	0.396556
					SE	0.0520199	0.105984

Table B-24: Quantification of qRT-PCR test by $2^{-\Delta\Delta}$ method for MEF WT (control) and MEF APP-APLP2 -/- cells.

No.	ΔCt control	ΔCt hmgcs1	Average, ΔCt control	ΔΔCt control	ΔΔCt hmgcs1	control	hmgcs1
1	4.18	4.98		-0.558	0.242	1.4722269	0.845572
2	5.05	4.92		0.312	0.182	0.8055243	0.88148
3	4.82	4.4		0.082	-0.338	0.944747	1.264003
4	4.81	5.59		0.072	0.852	0.9513183	0.554016
5	4.83	4.47	4.738	0.092	-0.268	0.9382212	1.204137
1	4.44	4.41		-0.084	-0.114	1.0599528	1.082225
2	4.55	4.81		0.026	0.286	0.9821396	0.820173
3	4.48	4.33		-0.044	-0.194	1.0309683	1.143931
4	4.75	4.8		0.226	0.276	0.8550022	0.825878
5	4.4	5.04	4.524	-0.124	0.516	1.0897521	0.699308
1	4.51	5.69		-0.1633333	1.016666667	1.1198716	0.494257
2	4.49	5.74		-0.1833333	1.066666667	1.1355044	0.477421
3	4.74	5.69		0.06666667	1.016666667	0.9548416	0.494257
4	4.66	5.62		-0.0133333	0.946666667	1.0092848	0.51883
5	4.85	5.58	4.673333	0.17666667	0.906666667	0.8847448	0.533416
6	4.79	5.57		0.11666667	0.896666667	0.9223162	0.537126
					Average	1.009776	0.773502
					SD	0.1541982	0.27761
					SE	0.0385495	0.069403
No.	ΔCt control	ΔCt hmgcs2	Average, ΔCt control	ΔΔCt control	ΔΔCt hmgcs2	control	hmgcs2
1	18.26	18.26		-0.224	-0.224	1.1679674	1.167967
2	19	19.11		0.516	0.626	0.699308	0.64797
3	18.73	19.08	18.484	0.246	0.596	0.8432311	0.661586
1	17.88	18.24		-0.05	0.31	1.0352649	0.806642

2	17.83	17.43		-0.1	-0.5	1.0717735	1.414214
3	18.04	17.04		0.11	-0.89	0.9265881	1.853176
4	18.33	17.63		0.4	-0.3	0.7578583	1.231144
5	17.57	17.51	17.93	-0.36	-0.42	1.2834259	1.337928
1	19.42	19.35		-0.78	-0.85	1.7171309	1.802501
2	21.13	19.35		0.93	-0.85	0.5248583	1.802501
3	20.61	19.93		0.41	-0.27	0.7526234	1.205808
4	19.99	19.8	20.2	-0.21	-0.4	1.1566882	1.319508
5	21.2	19.94		1	-0.26	0.5	1.197479
					Average	0.9566706	1.265263
					SD	0.3348294	0.400819
					SE	0.092865	0.111167
No.	ΔCt control	ΔCt hmgcr	Average, ΔCt control	ΔΔCt control	ΔΔCt hmgcr	control	hmgcr
1	4.51	5.31		-0.466	0.334	1.3812744	0.793334
2	5.26	5.21		0.284	0.234	0.8213107	0.850274
3	5.15	4.74		0.174	-0.236	0.8863817	1.177723
4	4.88	5.45		-0.096	0.474	1.068806	0.719966
5	5.08	4.82	4.976	0.104	-0.156	0.9304497	1.114194
1	5.38	5.86		0.2	0.68	0.8705506	0.624165
2	5.09	5.66		-0.09	0.48	1.0643702	0.716978
3	5.07	5.38		-0.11	0.2	1.0792282	0.870551
4	5.36	5.38		0.18	0.2	0.882703	0.870551
5	5	5.99	5.18	-0.18	0.81	1.1328839	0.570382
1	4.77	6.28		-0.13	1.38	1.0942937	0.384219
2	4.58	5.97		-0.32	1.07	1.2483305	0.476319
3	4.9	5.91		0	1.01	1	0.496546
4	4.99	5.88		0.09	0.98	0.9395227	0.50698
5	5	5.98	4.9	0.1	1.08	0.933033	0.473029
	5.16	6.04		0.26	1.14	0.8350879	0.45376
					Average	1.0105141	0.693686
					SD	0.1554572	0.238383
					SE	0.0388643	0.059596
No.	ΔCt control	ΔCt mvk	Average, ΔCt control	ΔΔCt control	ΔΔCt mvk	control	mvk
1	7.35	7.84		-0.254	0.236	1.1925089	0.849096
2	7.61	7.75		0.006	0.146	0.9958498	0.903753
3	7.92	7.74		0.316	0.136	0.803294	0.910039
4	7.54	8.19		-0.064	0.586	1.0453601	0.666187
5	7.6	7.81	7.604	-0.004	0.206	1.0027764	0.866938
1	7.65	7.65		-0.118	-0.118	1.0852294	1.085229
2	7.75	8.03		-0.018	0.262	1.0125548	0.833931
3	7.78	8.25		0.012	0.482	0.9917167	0.715984

4	7.72	8.1	7.768	-0.048	0.332	1.0338307	0.794434
1	7.31	8.54		-0.3466667	0.883333333	1.2716192	0.542113
2	7.31	8.51		-0.3466667	0.853333333	1.2716192	0.553504
3	7.62	8.43		-0.0366667	0.773333333	1.0257411	0.585064
4	8.25	8.47		0.59333333	0.813333333	0.6628097	0.569066
5	7.82	8.48	7.656667	0.16333333	0.823333333	0.8929595	0.565135
					Average	1.0205621	0.745748
					SD	0.1649994	0.170523
					SE	0.0440979	0.045574
No.	ΔCt control	ΔCt pmvk	Average, ΔCt control	ΔΔCt control	ΔΔCt pmvk	control	pmvk
1	16.83	20.26		-0.8	2.63	1.7411011	0.161544
2	17.57	18.48		-0.06	0.85	1.0424658	0.554785
3	18.06	17.81		0.43	0.18	0.7422618	0.882703
4	18.69	17.35	17.63	1.06	-0.28	0.4796321	1.214195
1	15.07	16		-0.18	0.75	1.1328839	0.594604
2	15.07	17.06		-0.18	1.81	1.1328839	0.285191
3	15.16	16.88		-0.09	1.63	1.0643702	0.323088
4	15.07	16.88	15.25	-0.18	1.63	1.1328839	0.323088
1	7.72	8.91		0.19333333	1.383333333	0.8745827	0.383332
2	7.5	8.96		-0.0266667	1.433333333	1.0186558	0.370274
3	7.13	8.76		-0.3966667	1.233333333	1.3164627	0.425334
4	7.74	8.69	7.526667	0.21333333	1.163333333	0.862542	0.44648
5	7.28	8.29		-0.2466667	0.763333333	1.1864626	0.589134
					Average	1.0559376	0.504135
					SD	0.2992457	0.27964
					SE	0.0829958	0.077558
No.	ΔCt control	ΔCt mvd	Average, ΔCt control	ΔΔCt control	ΔΔCt mvd	control	mvd
1	7.34	7.97		0.266	0.896	0.8316221	0.537375
2	7.33	6.77		0.256	-0.304	0.8374065	1.234563
3	6.83	8.11		-0.244	1.036	1.1842716	0.487678
4	7.09	7.65		0.016	0.576	0.9889709	0.670821
5	6.78	8.09	7.074	-0.294	1.016	1.2260349	0.494485
1	7.61	7.41		0.092	-0.108	0.9382212	1.077733
2	7.43	8.42		-0.088	0.902	1.0628957	0.535144
3	7.44	9.21		-0.078	1.692	1.0555537	0.309498
4	7.89	9.65		0.372	2.132	0.7727105	0.228141
5	7.22	8.75	7.518	-0.298	1.232	1.2294389	0.425727
1	6.87	8.82		-0.0466667	1.903333333	1.0328757	0.267325
2	7.25	9.1		0.33333333	2.183333333	0.7937005	0.220166
3	6.64	8.89		-0.2766667	1.973333333	1.2113927	0.254664
4	7.04	8.87		0.12333333	1.953333333	0.918064	0.258219

5	7.12	8.74	6.916667	0.20333333	1.823333333	0.8685415	0.282567
6	6.58	8.27		-0.3366667	1.353333333	1.2628355	0.391387
					Average	1.0134085	0.479718
					SD	0.1700287	0.29717
					SE	0.0425072	0.074293
No.	ΔCt control	ΔCt fdps	Average, ΔCt control	ΔΔCt control	ΔΔCt fdps	control	fdps
1	4.61	3.95		0.276	-0.384	0.8258777	1.304955
2	4.37	2.61		0.036	-1.724		
3	4.21	3.9		-0.124	-0.434	1.0897521	1.350974
4	4.37	3.34		0.036	-0.994	0.9753555	1.9917
5	4.11	4.49	4.334	-0.224	0.156	1.1679674	0.89751
1	4.18	4.78		-0.112	0.488	1.0807254	0.713013
2	4.3	5.11		0.008	0.818	0.9944702	0.567228
3	4.13	4.84		-0.162	0.548	1.1188371	0.683968
4	4.47	4.94		0.178	0.648	0.8839275	0.638164
5	4.38	4.74	4.292	0.088	0.448	0.9408261	0.733058
1	4.2	5.5		0.03333333	1.333333333	0.97716	0.39685
2	4.17	5.3		0.00333333	1.133333333	0.9976922	0.455861
3	3.68	5.77		-0.4866667	1.603333333	1.4012037	0.329116
4	4.78	4.92		0.61333333	0.753333333	0.6536846	0.593231
5	4.42	5.01	4.166667	0.25333333	0.843333333	0.8389558	0.557354
6	3.75	4.7		-0.4166667	0.533333333	1.3348399	0.690956
					Average	1.0187517	0.793596
					SD	0.1925473	0.439943
					SE	0.0497155	0.113593
No.	ΔCt control	ΔCt fdft	Average, ΔCt control	ΔΔCt control	ΔΔCt fdft	control	fdft
1	5.55	4.67		0.522	-0.358	0.6964057	1.281648
2	4.74	4.74		-0.288	-0.288	1.2209465	1.220947
3	5.27	4.42		0.242	-0.608	0.8455723	1.524145
4	4.6	5.07	5.028	-0.428	0.042	1.3453672	0.971307
1	4.58	4		0.23	-0.35	0.8526349	1.274561
2	3.85	4.59		-0.5	0.24	1.4142136	0.846745
3	4.47	4.75	4.35	0.12	0.4	0.9201877	0.757858
1	4.85	5.04		-0.1966667	-0.00666667	1.1460474	1.004632
2	5.24	5.93		0.19333333	0.883333333	0.8745827	0.542113
3	4.94	5.87		-0.1066667	0.823333333	1.0767376	0.565135
4	5.15	5.81		0.10333333	0.763333333	0.9308797	0.589134
5	4.89	5.72	5.046667	-0.1566667	0.673333333	1.1147086	0.627056
6	5.21	5.69		0.16333333	0.643333333	0.8929595	0.640232
					Average	1.0254803	0.911193

					SD	0.213634	0.32848
					SE	0.0592514	0.091104
No.	ΔCt control	ΔCt sqle	Average, ΔCt control	ΔΔCt control	ΔΔCt sqle	control	sqle
1	5.49	5.23		0.334	0.074	0.7933338	0.95
2	5	3.9		-0.156	-1.256	1.1141937	2.388326
3	5.3	5.54		0.144	0.384	0.9050065	0.76631
4	5.11	4.65		-0.046	-0.506	1.0323985	1.420107
5	4.88	5.47	5.156	-0.276	0.314	1.2108331	0.804408
1	6.88	6.02		-0.284	-1.144	1.217566	2.209929
2	6.51	5.91	7.164	-0.654	-1.254	1.5735249	2.385018
1	5.27	5.59		-0.1783333	0.141666667	1.1315759	0.906471
2	5.53	6.12		0.08166667	0.671666667	0.9449653	0.627781
3	5.13	6.32		-0.3183333	0.871666667	1.2468893	0.546515
4	5.69	6.17		0.24166667	0.721666667	0.8457677	0.606397
5	5.49	6.04	5.448333	0.04166667	0.591666667	0.9715319	0.663576
6	5.58	6.03		0.13166667	0.581666667	0.9127764	0.668191
					Average	1.0692587	1.149464
					SD	0.2116767	0.708416
					SE	0.0587086	0.196479
No.	ΔCt control	ΔCt lss	Average, ΔCt control	ΔΔCt control	ΔΔCt lss	control	lss
1	7.32	7.99		-0.026	0.644	1.0181852	0.639936
2	7.94	6.36		0.594	-0.986	0.6625035	1.980686
3	7.05	7.49		-0.296	0.144	1.2277357	0.905006
4	7.3	6.51		-0.046	-0.836	1.0323985	1.785094
5	7.12	7.3	7.346	-0.226	-0.046	1.1695877	1.032399
1	8.08	7.17		0.054	-0.856	0.9632619	1.810013
2	8.08	8.18		0.054	0.154	0.9632619	0.898755
3	7.86	8.37	8.026	-0.166	0.344	1.1219435	0.787854
1	7.1	7.98		0.025	0.905	0.9828206	0.534033
2	7.06	8.06		-0.015	0.985	1.0104514	0.505226
3	6.93	8.01		-0.145	0.935	1.1057307	0.523042
4	7.3	8.45		0.225	1.375	0.855595	0.385553
5	6.91	8.4	7.075	-0.165	1.325	1.1211661	0.399149
6	7.15	8.13		0.075	1.055	0.9493421	0.481297
					Average	1.0131417	0.90486
					SD	0.1416233	0.554667
					SE	0.0378504	0.148241

Table B-25: Quantification of qRT-PCR test by $2^{-\Delta\Delta}$ method for MEF PS1 rescue (control) and MEF PS1 -/- cells.

No.	ΔCt control	ΔCt hmgcs1	Average, ΔCt control	ΔΔCt control	ΔΔCt hmgcs1	control	hmgcs1
1	6.25	5.2		0.172	-0.878	0.8876113	1.837826
2	6.32	5.36		0.242	-0.718	0.8455723	1.6449
3	5.44	5.14		-0.638	-0.938	1.5561704	1.91587
4	6.08	5.73	6.078	0.002	-0.348	0.9986147	1.272795
1	5.28	5.1		-0.482	-0.662	1.3966785	1.582275
2	5.9	4.72		0.138	-1.042	0.9087781	2.05908
3	5.95	4.92		0.188	-0.842	0.8778218	1.792533
4	5.89	4.47		0.128	-1.292	0.9150992	2.448673
5	5.79	4.7	5.762	0.028	-1.062	0.980779	2.087824
1	5.53	4.73		-1.0366667	-1.83666667	2.0514822	3.571838
2	6.84	5.26		0.27333333	-1.30666667	0.8274056	2.473693
3	6.45	4.64		-0.1166667	-1.92666667	1.0842269	3.801758
4	6.37	5.11		-0.1966667	-1.45666667	1.1460474	2.744735
5	6.95	4.64		0.38333333	-1.92666667	0.7666642	3.801758
					Average	1.0887823	2.359683
					SD	0.3570909	0.753323
					SE	0.0954365	0.201334
No.	ΔCt control	ΔCt hmgcs2	Average, ΔCt control	ΔΔCt control	ΔΔCt hmgcs2	control	hmgcs2
1	19.45	19.33		0.414	0.294	0.7505395	0.815637
2	19.48	19.2		0.444	0.164	0.7350937	0.892547
3	18.87	19.22		-0.166	0.184	1.1219435	0.880259
4	19.02	18.34	19.036	-0.016	-0.696	1.0111521	1.620007
1	18.06	18.98		-0.518	0.402	1.4319687	0.756808
2	18.58	18.16		0.002	-0.418	0.9986147	1.336074
3	18.92	18.72		0.342	0.142	0.7889468	0.906262
4	18.77	18.91		0.192	0.332	0.8753913	0.794434
5	18.56	18.76	18.578	-0.018	0.182	1.0125548	0.88148
1	20.64	20.15		0.63	0.14	0.6461764	0.907519
2	19.66	18.99		-0.35	-1.02	1.2745606	2.027919
3	20.18	20.73		0.17	0.72	0.8888427	0.607097
					Average	0.9613154	1.035504
					SD	0.2314383	0.414057
					SE	0.0668105	0.119528
No.	ΔCt control	ΔCt hmgcr	Average, ΔCt control	ΔΔCt control	ΔΔCt hmgcr	control	hmgcr
1	6.95	6.02		0.33	-0.6	0.7955365	1.515717
2	6.73	6.03		0.11	-0.59	0.9265881	1.505247
3	6.29	5.76		-0.33	-0.86	1.2570134	1.815038

4	6.61	6.44	6.62	-0.01	-0.18	1.0069556	1.132884
1	5.82	5.95		-0.308	-0.178	1.2379903	1.131314
2	6.21	5.36		0.082	-0.768	0.944747	1.702907
3	6.22	5.03		0.092	-1.098	0.9382212	2.140577
4	6.07	5.55	6.128	-0.058	-0.578	1.0410216	1.492778
1	5.8	5.38		-0.8033333	-1.22333333	1.7451286	2.334856
2	7.05	6		0.44666667	-0.60333333	0.7337362	1.519223
3	6.96	5.31		0.35666667	-1.29333333	0.7809669	2.450937
4	6.75	6.19		0.14666667	-0.41333333	0.9033352	1.331759
5	6.98	5.9	6.603333	0.37666667	-0.70333333	0.7702151	1.628263
6	6.08	6.02		-0.5233333	-0.58333333	1.4372722	1.498307
					Average	1.037052	1.657129
					SD	0.2760154	0.417868
					SE	0.0737682	0.11168
No.	ΔCt control	ΔCt mvk	Average, ΔCt control	ΔΔCt control	ΔΔCt mvk	control	mvk
1	8.31	8.1		-0.02	-0.23	1.0139595	1.172835
2	8.31	8.37		-0.02	0.04	1.0139595	0.972655
3	8.25	7.85		-0.08	-0.48	1.057018	1.394744
4	8.21	8.39	8.33	-0.12	0.06	1.0867349	0.959264
1	7.64	7.79		-0.094	0.056	1.0673253	0.961927
2	7.87	7.7		0.136	-0.034	0.9100388	1.023847
3	7.75	8.37		0.016	0.636	0.9889709	0.643495
4	7.78	8.33		0.046	0.596	0.9686182	0.661586
5	7.63	8.17	7.734	-0.104	0.436	1.0747492	0.739181
1	7.51	8.47		-0.9866667	-0.02666667	1.9816012	1.018656
2	8.76	8.44		0.26333333	-0.05666667	0.8331607	1.04006
3	9.04	8.18	8.496667	0.54333333	-0.31666667	0.6861837	1.24545
4	8.64	8.15		0.14333333	-0.34666667	0.9054248	1.271619
					Average	1.0452111	1.008101
					SD	0.3135636	0.225562
					SE	0.0869669	0.06256
No.	ΔCt control	ΔCt pmvk	Average, ΔCt control	ΔΔCt control	ΔΔCt pmvk	control	pmvk
1	18.54	17.12		0.156	-1.264	0.8975101	2.401607
2	18.14	18.18		-0.244	-0.204	1.1842716	1.151888
3	19.34	17.96		0.956	-0.424	0.5154842	1.341642
4	18.26	19.44		-0.124	1.056	1.0897521	0.480964
5	17.64	18.91	18.384	-0.744	0.526	1.674813	0.694478
1	18.58	17.03		0.13	-1.42	0.9138315	2.675855
2	19.54	17.52		1.09	-0.93	0.4697614	1.905276
3	17.95	17.83	18.45	-0.5	-0.62	1.4142136	1.536875
1	7.06	8.83		-0.972	0.798	1.961558	0.575146
2	8.21	8.83		0.178	0.798	0.8839275	0.575146

3	7.9	7.95		-0.132	-0.082	1.0958118	1.058484
4	8.68	8.75		0.648	0.718	0.6381644	0.60794
5	8.31	7.88	8.032	0.278	-0.152	0.8247335	1.111109
					Average	1.0433717	1.239724
					SD	0.4365805	0.716862
					SE	0.1210856	0.198822
No.	ΔCt control	ΔCt mvd	Average, ΔCt control	ΔΔCt control	ΔΔCt mvd	control	mvd
1	7.81	8.16		-0.184	0.166	1.1360293	0.89131
2	8.02	7.59		0.026	-0.404	0.9821396	1.323171
3	8.26	8.15		0.266	0.156	0.8316221	0.89751
4	8.15	8.27		0.156	0.276	0.8975101	0.825878
5	7.73	7.83	7.994	-0.264	-0.164	1.2008034	1.120389
1	6.93	7.84		-0.68	0.23	1.6021398	0.852635
2	7.78	8.12		0.17	0.51	0.8888427	0.702222
3	7.82	7.95		0.21	0.34	0.8645372	0.790041
4	7.62	8	7.61	0.01	0.39	0.9930925	0.76313
1	7.24	7.33		-0.0633333	0.026666667	1.0448772	0.981686
2	7.18	6.85		-0.1233333	-0.45333333	1.0892487	1.3692
3	7.82	7.55	7.303333	0.51666667	0.246666667	0.698985	0.842842
4	7.61	6.96		0.30666667	-0.34333333	0.8085077	1.268684
					Average	1.0029488	0.971438
					SD	0.2311068	0.215187
					SE	0.0640975	0.059682
No.	ΔCt control	ΔCt fdps	Average, ΔCt control	ΔΔCt control	ΔΔCt fdps	control	fdps
1	6.04	5.52		0.128	-0.392	0.9150992	1.312211
2	6.41	5.51		0.498	-0.402	0.7080877	1.321338
3	6.04	5.81		0.128	-0.102	0.9150992	1.07326
4	5.12	5.08		-0.792	-0.832	1.7314731	1.780151
5	5.95	5.53	5.912	0.038	-0.382	0.9740043	1.303147
1	5.78	5.07		0.176	-0.534	0.8851538	1.447938
2	5.71	4.81		0.106	-0.794	0.9291607	1.733875
3	5.83	4.86		0.226	-0.744	0.8550022	1.674813
4	5.71	5.15	5.604	0.106	-0.454	0.9291607	1.369833
1	5.86	4.24		0.65	-0.97	0.6372803	1.958841
2	5.05	4.92		-0.16	-0.29	1.1172871	1.22264
3	4.87	4.5		-0.34	-0.71	1.2657566	1.635804
4	5.58	5.1	5.21	0.37	-0.11	0.7737825	1.079228
5	5.69	4.29		0.48	-0.92	0.7169776	1.892115
					Average	0.9538089	1.486085
					SD	0.2793681	0.278073

					SE	0.0746643	0.074318
No.	ΔCt control	ΔCt fdft	Average, ΔCt control	ΔΔCt control	ΔΔCt fdft	control	fdft
1	5.77	5.82		-0.046	0.004	1.0323985	0.997231
2	6.67	5.82		0.854	0.004	0.5532487	0.997231
3	5.94	5.84		0.124	0.024	0.9176399	0.983502
4	5.62	5.32	5.816	-0.196	-0.496	1.1455179	1.410298
1	5.81	5.41		0.422	0.022	0.7463892	0.984866
2	4.86	4.75		-0.528	-0.638	1.4419289	1.55617
3	5.38	5.13		-0.008	-0.258	1.0055606	1.19582
4	5.42	5.61		0.032	0.222	0.9780635	0.857376
5	5.47	5.19	5.388	0.082	-0.198	0.944747	1.147107
1	5.59	4.96		-0.3733333	-1.00333333	1.2953423	2.004626
2	6.08	5.73		0.11666667	-0.23333333	0.9223162	1.175548
3	5.96	5.81		-0.0033333	-0.15333333	1.0023132	1.112136
4	5.65	5.74		-0.3133333	-0.22333333	1.2425753	1.167428
5	6.2	4.99	5.963333	0.23666667	-0.97333333	0.848704	1.963372
					Average	1.0054818	1.253765
					SD	0.2309202	0.305977
					SE	0.061716	0.081776
No.	ΔCt control	ΔCt sqle	Average, ΔCt control	ΔΔCt control	ΔΔCt sqle	control	sqle
1	6.23	5.87		0.012	-0.348	0.9917167	1.272795
2	6.48	6.05		0.262	-0.168	0.833931	1.1235
3	6.55	6.2		0.332	-0.018	0.7944344	1.012555
4	5.63	5.7		-0.588	-0.518	1.5031615	1.431969
5	6.2	6.21	6.218	-0.018	-0.008	1.0125548	1.005561
1	6.24	5.85		-0.016	-0.406	1.0111521	1.325007
2	6.26	7.09		0.004	0.834	0.9972313	0.560972
3	6.3	5.3		0.044	-0.956	0.9699619	1.939924
4	5.99	5.22	6.256	-0.266	-1.036	1.2024692	2.050534
1	6.46	5.78		-0.6416667	-1.32166667	1.5601305	2.499547
2	6.47	3.07	7.101667	-0.6316667	-4.03166667	1.5493538	16.35508
3	6.24	5.13		-0.8616667	-1.97166667	1.8171363	3.92221
					Average	1.1869361	2.874971
					SD	0.282119	4.53592
					SE	0.0814407	1.309407
No.	ΔCt control	ΔCt lss	Average, ΔCt control	ΔΔCt control	ΔΔCt lss	control	lss
1	7.79	7.55		-0.202	-0.442	1.1502919	1.358486
2	8.52	7.91		0.528	-0.082	0.6935155	1.058484
3	7.93	7.79		-0.062	-0.202	1.0439119	1.150292

4	7.49	7.45		-0.502	-0.542	1.4161754	1.45599
5	8.23	8.17	7.992	0.238	0.178	0.84792	0.883928
1	8.07	7.87		0.192	-0.008	0.8753913	1.005561
2	8.23	8.34		0.352	0.462	0.7834972	0.725979
3	8.17	8.59		0.292	0.712	0.816769	0.610473
4	7.04	6.83	7.878	-0.838	-1.048	1.7875703	2.067661
1	9.63	7.14		-0.0283333	-2.51833333	1.0198333	5.729199
2	9.19	7.22	9.658333	-0.4683333	-2.43833333	1.3835103	5.420152
					Average	1.0743987	1.951473
					SD	0.3354105	1.507482
					SE	0.1011301	0.454523

Table B-26: Quantification of qRT-PCR test by $2^{-\Delta\Delta}$ method for MEF WT (control) and MEF APP Δ CT 15 cells (SREBP-1).

No.	ΔCt control	ΔCt srebf1	Average, ΔCt control	ΔΔCt control	ΔΔCt srebf1	control	srebf1
1	6.83	6.51		-0.334	-0.654	1.2605034	1.573525
2	6.96	6.73		-0.204	-0.434	1.1518876	1.350974
3	7.34	7.44		0.176	0.276	0.8851538	0.825878
4	7.25	6.38		0.086	-0.784	0.9421313	1.721898
5	7.44	6.93	7.164	0.276	-0.234	0.8258777	1.176091
					Average	1.0131107	1.329673
					SD	0.1850199	0.350412
					SE	0.0827434	0.156709
No.	ΔCt control	ΔCt srebf2	Average, ΔCt control	ΔΔCt control	ΔΔCt srebf2	control	srebf2
1	5.53	5.35		-0.316	-0.496	1.2448742	1.410298
2	6.09	5.88		0.244	0.034	0.8444009	0.976709
3	5.72	6.18		-0.126	0.334	1.0912639	0.793334
4	5.88	5.71		0.034	-0.136	0.9767085	1.098854
5	6.01	5.82	5.846	0.164	-0.026	0.892547	1.018185
					Average	1.0099589	1.059476
					SD	0.1613198	0.225839
					SE	0.0721444	0.100998
No.	ΔCt control	ΔCt scap	Average, ΔCt control	ΔΔCt control	ΔΔCt scap	control	scap
1	7.68	7.42		-0.046	-0.306	1.0323985	1.236275

2	7.81	7.05		0.084	-0.676	0.9434383	1.597704
3	7.78	7.04		0.054	-0.686	0.9632619	1.608817
4	7.63	6.97		-0.096	-0.756	1.068806	1.688802
5	7.73	7.77	7.726	0.004	0.044	0.9972313	0.969962
					Average	1.0010272	1.420312
					SD	0.0508312	0.306502
					SE	0.0227324	0.137072
No.	ΔCt control	ΔCt insing1	Average, ΔCt control	ΔΔCt control	ΔΔCt insig1	control	insig1
1	5.74	6.22		-0.416	0.064	1.3342232	0.956608
2	6.57	6.22		0.414	0.064	0.7505395	0.956608
3	6.12	6.73		-0.036	0.574	1.0252672	0.671752
4	6.03	5.88		-0.126	-0.276	1.0912639	1.210833
5	6.32	6.25	6.156	0.164	0.094	0.892547	0.936921
					Average	1.0187682	0.946545
					SD	0.2194813	0.190824
					SE	0.098155	0.085339
No.	ΔCt control	ΔCt s1p	Average, ΔCt control	ΔΔCt control	ΔΔCt s1p	control	s1p
1	6.78	6.14		-0.17	-0.81	1.1250585	1.753211
2	7.01	6.55		0.06	-0.4	0.9592641	1.319508
3	6.97	6.71		0.02	-0.24	0.9862327	1.180993
4	6.88	6.29		-0.07	-0.66	1.0497167	1.580083
5	7.11	6.51	6.95	0.16	-0.44	0.8950251	1.356604
					Average	1.0030594	1.43808
					SD	0.0879393	0.227082
					SE	0.0393276	0.101554

Table B-27: Quantification of qRT-PCR test by $2^{-\Delta\Delta}$ method for MEF WT (control) and MEF APP/APLP2 -/- cells (SREBP-1).

No.	ΔCt control	ΔCt srebf1	Average, ΔCt control	ΔΔCt control	ΔΔCt srebf1	control	srebf1
1	5.99	5.27		-0.5016667	-1.22166667	1.4158483	2.33216
2	6.6	6.35		0.10833333	-0.14166667	0.9276591	1.103179
3	6.71	6.26		0.21833333	-0.23166667	0.8595579	1.174191
4	6.52	5.62		0.02833333	-0.87166667	0.9805524	1.829776
5	6.66	6.12		0.16833333	-0.37166667	0.8898701	1.293847
6	6.47	5.87	6.491667	-0.0216667	-0.62166667	1.0151315	1.538652

					Average	1.0147699	1.545301
					SD	0.2046039	0.468304
					SE	0.0835292	0.191184
No.	ΔCt control	ΔCt srebf2	Average, ΔCt control	ΔΔCt control	ΔΔCt srebf2	control	srebf2
1	4.37	4.73		-0.7033333	-0.34333333	1.6282625	1.268684
2	5.28	5.92		0.20666667	0.846666667	0.866537	0.556068
3	5.07	5.56		-0.0033333	0.486666667	1.0023132	0.713672
4	5.08	5.13		0.00666667	0.056666667	0.9953897	0.961483
5	5.11	5.64		0.03666667	0.566666667	0.9749049	0.675175
6	5.53	5.65	5.073333	0.45666667	0.576666667	0.7286679	0.670511
					Average	1.0326792	0.807599
					SD	0.3099665	0.262564
					SE	0.1265433	0.107191
No.	ΔCt control	ΔCt scap	Average, ΔCt control	ΔΔCt control	ΔΔCt scap	control	scap
1	7.56	7.59		-0.02	0.01	1.0139595	0.993092
2	7.7	7.81		0.12	0.23	0.9201877	0.852635
3	7.37	8.02		-0.21	0.44	1.1566882	0.737135
4	7.59	7.87		0.01	0.29	0.9930925	0.817902
5	7.76	7.81		0.18	0.23	0.882703	0.852635
6	7.5	8.22	7.58	-0.08	0.64	1.057018	0.641713
					Average	1.0039415	0.815852
					SD	0.0980614	0.118866
					SE	0.0400334	0.048527
No.	ΔCt control	ΔCt insing1	Average, ΔCt control	ΔΔCt control	ΔΔCt insig1	control	insig1
1	5.59	6.8		-0.2866667	0.923333333	1.2198186	0.527289
2	5.95	6.74		0.07333333	0.863333333	0.9504395	0.549681
3	5.73	6.57		-0.1466667	0.693333333	1.1070088	0.618423
4	5.88	6.75		0.00333333	0.873333333	0.9976922	0.545884
5	6.15	6.74		0.27333333	0.863333333	0.8274056	0.549681
6	5.96	6.64	5.876667	0.08333333	0.763333333	0.9438743	0.589134
					Average	1.0077065	0.563349
					SD	0.1377064	0.033696
					SE	0.0562184	0.013756
No.	ΔCt control	ΔCt s1p	Average, ΔCt control	ΔΔCt control	ΔΔCt s1p	control	s1p
1	6.28	6.32		-0.35	-0.31	1.2745606	1.239708
2	6.75	7.51		0.12	0.88	0.9201877	0.543367
3	6.91	7.28		0.28	0.65	0.823591	0.63728
4	6.45	6.43		-0.18	-0.2	1.1328839	1.148698

5	6.53	7.1		-0.1	0.47	1.0717735	0.721965
6	6.86	7.01	6.63	0.23	0.38	0.8526349	0.768438
					Average	1.0126053	0.843243
					SD	0.1768877	0.28395
					SE	0.0722141	0.115922

Table B-28: Quantification of qRT-PCR test by $2^{-\Delta\Delta}$ method for MEF PS1 rescue (control) and MEF PS1/2 -/- cells (SREBP-1).

No.	ΔCt control	ΔCt srebf1	Average, ΔCt control	ΔΔCt control	ΔΔCt srebf1	control	srebf1
1	6.02	7.43		-0.266	1.144	1.2024692	0.452503
2	6.19	6.91		-0.096	0.624	1.068806	0.648869
3	6.23	6.97		-0.056	0.684	1.0395794	0.622437
4	6.74	7.05		0.454	0.764	0.730016	0.588861
5	6.25	7.17	6.286	-0.036	0.884	1.0252672	0.541863
					Average	1.0132276	0.570907
					SD	0.1731687	0.077329
					SE	0.0774434	0.034582
No.	ΔCt control	ΔCt srebf2	Average, ΔCt control	ΔΔCt control	ΔΔCt srebf2	control	srebf2
1	6.17	6.26		-0.396	-0.306	1.3158545	1.236275
2	6.49	6.29		-0.076	-0.276	1.0540914	1.210833
3	6.4	6.2		-0.166	-0.366	1.1219435	1.288775
4	6.93	6.28		0.364	-0.286	0.7770073	1.219255
5	6.84	6.28	6.566	0.274	-0.286	0.8270234	1.219255
					Average	1.019184	1.234879
					SD	0.2210015	0.031516
					SE	0.0988349	0.014095
No.	ΔCt control	ΔCt scap	Average, ΔCt control	ΔΔCt control	ΔΔCt scap	control	scap
1	7.95	8.26		-0.296	0.014	1.2277357	0.990343
2	8.9	8.25		0.654	0.004	0.6355158	0.997231
3	7.75	7.37		-0.496	-0.876	1.410298	1.83528
4	8.46	8.44		0.214	0.194	0.8621435	0.874179
5	8.17	8.88		-0.076	0.634	1.0540914	0.644387
6			8.246				
					Average	1.0379569	1.068284
					SD	0.3032257	0.451877
					SE	0.1356067	0.202086

No.	ΔCt control	ΔCt insing1	Average, ΔCt control	ΔΔCt control	ΔΔCt insig1	control	insig1
1	7.67	6.43		-0.096	-1.336	1.068806	2.524504
2	7.85	6.4		0.084	-1.366	0.9434383	2.577549
3	7.47	5.38		-0.296	-2.386	1.2277357	5.227061
4	8.16	6.51		0.394	-1.256	0.7610167	2.388326
5	7.68	6.83	7.766	-0.086	-0.936	1.0614232	1.913216
					Average	1.012484	2.926131
					SD	0.1731355	1.312662
					SE	0.0774286	0.58704
No.	ΔCt control	ΔCt s1p	Average, ΔCt control	ΔΔCt control	ΔΔCt s1p	control	s1p
1	7.2	7.64		0.04	0.48	0.9726549	0.716978
2	7.15	5.81		-0.01	-1.35	1.0069556	2.549121
3	7	7.66		-0.16	0.5	1.1172871	0.707107
4	7.16	7.33		0	0.17	1	0.888843
5	7.29	7.01	7.16	0.13	-0.15	0.9138315	1.109569
					Average	1.0021458	1.194324
					SD	0.0740851	0.774793
					SE	0.0331319	0.346498

Statistical Analysis

Normality test was performed before applying T-test by employing SPSS 25 software. Normally distributed data were tested by T-test while, Mann-Whitney U test was performed to non-normally distributed data.

Table B-29: Normality test of MEF WT (control) and MEF APP Δ CT 15 (sample) cells.

	Kolmogorov-Smirnov[a]			Shapiro-Wilk			
	Statistic	df	Sig.	Statistic	df	Sig.	Sig. Test
Hmgcs1-control	.134	14	.200*	.952	14	.594	T. test
Hmgcs1-sample	.183	14	.200*	.887	14	.074	
Hmgcs2-control	.273	14	.006	.698	14	.000	Mann-Whitney U test
Hmgcs2-sample	.114	14	.200*	.957	14	.680	
Hmgcr-control	.149	15	.200*	.969	15	.840	Mann-Whitney U test
Hmgcr-sample	.323	15	.000	.595	15	.000	
Mvk-control	.166	14	.200*	.954	14	.632	T. test
Mvk-sample	.181	14	.200*	.902	14	.119	
Pmvk-control	.186	14	.200*	.970	14	.872	T. test

Pmvk-sample	.165	14	.200*	.959	14	.700	
Mvd-control	.140	14	.200*	.912	14	.169	T. test
Mvd-sample	.176	14	.200*	.943	14	.463	
Fdps-control	.118	15	.200*	.976	15	.930	T. test
Fdps-sample	.184	15	.185	.931	15	.283	
Fdft-control	.215	13	.101	.921	13	.256	T. test
Fdft-sample	.123	13	.200*	.957	13	.709	
Sqle-control	.120	13	.200*	.971	13	.908	T. test
sqle-sample	.170	13	.200*	.950	13	.599	
Lss-control	.188	14	.194	.951	14	.575	T. test
Lss-sample	.217	14	.074	.896	14	.097	

Table B-30: Statistical significance (T.Test) of cholesterol genes in MEF APP Δ CT 15 cells.

Levene's Test for Equality of Variances			t-test for Equality of Means						
	F	Sig.	t	df	Sig. (2-tailed)	Mean Difference	Std. Error Difference	95% Confidence Interval of the Difference	
								Lower	Upper
	hmgcs1								
Equal variances assumed	35.297	.000	-.916-	26	.368	-.07228-	.07888	-.23443-	.08987
Equal variances not assumed			-.916-	15.172	.374	-.07228-	.07888	-.24025-	.09569
	mvk								
Equal variances assumed	8.713	.007	-2.075-	26	.048	-.17640-	.08502	-.35117-	-.00163-
Equal variances not assumed			-2.075-	16.072	.054	-.17640-	.08502	-.35657-	.00378
	pmvk								
Equal variances assumed	1.716	.202	3.616	26	.001	.39109	.10815	.16879	.61340
Equal variances not assumed			3.616	22.496	.001	.39109	.10815	.16709	.61509
	mvd								

Equal variances assumed	5.693	.025	2.893	26	.008	.26407	.09129	.07643	.45171
Equal variances not assumed			2.893	20.349	.009	.26407	.09129	.07386	.45428
	fdps								
Equal variances assumed	.320	.576	4.790	28	.000	.34467	.07196	.19727	.49206
Equal variances not assumed			4.790	26.583	.000	.34467	.07196	.19692	.49242
	fdft								
Equal variances assumed	3.372	.079	-2.259-	24	.033	-.25382-	.11238	-.48575-	-.02189-
Equal variances not assumed			-2.259-	20.111	.035	-.25382-	.11238	-.48815-	-.01950-
	sqle								
Equal variances assumed	2.789	.108	-1.907-	24	.069	-.28107-	.14737	-.58524-	.02309
Equal variances not assumed			-1.907-	19.101	.072	-.28107-	.14737	-.58942-	.02727
	lss								
Equal variances assumed	4.453	.045	.167	26	.869	.01973	.11806	-.22295-	.26241
Equal variances not assumed			.167	18.920	.869	.01973	.11806	-.22745-	.26691

Table B-31: Statistical significance (Mann-Whitney U test) of cholesterol genes in MEF APP Δ CT 15 cells.

	hmgcs2	hmgcr
Mann-Whitney U	13.000	18.000
Wilcoxon W	118.000	138.000
Z	-3.906-	-3.920-
Asymp. Sig. (2-tailed)	.000	.000
Exact Sig. [2*(1-tailed Sig.)]	.000	.000

Table B-32: Normality test of MEF WT (control) and MEF APP-APLP2 -/- (sample) cells.

	Kolmogorov-Smirnov[a]			Shapiro-Wilk			
	Statistic	df	Sig.	Statistic	df	Sig.	Sig. Test
Hmgcs1-control	.145	16	.200*	.852	16	.015	Mann-Whitney U test
Hmgcs1-sample	.223	16	.033	.872	16	.029	
Hmgcs2-control	.110	13	.200*	.951	13	.620	T.test
Hmgcs2-sample	.173	13	.200*	.916	13	.221	
Hmgcr-control	.176	16	.200	.919	16	.161	T.test
Hmgcr-sample	.158	16	.200*	.921	16	.174	
Mvk-control	.216	14	.075	.932	14	.323	T.test
Mvk-sample	.184	14	.200*	.912	14	.171	
Pmvk-control	.178	13	.200*	.943	13	.494	Mann-Whitney U test
Pmvk-sample	.219	13	.088	.858	13	.036	
Mvd-control	.155	16	.200*	.919	16	.161	Mann-Whitney U test
Mvd-sample	.236	16	.018	.790	16	.002	
Fdps-control	.144	15	.200*	.971	15	.867	Mann-Whitney U test
Fdps-sample	.288	15	.002	.811	15	.005	
Fdft-control	.210	13	.122	.943	13	.504	T.test
Fdft-sample	.180	13	.200*	.905	13	.159	
Sqle-control	.139	13	.200*	.927	13	.310	Mann-Whitney U test
sqle-sample	.303	13	.002	.752	13	.002	
Lss-control	.183	14	.200*	.933	14	.341	Mann-Whitney U test
Lss-sample	.214	14	.081	.809	14	.006	

Table B-33: Statistical significance (Mann-Whitney U test) of cholesterol genes in MEF APP/APLP2 -/- cells.

	hmgcs1	pmvk	mvk	Fdps	sqle	Lss
Mann-Whitney U	62.000	18.000	26.000	50.000	60.000	55.000
Wilcoxon W	198.000	109.000	162.000	170.000	151.000	160.500
Z	-2.488-	-3.413-	-3.844-	-2.592-	-1.256-	-1.953-
Asymp. Sig. (2-tailed)	.013	.001	.000	.010	.209	.051
Exact Sig. [2*(1-tailed Sig.)]	.012[b]	.000	.000	.009	.223	.050

Table B-34: Statistical significance (T. test)) of cholesterol genes in MEF APP/APLP2 -/- cells.

Levene's Test for Equality of Variances			t-test for Equality of Means						
	F	Sig.	t	df	Sig. (2-tailed)	Mean Difference	Std. Error Difference	95% Confidence Interval of the Difference	
								Lower	Upper
	hmgcs2								
Equal variances assumed	.181	.674	-2.130-	24	.044	-.30859-	.14485	-.60755-	-.00963-
Equal variances not assumed			-2.130-	23.263	.044	-.30859-	.14485	-.60805-	-.00913-
	hmgcr								
Equal variances assumed	3.409	.075	4.453	30	.000	.31683	.07115	.17152	.46213
Equal variances not assumed			4.453	25.804	.000	.31683	.07115	.17053	.46313
	mvk								
Equal variances assumed	.837	.369	4.333	26	.000	.27481	.06342	.14446	.40517
Equal variances not assumed			4.333	25.972	.000	.27481	.06342	.14445	.40518
	fdft								
Equal variances assumed	3.686	.067	1.052	24	.303	.11429	.10868	-.11001-	.33859
Equal variances not assumed			1.052	20.611	.305	.11429	.10868	-.11198-	.34055

Table B-35: Normality test of MEF PS1 rescue (control) and MEF PS1/2 -/- (sample) cells.

	Kolmogorov-Smirnov[a]			Shapiro-Wilk			
	Statistic	df	Sig.	Statistic	df	Sig.	Sig. Test
Hmgcs1-control	.243	14	.025	.781	14	.003	Mann-Whitney U test
Hmgcs1-sample	.199	14	.137	.884	14	.066	
Hmgcs2-control	.162	12	.200*	.950	12	.635	Mann-Whitney U test
Hmgcs2-sample	.371	12	.000	.775	12	.005	
Hmgcr-control	.209	14	.099	.870	14	.042	Mann-Whitney U test

Hmgcr-sample	.205	14	.114	.901	14	.117	
Mvk-control	.350	13	.000	.704	13	.001	Mann-Whitney U test
Mvk-sample	.162	13	.200*	.961	13	.777	
Pmvk-control	.155	13	.200*	.941	13	.469	T.test
Pmvk-sample	.164	13	.200*	.887	13	.089	
Mvd-control	.139	13	.200*	.891	13	.102	T. test
Mvd-sample	.244	13	.033	.873	13	.058	
Fdps-control	.257	14	.013	.824	14	.010	Mann-Whitney U test
Fdps-sample	.155	14	.200*	.940	14	.415	
Fdft-control	.167	14	.200*	.973	14	.917	Mann-Whitney U test
Fdft-sample	.279	14	.004	.825	14	.010	
Sqle-control	.302	11	.006	.858	11	.054	T.test
sqle-sample	.229	11	.113	.862	11	.062	
Lss-control	.199	10	.200*	.867	10	.093	T.test
Lss-sample	.149	10	.200*	.946	10	.617	

Table B-36: Statistical significance (Mann-Whitney U test) of cholesterol genes in MEF PS1/2 -/- cells.

	hmgcs1	hmgcs2	hmgcr	mvk	fdps	fdft
Mann-Whitney U	8.000	70.000	17.000	56.000	15.000	56.000
Wilcoxon W	113.000	148.000	122.000	147.000	120.000	161.000
Z	-4.136-	-.115-	-3.722-	-1.462-	-3.815-	-1.930-
Asymp. Sig. (2-tailed)	.000	.908	.000	.144	.000	.054
Exact Sig. [2*(1-tailed Sig.)]	.000[b]	.932	.000	.153	.000	.056

a. Grouping Variable: Grouping

b. Not corrected for ties.

Table B-37: Statistical significance (T.Test) of cholesterol genes in MEF PS1/2 -/- cells.

Levene's Test for Equality of Variances			t-test for Equality of Means						
	F	Sig.	t	df	Sig. (2-tailed)	Mean Difference	Std. Error Difference	95% Confidence Interval of the Difference	
								Lower	Upper
	pmvk								
Equal variances assumed	2.884	.102	-.843-	24	.407	-.19635-	.23279	-.67681-	.28411
Equal variances not assumed			-.843-	19.825	.409	-.19635-	.23279	-.68222-	.28952
	mvd								
Equal variances assumed	.182	.673	.354	24	.726	.03151	.08892	-.15202-	.21504
Equal variances not assumed			.354	23.991	.726	.03151	.08892	-.15202-	.21504
	sqle								
Equal variances assumed	5.382	.031	-1.661-	20	.112	-.49552-	.29841	-1.1179-	.12695
Equal variances not assumed			-1.661-	12.455	.122	-.49552-	.29841	-1.1430-	.15203
	lss								
Equal variances assumed	.467	.503	-.743-	18	.467	-.12655-	.17040	-.48454-	.23144
Equal variances not assumed			-.743-	17.132	.468	-.12655-	.17040	-.48584-	.23274

Table B-38: Normality test of MEF WT (control) and MEF APP Δ CT 15 (sample) cells (SREBP-1).

	Kolmogorov-Smirnov[a]			Shapiro-Wilk			
	Statistic	df	Sig.	Statistic	df	Sig.	Sig. Test
Srebf1-control	.249	5	.200*	.911	5	.475	T. test
Srebf1-sample	.157	5	.200*	.973	5	.897	
Srebf1-control	.182	5	.200*	.948	5	.723	T. test
Srebf2-sample	.231	5	.200*	.947	5	.716	
Scap-control	.171	5	.200*	.968	5	.861	T. test
Scap-sample	.319	5	.108	.858	5	.220	

Insig1-control	.171	5	.200*	.986	5	.964	T. test
Insig1-sample	.280	5	.200*	.905	5	.438	
S1p-control	.176	5	.200*	.987	5	.968	T. test
S1p-sample	.240	5	.200*	.952	5	.754	

Table B-39: Statistical significance (T.Test) of SREBP-1 genes in MEF APP Δ CT 15 cells.

Levene's Test for Equality of Variances			t-test for Equality of Means						
	F	Sig.	t	df	Sig. (2-tailed)	Mean Difference	Std. Error Difference	95% Confidence Interval of the Difference	
								Lower	Upper
	Srebpf1								
Equal variances assumed	1.443	.264	-1.786-	8	.112	-.31656-	.17721	-.72522-	.09209
Equal variances not assumed			-1.786-	6.069	.124	-.31656-	.17721	-.74899-	.11586
	Srebf2								
Equal variances assumed	.165	.695	-.399-	8	.700	-.04952-	.12412	-.33574-	.23670
Equal variances not assumed			-.399-	7.239	.701	-.04952-	.12412	-.34106-	.24203
	scap								
Equal variances assumed	16.287	.004	-3.018-	8	.017	-.41928-	.13894	-.73969-	-.09888-
Equal variances not assumed			-3.018-	4.220	.037	-.41928-	.13894	-.79726-	-.04131-
	Insig1								
Equal variances assumed	.260	.624	.555	8	.594	.07222	.13007	-.22771-	.37216
Equal variances not assumed			.555	7.848	.594	.07222	.13007	-.22872-	.37317
	S1p								
Equal variances assumed	5.634	.045	-3.995-	8	.004	-.43502-	.10890	-.68615-	-.18389-
Equal variances not assumed			-3.995-	5.173	.010	-.43502-	.10890	-.71217-	-.15787-

Table B-40: Normality test of MEF WT (control) and MEF APP/APLP2 -/- (sample) cells (SREBP-1).

	Kolmogorov-Smirnov[a]			Shapiro-Wilk			
	Statistic	df	Sig.	Statistic	df	Sig.	Sig. Test
Srebf1-control	.333	6	.037	.755	6	.022	Mann-Whitney U test
Srebf1-sample	.204	6	.200*	.904	6	.400	
Srebf1-control	.372	6	.009	.796	6	.054	T. test
Srebf2-sample	.306	6	.082	.856	6	.177	
Scap-control	.137	6	.200*	.974	6	.919	T. test
Scap-sample	.212	6	.200*	.967	6	.874	
Insig1-control	.196	6	.200*	.964	6	.847	T. test
Insig1-sample	.324	6	.048	.881	6	.276	
S1p-control	.199	6	.200*	.933	6	.602	T. test
S1p-sample	.271	6	.193	.879	6	.266	

Table B-41: Statistical significance (Mann-Whitney U test) of SREBP-1 genes in MEF APP/APLP2 -/- cells.

	Srebf1
Mann-Whitney U	3.000
Wilcoxon W	24.000
Z	-2.402-
Asymp. Sig. (2-tailed)	.016
Exact Sig. [2*(1-tailed Sig.)]	.015[b]

Table B-42: Statistical significance (T. test) of SREBP-1 genes in MEF APP/APLP2 -/- cells.

Levene's Test for Equality of Variances			t-test for Equality of Means						
	F	Sig.	t	df	Sig. (2-tailed)	Mean Difference	Std. Error Difference	95% Confidence Interval of the Difference	
								Lower	Upper
	Srebf2								
Equal variances assumed	.004	.953	1.357	10	.205	.22508	.16584	-.14444-	.59460
Equal variances not assumed			1.357	9.737	.205	.22508	.16584	-.14580-	.59596

	scap								
Equal variances assumed	.101	.757	2.990	10	.014	.18809	.06291	.04792	.32826
Equal variances not assumed			2.990	9.651	.014	.18809	.06291	.04723	.32895
	Insig1								
Equal variances assumed	5.628	.039	7.678	10	.000	.44436	.05788	.31540	.57332
Equal variances not assumed			7.678	5.597	.000	.44436	.05788	.30023	.58849
	S1p								
Equal variances assumed	2.235	.166	1.240	10	.243	.16936	.13658	-.13495-	.47367
Equal variances not assumed			1.240	8.373	.249	.16936	.13658	-.14316-	.48188

Table B-43: Normality test of MEF PS1 rescue (control) and MEF PS1/2 -/- (sample) cells (SREBP-1).

	Kolmogorov-Smirnov[a]			Shapiro-Wilk			
	Statistic	df	Sig.	Statistic	df	Sig.	Sig. Test
Srebf1-control	.328	5	.084	.878	5	.300	T. test
Srebf1-sample	.192	5	.200*	.940	5	.667	
Srebf1-control	.208	5	.200*	.943	5	.690	T. test
Srebf2-sample	.290	5	.197	.787	5	.063	
Scap-control	.134	5	.200*	.989	5	.977	T. test
Scap-sample	.362	5	.031	.826	5	.129	
Insig1-control	.211	5	.200*	.967	5	.854	Mann-Whitney U test
Insig1-sample	.405	5	.007	.733	5	.021	
S1p-control	.274	5	.200*	.938	5	.652	Mann-Whitney U test
S1p-sample	.344	5	.054	.725	5	.017	

Table B-44: Statistical significance (T.Test) of SREBP-1 genes in MEF PS1/2 -/- cells.

Levene's Test for Equality of Variances			t-test for Equality of Means						
	F	Sig.	t	df	Sig. (2-tailed)	Mean Difference	Std. Error Difference	95% Confidence Interval of the Difference	
								Lower	Upper
	Srebf1								
Equal variances assumed	3.453	.093	-2.543-	10	.029	-.53053-	.20863	-.9954-	-.06566-
Equal variances not assumed			-2.543-	6.842	.039	-.53053-	.20863	-1.0262-	-.03486-
	Srebf2								
Equal variances assumed	.004	.953	1.357	10	.205	.22508	.16584	-.14444-	.59460
Equal variances not assumed			1.357	9.737	.205	.22508	.16584	-.14580-	.59596
	scap								
Equal variances assumed	.101	.757	2.990	10	.014	.18809	.06291	.04792	.32826
Equal variances not assumed			2.990	9.651	.014	.18809	.06291	.04723	.32895

Table B-45: Statistical significance (Mann-Whitney U test) of SREBP-1 genes in MEF PS1/2 -/- cells.

	Insig1	S1p
Mann-Whitney U	.000	9.000
Wilcoxon W	15.000	24.000
Z	-2.449-	-.731-
Asymp. Sig. (2-tailed)	.014	.465
Exact Sig. [2*(1-tailed Sig.)]	.016	.548

Effect of cholesterol on IDE gene expression

N2a cells were used in the experiments. Untreated N2a cells were used as control, while cholesterol treated cells were used as a sample. Cholesterol concentration was 100 µM. Two housekeeping genes were used, β-actin and Polr2.

Table B-46: Quantification of gene expression for IDE gene on 04.10.2016 (first experiment).

Data step:	4		Show channel:	Thresholds:
Sample Group:	Default	Ch 1	No	
Method:	Threshold	Ch 2	No	
Smoothing:	ON	Ch 3	No	
Smoothing window:	5	Ch 4	No	
Baseline:	Trend	Ch 5	Yes	2218.23
Baseline range start:	3			
Baseline range end:	7			

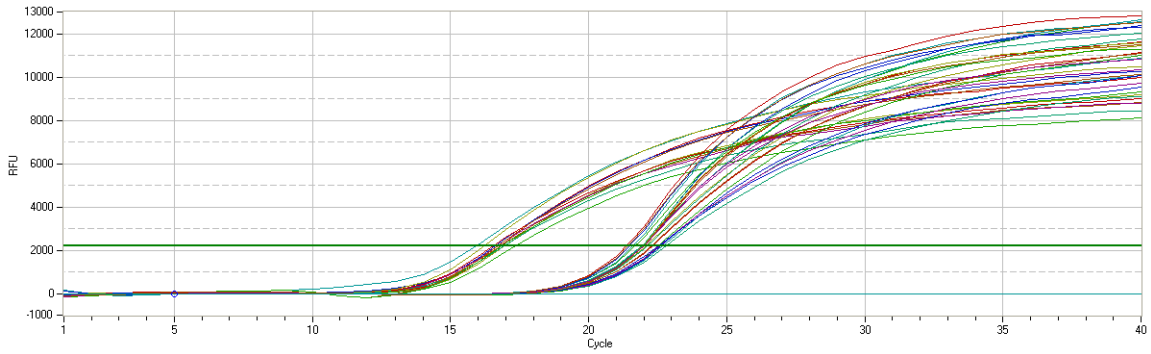

Well	Fluorophore	Sample Type	Sample Name	Target	Cq
A01-Ch5	SYBR	Empty	n2a sample	actin beta	16.92
A02-Ch5	SYBR	Empty	n2a sample	actin beta	16.94
A03-Ch5	SYBR	Empty	n2a sample	actin beta	16.98
A04-Ch5	SYBR	Empty	n2a sample	actin beta	17.36
A05-Ch5	SYBR	Empty	n2a sample	actin beta	16.96
A06-Ch5	SYBR	Empty	n2a sample	actin beta	15.98
A07-Ch5	SYBR	Empty	n2a sample	actin beta	16.65
A08-Ch5	SYBR	Empty	n2a control	actin beta	16.73
A09-Ch5	SYBR	Empty	n2a control	actin beta	16.49
A10-Ch5	SYBR	Empty	n2a control	actin beta	16.72
A11-Ch5	SYBR	Empty	n2a control	actin beta	16.25
A12-Ch5	SYBR	Empty	n2a control	actin beta	16.69
A13-Ch5	[none]	[none]			n. def.
A14-Ch5	[none]	[none]			n. def.
A15-Ch5	[none]	[none]			n. def.
A16-Ch5	[none]	[none]			n. def.
B01-Ch5	SYBR	Empty	n2a sample	polr2	22.54
B02-Ch5	SYBR	Empty	n2a sample	polr2	22.82

B03-Ch5	SYBR	Empty	n2a sample	polr2	22.68
B04-Ch5	SYBR	Empty	n2a sample	polr2	22.62
B05-Ch5	SYBR	Empty	n2a sample	polr2	22.58
B06-Ch5	SYBR	Empty	n2a sample	polr2	22.32
B07-Ch5	SYBR	Empty	n2a sample	polr2	22.28
B08-Ch5	SYBR	Empty	n2a control	polr2	22.1
B09-Ch5	SYBR	Empty	n2a control	polr2	21.92
B10-Ch5	SYBR	Empty	n2a control	polr2	22.15
B11-Ch5	SYBR	Empty	n2a control	polr2	21.95
B12-Ch5	SYBR	Empty	n2a control	polr2	22.56
B13-Ch5	[none]	[none]			n. def.
B14-Ch5	[none]	[none]			n. def.
B15-Ch5	[none]	[none]			n. def.
B16-Ch5	[none]	[none]			n. def.
C01-Ch5	SYBR	Empty	n2a sample	ide 59	21.94
C02-Ch5	SYBR	Empty	n2a sample	ide 59	22.02
C03-Ch5	SYBR	Empty	n2a sample	ide 59	21.96
C04-Ch5	SYBR	Empty	n2a sample	ide 59	22.01
C05-Ch5	SYBR	Empty	n2a sample	ide 59	21.69
C06-Ch5	SYBR	Empty	n2a sample	ide 59	21.69
C07-Ch5	SYBR	Empty	n2a sample	ide 59	21.93
C08-Ch5	SYBR	Empty	n2a control	ide 59	21.9
C09-Ch5	SYBR	Empty	n2a control	ide 59	21.77
C10-Ch5	SYBR	Empty	n2a control	ide 59	22.01
C11-Ch5	SYBR	Empty	n2a control	ide 59	21.37
C12-Ch5	SYBR	Empty	n2a control	ide 59	21.66

Table B-47: Quantification of gene expression for IDE gene on 12.10.2016 (second experiment).

Data step:	4		Show channel:	Thresholds:
Sample Group:	Default	Ch 1	No	
Method:	Threshold	Ch 2	No	
Smoothing:	ON	Ch 3	No	
Smoothing window:	5	Ch 4	No	
Baseline:	Trend	Ch 5	Yes	1573.2
Baseline range start:	3			
Baseline range end:	7			

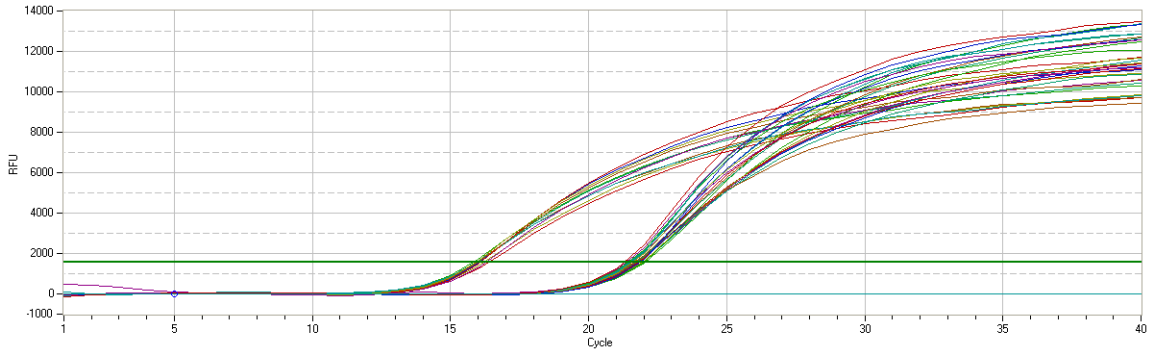

Well	Fluorophore	Sample Type	Sample Name	Target	Cq
A01-Ch5	SYBR	Empty	control	Actin Beta	16.4
A02-Ch5	SYBR	Empty	control	Actin Beta	15.92
A03-Ch5	SYBR	Empty	control	Actin Beta	16.23
A04-Ch5	SYBR	Empty	control	Actin Beta	15.82
A05-Ch5	SYBR	Empty	control	Actin Beta	16.01
A06-Ch5	SYBR	Empty	control	Actin Beta	15.95
A07-Ch5	SYBR	Empty	sample	Actin Beta	16.05
A08-Ch5	SYBR	Empty	sample	Actin Beta	16.27
A09-Ch5	SYBR	Empty	sample	Actin Beta	16.1
A10-Ch5	SYBR	Empty	sample	Actin Beta	16
A11-Ch5	SYBR	Empty	sample	Actin Beta	15.92
A12-Ch5	[none]	[none]			n. def.
A13-Ch5	[none]	[none]			n. def.
A14-Ch5	[none]	[none]			n. def.
A15-Ch5	[none]	[none]			n. def.
A16-Ch5	[none]	[none]			n. def.
B01-Ch5	SYBR	Empty	control	Polr2	22.04
B02-Ch5	SYBR	Empty	control	Polr2	21.74
B03-Ch5	SYBR	Empty	control	Polr2	21.94
B04-Ch5	SYBR	Empty	control	Polr2	21.77
B05-Ch5	SYBR	Empty	control	Polr2	21.91
B06-Ch5	SYBR	Empty	control	Polr2	21.7
B07-Ch5	SYBR	Empty	sample	Polr2	21.63
B08-Ch5	SYBR	Empty	sample	Polr2	21.92
B09-Ch5	SYBR	Empty	sample	Polr2	21.98
B10-Ch5	SYBR	Empty	sample	Polr2	21.71
B11-Ch5	SYBR	Empty	sample	Polr2	21.47
B12-Ch5	[none]	[none]			n. def.
B13-Ch5	[none]	[none]			n. def.
B14-Ch5	[none]	[none]			n. def.
B15-Ch5	[none]	[none]			n. def.
B16-Ch5	[none]	[none]			n. def.

C01-Ch5	SYBR	Empty	control	IDE 59	21.82
C02-Ch5	SYBR	Empty	control	IDE 59	21.56
C03-Ch5	SYBR	Empty	control	IDE 59	21.77
C04-Ch5	SYBR	Empty	control	IDE 59	21.71
C05-Ch5	SYBR	Empty	control	IDE 59	21.59
C06-Ch5	SYBR	Empty	control	IDE 59	21.42
C07-Ch5	SYBR	Empty	sample	IDE 59	21.48
C08-Ch5	SYBR	Empty	sample	IDE 59	21.52
C09-Ch5	SYBR	Empty	sample	IDE 59	21.84
C10-Ch5	SYBR	Empty	sample	IDE 59	21.36
C11-Ch5	SYBR	Empty	sample	IDE 59	21.27

Table B-48: Quantification of gene expression for IDE gene on 22.02.2017 (third experiment).

Data step:	4		Show channel:	Thresholds:
Sample Group:	Default	Ch 1	No	
Method:	Threshold	Ch 2	No	
Smoothing:	ON	Ch 3	No	
Smoothing window:	5	Ch 4	No	
Baseline:	Trend	Ch 5	Yes	1368.19
Baseline range start:	3			
Baseline range end:	7			

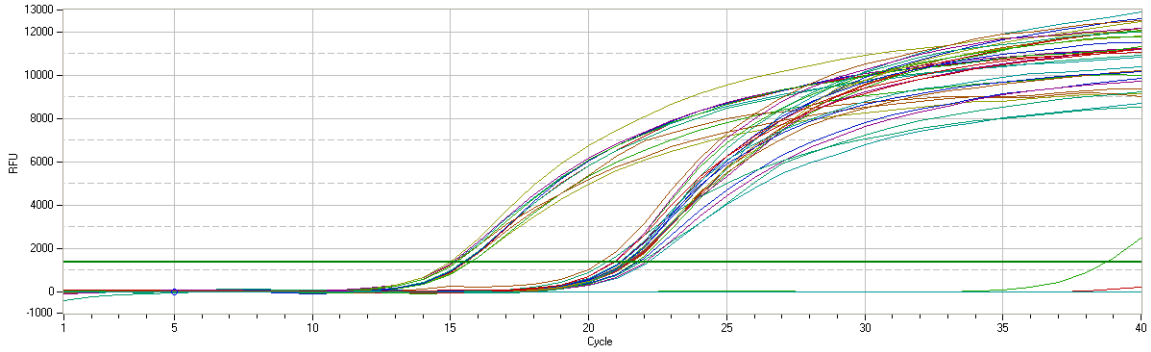

Well	Fluorophore	Sample Type	Sample Name	Target	Cq
A01-Ch5	SYBR	Empty	control	Actin Beta	15.59
A02-Ch5	SYBR	Empty	control	Actin Beta	15.55
A03-Ch5	SYBR	Empty	control	Actin Beta	15.71
A04-Ch5	SYBR	Empty	control	Actin Beta	15.76

A05-Ch5	SYBR	Empty	control	Actin Beta	15.47
A06-Ch5	SYBR	Empty	control	Actin Beta	15.16
A07-Ch5	SYBR	Empty	sample	Actin Beta	15.53
A08-Ch5	SYBR	Empty	sample	Actin Beta	15.11
A09-Ch5	SYBR	Empty	sample	Actin Beta	n. def.
A10-Ch5	SYBR	Empty	sample	Actin Beta	15.18
A11-Ch5	SYBR	Empty	sample	Actin Beta	15.03
A12-Ch5	SYBR	Empty	sample	Actin Beta	15.25
A13-Ch5	[none]	[none]			n. def.
A14-Ch5	[none]	[none]			n. def.
A15-Ch5	[none]	[none]			n. def.
A16-Ch5	[none]	[none]			n. def.
B01-Ch5	SYBR	Empty	control	polr2	21.7
B02-Ch5	SYBR	Empty	control	polr2	21.91
B03-Ch5	SYBR	Empty	control	polr2	22.14
B04-Ch5	SYBR	Empty	control	polr2	21.76
B05-Ch5	SYBR	Empty	control	polr2	22.04
B06-Ch5	SYBR	Empty	control	polr2	21.49
B07-Ch5	SYBR	Empty	sample	polr2	21.48
B08-Ch5	SYBR	Empty	sample	polr2	21.29
B09-Ch5	SYBR	Empty	sample	polr2	38.75
B10-Ch5	SYBR	Empty	sample	polr2	20.68
B11-Ch5	SYBR	Empty	sample	polr2	21.37
B12-Ch5	SYBR	Empty	sample	polr2	21.32
B13-Ch5	[none]	[none]			n. def.
B14-Ch5	[none]	[none]			n. def.
B15-Ch5	[none]	[none]			n. def.
B16-Ch5	[none]	[none]			n. def.
C01-Ch5	SYBR	Empty	control	IDE	21.63
C02-Ch5	SYBR	Empty	control	IDE	21.54
C03-Ch5	SYBR	Empty	control	IDE	21.14
C04-Ch5	SYBR	Empty	control	IDE	21.54
C05-Ch5	SYBR	Empty	control	IDE	21.41
C06-Ch5	SYBR	Empty	control	IDE	20.92
C07-Ch5	SYBR	Empty	sample	IDE	21.33
C08-Ch5	SYBR	Empty	sample	IDE	21.11
C09-Ch5	SYBR	Empty	sample	IDE	21.17
C10-Ch5	SYBR	Empty	sample	IDE	20.91
C11-Ch5	SYBR	Empty	sample	IDE	20.93
C12-Ch5	SYBR	Empty	sample	IDE	20.45

Table B-49: Quantification of qRT-PCR test by $2^{-\Delta\Delta}$ method for IDE gene (actin beta).

No.	ΔCt control	ΔCt IDE	Average, ΔCt control	ΔΔCt control	ΔΔCt IDE	control	IDE
1	5.17	5.02		0.004	-0.146	0.9972313	1.106497
2	5.28	5.08		0.114	-0.086	0.9240226	1.061423
3	5.29	4.98		0.124	-0.186	0.9176399	1.137605
4	5.12	4.65		-0.046	-0.516	1.0323985	1.429985
5	4.97	4.73	5.166	-0.196	-0.436	1.1455179	1.352848
6	5.42	5.43		-0.194	-0.184	1.143931	1.136029
7	5.64	5.25		0.026	-0.364	0.9821396	1.286989
8	5.54	5.74		-0.074	0.126	1.0526312	0.916369
9	5.89	5.36		0.276	-0.254	0.8258777	1.192509
10	5.58	5.35	5.614	-0.034	-0.264	1.0238469	1.200803
11	6.04	5.8		0.138	-0.102	0.9087781	1.07326
12	5.99	6		0.088	0.098	0.9408261	0.934327
13	5.78	5.73		-0.122	-0.172	1.0882424	1.126619
14	5.94	5.9		0.038	-0.002	0.9740043	1.001387
15	5.76	5.2	5.902	-0.142	-0.702	1.1034337	1.626758
					Avg,	1.0040347	1.172227
					Std.	0.0926671	0.189414
					SE	0.0239266	0.048906

Table B-50: Quantification of qRT-PCR test by $2^{-\Delta\Delta}$ method for IDE gene (Polr2).

No.	ΔCt control	ΔCt IDE	Average, ΔCt control	ΔΔCt control	ΔΔCt IDE	control	IDE
1	-0.2	-0.6		0.194	-0.206	0.8741786	1.153486
2	-0.15	-0.8		0.244	-0.406	0.8444009	1.325007
3	-0.14	-0.72		0.254	-0.326	0.8385682	1.253533
4	-0.58	-0.61		-0.186	-0.216	1.1376052	1.161509
5	-0.9	-0.89	-0.394	-0.506	-0.496	1.4201074	1.410298
6	-0.22	-0.15		-0.03	0.04	1.0210121	0.972655
7	-0.18	-0.4		0.01	-0.21	0.9930925	1.156688
8	-0.17	-0.14		0.02	0.05	0.9862327	0.965936
9	-0.06	-0.35		0.13	-0.16	0.9138315	1.117287
10	-0.32	-0.2	-0.19	-0.13	-0.01	1.0942937	1.006956
11	-0.37	-0.18		0.002	0.192	0.9986147	0.875391
12	-0.63	-0.44		-0.258	-0.068	1.1958198	1.048262
13	-0.57	-0.87	-0.372	-0.198	-0.498	1.147107	1.412254
					Avg,	1.0357588	1.14302
					Std.	0.1637802	0.170797
					SE	0.0454245	0.04737

Table B.51: Normality test of IDE gene expression experiments.

	Kolmogorov-Smirnov[a]			Shapiro-Wilk			
	Statistic	df	Sig.	Statistic	df	Sig.	Sig. Test
Srebf1-control	0.086	15	0.2	0.971	15	0.871	T. test
Srebf1-sample	0.173	15	0.2	0.934	15	0.317	
Srebf1-control	0.151	13	0.2	0.926	13	0.299	T. test
Srebf2-sample	0.149	13	0.2	0951	13	0.618	

Table B-52: Significance test (T. test) of IDE gene expression experiments with two housekeeping genes, β-actin and Polr2.

Levene's Test for Equality of Variances			t-test for Equality of Means						
	F	Sig.	t	df	Sig. (2-tailed)	Mean Difference	Std. Error Difference	95% Confidence Interval of the Difference	
								Lower	Upper
	B-actin								
Equal variances assumed	3.797	0.061	-3.089	28	0.004	-0.16819	0.05445	-0.27972	-0.05667
Equal variances not assumed			-3.089	20.339	0.006	-0.16819	0.05445	-0.28164	-0.05474
	Polr2								
Equal variances assumed	0.049	0.827	-1.634	24	.115	-.10726	.06563	-.24272	.02819
Equal variances not assumed			-1.634	23.958	.115	-.10726	.06563	-.24273	.02821

Appendix C

Results of western blot experiments

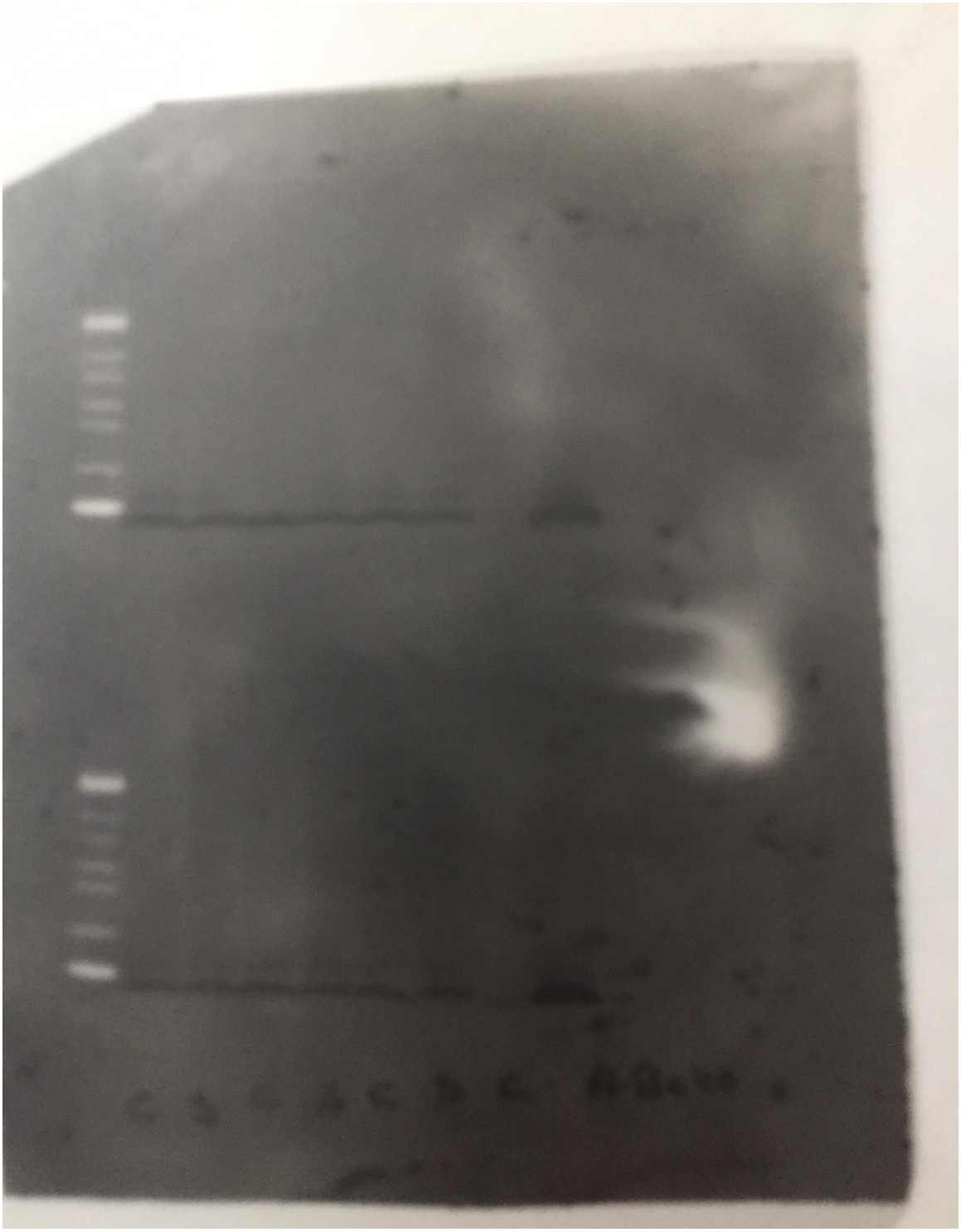

Figure C.1: Gel of Aβ degradation in N2a living cells on 22.06.2016.

Table C.1: Results of gel analysis by Image gauge, date of experiment 22.06.2016.

		Gel 1		Gel2	
Ln	Area Name	AU	AU-BG	AU	AU-BG
1	Control	1439198	117324.73	1255429	100418.5
2	Sample	1427673	115246.37	1374739	87774.95
3	Control	1604975	156830.82	1328147	105682.31
4	Sample	1489224	118341.89	1117720	73002.73
5	Control	1420658	118232.35	1235122	68953.93
6	Sample	1348353	96761.55	1281923	51679.81

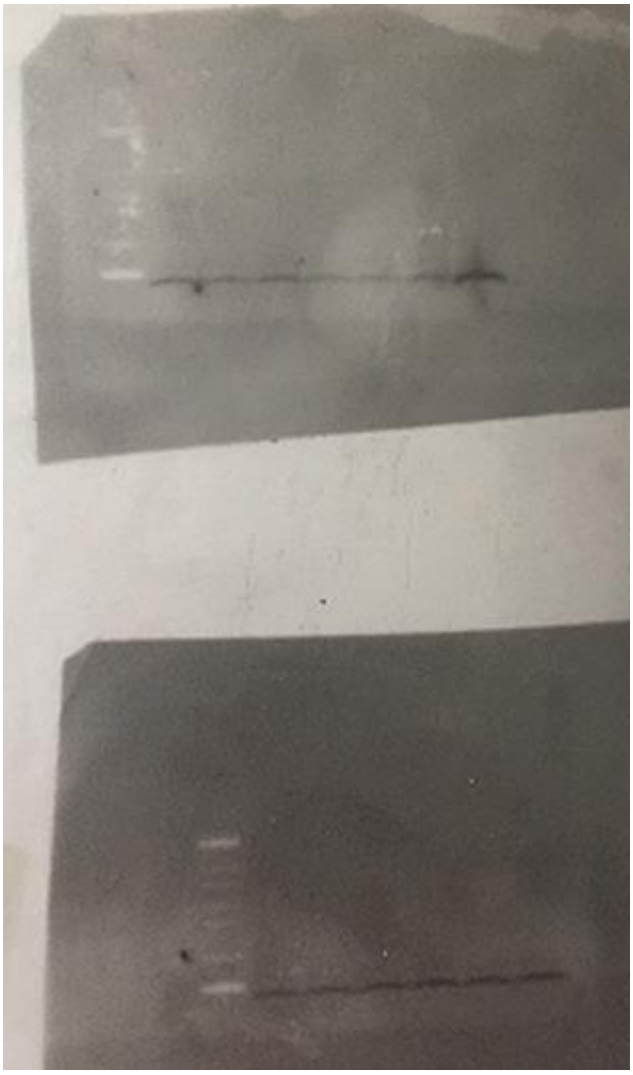

Figure C.2: Gels of Aβ degradation in N2a living cells on 26.06.2016.

Table C.2: Results of gel analysis by Image gauge, date of experiment 26.06.2016.

	Gel1			Gel2		
Ln	Area Name	AU	AU-BG	Area Name	AU	AU-BG
1	control	5587406	758865.1	sample	5009953	425863.6
2	sample	5307325	467291.4	control	5165016	543389.2
3	control	6234141	575775.9	sample	5603951	609008.5
4	sample	4630562	475210.3	control	5550052	635950.8
5	control	4499575	527447.5	sample	6010676	675323.2
6	sample	7406998	753780.9	control	6803584	790098.3

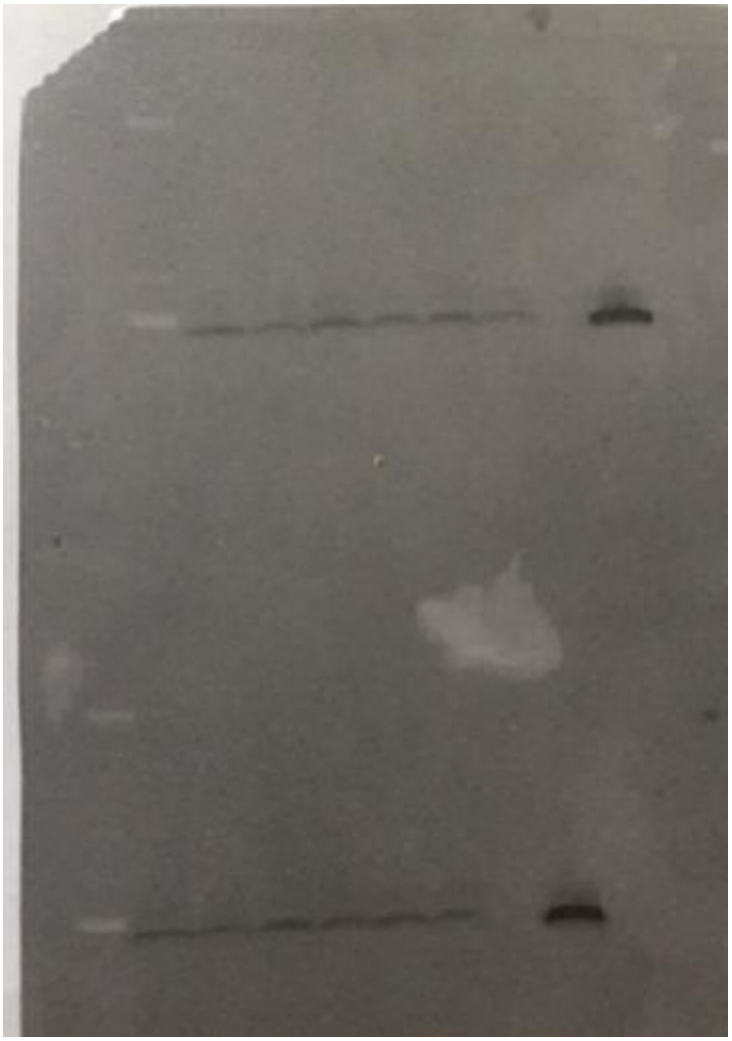

Figure C.3: Gels of N2a degradation in living cells on 27.06.2016.

Table C.3: Results of gel analysis by Image gauge, date of experiment 27.06.2016.

		Gel1		Gel2	
Ln	Area Name	AU	AU-BG	AU	AU-BG
1	Control	1157456	85608.5	1209656	87349.69
2	Sample	1155463	65002.16	1072515	53589.15
3	Control	1070402	66621.12	1098202	72040.7
4	Sample	1092584	70821.29	1063912	64246.09
5	Control	1073482	79173.7	1100330	81272.19
6	Sample	1036097	51241.76	1066814	54938.38

Table C 4: Data analysis of Aβ degradation in N2a living cells.

Control	Sample	Average	Factor	Adjusted* Control	Adjusted** Sample
117324.7	115246.4	116285.6	89.65	90.45115	88.84885
156830.8	118341.9	137586.4		102.1895	77.11048
118232.4	96761.55	107497		98.60308	80.69692
100418.5	87774.95	94096.73		95.67303	83.62697
105682.3	73002.73	89342.52	*Control×factor	106.046	73.25398
68953.93	51679.81	60316.87	Area	102.4874	76.81259
85608.5	65002.16	75305.33		101.9158	77.38421
66621.12	70821.29	68721.21	**Sample×factor	86.91034	92.38966
79173.7	51241.76	65207.73	Area	108.8509	70.44907
87349.69	53589.15	70469.42		111.1248	68.17521
72040.7	64246.09	68143.4		94.77733	84.52267
81272.19	54938.38	68105.29		106.9822	72.31782
753780.9	527447.5	640614.2		105.487	73.81301
543389.2	425863.6	484626.4		100.5204	78.77959
635950.8	609008.5	622479.7		91.59013	87.70987
790098.3	675323.2	732710.8		96.67159	82.62841
n= 16	n= 16		Average	100.0175	79.28246
			Std. Dev.	6.950798	6.950798
			Std. Error	1.7377	1.7377

Table C.5: Normality test of N2a degradation test.

	Kolmogorov-Smirnov[a]			Shapiro-Wilk		
	Statistic	df	Sig.	Statistic	df	Sig.
Control	.108	16	.200*	.977	16	.934
Cholesterol	.108	16	.200*	.977	16	.934

Table C.6: Significance test (T. test) of Aβ degradation in N2a living cells.

			t-test for Equality of Means						
								95% Confidence Interval of the Difference	
Levene's Test for Equality of Variances	F	Sig.	t	df	Sig. (2-tailed)	Mean Difference	Std. Error Difference	Lower	Upper
Equal variances assumed	.000	1.000	8.438	30	.000	20.73508	2.45748	15.71624	25.75392
Equal variances not assumed			8.438	30	.000	20.73508	2.45748	15.71624	25.75392

Figure C.4: Gel of Aβ degradation in N2a culture medium on 22.07.2016 (test).

Table C.7: Results of gel analysis of Aβ degradation at different times by Image gauge.

NO.	Ln	Area Name	AU	AU-BG	Ratio	% of Lane	Dist (px)	C-Dist (px)	RF
1	5	Po. Ctrl.	2422135.05	1587921	-------	100	36	-----	0.59
1	4	30h	1248697.43	535212.4	-------	100	31	-------	0.52
1	3	8h	1669695.01	799803.9	-------	100	21	-----	0.36
1	2	24h	1314550.19	544132.1	-------	100	21	-----	0.31
1	1	12h	1499064.43	675714.2	-------	100	19	-----	0.33

Table C.8: Data analysis of Aβ degradation at different times.

Positive control	8h	12h	24h	30h	MBV	Factor
1587921	799803.9	675714.2	544132.1	535212.37	828556.7	52.18
100.0025	50.36924	42.55444	34.2678	33.70606158		

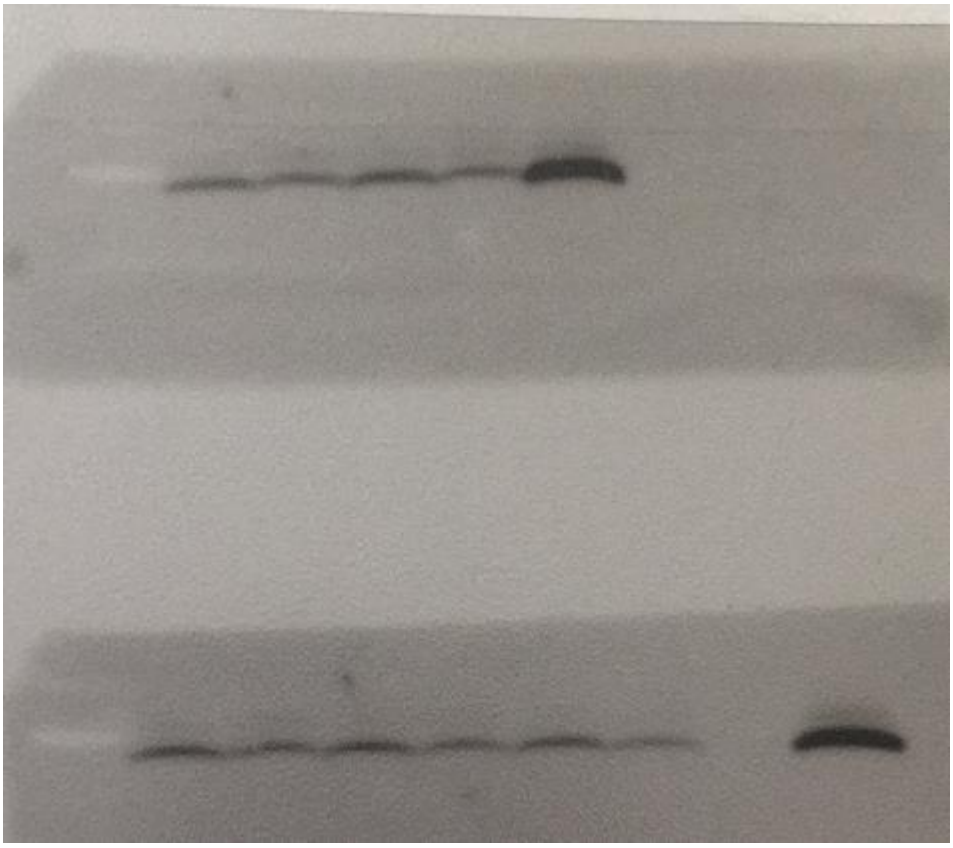

Figure C.5: Gel of Aβ degradation in N2a culture medium on 26.07.2016.

Table C.9: Data analysis of Aβ degradation in N2a culture medium by Image gauge on 26.07.2016.

NO.	Ln	Area Name	AU	AU-BG	Ratio	% of Lane	Dist (px)	C-Dist (px)	RF
1	1	Control	665551	275493	-------	100	29	------	0.49
1	2	Sample	551600	185533.6	-------	100	28	-------	0.47
1	3	Control	568755	227877.9	-------	100	31	------	0.53
1	4	Sample	436929	142111.8	-------	100	30	------	0.51
1	5	Control	528936	207464	-------	100	27	------	0.46
1	6	Sample	409305	115733	-------	100	29	------	0.49
1	7	Pos. Ctrl.	1764449	1042212	-------	100	42	------	0.47

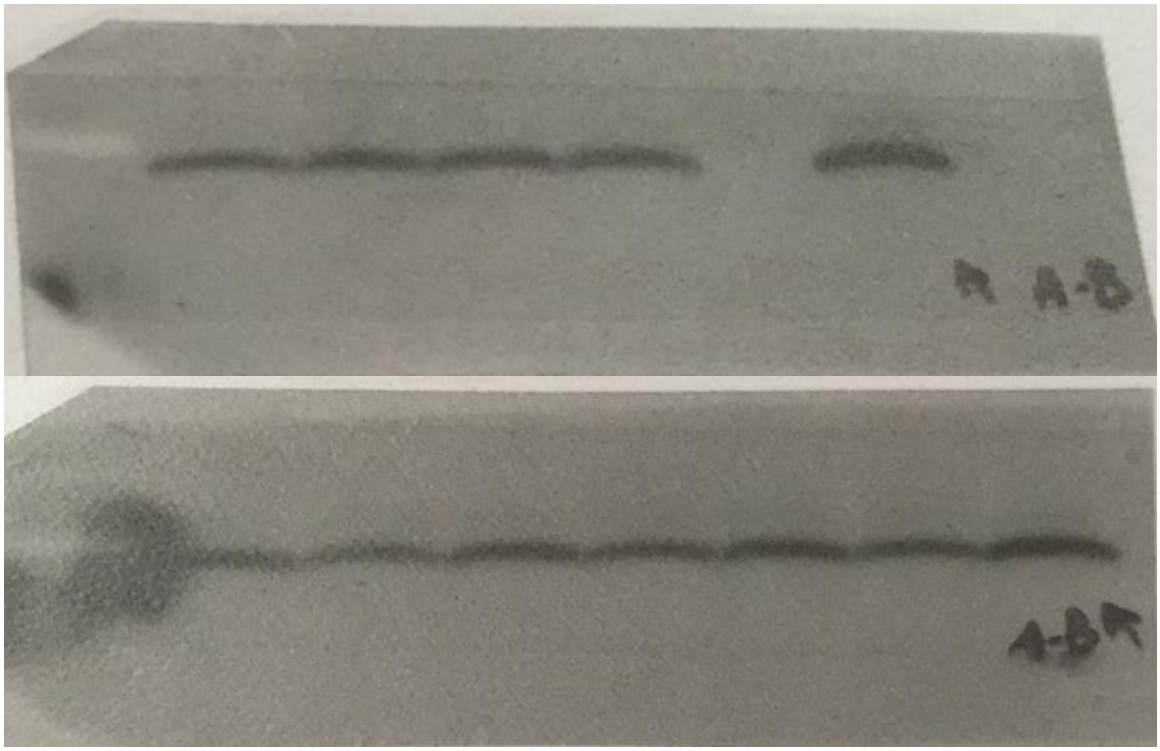

Figure C.6: Gel of Aβ degradation in N2a culture medium on 28.07.2016.

Table C.10: Data analysis of Aβ degradation in N2a culture medium by Image gauge on 28.07.2016.

NO.	Ln	Area Name	AU	AU-BG	Ratio	% of Lane	Dist (px)	C-Dist (px)	RF
1	1	Control	1644177	375184	-------	100	42	------	0.5
1	2	Sample	1366264	379722.1	-------	100	38	-------	0.45
1	3	Control	1399059	452008	-------	100	41	------	0.49
1	4	Sample	1311806	377304	-------	100	36	------	0.43
1	5	Control	1549441	505586	-------	100	38	------	0.45
1	6	Sample	1401487	434421.2	-------	100	37	------	0.44
1	7	Pos. Ctrl.	1572990	619443.4	-------	100	33	------	0.39
1	8	Control	1032179	387231.3	-------	100	50	------	0.44
1	9	Sample	1271509	477675	-------	100	45	------	0.39
1	10	Control	1289560	480904	-------	100	44	------	0.39
1	11	Sample	1417251	511439.4	-------	100	42	------	0.37
1	12	Pos. Ctrl.	1910090	701870.2	-------	100	39	------	0.34

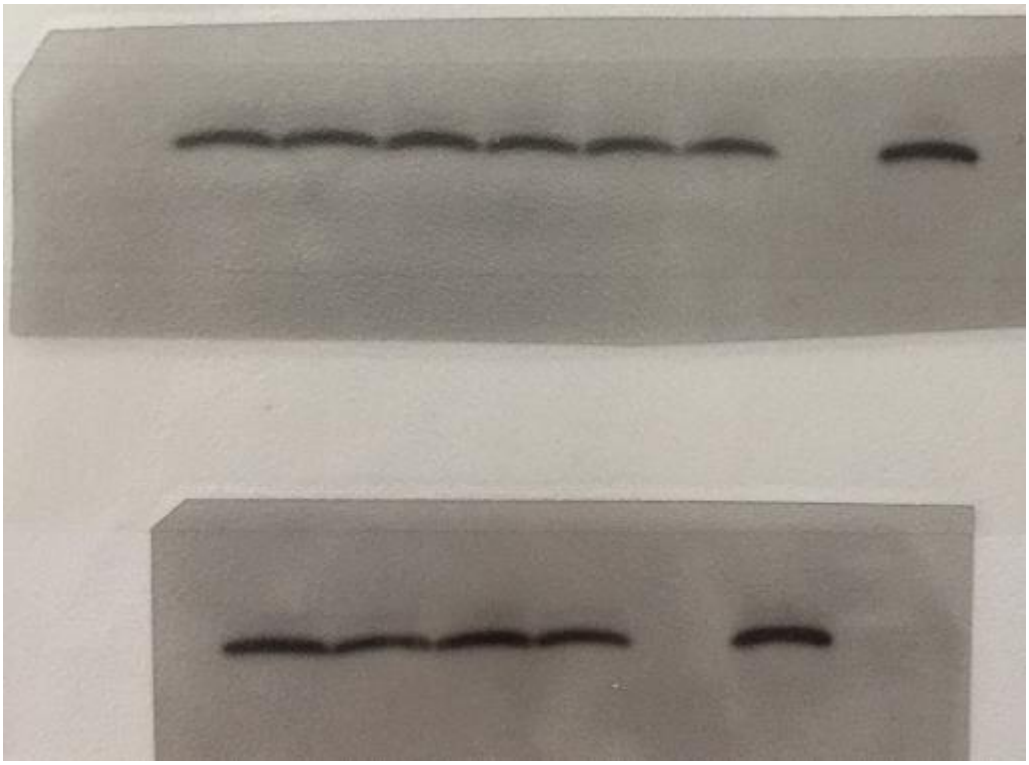

Figure C.7: Gel of Aβ degradation in N2a culture medium on 15.08.2016.

Table C.11: Data analysis of Aβ degradation in N2a culture medium by Image gauge on 15.08.2016.

NO.	Ln	Area Name	AU	AU-BG	Ratio	% of Lane	Dist (px)	C-Dist (px)	RF
1	1	Control	1191096	504710	-------	100	63	------	0.51
1	2	Sample	1152896	475437.8	-------	100	58	-------	0.47
1	3	Control	1115939	475912	-------	100	52	------	0.42
1	4	Sample	1006545	378708.4	-------	100	49	------	0.4
1	5	Control	1000149	353512	-------	100	46	------	0.37
1	6	Sample	838334	300666	-------	100	47	------	0.38
1	7	Pos. Ctrl.	1389879	601135	-------	100	55	------	0.44
1	8	Control	1306717	472502.7	-------	100	58	------	0.5
1	9	Sample	1002967	289481.9	-------	100	57	------	0.49
1	10	Control	1294801	424910	-------	100	57	------	0.49
1	11	Sample	1111520	341102	-------	100	55	------	0.47
1	12	Pos. Ctrl.	1336066	512716	-------	100	53	------	0.46

Table C 12: Data analysis of Aβ degradation in N2a culture medium.

Control	Sample	Mean	Factor	Adjusted* Control	Adjusted** Sample
275493.23	185533.59	230513.41	90.3	107.920136	72.67986351
227877.85	142111.82	184994.835		111.232132	69.36786828
207464.2	115733.12	161598.66		115.929286	64.67071408
321769.51	298625.07	310197.29		93.6687318	86.93126823
416260.31	318671.48	367465.895	*Control×factor	102.290598	78.30940241
429405.37	367148.8	398277.085	Mean	97.3576095	83.24239051

358854.67	420161.2	389507.935		83.193624	97.40637597
405289.5	451102.67	428196.085	**Sample×factor	85.4693519	95.13064815
504710.43	475437.83	490074.13	Mean	92.996853	87.603147
475912.46	378708.39	427310.425		100.570669	80.02933141
353512.47	300665.76	327089.115		97.5947367	83.00526335
472502.71	289481.94	380992.325		111.989119	68.61088129
424909.84	341101.89	383005.865		100.179559	80.42044126
n= 13	n= 13		Average	100.0175	79.28246
			Std. Dev.	6.950798	6.950798
			Std. Error	1.7377	1.7377

Table C.13: Normality test of Aβ degradation in N2a culture medium.

	Kolmogorov-Smirnov[a]			Shapiro-Wilk		
	Statistic	df	Sig.	Statistic	df	Sig.
Control	.102	13	.200*	.967	13	.861
Cholesterol	.102	13	.200*	.967	13	.861

Table C.14: Significance test (T. test) of Aβ degradation in N2a culture medium.

	Levene's Test for Equality of Variances		t-test for Equality of Means						
	F	Sig.	t	df	Sig. (2-tailed)	Mean Difference	Std. Error Difference	95% Confidence Interval of the Difference	
								Lower	Upper
Equal variances assumed	.000	1.000	4.988	24	.000	19.46037	3.90176	11.4075	27.5132
Equal variances not assumed			4.988	24.000	.000	19.46037	3.90176	11.4075	27.5132

Figure C.8: Gel of Aβ degradation in N2a IDE knock down living cells on 07.07.2016.

Table C.15: Data analysis of Aβ degradation in N2a IDE knock-down living cells by Image gauge on 07.07.2016.

NO.	Ln	Area Name	AU	AU-BG	Ratio	% of Lane	Dist (px)	C-Dist (px)	RF
1	1	Control	990292	524566.11	-----	100	57	------	0.47
1	2	Sample	1365796	771508.88	-----	100	60	-------	0.5
1	3	Control	1402848	795290.69	-----	100	55	------	0.46
1	4	Sample	1460101	857778.28	-----	100	42	------	0.35
1	5	Control	1412384	817909.94	-----	100	54	------	0.45
1	6	Sample	1043021	556937.18	-----	100	56	------	0.47
1	7	Control	1322214	579899.12	-----	100	55	------	0.49
1	8	Sample	1515306	672489.8	-----	100	58	------	0.52
1	9	Control	1582087	717753.38	-----	100	51	------	0.46
1	10	Sample	1592724	771843.76	-----	100	50	------	0.45
1	11	Control	1240434	585594.61	-----	100	60	------	0.54
1	12	Sample	1175777	535338.9	-----	100	61	------	0.54

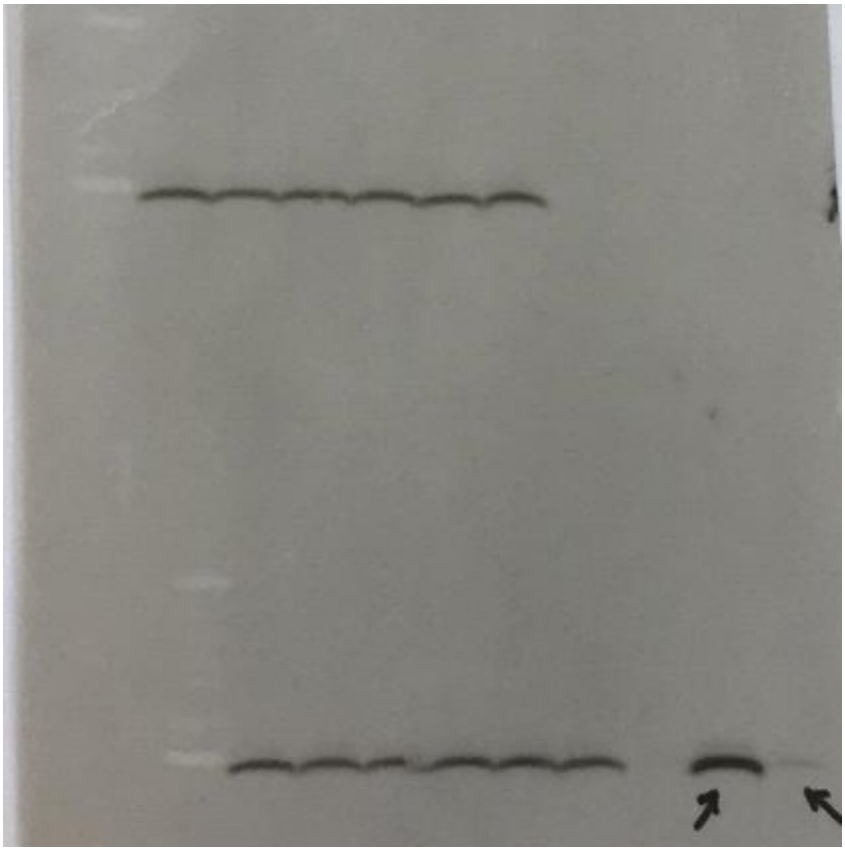

Figure C.9: Gel of Aβ degradation in N2a IDE knock down living cells on 09.07.2016.

Table C.16: Data analysis of Aβ degradation in N2a IDE knock-down living cells by Image gauge on 09.07.2016.

NO.	Ln	Area Name	AU	AU-BG	Ratio	% of Lane	Dist (px)	C-Dist (px)	RF
1	1	Control	1563580	459931.79	-----	100	47	------	0.44
1	2	Sample	1531823	395447.68	-----	100	53	-------	0.49
1	3	Control	1566971	386060.69	-----	100	61	------	0.56
1	4	Sample	1572988	398463.39	-----	100	57	------	0.53
1	5	Control	1585782	419040.02	-----	100	54	------	0.5
1	6	Sample	1544350	398361.53	-----	100	47	------	0.44
1	7	Control	1436537	416346.1	-----	100	51	------	0.47
1	8	Sample	1491167	378900.7	-----	100	47	------	0.44
1	9	Control	1505112	332906.7	-----	100	48	------	0.44
1	10	Sample	1538252	414418.3	-----	100	53	------	0.49
1	11	Control	1583717	433353.3	-----	100	53	------	0.49
1	12	Sample	1476466	377432.7	-----	100	55	------	0.51

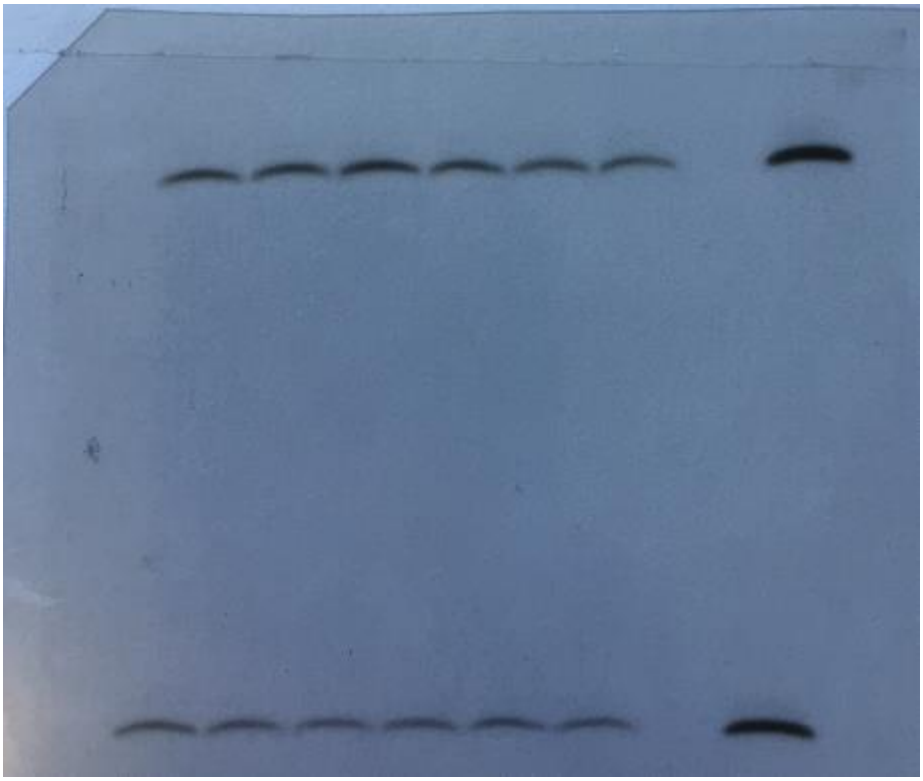

Figure C.10: Gel of Aβ degradation in N2a knock down living cells on 14.12.2016.

Table C.17: Data analysis of Aβ degradation in N2a IDE knock-down living cells by Image gauge on 14.12.2016.

NO.	Ln	Area Name	AU	AU-BG	Ratio	% of Lane	Dist (px)	C-Dist (px)	RF
1	1	Control	531837	299715.36	-----	100	51	------	0.44
1	2	Sample	537698	315162.35	-----	100	53	-------	0.46
1	3	Control	623610	401214.12	-----	100	45	------	0.39
1	4	Sample	469937	292427.26	-----	100	44	------	0.38
1	5	Control	447225	266240.16	-----	100	43	------	0.37
1	6	Sample	378596	214336.48	-----	100	40	------	0.34
1	7	Control	426791	232883.37	-----	100	51	------	0.41
1	8	Sample	411479	210115.82	-----	100	52	------	0.42
1	9	Control	349445	189206.68	-----	100	49	------	0.4
1	10	Sample	384954	210789.87	-----	100	58	------	0.47
1	11	Control	384301	235899.66	-----	100	61	------	0.49
1	12	Sample	357003	201759.7	-----	100	56	------	0.45

Table C 18: Data analysis of Aβ degradation in N2a IDE knock down living cells.

Control	Sample	Mean	Factor	Adjusted* Control	Adjusted** Sample
795290.69	771508.88	783399.785	97.4	98.8783948	95.9216052
817909.94	857778.28	837844.11		95.0826379	99.7173621
579899.12	672489.8	626194.46		90.1990961	104.600904
717753.38	771843.76	744798.57		93.8632028	100.936797
585594.61	535338.9	560466.755	*Control×factor	101.766812	93.0331878
459931.79	395447.68	427689.735	Mean	104.74265	90.0573497
386060.69	398463.39	392262.04		95.8601837	98.9398163
419040.02	398361.53	408700.775	**Sample×factor	99.8640092	94.9359908
416346.11	378900.66	397623.385	Mean	101.986233	92.8137672
433353.34	377432.73	405393.035		104.117761	90.6822385
299715.36	315162.35	307438.855		94.9531121	99.8468879
401214.12	292427.26	346820.69		112.675675	82.1243252
266240.16	214336.48	240288.32		107.919484	86.8805157
232883.37	210115.82	221499.595		102.405787	92.3942135
189206.68	210789.87	199998.275		92.1444479	102.655552
235899.66	201759.7	218829.68		104.997763	89.802237
n= 16	n= 16		Average	100.091078	94.7089219
			Std. Dev.	6.13206282	6.13206282
			Std. Error	1.5330157	1.5330157

Table C.19: Normality test of Aβ degradation in N2a IDE knock down living cells.

	Kolmogorov-Smirnov[a]			Shapiro-Wilk		
	Statistic	df	Sig.	Statistic	df	Sig.
Control	.130	16	.200*	.975	16	.909
Cholesterol	.130	16	.200*	.975	16	.909

Table C.20: Significance test (T. test) of Aβ degradation in N2a IDE knock down living cells.

			t-test for Equality of Means						
					Sig. (2-tailed)	Mean Difference	Std. Error Difference	95% Confidence Interval of the Difference	
Levene's Test for Equality of Variances	F	Sig.	t	df				Lower	Upper
Equal variances assumed	.000	1.000	2.483	30	.019	5.38216	2.16801	.95449	9.80983
Equal variances not assumed			2.483	30.000	.019	5.38216	2.16801	.95449	9.80983

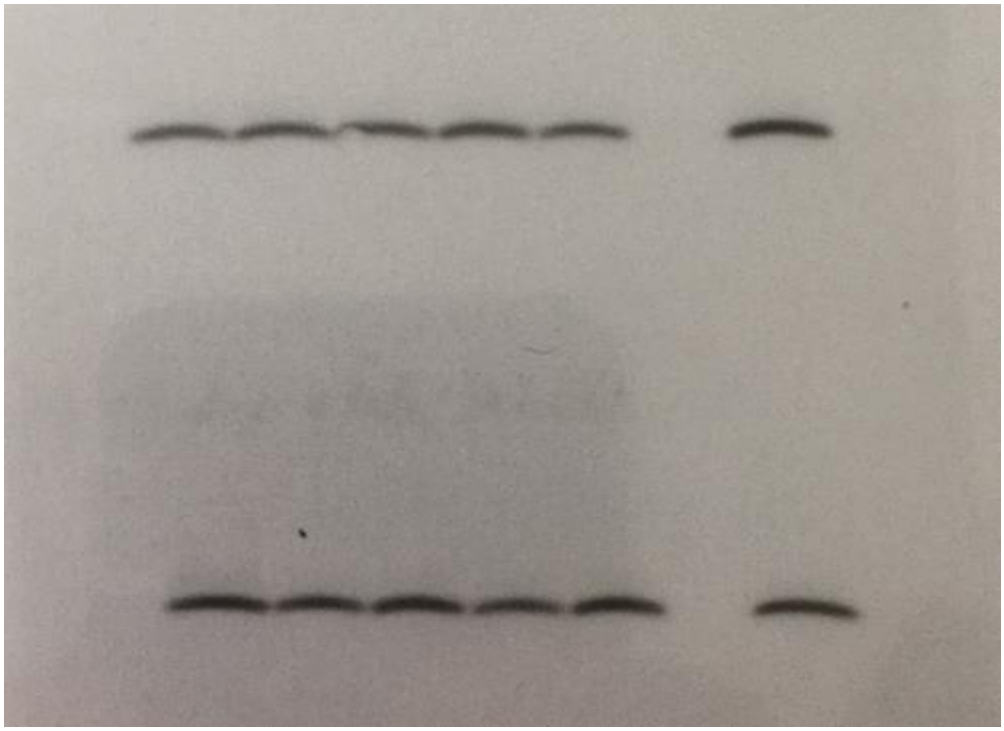

Figure C.11: Gel of Aβ degradation in N2a IDE knock down culture medium on 15.12.2016.

Table C.21: Data analysis of Aβ degradation in N2a IDE knock-down culture medium by Image gauge on 15.12.2016.

NO.	Ln	Area Name	AU	AU-BG	Ratio	% of Lane	Dist (px)	C-Dist (px)	RF
1	1	Control	836235.46	271351	-----	100	55	------	0.46
1	2	Sample	1079152.43	438609.5	-----	100	60	-------	0.5
1	3	Control	1219141.64	515873.8	-----	100	55	------	0.46
1	4	Sample	1299357.37	588597.1	-----	100	43	------	0.42
1	5	Control	1157699.76	454379.2	-----	100	54	------	0.45
1	6	Pos. ctrl.	1215394.9	525055.32	-----	100	60	------	0.54
1	7	Sample	903665.00	338911.49	-----	100	55	------	0.49
1	8	Control	928371.00	287963.07	-----	100	58	------	0.52
1	9	Sample	1041088.00	337942.14	-----	100	51	------	0.46
1	10	Control	1045749.00	335103.75	-----	100	50	------	0.45
1	11	Sample	1152047.00	448866.41	-----	100	60	------	0.54
1	12	Pos. ctrl.	1215276.00	525198.12	-----	100	61	------	0.54

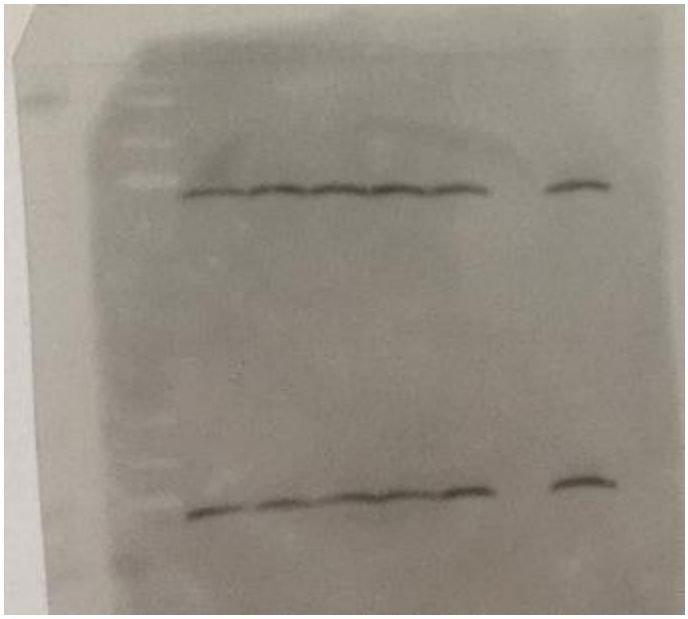

Figure C.12: Gel of Aβ degradation in N2a culture medium on 16.12.2016.

Table C.22: Data analysis of Aβ degradation in N2a IDE knock-down culture medium by Image gauge on 16.12.2016.

NO.	Ln	Area Name	AU	AU-BG	Ratio	% of Lane	Dist (px)	C-Dist (px)	RF
1	1	Control	602047	436068.5	-----	100	46	------	0.46
1	2	Sample	685828	522977.1	-----	100	40	-------	0.4
1	3	Control	600052	441892	-----	100	37	------	0.37
1	4	Sample	695801	557671.78	-----	100	41	------	0.41
1	5	Control	578717	451180.04	-----	100	45	------	0.45
1	6	Pos. ctrl.	893157	725671.64	-----	100	52	------	0.52
1	7	Sample	801280	570109.34	-----	100	55	------	0.47
1	8	Control	683845	490484.97	-----	100	51	------	0.44
1	9	Sample	758160	559059.67	-----	100	47	------	0.41
1	10	Control	595521	425572	-----	100	53	------	0.46
1	11	Sample	804564	611187.12	-----	100	58	------	0.5
1	12	Pos. ctrl.	886135	696017.61	-----	100	71	------	0.61

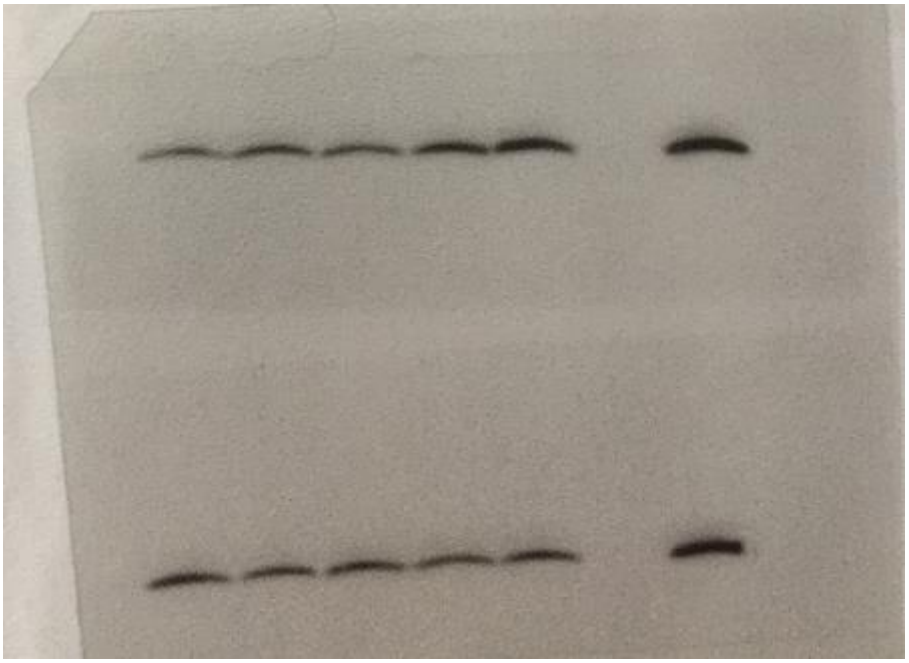

Figure C.13: Gel of Aβ degradation in N2a culture medium on 22.12.2016.

Table C.23: Data analysis of Aβ degradation in N2a IDE knock-down culture medium by Image gauge on 22.12.2016.

NO.	Ln	Area Name	AU	AU-BG	Ratio	% of Lane	Dist (px)	C-Dist (px)	RF
1	1	Control	295849	176169.4	-----	100	36	------	0.46
1	2	Sample	402122	252506.8	-----	100	30	-------	0.38
1	3	Control	358545	229148.69	-----	100	32	------	0.41
1	4	Sample	546564	369544.68	-----	100	34	------	0.44
1	5	Control	720619	528927.54	-----	100	36	------	0.46
1	6	Pos. ctrl.	929065	752009.67	-----	100	33	------	0.42
1	7	Sample	548470	369619.52	-----	100	45	------	0.44
1	8	Control	417388	239259.66	-----	100	42	------	0.41
1	9	Sample	452845	279887.29	-----	100	48	------	0.47
1	10	Control	388371	222755.44	-----	100	49	------	0.48
1	11	Sample	408780	271738.29	-----	100	47	------	0.46
1	12	Pos. ctrl.	883170	668667.15	-----	100	37	------	0.36

Table C.24: Data analysis of Aβ degradation in N2a IDE knock down culture medium.

Control	Sample	Mean	Factor	Adjusted* Control	Adjusted** Sample
271350.95	438609.5	354980.225	114.9	87.8308761	141.969124
515873.78	588597.12	552235.45		107.334466	122.465534
287963.07	337942.14	312952.605		105.725136	124.074864
335103.75	448866.41	391985.08	*Control×factor	98.2267511	131.573249
436068.48	522977.12	479522.8	Mean	104.487771	125.312229
441892.04	557671.78	499781.91		101.591103	128.208897
451180.04	570109.34	510644.69	**Sample×factor	101.519878	128.280122
490484.97	559059.67	524772.32	Mean	107.392713	122.407287
425572	611187.12	518379.56		94.3289948	135.471005
176169.4	252506.75	214338.075		94.4389561	135.361044
229148.69	369544.68	299346.685		87.9554904	141.84451
239259.66	279887.29	259573.475		105.908105	123.891895
222755.44	271738.29	247246.865		103.518401	126.281599
n= 13	n= 13		Average	100.019895	129.780105
			Std. Dev.	6.90937118	6.90937118
			Std. Error	1.91631477	1.91631477

Table C.25: Normality test of Aβ degradation in N2a IDE knock down culture medium.

	Kolmogorov-Smirnov[a]			Shapiro-Wilk		
	Statistic	df	Sig.	Statistic	df	Sig.
Control	.201	13	.154	.879	13	.070
Cholesterol	.201	13	.154	.879	13	.070

Table C.26: Significance test (T. test) of Aβ degradation in N2a IDE knock down culture medium.

			t-test for Equality of Means						
								95% Confidence Interval of the Difference	
Levene's Test for Equality of Variances	F	Sig.	t	df	Sig. (2-tailed)	Mean Difference	Std. Error Difference	Lower	Upper
Equal variances assumed	.000	1.000	-10.98	24	.000	-29.76021	2.71008	-35.35354	-24.16688
Equal variances not assumed			-10.98	24.	.000	-29.76021	2.71008	-35.35354	-24.16688

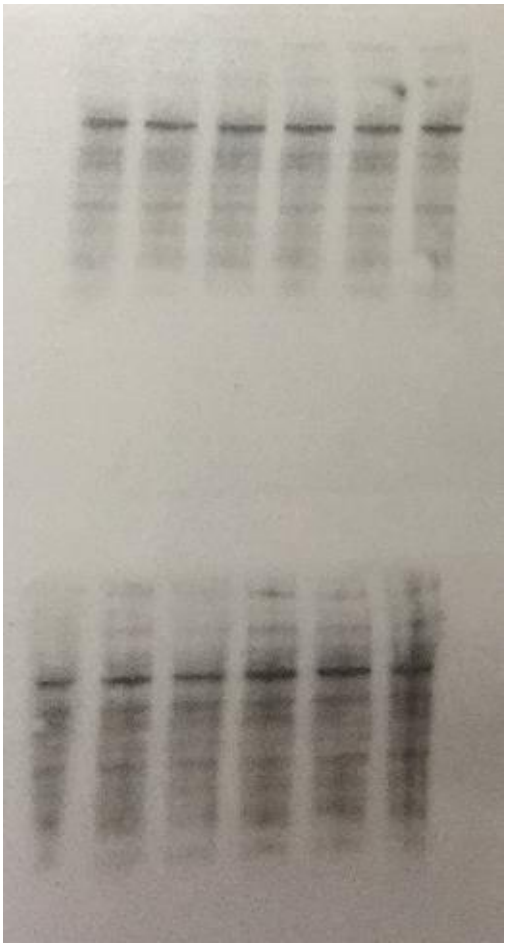

Figure C.14: Gel of intracellular IDE level experiment on 14.11.2016.

Table C.27: Data analysis of intracellular IDE level by Image gauge on 14.11.2016.

NO.	Ln	Area Name	AU	AU-BG	Ratio	% of Lane	Dist (px)	C-Dist (px)	RF
1	1	Control	504865	220003.1	-----	100	28	------	0.48
1	2	Sample	534665	265261.4	-----	100	28	-------	0.48
1	3	Control	455824	169778.4	-----	100	22	------	0.38
1	4	Sample	520694	234586.3	-----	100	29	------	0.5
1	5	Control	416955	158351	-----	100	35	------	0.6
1	6	Sample	436303	183488.6	-----	100	31	------	0.53
1	7	Control	346464	103522.4	-----	100	36	------	0.56
1	8	Sample	476908	184662.2	-----	100	22	------	0.34
1	9	Control	426424	142437.7	-----	100	30	------	0.47
1	10	Sample	719592	281510.5	-----	100	29	------	0.45
1	11	Control	516389	188146	-----	100	31	------	0.48
1	12	Sample	505748	106927.3	-----	100	28	------	0.44

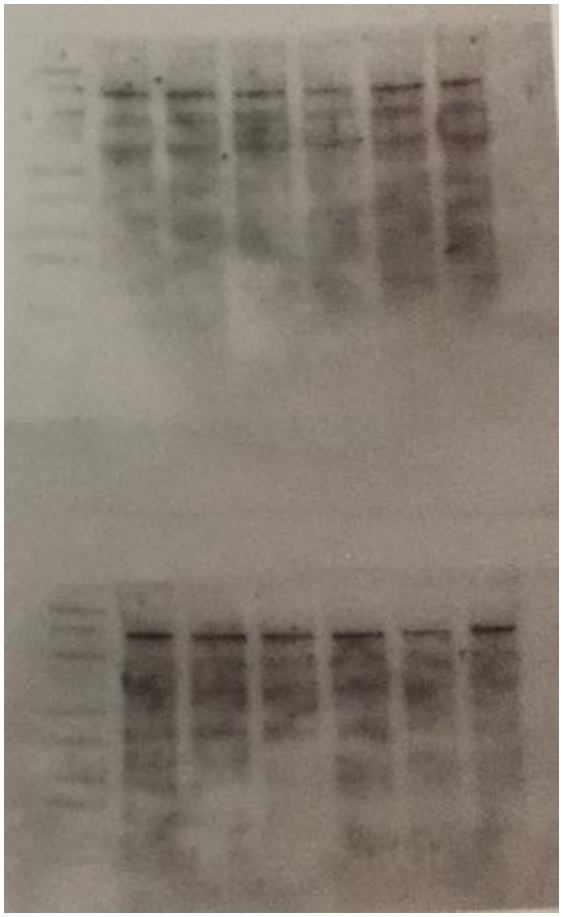

Figure C.15: Gel of extracellular IDE level experiment on 18.11.2016.

Table C.28: Data analysis of extracellular IDE level by Image gauge on 18.11.2016.

NO.	Ln	Area Name	AU	AU-BG	Ratio	% of Lane	Dist (px)	C-Dist (px)	RF
1	1	Control	1609771	538131.6	-----	100	68	------	0.46
1	2	Sample	1441178	484345.3	-----	100	73	-------	0.49
1	3	Control	1282271	413151.7	-----	100	76	------	0.51
1	4	Sample	898382	211983	-----	100	66	------	0.45
1	5	Control	1272527	367072.9	-----	100	77	------	0.52
1	6	Sample	1225284	354556.6	-----	100	82	------	0.55
1	7	Control	2464837	948945.9	-----	100	53.57	------	0.43
1	8	Sample	2347570	650705.4	-----	100	64.48	------	0.52
1	9	Control	2327348	760800.8	-----	100	62.5	------	0.5
1	10	Sample	1391520	325513	-----	100	52.58	------	0.42
1	11	Control	2403769	645972.1	-----	100	68.45	------	0.55
1	12	Sample	2427441	790785.6	-----	100	54.56	------	0.44

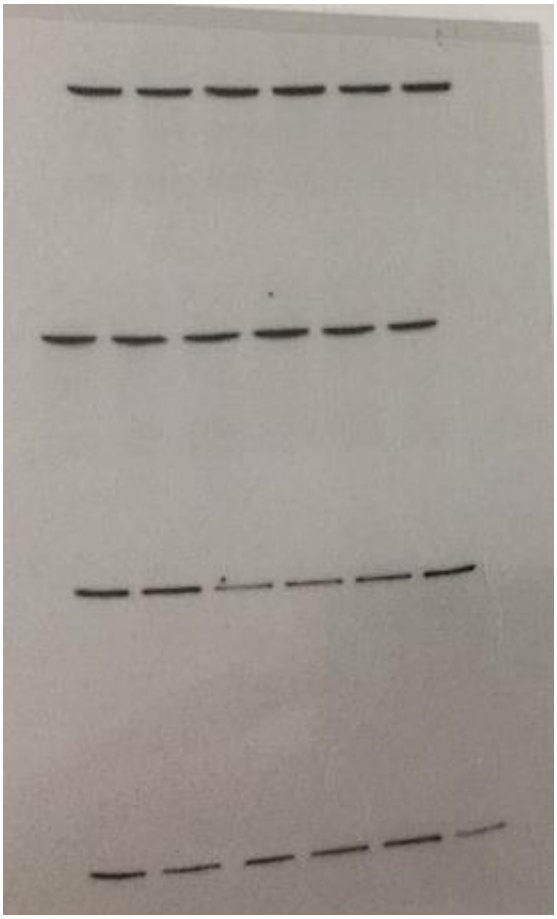

Figure C.16: Gel of intracellular (above) and extracellular (below) IDE level experiment on 28.11.2016.

Table C.29: Data analysis of intracellular IDE level by Image gauge on 28.11.2016.

NO.	Ln	Area Name	AU	AU-BG	Ratio	% of Lane	Dist (px)	C-Dist (px)	RF
1	1	Control	511963	365037.8	-----	100	44	------	0.59
1	2	Sample	493484	339787.3	-----	100	43	-------	0.58
1	3	Control	535562	375865.9	-----	100	45	------	0.61
1	4	Sample	613624	447413.4	-----	100	45	------	0.61
1	5	Control	492618	341469.1	-----	100	42	------	0.57
1	6	Sample	560919	396887.9	-----	100	46	------	0.62
1	7	Control	644444	409930.7	-----	100	46	------	0.49
1	8	Sample	631546	386227.5	-----	100	47	------	0.5
1	9	Control	533024	346858.2	-----	100	49	------	0.52
1	10	Sample	654538	423788.6	-----	100	50	------	0.53
1	11	Control	544385	343837.2	-----	100	51	------	0.54
1	12	Sample	464081	287947.5	-----	100	49	------	0.52

Table C.30: Data analysis of extracellular IDE level by Image gauge on 28.11.2016.

NO.	Ln	Area Name	AU	AU-BG	Ratio	% of Lane	Dist (px)	C-Dist (px)	RF
1	1	Control	516768	281633.3	-----	100	41	------	0.47
1	2	Sample	490387	283608.9	-----	100	50	-------	0.57
1	3	Control	211123	78622.21	-----	100	41	------	0.47
1	4	Sample	256100	114719.3	-----	100	40	------	0.45
1	5	Control	251969	117940.6	-----	100	49	------	0.56
1	6	Sample	394152	199744.4	-----	100	53	------	0.6
1	7	Control	474920.8	239786.1	-----	100	52	------	0.58
1	8	Sample	314185.5	172804.8	-----	100	49	------	0.55
1	9	Control	311114.1	177085.7	-----	100	50	------	0.56
1	10	Sample	300293.4	167792.6	-----	100	48	------	0.54
1	11	Control	342813	208784.5	-----	100	51	------	0.57
1	12	Sample	265680.8	71273.2	-----	100	42	------	0.49

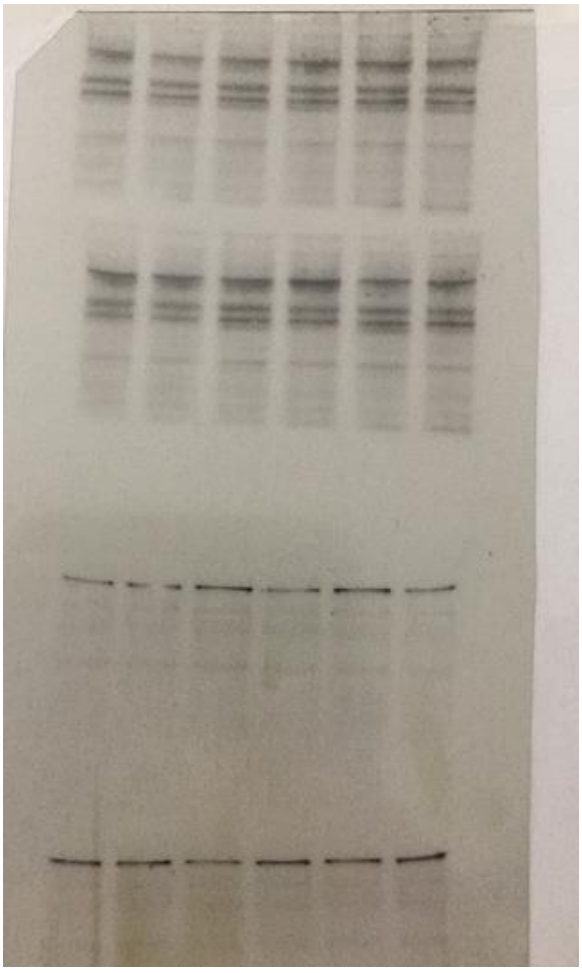

Figure C.17: Gel of intracellular (above) and extracellular (below) IDE level experiment on 02.12.2016.

Table C.31: Data analysis of intracellular IDE level by Image gauge on 02.12.2016.

NO.	Ln	Area Name	AU	AU-BG	Ratio	% of Lane	Dist (px)	C-Dist (px)	RF
1	1	Control	902232.8	302674.6	-----	100	53	------	0.62
1	2	Sample	962881.6	281177.3	-----	100	48	-------	0.56
1	3	Control	978921.2	352579.7	-----	100	43	------	0.51
1	4	Sample	1062623	419248.8	-----	100	50	------	0.58
1	5	Control	1242785	413519.1	-----	100	49	------	0.57
1	6	Sample	937629.5	334817.3	-----	100	55	------	0.65
1	7	Control	1165286	333506.3	-----	100	53	------	0.62
1	8	Sample	1007403	357442	-----	100	45	------	0.53
1	9	Control	1079120	409194	-----	100	44	------	0.52
1	10	Sample	1263176	441773.5	-----	100	51	------	0.59
1	11	Control	854582.1	253325.1	-----	100	50	------	0.58
1	12	Sample	899621.7	270074.7	-----	100	49	------	0.57

Table C.32: Data analysis of extracellular IDE level by Image gauge on 02.12.2016.

NO.	Ln	Area Name	AU	AU-BG	Ratio	% of Lane	Dist (px)	C-Dist (px)	RF
1	1	Control	1280394.7	208755.2	-----	100	68	------	0.46
1	2	Sample	1151057.6	194224.8	-----	100	73	-------	0.49
1	3	Control	1189151.6	320032.3	-----	100	76	------	0.51
1	4	Sample	858860.53	172461.5	-----	100	66	------	0.45
1	5	Control	1270240.4	364786.3	-----	100	77	------	0.52
1	6	Sample	1090289.4	219562.1	-----	100	82	------	0.55
1	7	Control	1825434.8	309543.8	-----	100	53.57	------	0.43
1	8	Sample	1980332.8	283468.2	-----	100	64.48	------	0.52
1	9	Control	1762816.5	196269.3	-----	100	62.5	------	0.5
1	10	Sample	1365797.9	299790.9	-----	100	52.58	------	0.42
1	11	Control	2051088.9	293292	-----	100	68.45	------	0.55
1	12	Sample	1942838.6	306183.1	-----	100	54.56	------	0.44

Table C.33: Data analysis of intracellular IDE level.

Control	Sample	Mean	Factor	Adjusted* Control	Adjusted** Sample
220003.1	265261.39	242632.245	107.75	98.8340931	119.165907
169778.39	234586.29	202182.34		91.5304695	126.46953
158350.98	183488.6	170919.79	*Control×factor	100.984543	117.015457
103522.35	184662.19	144092.27	Mean	78.3104892	139.689511
142437.72	281510.48	211974.1		73.2434362	144.756564
375865.93	447413.38	411639.655	**Sample×factor	99.5273071	118.472693
341469.07	396887.89	369178.48	Mean	100.818793	117.181207
409930.71	386227.46	398079.085		112.245152	105.754848
346858.23	423788.59	385323.41		98.1189985	119.881002
343837.2	287947.51	315892.355		118.642488	99.3575124

302674.61	281177.34	291925.975		113.01335	104.98665
352579.72	419248.83	385914.275		99.5847834	118.415217
333506.27	357442.02	345474.145		105.224035	112.775965
409193.97	441773.51	425483.74		104.826903	113.173097
253325.14	270074.66	261699.9		105.511849	112.488151
n= 15	n= 15		Average	100.027779	117.972221
			Std. Dev.	11.9904916	11.9904916
			Std. Error	3.09593161	3.09593161

Table C.34: Normality test of intracellular IDE level experiments.

	Kolmogorov-Smirnov[a]			Shapiro-Wilk		
	Statistic	df	Sig.	Statistic	df	Sig.
Control	.237	15	.023	.910	15	.136
Cholesterol	.237	15	.023	.910	15	.136

Table C.35: Significance test (T. test) of intracellular IDE level experiments.

			t-test for Equality of Means						
								95% Confidence Interval of the Difference	
Levene's Test for Equality of Variances	F	Sig.	t	df	Sig. (2-tailed)	Mean Difference	Std. Error Difference	Lower	Upper
Equal variances assumed	.000	1.000	-4.098	28	.000	-17.94444	4.37831	-26.91300	-8.97588-
Equal variances not assumed			-4.098	28.	.000	-17.94444	4.37831	-26.91300	-8.97588-

Table C.36: Data analysis of extracellular IDE level experiments.

Control	Sample	Mean	Factor	Adjusted* Control	Adjusted** Sample
538131.57	484345.25	511238.41	107.75	113.418076	102.081924
367072.94	354556.64	360814.79		109.618869	105.881131
645972.12	790785.55	718378.835	*Control×factor	96.8896807	118.610319
650705.39	760800.75	705753.07	Mean	99.3456618	116.154338
325513	948945.94	637229.47		55.041437	160.458563
281633.28	283608.9	282621.09	**Sample×factor	107.373395	108.126605
78622.21	114719.31	96670.76	Mean	87.6329422	127.867058
117940.58	199744.36	158842.47		80.0044062	135.495594
239786.1	172804.79	206295.445		125.242476	90.2575242
177085.7	167792.6	172439.15		110.653434	104.846566
208755.24	194224.8	201490.02		111.635192	103.864808

309543.78	283468.17	296505.975		112.487926	103.012074
196269.25	299790.9	248030.075		85.2639007	130.236099
293292	306183.12	299737.56		105.432943	110.067057
n= 14	n= 14		Average	100.002881	115.497119
			Std. Dev.	17.9738068	17.9738068
			Std. Error	4.80370192	4.80370192

Table C.37: Normality test of extracellular IDE level experiments.

	Kolmogorov-Smirnov[a]			Shapiro-Wilk		
	Statistic	df	Sig.	Statistic	df	Sig.
Control	.190	14	.183	.900	14	.112
Cholesterol	.190	14	.183	.900	14	.112

Table C.38: Significance test (T. test) of extracellular IDE level experiments.

			t-test for Equality of Means						
								95% Confidence Interval of the Difference	
Levene's Test for Equality of Variances	F	Sig.	t	df	Sig. (2-tailed)	Mean Difference	Std. Error Difference	Lower	Upper
Equal variances assumed	.000	1.000	-2.281	26	.031	-15.49424	6.79346	-29.45840	-1.53008-
Equal variances not assumed			-2.281	26.	.031	-15.49424	6.79346	-29.45840	-1.53008-

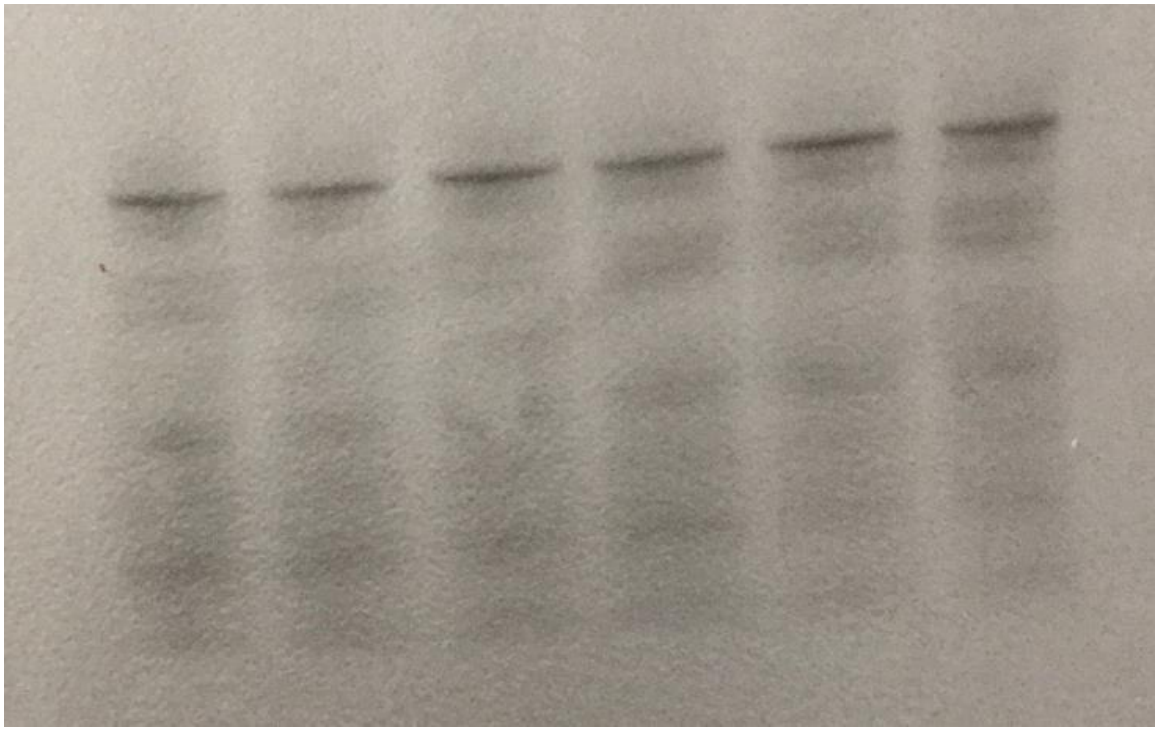

Figure C.18: Gel of intracellular IDE stability experiment on 26.12.2016.

Table C.39: Data analysis of intracellular IDE stability by Image gauge on 26.12.2016.

NO.	Ln	Area Name	AU	AU-BG	Ratio	% of Lane	Dist (px)	C-Dist (px)	RF
1	1	Control	467928	186286.3	------	100	59	------	0.61
1	2	Sample	427552	154503.6	------	100	51	-------	0.53
1	3	Control	478562	186978.3	------	100	51	------	0.53
1	4	Sample	527386	181624.2	------	100	55	------	0.57
1	5	Control	520696	183593.5	------	100	47	------	0.49
1	6	Sample	515330	175161.7	------	100	39	------	0.41

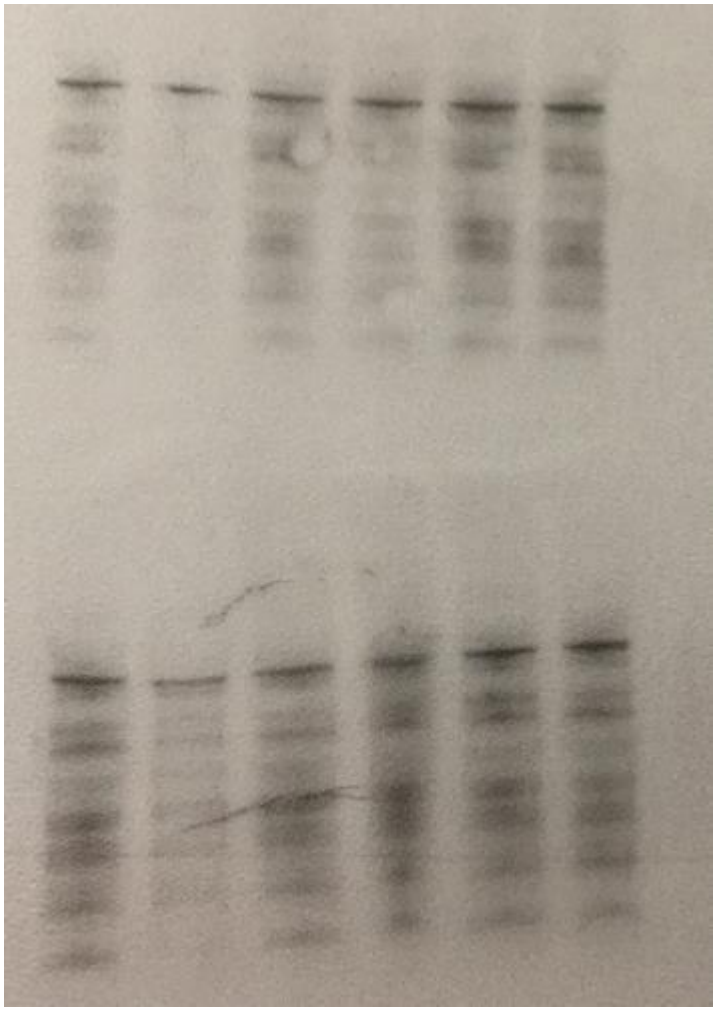

Figure C.19: Gel of intracellular IDE stability experiment on 27.12.2016.

Table C.40: Data analysis of intracellular IDE stability by Image gauge on 27.12.2016.

NO.	Ln	Area Name	AU	AU-BG	Ratio	% of Lane	Dist (px)	C-Dist (px)	RF
1	1	Control	516216	94479.7	------	100	56	------	0.5
1	2	Sample	1199879	330916.4	------	100	59	-------	0.53
1	3	Control	952195	252961	------	100	67	------	0.6
1	4	Sample	891557	242337.9	------	100	64	------	0.57
1	5	Control	600182	142775	------	100	55	------	0.49
1	6	Sample	657027	191378.6	------	100	54	------	0.48
1	7	Control	736706	180202.4	------	100	55	------	0.47
1	8	Sample	1172724	357286.3	------	100	67	-------	0.58
1	9	Control	1161735	301111.4	------	100	62	------	0.53
1	10	Sample	1179689	314244.8	------	100	63	------	0.54
1	11	Control	723720	136623.5	------	100	62	------	0.53
1	12	Sample	1075082	318778.7	------	100	70	------	0.6

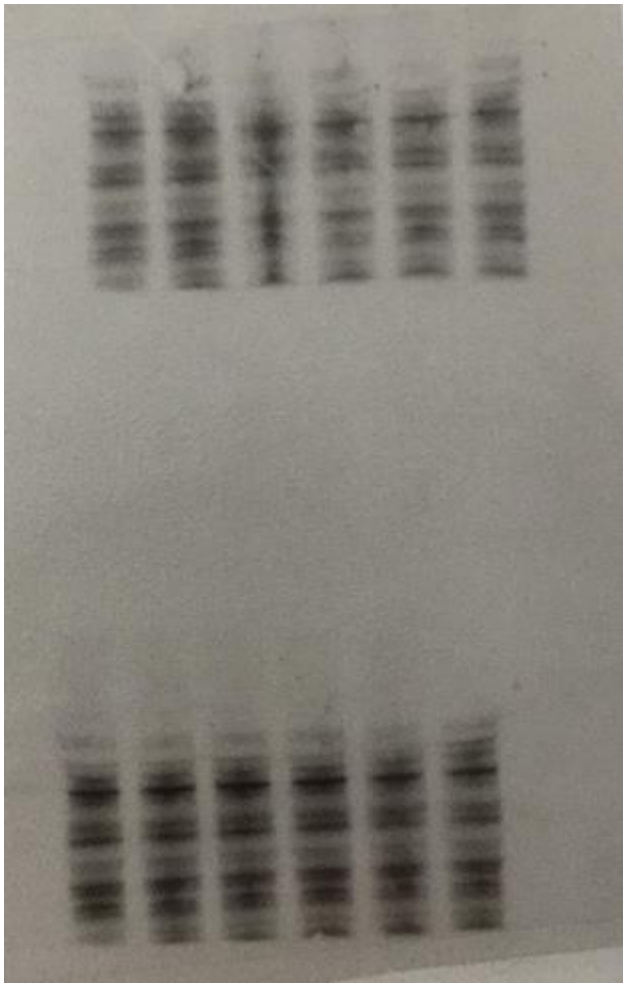

Figure C.20: Gel of intracellular IDE stability experiment on 21.01.2017.

Table C.41: Data analysis of intracellular IDE stability by Image gauge on 21.01.2017.

NO.	Ln	Area Name	AU	AU-BG	Ratio	% of Lane	Dist (px)	C-Dist (px)	RF
1	1	Control	357252	115833.9	------	100	50	------	0.5
1	2	Sample	515614	184511.5	------	100	54	-------	0.54
1	3	Control	617602	221483	------	100	47	------	0.47
1	4	Sample	1070386	440341	------	100	53	------	0.53
1	5	Control	803044	274368	------	100	45	------	0.45
1	6	Sample	874579	304551.1	------	100	44	------	0.44
1	7	Control	448088	224048.5	------	100	144	------	0.72
1	8	Sample	747993	428693	------	100	132	-------	0.66
1	9	Control	481626	212111	------	100	120	------	0.6
1	10	Sample	695452	380517.6	------	100	100	------	0.5
1	11	Control	629167	298716.9	------	100	78	------	0.39
1	12	Sample	582447	263274.5	------	100	59	------	0.29

Table C.42: Data analysis of intracellular IDE stability experiments.

Control	Cholesterol	Average	Factor		Normalized Control	Normalized Sample
115833.89	184511.49	150172.69	114.6		88.3953254	140.804675
221483.03	440341.01	330912.02			76.7030319	152.496968
274367.99	304551.11	289459.55			108.625097	120.574903
224048.5	428693.02	326370.76			78.6711349	150.528865
212111.03	380517.63	296314.33			82.0342507	147.165749
298716.89	263274.51	280995.7			121.827329	107.372671
94479.7	330916.4	212698.05			50.9049031	178.295097
252960.96	242337.92	247649.44			117.057911	112.142089
142775.02	191378.56	167076.79			97.9311207	131.268879
318778.65	357286.26	338032.455			108.072562	121.127438
301111.4	314244.84	307678.12			112.154112	117.045888
136623.46	180202.37	158412.915			98.8369447	130.363055
186286.3	154503.56	170394.93			125.287824	103.912176
186978.27	181624.24	184301.255			116.264589	112.935411
183593.46	175161.67	179377.565			117.293434	111.906566
n=15	n=15					
				Average	100.003971	129.196029
				Std	20.9230332	20.9230332
				SE	5.40230394	5.40230394

Table C.43: Normality test of intracellular IDE stability experiments.

	Kolmogorov-Smirnov[a]			Shapiro-Wilk		
	Statistic	df	Sig.	Statistic	df	Sig.
Control	.183	15	.186	.915	15	.162
Cholesterol	.183	15	.186	.915	15	.162

Table C.44: Significance test (T. test) of intracellular IDE stability experiments.

			t-test for Equality of Means						
								95% Confidence Interval of the Difference	
Levene's Test for Equality of Variances	F	Sig.	t	df	Sig. (2-tailed)	Mean Difference	Std. Error Difference	Lower	Upper
Equal variances assumed	.000	1.000	-3.821	28	.001	-29.19206	7.64001	-44.84191	-13.54220
Equal variances not assumed			-3.821	28.	.001	-29.19206	7.64001	-44.84191	-13.54220

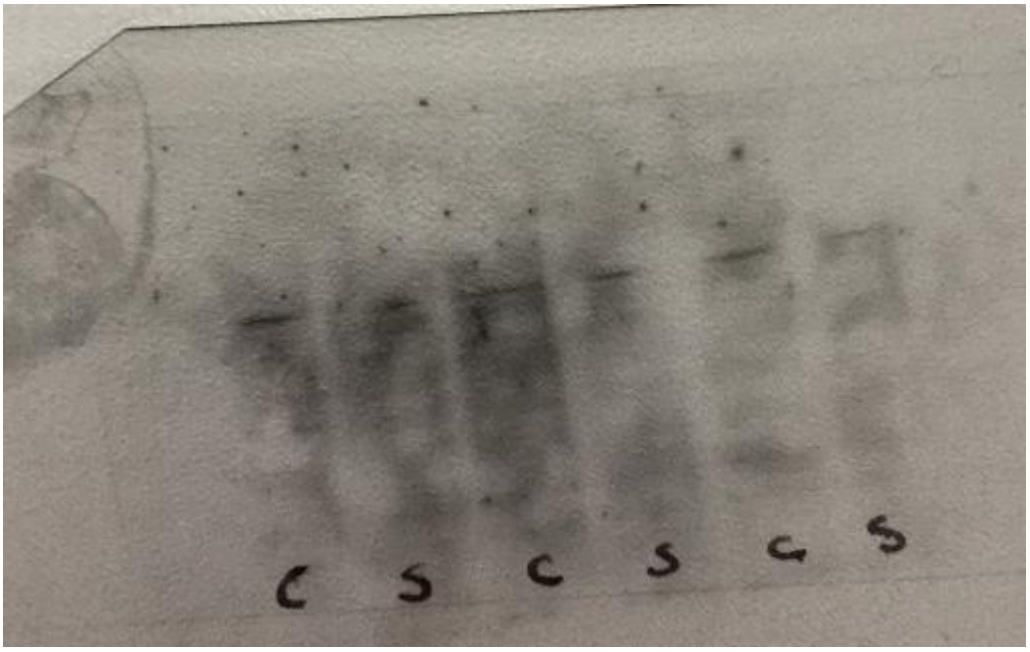

Figure C.21: Gel of extracellular IDE stability experiment on 26.12.2016.

Table C.45: Data analysis of extracellular IDE stability by Image gauge on 21.01.2017.

NO.	Ln	Area Name	AU	AU-BG	Ratio	% of Lane	Dist (px)	C-Dist (px)	RF
1	1	Control	461193	162439.25	------	100	37.00	------	0.42
1	2	Sample	442811	147188.31	------	100	41.00	-------	0.51
1	3	Control	437486	138029.14	------	100	40.00	------	0.49
1	4	Sample	479524	191199.24	------	100	38.00	------	0.47
1	5	Control	489217	197539.94	------	100	35.00	------	0.53
1	6	Sample	520155	214711.61	------	100	36.00	------	0.45

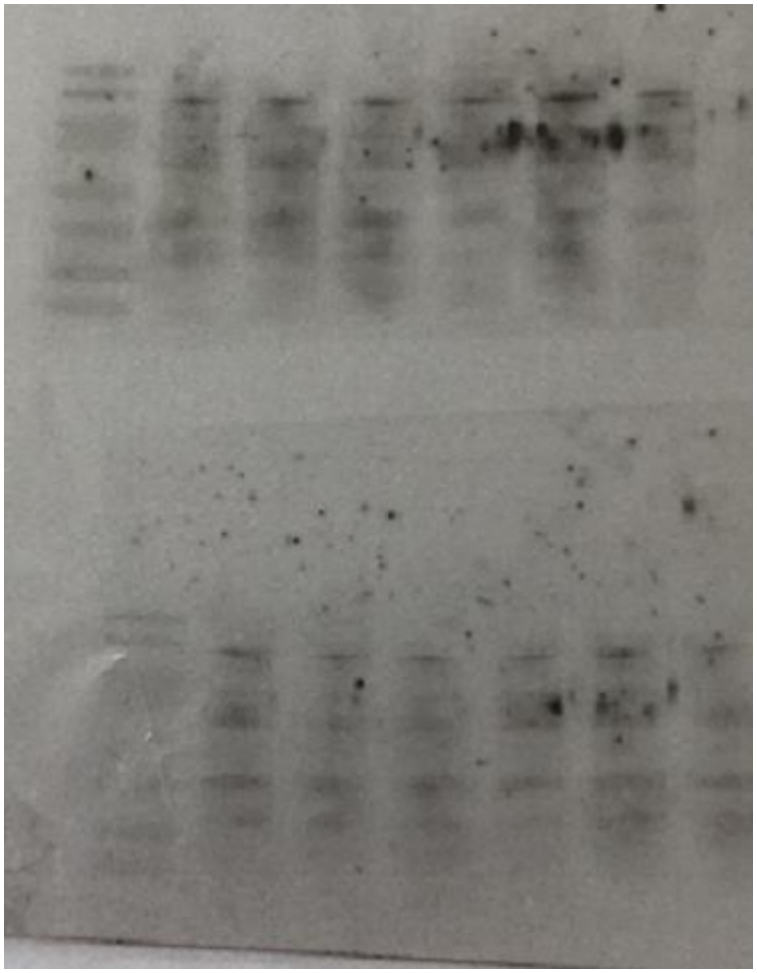

Figure C.22: Gel of extracellular IDE stability experiment on 27.12.2016.

Table C.46: Data analysis of extracellular IDE stability by Image gauge on 27.12.2016.

NO.	Ln	Area Name	AU	AU-BG	Ratio	% of Lane	Dist (px)	C-Dist (px)	RF
1	1	Control	239566.00	54848.29	------	100	35.00	------	0.47
1	2	Sample	184602.00	37755.09	------	100	46.00	-------	0.62
1	3	Control	185399.00	44292.17	------	100	45.00	------	0.61
1	4	Sample	269087.00	44164.62	------	100	37.00	------	0.50
1	5	Control	440571.00	100253.92	------	100	40.00	------	0.54
1	6	Sample	157036.00	25642.42	------	100	36.00	------	0.49
1	7	Control	253547.00	36987.49	------	100	37.00	------	0.50
1	8	Sample	294715.00	38271.52	------	100	40.00	-------	0.54
1	9	Control	282137.00	36303.28	------	100	44.00	------	0.59
1	10	Sample	314057.00	32713.42	------	100	47.00	------	0.64
1	11	Control	400504.00	71177.98	------	100	43.00	------	0.58
1	12	Sample	314723.00	37877.16	------	100	38.00	------	0.51

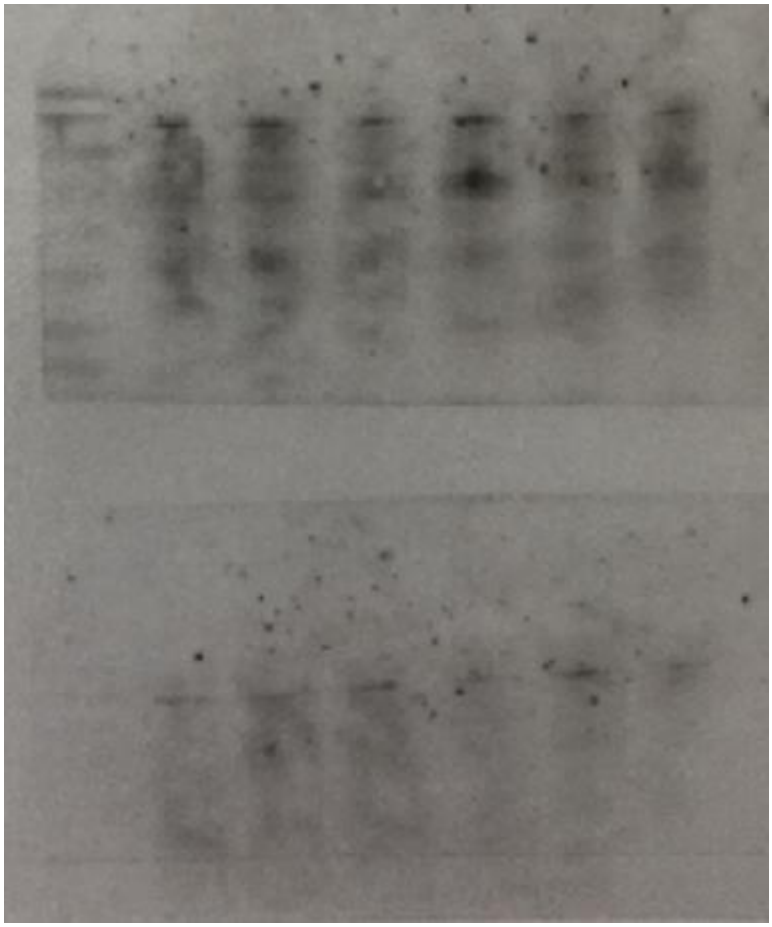

Figure C.23: Gel of extracellular IDE stability experiment on 23.01.2017.

Table C.47: Data analysis of extracellular IDE stability by Image gauge on 23.01.2017.

NO.	Ln	Area Name	AU	AU-BG	Ratio	% of Lane	Dist (px)	C-Dist (px)	RF
1	1	Control	439441.00	65425.20	------	100	45.00	------	0.51
1	2	Sample	858931.00	159322.10	------	100	45.00	-------	0.51
1	3	Control	439875.00	40363.10	------	100	53.00	------	0.60
1	4	Sample	679251.00	118773.73	------	100	51.00	------	0.58
1	5	Control	496841.00	45699.94	------	100	52.00	------	0.59
1	6	Sample	626260.00	47043.55	------	100	35.00	------	0.40
1	7	Control	624954.00	58272.84	------	100	75.00	------	0.59
1	8	Sample	841787.00	81457.33	------	100	81.00	-------	0.63
1	9	Control	907425.00	86077.42	------	100	64.00	------	0.50
1	10	Sample	887089.00	59595.09	------	100	53.00	------	0.41
1	11	Control	1280331.00	194393.07	------	100	56.00	------	0.44
1	12	Sample	1290628.00	127728.85	------	100	56.00	------	0.44

Table C.48: Data analysis of extracellular IDE stability experiments.

Control	Cholesterol	Average	Factor		Normalized Control	Normalized Sample
65425.2	159322.1	112373.7	115.2		67.07073	163.3293
40363.1	118773.7	79568.42			58.43813	171.9619
45699.94	47043.55	46371.75			113.5311	116.8689
58272.84	81457.33	69865.09			96.08564	134.3144
86077.42	59595.09	72836.26			136.1426	94.25738
194393.1	127728.9	161061			139.041	91.35897
162.439	147.18	154.8095			120.8774	109.5226
138.029	191.199	164.614			96.59531	133.8047
197.539	214.711	206.125			110.4014	119.9986
37755.09	54848.29	46301.69			93.9358	136.4642
44164.62	44292.17	44228.4			115.0339	115.3661
25642.42	100253.9	62948.17			46.9276	183.4724
38271.52	36987.49	37629.51			117.1655	113.2345
32713.42	36303.28	34508.35			109.2079	121.1921
37877.16	71177.98	54527.57			80.0228	150.3772
n=15	n=15					
				Average	100.0318	130.3682
				Std	27.06376	27.06376
				SE	6.987834	6.987834

Table C.49: Normality test of extracellular IDE stability experiments.

	Kolmogorov-Smirnov[a]			Shapiro-Wilk		
	Statistic	df	Sig.	Statistic	df	Sig.
Control	.166	15	.200*	.947	15	.472
Cholesterol	.166	15	.200*	.947	15	.472

Table C.50: Significance test (T. test) of intracellular IDE stability experiments.

Levene's Test for Equality of Variances			t-test for Equality of Means						
	F	Sig.	t	df	Sig. (2-tailed)	Mean Difference	Std. Error Difference	95% Confidence Interval of the Difference	
								Lower	Upper
Equal variances assumed	.000	1.000	-3.070	28	0.005	-30.33643	9.88229	-50.57938	-10.09348
Equal variances not assumed			-3.070	28	0.005	-30.33643	9.88229	-50.57938	-10.09348

Appendix D

Results of IDE promoter assay experiments

Table D.1: Results of IDE promoter assay on 03.02.2017

Zeit:	13:18:43										
System				SAFIRE2							
Anwender				SAFIRE2\Safire							
Platte				Nunclon 96 Flat Bottom White Polystyrol LumiNunc FluoroNunc [NUN96fw_LumiNunc FluoroNunc.pdfx]							
Platten-ID (Stapler)											
Label: Label1											
Modus				Lumineszenz							
Abschwächung				AUTOMATIC							
Farbe für OD2 Abschwächung											
Integrationszeit				500	ms						
Ruhezeit				10	ms						
Bereich der Platte				D1-E12							
Startzeit:	03.02.2017 13:18:52										
	Temperatur: 22.5 °C										
<>	1	2	3	4	5	6	7	8	9	10	11
Control	5059	6811	4871	257	1106034	429	63	35	43	37	49
Sample	7085	5623	5129	97	269	95	43	43	25	19	41
Endzeit:	03.02.2017 13:19:19										

Datum:	03.02.2017										
Zeit:	12:54:42										
System				SAFIRE2							
Anwender				SAFIRE2\Safire							
Platte				Nunclon 96 Flat Bottom White Polystyrol LumiNunc FluoroNunc [NUN96fw_LumiNunc FluoroNunc.pdfx]							
Platten-ID (Stapler)											
Label: Label1											
Modus				Lumineszenz							
Abschwächung				AUTOMATIC							
Farbe für OD2 Abschwächung											
Integrationszeit				500	ms						
Ruhezeit				10	ms						
Bereich der Platte				A1-B12							
Startzeit:	03.02.2017 12:54:51										
	Temperatur: 21.4 °C										
<>	1	2	3	4	5	6	7	8	9	10	11
Control	272	402	306	194	5032	10	38	26	28	22	26
Sample	266	200	166	148	5216	24	14	42	32	24	30
Endzeit:	03.02.2017 12:55:19										

Table D.2: Results of IDE promoter assay on 21.03.2017

Programm: Tecan i-control				Tecan i-control , 1.9.17.0							
Gerät: infinite M1000Pro				Seriennummer: 1210001738							
Firmware: V_1.05_11/2011_S3LCE_ALPHA (Nov 3 2011/09.27.24)				MAI, V_1.05_11/2011_S3LCE_ALPHA (Nov 3 2011/09.27.24)							
Datum:	21.03.2017										
Zeit:	12:24:52										
System				SAFIRE2							
Anwender				SAFIRE2\Safire							
Platte				Nunclon 96 Flat Bottom White Polystyrol LumiNunc FluoroNunc [NUN96fw_LumiNunc FluoroNunc.pdfx]							
Platten-ID (Stapler)											
Label: Label1											
Modus				Lumineszenz							
Abschwächung				AUTOMATIC							
Farbe für OD2 Abschwächung											
Integrationszeit				500	ms						
Ruhezeit				10	ms						
Bereich der Platte				A6-C12							
Startzeit:	21.03.2017 12:25:01										
	Temperatur: 22.4 °C										
<>	6	7	8	9	10	11	12				
Control	38865	25240	25329	31376	32480	54617	143940				
Sample	45812	43939	42861	36181	37849	44579	118296				
C	57	81	61	93	59	53	16563				
Endzeit:	21.03.2017 12:25:26										

Programm: Tecan i-control				Tecan i-control , 1.9.17.0							
Gerät: infinite M1000Pro				Seriennummer: 1210001738							
Firmware: V_1.05_11/2011_S3LCE_ALPHA (Nov 3 2011/09.27.24)				MAI, V_1.05_11/2011_S3LCE_ALPHA (Nov 3 2011/09.27.24)							
Datum:	21.03.2017										
Zeit:	11:59:52										
System				SAFIRE2							
Anwender				SAFIRE2\Safire							
Platte				Nunclon 96 Flat Bottom White Polystyrol LumiNunc FluoroNunc [NUN96fw_LumiNunc FluoroNunc.pdfx]							
Platten-ID (Stapler)											
Label: Label1											
Modus				Lumineszenz							
Abschwächung				AUTOMATIC							
Farbe für OD2 Abschwächung											
Integrationszeit				500	ms						
Ruhezeit				10	ms						
Bereich der Platte				F1-G12							
Startzeit:	21.03.2017 12:00:01										
	Temperatur: 21.1 °C										
<>	1	2	3	4	5	6	7	8	9	10	11
Control	60070	36432	37804	40125	44479	66831	48001	35	25	19	31
Sample	50569	56896	54087	46733	54730	62817	36844	45	33	33	15
Endzeit:	21.03.2017 12:00:29										

Table D.3: Results of IDE promoter assay on 28.03.2017

Programm: Tecan i-control				Tecan i-control , 1.9.17.0					
Gerät: infinite M1000Pro				Seriennummer: 1210001738					
Firmware: V_1.05_11/2011_S3LCE_ALPHA (Nov 3 2011/09.27.24)				MAI, V_1.05_11/2011_S3LCE_ALPHA (Nov 3 2011/09.27.24)					
Datum:	28.03.2017								
Zeit:	12:11:05								
System				SAFIRE2					
Anwender				SAFIRE2\Safire					
Platte				Corning 96 Flat Bottom Black Polystyrol [COS96fb.pdfx]					
Platten-ID (Stapler)									
Label: Label1									
Modus				Lumineszenz					
Abschwächung				AUTOMATIC					
Farbe für OD2 Abschwächung									
Integrationszeit				500	ms				
Ruhezeit				0	ms				
Bereich der Platte				C1-D12					
Startzeit:	28.03.2017 12:11:15								
	Temperatur: 22.2 °C								
<>	1	2	3	4	5	6	7	8	12
Control	3070	2682	3094	3110	3633	4869	270	170	64
Sample	3158	3312	3144	3482	3817	5042	2472337	206	86
Endzeit:	28.03.2017 12:11:42								

Programm: Tecan i-control				Tecan i-control , 1.9.17.0				
Gerät: infinite M1000Pro				Seriennummer: 1210001738				
Firmware: V_1.05_11/2011_S3LCE_ALPHA (Nov 3 2011/09.27.24)				MAI, V_1.05_11/2011_S3LCE_ALPHA (Nov 3 2011/09.27.24)				
Datum:	28.03.2017							
Zeit:	11:54:54							
System				SAFIRE2				
Anwender				SAFIRE2\Safire				
Platte				Corning 96 Flat Bottom Black Polystyrol [COS96fb.pdfx]				
Platten-ID (Stapler)								
Label: Label1								
Modus				Lumineszenz				
Abschwächung				AUTOMATIC				
Farbe für OD2 Abschwächung								
Integrationszeit				500	ms			
Ruhezeit				0	ms			
Bereich der Platte				A1-B12				
Startzeit:	28.03.2017 11:55:03							
	Temperatur: 21.4 °C							
<>	1	2	3	4	5	6	7	8
A	9959	6392	8358	8134	8917	11792	56559	47
B	8485	7902	7493	8595	9524	11149	25	55
Endzeit:	28.03.2017 11:55:31							

Table D.4: Data analysis of IDE promoter assay experiments.

Control	Sample	Mean	Factor	Adjusted* Control	Adjusted** Sample
18.59926	26.63533835	22.6173	111.9	92.0206	131.7793972
16.94279	28.115	22.52889		84.15406	139.6459424
15.9183	30.89759036	23.40795		76.09629	147.7037086
0.646995	0.905930511	0.776463	*Control×factor	93.24176	130.5582428
0.692798	0.772268701	0.732533	Mean	105.8301	117.9699118
0.670008	0.792445504	0.731227		102.5317	121.2682981
0.308264	0.372186211	0.340225	**Sample×factor	101.388	122.4120253
0.419587	0.419134396	0.419361	Mean	111.9604	111.839617
0.370184	0.419591619	0.394888		104.8997	118.9003203
0.382346	0.405119255	0.393732		108.6638	115.1361564
0.407424	0.400776984	0.404101		112.8203	110.9796801
0.412907	0.452237869	0.432572		106.8129	116.9871454
n= 12	n= 12		Average	100.035	123.7650371
			Std. Dev.	11.38992	11.38991758

Table D.5: Normality test of IDE promoter assay.

	Kolmogorov-Smirnov[a]			Shapiro-Wilk		
	Statistic	df	Sig.	Statistic	df	Sig.
Control	.214	12	.135	.903	12	.172
Cholesterol	.214	12	.135	.903	12	.172

Table D.6: Significance test (T. test) of IDE promoter assay.

			t-test for Equality of Means						
								95% Confidence Interval of the Difference	
Levene's Test for Equality of Variances	F	Sig.	t	df	Sig. (2-tailed)	Mean Difference	Std. Error Difference	Lower	Upper
Equal variances assumed	.000	1.000	-5.103	22	.000	-23.73007	4.64991	-33.37340	-14.08674
Equal variances not assumed			-5.103	22	.000	-23.73007	4.64991	-33.37340	-14.08674

Appendix E

Results of IDE activity experiments

Table E.1: Results of IDE activity experiment on 24.08.2016 with 150 µM PC 18:0.

SAFIRE II; Serial number: 506000019; Firmware: V 2.10 12/2007 Safire2; XFLUOR4SAFIREII Version: V 4.62n											
Date:					23/8/16						
Time:					11:57						
Measurement mode:					Fluorescence						
Excitation wavelength:					320	nm					
Emission wavelength:					405	nm					
Excitation bandwidth:					10	nm					
Emission bandwidth:					10	nm					
Gain (Manual):					100						
Number of reads:					10						
FlashMode:					High sensitivity						
Integration time:					40	µs					
Lag time:					0	µs					
Plate definition file:					COS96fb.pdf						
Part of the plate:					A1 - B7						
Z-Position (Calc. from Well A1):					5720	µm					
Number of kinetic cycles:					1000						
Kinetic interval (Minimal):					40	s					
Valid temperature range:					37 - 38	°C					
Shake duration (Orbital Medium):					10	s					
Shake duration between cycles (Orbital Medium):					30	s					
Target Temperature:					37	°C					
Current Temperature:					37.2	°C					
Rawdata (RFU)					Temperature:			37	°C		
Cycle No.	Time (s)	Temp (°C)	Ctr;l.	Sample	C	S	C	S	A7	Mean C	Mean S
1	0	37.0	1391	1109	1167	1143	1016	979	57	1191	1077
2	40	37,1	1332	1159	1237	1139	1079	1080	57	1216	1126
3	81	37.0	1554	1297	1436	1323	1253	1252	55	1414	1291
4	121	37,1	1734	1419	1617	1516	1395	1385	54	1582	1440
5	161	37,1	1910	1522	1750	1636	1559	1519	56	1740	1559
6	201	37,1	2077	1609	1859	1757	1697	1621	56	1878	1662
7	241	37.0	2186	1676	1993	1880	1806	1718	55	1995	1758
8	281	37.0	2284	1741	2081	1983	1913	1780	58	2093	1835
9	322	37,1	2375	1840	2168	2040	1982	1870	56	2175	1917
10	362	37.0	2476	1879	2230	2097	2063	1936	54	2256	1971
11	402	37,1	2542	1946	2298	2148	2149	1994	55	2330	2029
12	442	37.0	2614	1971	2360	2198	2208	2034	56	2394	2068
13	483	37,1	2658	2035	2407	2233	2239	2089	55	2435	2119
14	523	37.0	2701	2056	2439	2247	2307	2145	54	2482	2149
15	563	37,1	2745	2095	2484	2303	2333	2165	54	2521	2188
16	603	37,1	2761	2133	2508	2320	2371	2209	56	2547	2221

17	644	37.0	2801	2164	2538	2372	2420	2256	55	2586	2264
18	684	37,2	2857	2185	2569	2374	2425	2266	54	2617	2275
19	724	37,1	2853	2209	2568	2383	2407	2297	55	2609	2296
20	764	37,1	2878	2232	2587	2435	2453	2353	53	2639	2340
21	804	37,1	2888	2264	2626	2482	2478	2374	52	2664	2373
22	845	37.0	2937	2283	2661	2490	2501	2389	52	2700	2387
23	885	37,2	2944	2319	2660	2539	2529	2428	57	2711	2429
24	925	36,9	2952	2340	2657	2569	2527	2432	55	2712	2447
25	965	37,1	2964	2356	2672	2580	2546	2446	59	2727	2461
26	1005	37,1	2964	2358	2690	2610	2561	2479	55	2738	2482
27	1046	36,9	3006	2394	2700	2627	2560	2489	56	2755	2503
28	1086	37,2	3001	2402	2718	2649	2561	2498	55	2760	2516
29	1126	37,1	3019	2406	2711	2666	2576	2534	54	2769	2535
30	1166	37,1	2985	2441	2734	2700	2587	2531	55	2769	2557
31	1206	37.0	3024	2434	2754	2741	2590	2549	55	2789	2575
32	1246	36,9	3023	2437	2753	2770	2613	2582	55	2796	2596
33	1287	37,2	2992	2437	2740	2758	2617	2568	56	2783	2588
34	1327	37,1	3045	2463	2735	2771	2621	2577	54	2800	2604
35	1367	36,9	3024	2466	2735	2746	2617	2601	56	2792	2604
36	1407	37,2	3021	2466	2737	2797	2587	2603	54	2782	2622
37	1447	37.0	3027	2463	2777	2799	2623	2605	55	2809	2622
38	1487	37.0	3033	2506	2767	2825	2619	2638	54	2806	2656
39	1528	37,2	3031	2499	2786	2834	2630	2650	53	2816	2661
40	1568	37.0	3019	2522	2781	2830	2629	2671	55	2810	2674
41	1608	36,9	3031	2531	2761	2848	2638	2656	55	2810	2678
42	1648	37,1	3026	2551	2786	2862	2648	2716	58	2820	2710
43	1688	36,9	3023	2534	2783	2872	2650	2685	55	2819	2697
44	1728	37,2	3028	2535	2753	2861	2649	2723	55	2810	2706
45	1768	37,1	3054	2542	2783	2920	2673	2755	55	2837	2739
46	1809	37.0	3043	2564	2798	2980	2683	2777	57	2841	2774
47	1849	37,3	3047	2570	2792	2932	2668	2749	56	2836	2750
48	1889	36,9	3041	2563	2793	2985	2647	2761	53	2827	2770
49	1929	37,1	3074	2603	2792	2981	2680	2774	53	2849	2786
50	1970	37,1	3030	2585	2799	2990	2653	2786	57	2827	2787
51	2010	37.0	3058	2605	2786	3040	2661	2773	58	2835	2806
52	2050	37,2	3036	2632	2796	3009	2654	2803	54	2829	2815
53	2090	37,1	3045	2631	2805	3044	2664	2809	54	2838	2828
54	2130	37.0	3047	2657	2790	3052	2671	2840	52	2836	2850
55	2170	37,2	3038	2627	2797	3046	2668	2845	57	2834	2839
56	2211	36,9	3063	2679	2793	3025	2661	2848	56	2839	2851
57	2251	37,1	3055	2644	2802	3011	2662	2874	55	2840	2843
58	2291	37,1	3064	2657	2799	3029	2656	2885	53	2840	2857
59	2331	36,9	3064	2647	2782	3025	2648	2901	56	2831	2858
60	2371	37,2	3039	2660	2799	3033	2646	2898	56	2828	2864
61	2411	37,1	3042	2680	2789	3029	2670	2928	52	2834	2879
62	2451	37,1	3015	2698	2829	3029	2652	2901	57	2832	2876
63	2492	37,1	3067	2686	2796	3018	2651	2897	51	2838	2867
64	2532	37.0	3057	2670	2811	3051	2634	2880	57	2834	2867
65	2572	37.0	3017	2697	2785	3001	2653	2887	53	2818	2862
66	2612	37,1	3067	2670	2805	3030	2654	2917	55	2842	2872
67	2652	37.0	3062	2702	2801	3020	2641	2886	57	2835	2869
68	2692	37.0	3059	2710	2803	3025	2645	2919	55	2836	2885

69	2733	37.0	3052	2698	2800	3053	2636	2934	53	2829	2895
70	2773	37.0	3025	2682	2787	3050	2640	2960	57	2817	2897
	Slope		0.461	0.498	0.437	0.630	0.455	0.601			

Table E.2: Test of normality of IDE activity exprement with 150 µM PC 18:0.

	Kolmogorov-Smirnov[a]			Shapiro-Wilk		
	Statistic	df	Sig.	Statistic	df	Sig.
Control	.270	3	.	.949	3	.565
Cholesterol	.270	3	.	.949	3	.565

Table E.3: Data analysis IDE activity with 150 µM PC 18:0

	Control	Sample	mean	Factor
	0.461205	0.498868	0.480036	113.6
	0.437001	0.630287	0.533644	113.6
	0.455084	0.601608	0.528346	113.6
	*	**		
	109.1436	118.0564	* control × factor	
	93.02704	134.173	mean	
	97.84789	129.3521	** Sample × Factor	
			mean	
Avg	100.0062	127.1938		
Std	8.272189	8.272189		
SE	4.77595	4.77595		
T.test		0.015795		

Table E.4: IDE activity 24.08.2016 without PC

Time (s)	Control	Sample	C	S	C	S	Mean C	Mean S	Std. C	Std. S
0	221	374	284	408	251	369	252	384	32	21
40	204	349	232	380	215	368	217	366	14	16
81	206	379	225	416	230	397	220	397	13	19
121	203	412	232	449	233	428	223	430	17	19
161	206	430	228	482	232	455	222	456	14	26
201	207	449	227	514	240	477	225	480	17	33
241	206	474	223	542	232	504	220	507	13	34
281	204	476	227	556	239	532	223	521	18	41
322	206	496	228	580	235	555	223	544	15	43
362	209	513	231	594	237	573	226	560	15	42
402	205	513	228	605	234	588	222	569	15	49
442	209	525	230	623	238	605	226	584	15	52
483	209	522	227	637	238	611	225	590	15	60
523	207	534	230	647	239	626	225	602	17	60
563	207	544	228	651	246	646	227	614	20	60
603	202	553	232	667	238	652	224	624	19	62
644	204	557	228	675	237	653	223	628	17	63

684	204	553	234	679	242	653	227	628	20	67
724	211	568	234	680	244	666	230	638	17	61
764	207	568	234	680	238	667	226	638	17	61
804	211	576	232	685	239	682	227	648	15	62
845	212	567	232	688	235	680	226	645	13	68
885	209	573	239	710	240	680	229	654	18	72
925	210	579	232	702	234	691	225	657	13	68
965	211	586	227	707	232	696	223	663	11	67
1005	206	588	225	701	233	698	221	662	14	64
1046	213	584	228	704	230	712	224	667	9	72
1086	206	592	226	704	236	687	223	661	15	60
1126	211	592	227	699	228	715	222	669	10	67
1166	206	591	225	713	233	720	221	675	14	73
1206	210	601	225	709	231	711	222	674	11	63
1246	215	598	227	721	233	708	225	676	9	68
1287	214	602	219	709	231	706	221	672	9	61
1327	195	599	218	713	232	709	215	674	19	65
1367	211	600	222	716	230	704	221	673	10	64
1407	210	608	223	708	229	715	221	677	10	60
1447	205	608	219	712	226	720	217	680	11	62
1487	202	610	220	726	226	726	216	687	12	67
1528	205	606	215	729	232	710	217	682	14	66
1568	206	611	217	731	230	705	218	682	12	63
1608	212	613	217	720	225	721	218	685	7	62
1648	210	625	223	725	226	725	220	692	9	58
1688	208	623	216	719	226	723	217	688	9	57
1728	203	624	220	738	232	730	218	697	15	64
1768	211	611	214	729	224	734	216	691	7	70
1809	208	613	219	733	223	738	217	695	8	71
1849	204	623	221	733	217	724	214	693	9	61
1889	209	633	217	736	233	731	220	700	12	58
1929	205	636	214	731	231	739	217	702	13	57
1970	207	622	217	738	224	729	216	696	9	65
2010	208	628	214	727	222	732	215	696	7	59
2050	203	623	215	733	222	739	213	698	10	65
2090	203	624	215	736	223	748	214	703	10	68
2130	205	643	215	733	228	736	216	704	12	53
2170	208	628	210	734	224	736	214	699	9	62
2211	202	630	216	739	220	724	213	698	9	59
2251	210	633	214	745	223	739	216	706	7	63
2291	205	627	216	747	219	738	213	704	7	67
2331	201	629	213	731	228	733	214	698	14	59
2371	203	638	213	745	219	739	212	707	8	60
2411	206	641	210	733	224	734	213	703	9	53
2451	206	646	215	734	224	744	215	708	9	54
2492	201	643	211	738	222	732	211	704	11	53
2532	204	645	206	738	223	740	211	708	10	54
2572	204	639	213	749	220	730	212	706	8	59
2612	204	640	210	748	222	743	212	710	9	61
2652	202	638	212	740	224	739	213	706	11	59
2692	206	648	210	748	224	738	213	711	9	55
2733	200	641	208	749	220	740	209	710	10	60
2773	203	647	211	743	220	745	211	712	9	56
Slope	0.002	0.087	0.011	0.103	0.007	0.115				

Table E.5: Test of normality of IDE activity exprement without PC 18:0.

	Kolmogorov-Smirnov[a]			Shapiro-Wilk		
	Statistic	df	Sig.	Statistic	df	Sig.
Control	.177	3	.	1.000	3	.966
Cholesterol	.177	3	.	1.000	3	.966

Table E.6: Data analysis IDE activity without PC 18:0

	Control	Sample	MBV	Factor
	0.001016893	0.087205	0.043094	785
	0.010623266	0.103366	0.046372	
	0.007021257	0.115413	0.054196	
	18.5237793	1588.524		
	179.8355406	1749.836		
	101.699767	1671.7		
Avg	100.0196956	1670.02		
std	80.6690031	80.669		
SE	46.57427066	46.57427		
t.test		0.334703		